6-1-2021

Flaxseed's paradoxical role in extending lifespan and reproductive capacity in White Leghorn laying hens; and the effect of polyunsaturated fatty acids (PUFAs) on lipid metabolism, mitochondrial bioenergetics and E-cadherin expression in laying hen ovarian tumors

William Christopher Weston
Southern Illinois University Carbondale, william.c.weston1@gmail.com

FLAXSEED'S PARADOXICAL ROLE IN EXTENDING LIFESPAN AND REPRODUCTIVE CAPACITY IN WHITE LEGHORN LAYING HENS; AND THE EFFECT OF POLYUNSATURATED FATTY ACIDS (PUFAS) ON LIPID METABOLISM, MITOCHONDRIAL BIOENERGETICS AND E-CADHERIN EXPRESSION IN LAYING HEN OVARIAN TUMORS

by

William Christopher "Chris" Weston

B.A., Southern Illinois University, 2005
M.S., Southern Illinois University, 2012

A Dissertation
Submitted in Partial Fulfillment of the Requirements for the
Doctor of Philosophy Degree

Department of Molecular, Cellular and Systemic Physiology
in the Graduate School
Southern Illinois University Carbondale
May 2021

DISSERTATION APPROVAL

FLAXSEED'S PARADOXICAL ROLE IN EXTENDING LIFESPAN AND REPRODUCTIVE CAPACITY IN WHITE LEGHORN LAYING HENS; AND THE EFFECT OF POLYUNSATURATED FATTY ACIDS (PUFAS) ON LIPID METABOLISM, MITOCHONDRIAL BIOENERGETICS AND E-CADHERIN EXPRESSION IN LAYING HEN OVARIAN TUMORS

by

William Christopher "Chris" Weston

A Dissertation Submitted in Partial

Fulfillment of the Requirements

for the Degree of

Doctor of Philosophy

in the field of Molecular, Cellular and Systemic Physiology

Approved by:

Dr. Dale B. Hales, Chair

Dr. Karen H. Hales

Dr. Brent M. Bany

Dr. Matthew J. Young

Dr. Philip J. Jensik

Graduate School
Southern Illinois University Carbondale
December 11, 2020

AN ABSTRACT OF THE DISSERTATION OF

Chris Weston, for the Doctor of Philosophy degree in Molecular, Cellular and Systemic Physiology, presented on December 11, 2020, at Southern Illinois University Carbondale.

TITLE: FLAXSEED'S PARADOXICAL ROLE IN EXTENDING LIFESPAN AND REPRODUCTIVE CAPACITY IN WHITE LEGHORN LAYING HENS; AND THE EFFECT OF POLYUNSATURATED FATTY ACIDS (PUFAS) ON LIPID METABOLISM, MITOCHONDRIAL BIOENERGETICS AND E-CADHERIN EXPRESSION IN LAYING HEN OVARIAN TUMORS

MAJOR PROFESSOR: Dr. Dale Buchanan Hales

We are the first lab to report the occurrence of a diet-induced transsulfuration (TS) blockade associating with elevated S-adenosylmethionine (SAM) synthesis, enhanced lifespan and enhanced reproductive capacity, in a vertebrate animal model. In this paradoxical study, we used LC-MS/MS-derived metabolomics data to report the effects of flaxseed (*Linum usitatissimum*) on one-carbon metabolism in White Leghorn laying hens (*Gallus gallus*). Flaxseed contains a vitamin B6-antagonizing molecule called "linatine" that is particularly effective at reducing vitamin B6 levels in small rodents and poultry. Linatine reduces TS flux due to its inhibition of the vitamin B6-dependent enzymes cystathionine beta synthase (CBS) and cystathionine gamma lyase (CSE). In this study, our flaxseed-fed hens displayed decreased 4-pyridoxic acid and decreased pyridoxamine, concomitant with over 15-fold elevated cystathionine. Homocysteine levels were stable in flaxseed-fed hens despite such highly elevated cystathionine. This is an astonishing finding, because mammalian models would predict the induction of hyperhomocysteinemia (i.e. elevated homocysteine) when cystathionine is so highly elevated (1). We are therefore reporting a phenomenon that might be unique to birds. Our metabolomics data indicate increased consumption of one-carbon donor molecules (e.g. choline, betaine, dimethylglycine, serine, etc) in flaxseed-fed hens, probably as a means of fueling the betaine homocysteine methyltransferase (BHMT) and methionine synthase-B12 (MS-B12) reactions.

This modeling approach provides a rationale that flaxseed-fed hens increase their rate of homocysteine remethylation via BHMT and MS-B12, and in turn this would maintain stable homocysteine levels in the animal. We observed that the culminating outcome is elevated synthesis of SAM and an elevated SAM:SAH ratio. The associated biological outcomes are extended lifespan and increased reproductive capacity (i.e. increased daily egg laying) in flaxseed-fed hens. Our data further indicate that flaxseed tremendously stimulates a glucagon-like phenotype in hens. Specifically, flaxseed-fed hens exhibit 3-fold elevated glycated hemoglobin (HbA1c) (2), 2-fold elevated serum free fatty acids (FFAs), 10 to 14% reduced body weight, and slightly reduced plasma pyruvate. Interestingly, the HbA1c level of our flaxseed-fed hens (i.e. 6.2% HbA1c) (2) represents the highest HbA1c level ever reported in a wild-type avian species. These phenotypic markers suggest that elevated glucagon release could play a synergistic role in enhancing lifespan and reproductive capacity in flaxseed-fed hens. We suspect that linatine is responsible for stimulating this glucagon-like phenotype. Therefore, we conclude that the vitamin B6-antagonizing effects of linatine (via flaxseed dieting) improve liver function, body leanness, egg laying performance and animal survival, in a manner associated with increased SAM synthesis, increased blood FFAs and increased blood glucose, in laying hens.

The second part of this dissertation is used to test the hypothesis that polyunsaturated fatty acids (PUFAs) regulate lipid metabolism, increase mitochondrial respiration and decrease E-cadherin expression, in laying hen ovarian tumors. Researchers are unaware of the mitochondrial effects of PUFAs within laying hen ovarian tumors, and only a few publications exist regarding the analysis of E-cadherin in laying hen ovarian cancer. The results of this present work suggest that dietary PUFAs accumulate within laying hen ovarian tumors, and these same tumors exhibit decreased gene transcripts that govern *de novo* lipogenesis (i.e. *FASN*). Simultaneously, these

tumors exhibit elevated transcripts for oxidative phosphorylation (OXPHOS) and decreased transcripts for phase 2 antioxidant enzymes. These patterns associated with decreased transcript levels of *CDH1* (the gene for E-cadherin) in ovarian tumors, but no effect on full length 120kDa protein was observed by PUFAs versus our control diet. Interestingly, the effect of PUFAs on E-cadherin occurred at the level of the cleaved 37kDa and 80kDa E-cadherin fragments, such that PUFAs reduced their levels in hen ovarian tumors. We therefore developed a system for depleting the 80kDa E-cadherin fragment from hen ascites fluid (i.e. fluid from a hen that had ovarian cancer), so that we could test our hypothesis that the 80kDa E-cadherin fragment is important for supporting mitochondrial respiration in normal ovarian surface epithelial cells (IOSE80s). Mitochondrial membrane potential was decreased in IOSE80s when the 80kDa fragment was removed from the ascites; however, there was no effect on basal oxygen consumption in subsequent tests using extracellular flux analysis with Seahorse XF_p. During our analysis of microRNA-200a-3p (miR-200a) we did not observe any effect of diet on miR-200a within hen ovarian tumors; however, we did observe that miR-200a levels increased within the tumor when going from stage 2 to stage 4 disease. Overall, we observed reduced risk of ovarian cancer, stage 4 ovarian cancer, multiple peritoneal tumor involvement and cancer-associated mortality, in laying hens that consumed a diet that was supplemented with PUFAs.

ACKNOWLEDGEMENTS

This research was made possible by the commitment, mentorship and friendship of numerous people. A significant amount of chronological time transpires during a student's time within a PhD program, and with that it becomes imperative for friends, family, mentors, professors and colleagues, to be supportive in a myriad of ways.

Firstly, I want to acknowledge the commitments and sacrifices that were displayed by family and friends during this journey. The long nights and extended periods of unavailability were a challenge for everyone, and I acknowledge that this was encountered by everyone. This was a unique experience for everyone. Dorian and Odin (my kids), I hope that you benefit from observing your dad complete a PhD. You both had a rare perspective during this process, because you are wide-awake teenagers. Therefore, you were able to get a first-hand glimpse of what it means to be a graduate student and in particular a PhD student. My only wish is that you realize that your potential as human beings is without limitation, and you get to choose your own vision and excitement about your own life.

Without equivocation, I completed this research and received a PhD in part due to the confidence and support of my research committee. My PhD advisor, Dr. Dale B. Hales ("Buck"), has been a friend to me for quite some time, and I could not have had a more trusting and dedicated mentor. Buck supported me in a plethora of ways, both inside and outside of the lab. I will always be grateful for Buck's commitment during my time as his PhD student. I am confident that Buck enabled me to take radical ownership of my research, which truly enabled me to bring forth my most creative and bold research. We discovered several unique things within our research model, and I am confident that these discoveries would never have arisen had Buck not placed such high confidence in my analytical abilities. Furthermore, it is always a joy

to share with anyone who loves mitochondria. May the ‘mitochondriacs’ lead the way! Thank you for your mentorship and friendship, Buck. Your impression will be left on everything that I do moving forward. I look forward to opportunities to continue collaborating as scientists and as friends. If there was one thing that I learned from you, it was that “right now in the moment” we have the ability to see a situation for what it is and then to act in the most tactful and helpful manner possible. Ryder is lucky to have you as his dad.

To Dr. Karen Hales, I appreciate your ability to relentlessly ask provoking questions about science. I acknowledge your confidence to ask the “exact” question that is on your mind. This is where I think many scientists struggle. You are the exemplification of confidence. As a PhD student, I always felt like I wanted to make scientific discoveries that supported your scientific pursuits. It seemed like I was doing something important if it fit into your lane of study. This is my humble way of saying you are an inspiration to me. I also appreciate your ability to help me to stay calm during key moments of the PhD process. Also, long live Carbondale New School! I would not have landed in Buck’s lab and your lab had Ryder not attended school with Dorian. Dorian is a young musician too, so maybe he and Ryder can collaborate in the future.

To Dr. Matt Young, I practically lived in your lab half of the time that I was in this PhD program. I appreciate your ability to support the experiments that I conducted. The high-quality standards that you displayed helped me to expect more from myself in terms of experimental consistency and accuracy. You and Carolyn are experts at making students feel at home in your lab. That is priceless. I hope that you keep this tradition in your lab. You are an expert of your field of study. My perspective as a physiologist was expanded exponentially through our pursuits as researchers of mitochondrial metabolism. Thank you for supporting me during committee meetings, because I know that the mitochondrial language is not spoken by all people. You know

this. I have no doubt in my mind that you are a leader in your field of study.

To Dr. Brent Bany, the conversations that we shared about family and life meant just as much to me as your advice about primer efficiencies while conducting qPCR. Thank you so much for being a part of this process. I will always remember your question during my preliminary examination, "what is one of the major assumptions about variance during one-way ANOVA?" It is humbling to realize that, as much as I think I know, there is always more to remember, learn and realize. Thank you, Brent. Also, I learned a lot about being an "analyst" from you; specifically with regard to appreciating the notion of a "big biological effect." This was a tremendous conceptual contribution to my research.

To Dr. Phil Jensik, I acknowledge that you are a very refined molecular biologist. I also acknowledge the passion that you have for your research. I would trust you as a trustworthy colleague and collaborator. One of the most valuable moments of my research was when you convinced me to not pursue certain molecular experiments. Sometimes it seems tempting as a researcher to try certain techniques that, quite simply, are way more complicated than they appear at face value. So thank you for being very frank with me about several molecular techniques. I once heard that it is just as valuable in life to know three things: 1) what to start, 2) what to quit, and 3) what to never start. My path was made much clearer by your experience. Thank you, Phil.

I am grateful to all of my committee members for ensuring that my scientific approaches were grounded in reliable scientific practices. You were strongly committed to my ability to utilize well-calibrated techniques that produce the most repeatable results. At times it felt like the school of hard knocks, but that's biological science. I acknowledge that each of you had open-door "locker room" talks with me that helped both my personal and professional development. I

appreciate all of you being able to share with me the finer intricacies of science and life.

To Dr. Purab Pal ("Purab, my mate"), my friend and labmate, you were such an important friend to me during the process of my studies. We shared many important coffee talks. Also, your technical experience in the lab was a great help. Thank you so much. And as always, "thaw it in the window." I look forward to keeping in touch, man.

To Kara Starkweather, I wanted to say thank you for being a good friend in the lab. I appreciate your experience in cell culture and in western blotting. You worked in the lab longer than anyone, throughout your bachelors and masters. Thank you for being you.

To Angie Raymer, thank you so much for being an excellent instructor and course director. Your efforts helped to ensure the welfare and funding of graduate students, particularly because you directed the undergraduate courses that provided TA opportunities for graduate students. This is a very integral contribution to the department. Said concisely, the department would not have a functional graduate program without your efforts. Thank you.

To Susan Sugawara, thank you for your support in helping with all matters related to the program. You are without question one of the most talented people in our department, given the wide variety of things that you are tasks with. You're also a very strong person whom I have seen overcome many challenges. Thank you for being a kind person who sets a good example. Also, your appreciation of animals is very well received.

To Carolyn Skouby, thank you for helping to facilitate all of our purchasing and acquisitions, and also for securing our semesterly contracts. These were indispensable aspects of being in a successful laboratory. Also, no graduate student could survive without a funded contract, and this is another way that you made a tremendous impact. Thank you for being a true professional and kind person to work with.

To Dr. Denise Zaczek, I want to mention that you were my first physiology instructor (back in 2009, before I entered graduate school). You elevated my interest and appreciation of physiological and biological studies. Your method of teaching, in particular with regard to endocrinology and gastrointestinal physiology, clicks with my train of thought. Also, thank you for sharing your ideas and references as I crafted my PhD research. Your encouragement helped me to be an authentic researcher who acted boldly and with excitement.

To the late Terence Mckenna, thank you for the work that you did during your career. I wish that you could be here to see how the world has unfolded since the start of the new millennium. You would be excited to know that the United States is abolishing its restrictions on mind-altering substances and embracing the usage of these substances medicinally. We are making big strides in remembering what it means to be human. Thank you for your courage, Terence.

Finally, I would like to acknowledge my kids and myself for the tremendous courage that we demonstrated during the completion of this PhD program. Thank you, Odin and Dorian.
We made it! We are strong. I also acknowledge your courage and sacrifices, too, Heather, Tisha, Karen, Jose, Michel, Dad and Renee. I'll even throw ex-girlfriends in there, too. Thank you all for helping me. And as always, you're welcome!

DEDICATION

I dedicate this work to ‘a hope’ that humans will be courageous enough to step outside of cultural ways of thinking. I want all people be brave enough to ask questions that are not limited by the dominating gravity of ideologies and institutions. May all scientists act as individuals who represent their own purpose and vision. As scientists in the free nation of the United States of America, we have a responsibility to the world to develop bold and authentic hypotheses that are not limited by dogmatic religious beliefs or otherwise oppressive laws that exist elsewhere.

I dedicate this work to ‘an intention’ that science will be used to sustain and protect Earth’s natural resources. Science’s purpose is not to fuel tidal waves of economic growth. Humans do not need the next generation of cell phones or computers; humans do not need the next generation of social media; humans do not need the next generation of advanced instruments that alienate humans from nature; humans do not need one billion more inhabitants on this planet.

I dedicate this work to ‘a vision’ that science will empower researchers as authentic individuals whose provisional understandings of the world mean everything to science.

I dedicate this work to the individual who seeks truth from nature and not from culture.

I dedicate this work to the individual who seeks wisdom from individual experience.

I dedicate this work to the individual who accepts that the human brain has its own limitations. Some things cannot be known.

I dedicate this work to the individual who lives within this world, within their own body.

I dedicate this work to the individual whose favorite question is, “what are we?”

I dedicate this work to the extremely rare opportunity to be alive.

I dedicate this work to the individual whose purpose is Self and nature.

I dedicate this work to the individual who eats the fruit of the tree of knowledge.

TABLE OF CONTENTS

LIST OF TABLES

TABLE PAGE

LIST OF FIGURES

LIST OF ABBREVIATIONS

Abbreviation	Complete term
1ADP	1-amino D-proline
2-MOE	2-methoxyestradiol
4PA	4-pyridoxic acid
5,10-CH_2THF	N5,N10-methylene-tetrahydrofolate
5-CH_3THF	N5-methyl-tetrahydrofolate
AA	Arachidonic acid
ACC	Acetyl CoA Carboxylase
ACYL	ATP citrate lyase
AKA	Also known as
ALA	Alpha-linolenic acid
AST	Aspartate aminotransferase
ATP5B	ATP synthase subunit 5b
B6	Vitamin B6
BHMT	Betaine homocysteine methyltransferase
CAT	Catalase
CBS	Cystathionine beta synthase
CHDH	Choline dehydrogenase
CoA	Coenzyme A
COMT	Catechol-O-methyltransferase
CPT1	Carnitine palmitoyl transferase 1
CPT2	Carnitine palmitoyl transferase 2

CRN	Corn oil diet
CSE	Cystathionine gamma lyase (AKA Cystathionase)
CTL	Control diet
dcSAM	Decarboxylated SAM
DF	Defatted flaxseed diet
DHA	Docosahexaenoic acid
DMEM	Dulbecco's Modified Eagles Medium
DMG	Dimethylglycine
DMGDH	Dimethylglycine Dehydrogenase
DNAse	DNA cleavage enzyme
DNM1L	Dynamin-like protein 1 (DRP1)
dTMP	Deoxythymidine monophosphoate
dTTP	Deoxythymidine triphosphate
dUMP	Deoxyuriacil monophosphate
EGF	Epidermal growth factor
EPA	Eicosapentaenoic acid
ETC	Electron transport chain
FAD	Flavin adenine dinucleotide
FASN	Fatty acid synthase
FFA	Free fatty acid (ie non-esterified fatty acid)
FSH	Fish oil diet
FXO	Flaxseed oil diet
GCS	Glycine cleavage system

GPX	Glutathione peroxidase
GSH	glutathione
GSSG	Reduced glutathione
H&E	Hematoxylin and eosin
HbA1c	Glycated hemoglobin
Hcy	Homocysteine
HO1	Heme oxygenase 1
HyperHcy	Hyperhomocysteinemia
IMS	Intermembrane space
LA	Linoleic acid
L-CAM	Liver-cell adhesion molecule (AKA CDH1)
MAM	Mitochondria-associated membrane
MAT	Methionine adenosyl transferase
Met	Methionine
miRNA	micro RNA
mRNA	messenger RNA
MS-B12	Methionine Synthase-B12 (cobalamin) complex
MTA	Methylthioadenosine
MT-COX1	Cytochrome c oxidase subunit 1, mitochondrial encoded
MT-COX2	Cytochrome c oxidase subunit 2, mitochondrial encoded
MT-COX3	Cytochrome c oxidase subunit 3, mitochondrial encoded
MT-CYTB	Cytochrome b, mitochondrial encoded
MTHFR	Methlene tetrahydrofolate reductase

MTHFD2	Methylene tetrahydrofolate dehydrogenase 2, bidirectional
NAFLD	Non-alcoholic fatty liver disease
NOS2	Inducible nitric oxide synthase
NQO1	NAD(P)H Quinone Dehydrogenase 1
OCR	Oxygen consumption rate
OvCa	Ovarian cancer
OXPHOS	Oxidative phosphorylation
PC or PtdChl	Phosphatidylcholine
PE or PtdEth	Phosphatidylethanolamine
PEMT	Phosphatidylethanolamine methyltransferase
PEPCK	Phosphoenoylpyruvate carboxykinase
PLC	Phospholipase C
PLD	Phospholipase D
PLP	Pyridoxal 5' phosphate
PRX	Peroxinredoxin
PUFA	Polyunsaturated fatty acid
PVDF	Polyvinylidene difluoride membrane
ROS	Reactive oxygen species
RT	Room temperature
SAH	S-adenosylhomocysteine
SAM	S-adenosylmethionine
SCD1	Sterol CoA desaturase 1
SDH	Sarcosine dehydrogenase

SHMT1	Serine hydroxymethyltransferase 1 (cytosolic)
SHMT2	Serine hydroxymethyltransferase 2 (mitochondrial)
SLC25A4	ADP/ATP Translocase 1
SNAI2	Slug
SOD1	Superoxide dismutase (cytosolic)
SOD2	Superoxide dismutase (mitochondrial)
SREBP1	Sterol regulatory element binding protein
THF	Tetrahydofoloate
TK	Thymidine kinase
TS	Transsulfuration
TYMS	Thymidylate synthase
WF	Whole flaxseed diet
ZEB1	zinc finger E-box binding homeobox 1

CHAPTER 1

INTRODUCTION

1.1 Ovarian Cancer

Ovarian cancer is the 7th most common cancer in women worldwide and the 8th most common cause of cancer-related death in women. In 2012, ovarian cancer accounted for 239,000 new cancer cases and 152,000 cancer-related deaths worldwide (3). The 5-year survival rate for a patient diagnosed with ovarian cancer has remained consistently low, averaging between 30-50% in most countries (4). In the United States, a woman's lifetime chance of developing ovarian cancer is 1 in 75, and meanwhile a woman's lifetime chance of dying from ovarian cancer is almost equivalent at 1 in 100 (5). Said concisely, morbidity from ovarian cancer is tightly coupled to individual mortality. Ovarian cancer's low survival rate is the result of late stage detection when the survival probability beyond five years reaches an abysmal 29% (5). In 1979, the etiology of ovarian cancer was argued as stemming from incessant (monthly) ovulation, whereby genetic mutations accrue over the reproductive lifetime of a woman in response to menstrual cycle-associated healing of the ovarian surface epithelium (6). In support of this hypothesis, the risk of ovarian cancer is inversely correlated with parity and the usage of pharmaceutical birth control (7,8). Therefore, a probable best route to deal with ovarian cancer is disease prevention and disease severity reduction, which our lab has pursued by employing the laying hen model for ovarian cancer and the flaxseed dietary intervention strategy. A valuable animal model for studying ovarian cancer is the egg laying hen model, because laying hens spontaneously develop ovarian cancer at around 2 years of age, an age when hens have ovulated nearly as many times as a woman approaching menopause (9–13). The incessant ovulation phenomenon was recapitulated in a study showing that restricted ovulation mutant hens develop

significantly less ovarian cancer than wild type laying hens (13). Furthermore, human epithelial ovarian cancer histotypes (e.g. serous, endometrioid, mucinous, etc) can be identified in hen ovarian cancer (9). Our lab has spent a number of years engaging the laying hen ovarian cancer model with a particular focus on pathological prevention and intervention through dietary enrichment with polyunsaturated fatty acids (PUFAs).

1.2 Flaxseed for ovarian cancer

Our lab has shown that dietary flaxseed reduces the severity of ovarian cancer by regulating prostaglandin synthesis, steroid metabolism, cytochrome P450 enzymes, angiogenesis and intrinsic apoptosis in laying hen ovarian tumors (14–17). We observed that dietary whole flaxseed (WF), which is a rich source of alpha-linolenic acid (ALA), reduces ovarian cancer severity in laying hens via altering inflammatory activation and estrogenic signaling (15–19). Knowing that ALA can be desaturated and elongated several times until becoming docosahexaenoic acid (DHA), we have also sought to uncover the anti-ovarian cancer effects of DHA-rich sources such as fish oil (FSH). We observed that dietary FSH decreases inflammatory protein expression in pre-cancerous (normal) hen ovaries, suggesting a potential role in preventing ovarian carcinogenesis (20). Very recently we showed that DHA as well as WF exhibit anti-angiogenic and pro-apoptotic properties in the context of chicken embryogenesis and laying hen ovarian cancer (21). Our lab's works indicate that WF's mechanisms of action operate discretely and synergistically through WF's omega-3 PUFA-rich component and lignan/fiber-rich component.

1.3 Major components of flaxseed

Flax (*Linum usitatissimum*) is a highly nutritious annual crop that provides fibers and oils to humans all over the world (22). Between 38 to 50% of the seed content of flax (i.e. flaxseed)

consists of oil (23–25), which is composed of ~50% ALA, ~20% oleic acid, ~15% linoleic acid (LA), 6% palmitic acid and 4% stearic acid (26,27). Thanks to novel work from George Burr and Mildred Burr in the early 20th century, we now observe that LA (28) and ALA (29) are essential fatty acids that must be derived from the diet (30). A myriad of long-chain omega-3 and omega-6 polyunsaturated fatty acids (PUFAs) can be synthesized from ALA or LA through the activities of desaturase and elongase enzymes (31,32). It is through these elongation and desaturation activities that PUFAs such as eicosapentaenoic acid (EPA) and docosahexaenoic acid (DHA) can be derived.

Flaxseed consists of 20-30% protein by mass, with an amino acid index mostly similar to soybeans (33,34). Compared to soy, flaxseed contains more arginine, glutamic acid, glycine and methionine; however, flaxseed is less concentrated with lysine, aspartic acid, leucine and tyrosine (23,24,35); Flaxseed is sometimes referred to as a 'protein-limited' food due to its lower lysine content (35) and lower lysine:arginine ratio (36); however, the overall bioactivity of flaxseed proteins is high (>70%) (37), meaning that flaxseed proteins are efficiently digested and integrated into the metabolism. Defatted flaxseed (DF) varieties likely have the best protein digestibility, because the extraction of mucilage and oil during the defatting process improves the digestibility coefficient of flaxseed proteins (38). It is worth noting that chickens (like other avian species) have a gizzard to grind seed material (39), so they are ideal animals for consuming WF. This is a marked difference from mammals, because mammals lack a gizzard and therefore rely on the mastication (i.e. chewing) process to forcefully grind food. It's as though the mammalian mouth is functionally analogous to the avian gizzard.

1.4 Food toxins as a normal part of life

Food toxicity researcher Bruce Ames illustrated that humans receive the majority of their

biological pesticides from everyday foods (40), suggesting that exposure to plant-based toxins is a normal part of being an omnivorous animal. Plants contain a myriad of socalled 'toxic' molecules that protect them from predation, and animals have thankfully evolved detoxification systems to allow the safe digestion of many of these plant molecules (40,41). Such a detoxification regime requires the activity of cytochrome P450 (CYP450) enzymes in the liver (42). In humans, most prescription drugs are cleared from the liver by CYP450 enzymes, with CYP3A4 and CYP3A5 accounting for 37% of all drug clearance (43). Our lab has illustrated that flaxseed influences CYP1A1 and CYP3A4 expression, respectively, in the liver and ovary of the laying hen (16), suggesting that the components of flaxseed influence detoxification systems in chickens. Flaxseed contains numerous molecules that are recorded as toxic in the literature, such as linatine, cyanogenic glycosides, phytic acid and trypsin inhibitors (35,44). In Europe, a heated debate currently exists as to whether the cyanogenic glycosides in flaxseed are toxic to humans and, in particular, toxic to children (45). Cyanogenic glycosides, when catabolized by β-galactosidase, can contribute to the formation of hydrogen cyanide within the animal (46). However, it is important to consider that cyanide is a commonly occurring molecule in many human foods (47,48), including flaxseed (49), suggesting that dietary cyanide might be an equivocal concern. A human study revealed that flaxseed does not elevate physiological cyanide levels to an appreciable concentration (50).

1.5 Vitamin B6 metabolism

The discovery and elucidation of vitamin B6 happened in 1934, at a time when B vitamins were investigated in relation to "rat pellagra prevention factor" (51). The *de novo* synthesis of vitamin B6 occurs in plants, fungi and bacteria, but not in animals which makes B6 essential in the animal diet (52). The term 'vitamin B6' refers to six different B6 vitamer molecules that are

based on three structures: pyridoxine, pyridoxal and pyridoxamine. These three structures are differentiated based on the chemistry of the 4' carbon of the pyridine ring. At the 4' carbon, pyridoxine contains alcohol, pyridoxal contains aldehyde, and pyridoxamine contains amine (52). The naming of the B6 vitamer is based on the chemistry of the 4' carbon; for example, pyridoxal has an "-al" suffix because of aldehyde at the 4' carbon. These three B6 vitamers (pyridoxine, pyridoxal and pyridoxamine) can be further divided into two groups based on the phosphorylation status of their 5' carbon. The three phosphorylated vitamers are: pyridoxine 5' phosphate, pyridoxal 5' phosphate (PLP), and pyridoxamine 5' phosphate (53). A seventh molecule called 4-pyridoxic acid, which contains carboxyl at the 4' carbon, represents an end-point urinary excretion molecule among B6 vitamers. PLP is the active cofactor for B6-dependent reactions (53). The aldehyde of PLP is necessary for forming a 'Schiff base' with the ε-amino group (i.e. C=N) on a lysine residue located on the exterior the B6-dependent enzyme. The formation of the Schiff base constitutes an internal aldimine whereby PLP is bound to the B6-dependent enzyme (54). An incoming amine-containing substrate (e.g. tyrosine) can then displace the lysine ε-group in the internal aldimine, producing an external aldimine that consists of PLP and the incoming amine substrate (e.g. PLP-tyrosine). This external aldimine can then use the amine substrate in a myriad of reactions (decarboxylation, racemization, transamination, α/β elimination, retro aldol cleavage, etc) to yield the final modified product plus pyridoxamine 5' phosphate (54). Two critical B6-dependent reactions within our current research include the two primary reactions of the transsulfuration (TS) pathway:

Cystathionine beta synthase (CBS): Homocysteine + Serine → Cystathionine + H_2O

Cystathionine gamma lyase (CSE): Cystathionine + H_2O → Cysteine + α-ketoglutarate + NH_4^+

Over 140 PLP-dependent enzymatic reactions are known in biology, comprising 4% of all

known enzymatic reactions (55). B6 vitamers also have roles outside of B6-dependent enzymatic reactions. For example, B6 vitamers function as potent reactive oxygen species (ROS) scavengers (56,57), similar to the activity of ascorbic acid and α-tocopherol.

1.6 Linatine, a naturally-occurring vitamin B6-antagonist in flaxseed

Nature provides a myriad of direct and indirect ways for animals to encounter vitamin B6 antagonism (i.e. molecules that reduce B6 levels in the animal) (58). Linatine, the putative vitamin B6-antagonizing molecule in flaxseed, was first isolated and characterized in 1967 (59). The cotyledon portion of flaxseed (as opposed to the mucilage or hull portion) is responsible for exerting flaxseed's anti-growth effect (60). Linatine was named according to its discovery in 'linseed' (AKA flaxseed) and according to the fact that the linatine molecule is a dipeptide (thus the "-ine" suffix). Klosterman *et al.* characterized linatine as 1-[(N-γ-L-glutamyl)amino]-D-proline, which is essentially a glutamic acid associated with a D-proline through the γ-carboxyl of the glutamic acid (59). Upon acid hydrolysis, linatine disassociates into glutamic acid and 1-amino D-proline (1ADP). The canonical B6-antagonizing effect is exerted through 1ADP's ability to form an inert hydrazone with pyridoxal 5' phosphate (PLP), thus removing PLP from the metabolism. 1ADP's anti-growth properties are 50 times stronger than the L-proline enantiomer in terms of inhibiting growth (59). The first observation that flaxseed exerted anti-growth effects was made in a study of flaxseed-fed chickens (chicks) in 1928 (61). By 1948, researchers realized that flaxseed's anti-growth properties can be eradicated by soaking flaxseed meal in water for 18 to 24 hours prior to feeding chicks (62,63). At the same time, researchers discovered that pyridoxine supplementation ablates flaxseed's antigrowth properties in chicks (62) and in turkey poults (64), suggesting that flaxseed's anti-growth mechanism is mediated through antagonism of vitamin B6 (62,64). Later, in the 1980s, 1ADP was observed to interrupt

the synthesis of carnitine in perfused rat liver, indicating that carnitine synthesis is vitamin B6-dependent (65). More recently, flaxseed extracts as well as synthetic 1ADP were studied as dietary constituents in rat models of vitamin B6 deficiency (1,66). The researchers wanted to investigate if flaxseed extracts or 1ADP are toxic to rats when the rats are provided a B6-replete diet or a B6-insufficient diet. The results of those works suggest that flaxseed extracts or synthetic 1ADP reduce the activities of CBS and CSE in hepatocytes *in vitro* and *in vivo* (1,66). Simultaneously, the same group of researchers observed that 1ADP decreased 4-pyridoxic acid levels while increasing cystathionine levels (a marker of TS inhibition) in rats consuming a B6-sufficient diet. However, when 1ADP was combined with a B6-deficient diet, the rats exhibited lower body weight and they developed severe hyperhomocysteinemia (hyperHcy) and liver pathology (1,66). The conclusion from their work was that 1ADP perturbs TS even in B6-sufficient rats, and the perturbation amplifies exponentially when the animal is fed a B6-deficient diet.

1.7 One-carbon metabolism

One-carbon metabolism is the process of bio-synthesizing, donating, modifying and transferring single carbon units within, but not limited to, the folate cycle, the methionine (Met) cycle, TS, and phosphatidylcholine (PC) metabolism (67,68). One-carbon metabolism means something different depending on the pathway being considered, but in general it refers to the transfer and modification of a single carbon group bearing one to three hydrogen bonds. A wide variety and great number of reactions are supported by one-carbon metabolism. Homocysteine (Hcy) is arguably the most central molecule within one-carbon metabolic pathways, linking the folate cycle, Met cycle, TS, and PC metabolism. A model for one-carbon metabolism that relates specifically to the integration of these pathways can be seen in Figure 1.1. An in-depth one-

carbon metabolic model that illustrates how these pathways are compartmentalized (i.e. cytosolic versus mitochondrial), minus TS, can be seen in Figure 1.2.

In most circumstances, Hcy is subject to one of two primary fates. One of these fates involves the remethylation of Hcy to form Met, depending on the methylation needs of the cell. This remethylation is performed by either betaine homocysteine methyltransferase (BHMT) or methionine synthase-B12 (MS-B12) complex. The second fate of Hcy is the irreversible conversion of Hcy to cystathionine via the TS pathway. Some authors have noted that Hcy is catabolized through the TS pathway depending on the redox status of the cell, suggesting an oscillation between cellular methylation needs and cellular redox state (69). Interestingly, Hcy is an exceptionally toxic molecule when it accumulates and induces a condition referred to as HyperHcy (70). HyperHcy inflicts its damage directly on the mitochondria by insulting mitochondrial polarization, culminating in mitochondrial dysfunction and intrinsic cell apoptosis (71–74). HyperHcy results in damage to vascular endothelial cells and cardiovascular smooth muscle which in turn drives a plethora of cardiovascular complications (75). One-carbon metabolism is wired to permit the continual movement of Hcy, whether the Hcy is moving through the Met cycle, TS, polyamine synthesis, protein translation initiation, protein autophagy, etcetera. This continual movement of Hcy prevents HyperHcy, but it requires a variety of essential cofactors (B3, B6, B12, FAD), minerals (Zn^{2+}), and nutrients (folate), that must be derived from the diet.

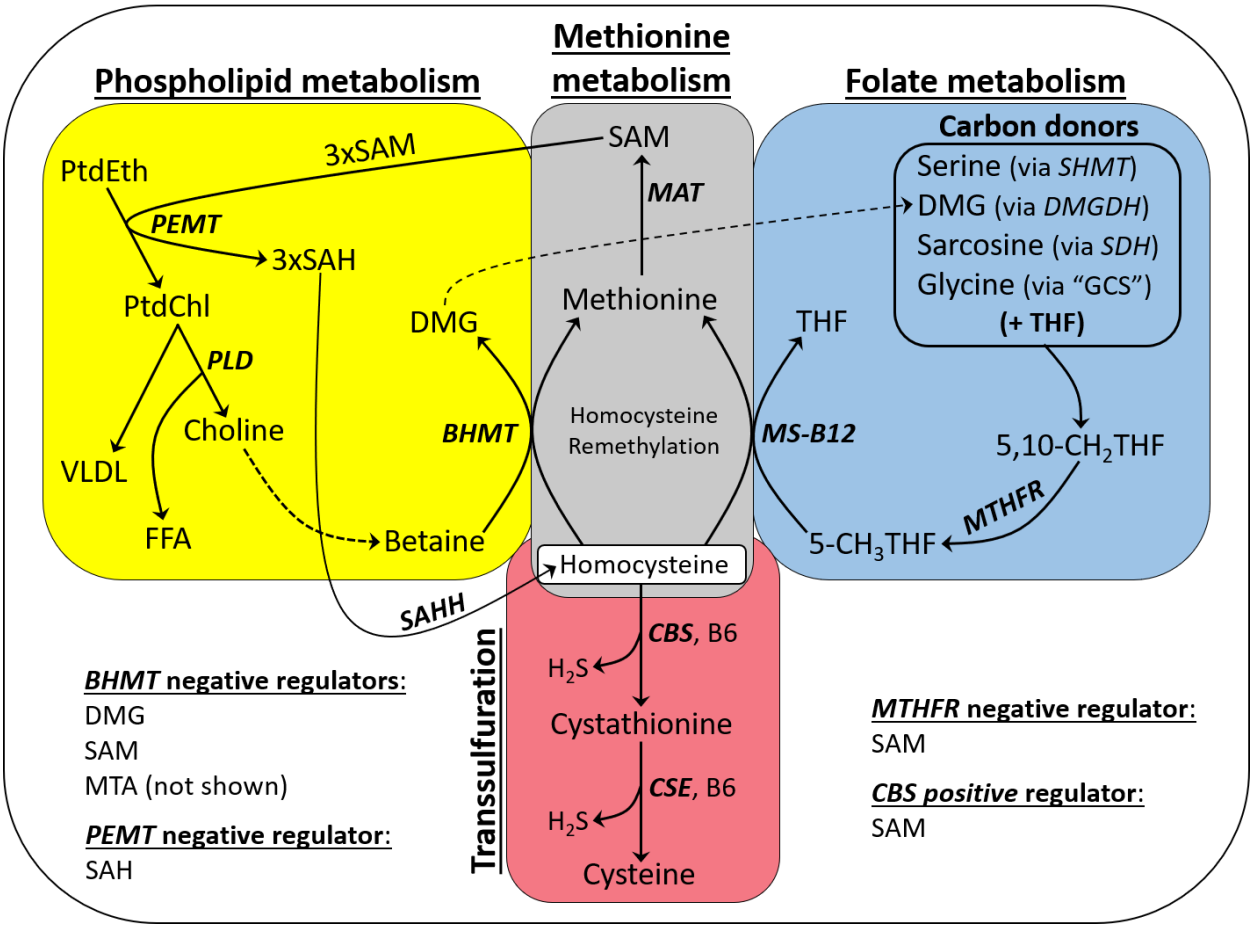

Figure 1.1. Model of one-carbon metabolism, illustrating the integration of phospholipid metabolism, methionine metabolism, folate metabolism and transsulfuration.

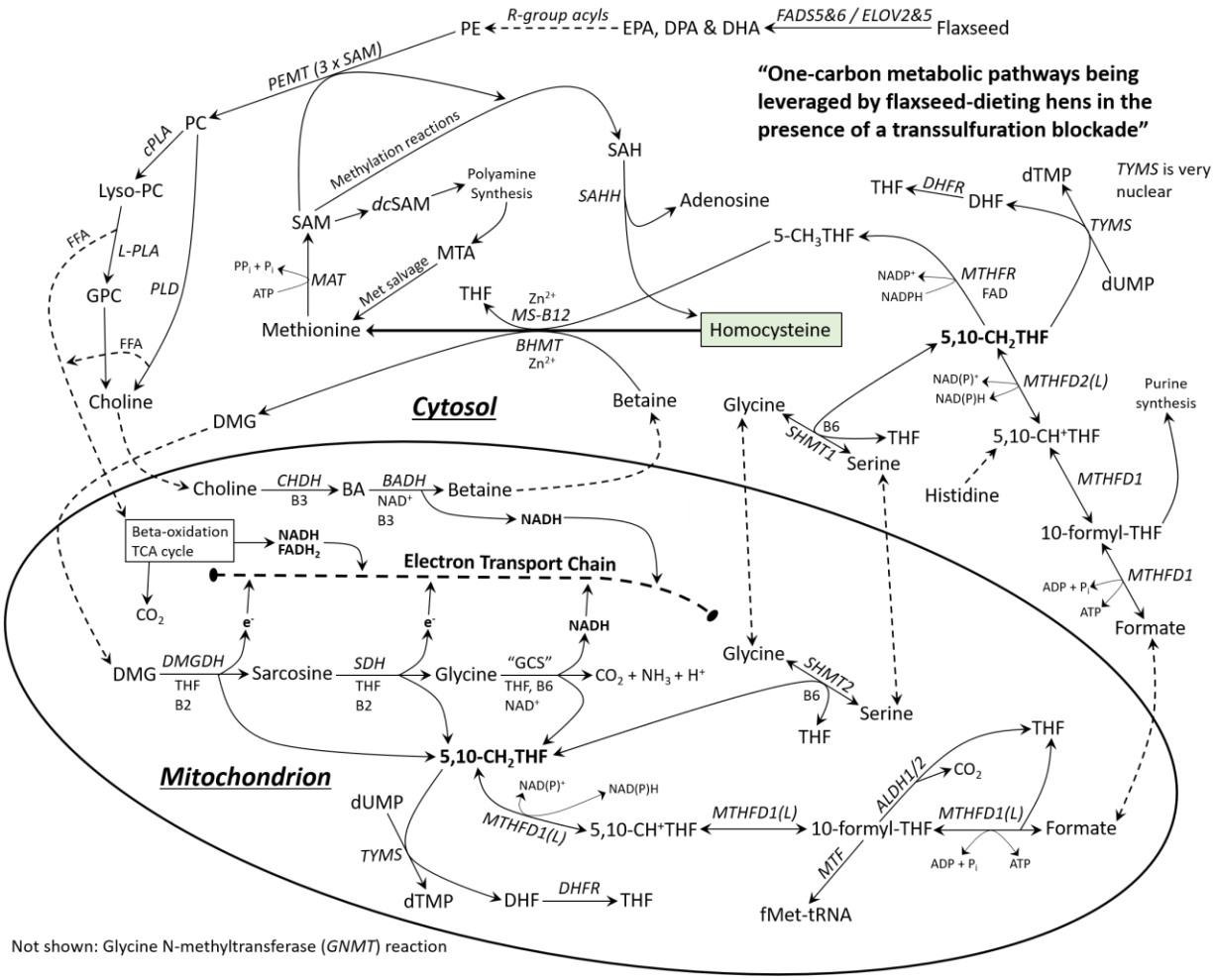

Figure 1.2. Expanded model illustrating one-carbon metabolism at depth (minus TS), focusing on the role of phospholipid metabolism, folate cycle and methionine cycle. The image also allows the visualization of these pathways with regard to cytosolic and mitochondrial compartmentalization.

1.8 Phospholipid metabolism: an emerging giant in the field of one-carbon metabolism

Phosphatidylethanolamine N-methyltransferase (PEMT) is the only known enzyme to provide *de novo* choline synthesis in biology, by way of converting phosphatidylethanolamine (PE) to PC. PEMT synthesizes PC from PE by using three S-adenosylmethionine (SAM) molecules to tri-methylate PE, converting PE's NH_2 terminal to a 'nitrogen hub' with three methyl groups,

N-$(CH_3)_3$ (76). The PEMT reaction is argued to be the greatest consumer of SAM in physiology (77–79). Therefore, PE is considered the primary 'sink' for excess SAM in physiology; a function that protects histones from hypermethylation (77). The CDP-choline "Kennedy" pathway, in contrast to the PEMT pathway, utilizes pre-existing choline to synthesize PC. Therefore, the Kennedy pathway does not provide choline biosynthesis. The PEMT pathway is how choline is made in physiology, even in algae (80). PEMT has been illustrated as a sensor of the choline status in mammals (81). When dietary choline is insufficient, PEMT is critical for synthesizing PC and protecting the animal from choline deficiency-associated liver pathology and starvation (82). PEMT's evolutionary role is suspected to be the maintenance of PC levels during periods of starvation, pregnancy and lactation, in order to sustain processes such as bile secretion and lipoprotein formation (82). PEMT is almost entirely expressed in the liver. In non-hepatic mammalian tissues, the activity of PEMT is usually less than 1% of what is observed in the liver (83,84). PEMT is located in the endoplasmic reticulum as well as in a membrane fraction associated with mitochondria but not physically a part of mitochondria (85), referred to as the mitochondria associated membrane (MAM). The rate of PEMT activity is dependent on the concentration of PEMT's two primary substrates, PE and SAM (86,87). For these reasons, the researchers in (86,87) saw increased PEMT activity when ethanolamine (increasing PE synthesis) or methionine (increasing SAM synthesis) were added to their culture system. Murine hepatocytes derive 30% of their PC from PEMT, while the other 70% of PC is derived from the CDP-choline (Kennedy) pathway (88). Previous work indicates that choline deficiency strongly induces PEMT activity and in turn increases SAM consumption (81,89).

1.9 The methionine cycle: how sulfur-based amino acids regulate methylation capacity

It is helpful to realize that Met is, simply, methylated Hcy (i.e. Met = CH_3Hcy). Hcy is the primary molecular scaffold for every molecule in the Met cycle. If we thought about the 'Met cycle' as a 'Hcy cycle', this is how the molecules would appear, in their order of reaction:

'Hcy cycle' instead of 'Met cycle': **Hcy** → CH_3**Hcy** → Adenosyl-CH_3**Hcy** → Adenosyl-**Hcy** → **Hcy**

Notice that Hcy is present in every molecule and that the cycle begins and ends with Hcy. This is a helpful way to understand that the Met cycle is based on the utilization of Hcy as a primary constituent. All molecules within the Met cycle contain Hcy. In contrast, this is how the canonical 'Met cycle' appears in common literature:

'Met cycle' as it is taught today: Hcy → **Met** → Adenosyl-**Met** → Adenosyl-Hcy → Hcy

Notice that Met is a transient molecule that depends solely on the methylation status of Hcy. The remethylation of Hcy is possible because of the sulfonium center in Hcy that receives a methyl group during remethylation (90).

Animals are auxotroph for Met; they must acquire Met from the diet. The reason for this is that animals do not fix inorganic sulfur into amino acids to form cysteine or Hcy (plants do this) (91,92). Animals create Met only by remethylating Hcy; however, that Hcy molecule was first created by a plant (or bacterium or protist). In animals, the remethylation of Hcy is performed either via MS-B12 or BHMT, yielding Met (68,93). MS-B12 is a zinc-dependent matalloenzyme that utilizes 5-CH_3THF as a methyl donor to conduct the remethyaltion of Hcy (94). MS-B12 is expressed in all tissues throughout the body, whereas BHMT expression is mainly restricted to the liver and kidney (95,96). BHMT is also zinc-dependent, like MS-B12, but it utilizes betaine as a methyl group donor to facilitate the remethylation of Hcy (96). After dietary provision of

betaine is depleted, all betaine must be derived from choline. In the liver, BHMT facilitates 50% of Hcy remethylation (97–100), the other 50% being facilitated by MS-B12. BHMT depletion culminates in HyperHcy within the animal, indicating the critical importance of this enzyme in the liver (101). Interestingly, BHMT expression increased 1.8-fold in the brains of late stage hibernating bats, likely because MS-B12 activity declines due to nutrient, cofactor or mineral deficiency during later stages of hibernation (102), indicating that the tissue expression of BHMT is context-dependent in mammals.

The majority of excess Met is acted on by methionine adenosyl transferase (MAT), an enzyme that consumes ATP as a cosubstrate to drive the adenosylation of Met, thereby forming SAM (103). In 1953, SAM was characterized as the adenosylated (i.e. 'active') form of Met that can transfer a methyl group to a receiving molecule due to the high energy nature of the sulfonium center to which the labile methyl group is bound (90). The liver is the primary organ of SAM synthesis given that 50% of methionine metabolism and 85% of all transmethylation reactions occur hepatically (103,104). In the methionine cycle, one-carbon metabolism is centered on several thousand methylation reactions that utilize SAM as the cell's master methyl donor (103). SAM is the methyl donor for a plethora of methyltransferase reactions involving, but not limited to, PC synthesis (84), creatine synthesis (104), sarcosine synthesis (105), histone protein methylation (77), 5-methylcytosine DNA or RNA methylation (106,107), N6-methyladenosine RNA methylation (108), catechol structure methylation (109), and many other molecular targets. S-adenosylhomocysteine (SAH) is produced after the completion of a SAM-dependent methyltransferase reaction. SAH induces allosteric inhibition of numerous methyltransferase reactions (110), illustrating why the SAM:SAH ratio is important for determining the methylation index for lipid, RNA, DNA and protein methylation (111,112). The

enzyme S-adenosylhomocysteine hydrolase (SAHH) is essential for preventing the accumulation of SAH, because SAHH hydrolyzes SAH into Hcy and adenosine (112). In addition to methyltransferase reactions, SAM can also be catabolized in support of polyamine synthesis. The decarboxylated form of SAM (*dc*SAM) is required for polyamine synthesis (113). The rate limiting enzyme for polyamine synthesis is ornithine decarboxylase (ODC), a vitamin B6-dependent enzyme that converts ornithine to putrescine. *dc*SAM can react with putrescine to produce the polyamine spermidine, and in turn another molecule of *dc*SAM can react with spermidine to produce the polyamine spermine. Reaction with either putrescine or spermidine causes *dc*SAM to be converted to methylthioadenosine (MTA), the first molecule of the Met salvage pathway (114). MTA, aside from being the first molecule of Met salvaging, is a cell-permeable pan methyltransferase inhibitor (115) that has been used to inhibit enzymes such as protein arginine methyltransferase 5 (PRMT5), a histone methyltransferase implicated in numerous forms of cancer (116–118).

1.10 The folate cycle: a super-highway of one-carbon metabolism

The folate cycle is crucial for the proper engagement of numerous physiological reactions throughout the cell. The name folate was derived because it was understood that the benefits of folate were obtained by eating green, leafy ‘foliage’ (119). As such, plants can biosynthesize folate, whereas animals cannot and therefore must consume it dietarily. Molecular folate (vitamin B9) is complex in terms of how it must be processed to become bioactive (120). Bioactive folate is referred to as tetrahydrofolate (THF). THF exists in its bioactive form as 2-amino-4-hydroxy-pterdine linked to p-aminobenzoic acid conjugated with anywhere from one to nine glutamic acid residues (i.e. polyglutamate tail) (121). The majority of folate exists with a monoglutamate tail in order to favor entry into the cell, and furthermore, this folate is mostly

represented by 5-CH_3THF (122). Once inside the cell, the folate molecule is converted to the polyglutamyl form so that the molecule can be retained intracellularly (93). Biological outcomes from the folate cycle appear when THF receives a one-carbon unit such as formyl (-HCO), methylene (CH_2) or methyl (CH_3), yielding the formation of 10-formyl-THF, 5,10-CH_2THF and 5-CH_3THF, respectively. The prefixes '5' and '10' refer to the 5-nitrogen and 10-nitrogen within the THF moiety, both of which share a covalent bond with the newly introduced carbon unit (120). 5,10-CH_2THF has been long considered the 'active formaldehyde' of the folate cycle (123), because 5,10-CH_2THF is the immediate substrate for numerous enzymatic reactions such as methylene tetrahydrofolate reductase (MTHFR), thymidylate synthase (TYMS), serine hydroxymethyltransferase (SHMT), and bidirectional methylene tetrahydrofolate dehydrogenase (MTHFD2) (120).

MTHFR is a cytosolic FAD-dependent enzyme that uses NADPH to reduce 5,10-CH_2THF to 5-CH_3THF. This is the only place in the metabolism where 5-CH_3THF is found (121). The CH_3 group from 5-CH_3THF is used by MS-B12 to remethylate Hcy, in a reaction that produces Met and THF. Methionine synthase (MS) must complex with cobalamin (B12), so that B12 can receive the methyl group from 5-CH_3THF prior to passing this methyl group to Hcy (thus facilitating the remethylation of Hcy) (124). In this manner, the folate cycle supports Hcy remethylation, ensuring that SAM levels are high enough to sustain methyltransferases (125).

Serine, via SHMT, is the major carbon donor for the synthesis of 5,10-CH_2THF. SHMT is a B6-dependent enzyme that consumes serine and THF as substrates in a reversible reaction that yields 5,10-CH_2THF and glycine. SHMT includes a cytosolic (SHMT1) and a mitochondrial (SHMT2) isoform. SHMT2 is critical for determining the fate of cytoplasmic folate (126). Therefore, the remethylation capacity of the cell is heavily influenced by mitochondrial SHMT

The mitochondrial compartmentalization of SHMT2 might help to protect SHMT2's catalytic activity, because SHMT2 exhibits 50% of maximum catalytic activity (i.e. 50% of Vmax) at a pH that is characteristic of the mitochondrial matrix (i.e. pH 7.8) where SHMT2 is located (127). Furthermore, SHMT2's 100% V_{max} was observed at pH 8.5 (127), suggesting that mitochondrial hyperpolarization might help to enhance SHMT2 catalytic activity and/or compensate for B6 deficiency.

Several other enzymes are responsible for generating 5,10-CH_2THF; those enzymes are dimethylglycine dehydrogenase (DMGDH) and sarcosine dehydrogenase (SDH) and the 4-protein glycine cleavage system (GCS) (128,129). The BHMT reaction and the folate cycle are inextricably linked, because DMG (a product of the BHMT reaction) is catabolized along with THF via DMGDH to yield 5,10-CH_2THF and sarcosine. Sarcosine is then catabolized via SDH in a reaction very similar to DMGDH, producing another molecule of 5,10-CH_2THF and a molecule of glycine (128). Glycine then through the GCS produces another molecule of 5,10-CH_2THF (129). It is in this manner that the full oxidation of choline (oxidized all the way through DMG, sarcosine and glycine) forms three molecules of 5,10-CH_2THF. DMGDH and SDH are flavoprotein-dependent enzymes located in the inner-mitochondrial membrane. The DMGDH and SDH reactions each result in the direct transfer of a single electron into the ubiquinone pool, skipping complexes 1 and 2 of the electron transport chain (ETC) (123,130). Researchers showed that this electron from DMGDH as well as the NADH from betaine aldehyde dehydrogenase (BADH), boost the production of ROS and ATP in the mitochondria (130). This is how choline oxidation and the BHMT reaction contribute indirectly to mitochondrial metabolism in a major way.

Another major enzyme in the folate cycle is thymidylate synthase (TYMS), which uses 5,10-

CH_2THF and 2'-deoxyuracil 5'-monophosphate (dUMP) to synthesize 2'-deoxythymidine 5'-monophopshate (dTMP) and DHF (131). 5-fluorouracil (5-FU) is a popular chemotherapeutic drug that challenges DNA replication in cancer cells by inhibiting TS (131). TS is essential for providing ample dTMP to support nuclear and mitochondrial polymerization of thymidine into DNA (132). dTMP, after two subsequent phosphorylation events, is leveraged by DNA polymerases in the form of 2'-deoxythymidine triphosphate (dTTP) to drive the incorporation of thymidine into DNA (133). A supplemental pathway via thymidine kinase (TK) is available to supplement the cell's dTMP needs. TK, in the form of TK1 or TK2, uses thymidine and ATP as substrates to yield dTMP (134). TK is primarily responsible for supplementing dTMP during the S-phase of the cell cycle, depending on the availability of ATP and the capacity of TS to meet the cell's initial dTMP needs (134–136).

1.11 Transsulfuration: a vitamin B6-dependent exit route from one-carbon metabolism

TS is a short, two-step pathway that is important for providing the cell with cysteine and hydrogen sulfide (H_2S) (137). Besides remethylation via BHMT or MS-B12, the alternate fate of Hcy is the irreversible conversion of Hcy to cystathionine. Cystathionine is produced when Hcy and serine are catabolized by the B6-dependent enzyme cystathionine beta synthase (CBS) (138). Cystathionine is then converted to cysteine through the B6-dependent enzyme cystathionine gamma lyase (CSE). Elevated cystathionine is a classic symptom of B6 deficiency (139,140), due to CSE's acute loss of catalytic activity when B6 levels are insufficient (141,142). An additional factor is that B6 deficiency accelerates the lysosomal degradation of apo-CSE (143), further driving the accumulation of cystathionine. Another name for CSE is 'cystathionase', thus explaining the three-letter acronym, CSE. The CBS and CSE reactions serve as a significant sources of the gasotransmitter signaling molecule hydrogen sulfide (H_2S) (144). H_2S availability

affects a myriad of physiological outcomes and processes such as hypertension (145), atherosclerosis (146), blood sugar (147), mitochondrial bioenergetics (148) and cancer metabolism (149). Recently, CBS was recognized as an important enzyme in several kinds of cancer with a particularly crucial role in the advancement of ovarian cancer (150–152). The TS pathway is the reason why cysteine is considered a non-essential amino acid in animals. Cysteine can be synthesized via CSE or it can be introduced to the metabolism through dietary cysteine. Given that cysteine is the rate-limiting substrate for the synthesis of glutathione (GSH), it can be argued that TS serves an imperative role in maintaining redox stability in the context of dietary sulfur amino acid insufficiency (153).

1.12 The regulation of blood sugar and blood lipids in birds: the major role of glucagon

Avian species exhibit exceptionally high "normal" blood glucose (normal = 200 to 400mg/dL) compared to mammals where normal is 90mg/dL (154–156). After controlling for body mass, birds still have exceptionally higher blood glucose than mammals (157). Researchers have proposed using birds as a model for pathology-free diabetes, given elevated blood glucose in the absence of diabetic pathology (158). Male White Leghorn chickens were observed to have fasted blood glucose levels of 218mg/dL (159). Despite having high blood glucose, chickens have low percentages of glycated hemoglobin (% HbA1c), between 1% and 2% HbA1c (2,160). This appears to be a common pattern in birds, where blood glucose levels are high while HbA1c is low. As an extreme example, hummingbirds have blood glucose levels ranging from 504 to 756mg/dL after feeding, and these levels decline to about 306mg/dL in the fasted state (161). Surprisingly, those same hummingbirds have HbA1c ranging from only 3.7 to 4.6%!! These are low HbA1c values considering the high blood glucose level of the hummingbird. Therefore, birds appear to be less susceptible to advanced glycation end products than mammals, possibly

indicating why birds are protected from the canonical effects of diabetes. It is commonly understood that human diabetics have HbA1c exceeding 6.5%, meaning that a hummingbird with super-hyperglycemic blood sugar has an HbA1c value well below the threshold for diabetes in humans. The authors in (161) claim that the HbA1c values of their hummingbirds (i.e. 3 to 4.6% HbA1c) are the highest HbA1c values ever recorded in birds. However, our lab observed that White Leghorn hens fed either 15% defatted flaxseed (DF) or 15% whole flaxseed (WF) have HbA1c values of 5.3% and 6.2%, respectively (2). Our control-fed hens had an HbA1c value of 1.9% (2). The HbA1c values that we reported for our flaxseed-fed hens are the highest HbA1c values ever reported in a wild-type bird. If birds provide a good animal model for the study of non-pathological diabetes, then the flaxseed-fed hen could be a diamond opportunity for metabolic researchers and cancer researchers, alike. All of this begs the question, "is a flaxseed-fed hen actually a hummingbird dressed up in a chicken costume?"

How is blood sugar regulated in birds? Birds, in contrast to mammals, have greater dependence on glucagon than on insulin to regulate blood glucose. β-cells of the avian pancreas can be considered non-responsive to glucose, because "avian hyperglycemia" (~500mg/dL) is required to stimulate insulin release (162). Chickens have far more α-cells (glucagon releasing cells) than β-cells (insulin releasing cells) in the pancreatic islet; therefore, birds have exceptionally higher glucagon levels (~10 times higher) and exceptionally lower insulin levels (~10 times lower) compared to mammals (163,164). Somatostatin from the δ-cells of the pancreas is critical for negatively regulating glucagon release from the chicken pancreas (165). Therefore, somatostatin in the bird is analogous to insulin in the mammal, in terms of negatively regulating blood glucose levels.

Glucagon is used by chickens to dramatically stimulate glycogenolysis, gluconeogenesis and

lipolysis, and in turn this ensures that the animal has sufficient blood glucose and blood lipids (162). Intracardiac glucagon injection in chickens was shown to cause a 2-fold elevation in blood glucose and a 6-fold elevation in circulating FFAs (166), indicating that glucagon simultaneously elevates blood glucose and blood lipids in chickens. In geese and ducks, an infusion of glucagon increases plasma glucose, plasma FFAs, plasma TG and liver TG deposition (167). Similar lipolytic effects of glucagon were observed in fasting king penguins (168). Clearly, glucagon is a major stimulator of glucose formation and lipid mobilization in class aves. The baseline message from all of this is that birds, in particular chickens, depend on glucagon to maintain their normal hyperglycemic state. Fortunately for our lab, most of the research in avian metabolism is based on studies of chickens (i.e. domestic fowl).

1.13 Mitochondrial metabolism

In the 1960s, mitochondria were appreciated as organelles that exert a biological effect through a coupled chemiosmotic system culminating in the production of energy-rich molecules such as ATP (169). Today we understand that mitochondria serve a myriad of roles that are essential to the proper maintenance of cell physiology, including bioenergetics, cell death, ROS signaling, calcium homeostasis, and macromolecule synthesis (170). Morphologically, the mitochondria consist of an outer membrane, inner membrane, intermembrane space (IMS), and unique tubular cristae that extend into a central space called the matrix (171,172). The IMS is rich with protons but overall represents the molecular composition of the cytosol, whereas the mitochondrial matrix consists of a unique subset of molecules geared toward the maintenance of chemiosmotic force (173,174). The inner membrane is impermeable to ions which aids in the maintenance of a high membrane potential of approximately -180mv, which is far more negative than typical transmembrane charges in biology. This impermeability of ions is likely due to a

uniquely high concentration of cardiolipin, a highly specialized glyceride molecule consisting of four LA (C18:2ω6) acyls (173,175). Cardiolipin is required for the formation of respiratory supercomplexes in the inner-mitochondrial membrane, including complexes 1, 2, 3 and 4 of the electron transport chain (ETC), as well as ATP synthase and ADP/ATP translocase (176). The chicken mitochondrial genome consists of 16,775 base pairs encoding 13 proteins, 2rRNAs, and 22 tRNAs, all of which are found in the mitochondrial genomes of other vertebrates (177). Every protein that is encoded in the mitochondrial genome is required for proper functioning of the ETC (178). The chicken mitochondrial genome, similar to other vertebrates, encodes seven subunits for complex 1 (ND1, ND2, ND3, ND4, ND4L, ND5 and ND6); one catalytic subunit for complex 3 (CYTB); three catalytic subunits for complex 4 (COX1, COX2 and COX3) and two subunits for ATP synthase (ATP6 and ATP8) (179). The chicken nuclear genome consists of 8 pairs of macrochromosomes, 30 pairs of microchromosomes and 1 pair of sex chromosomes (ZZ for male and WZ for female) (180). Among these chromosomes only 14 mitochondrial pseudogenes (i.e. impartial, non-coding mitochondrial DNA sequences) can be found (179). This is in comparison to the human nuclear genome which has possibly more than 1,000 mitochondrial pseudogenes (181,182).

In 1904, biochemists observed that fatty acids undergo an oxidative reaction called beta-oxidation, whereby two carbon units are successfully removed from the acyl molecule (183). Beta-oxidation, or fatty acid oxidation (FAO), occurs primarily in the mitochondria and to a lesser extent in peroxisomes. Peroxisomes contribute an important but minor role to total FAO (184,185). Peroxisomes help to produce medium and short-chain fatty acids that passively diffuse into mitochondria skipping the facilitative activity of carnitine palmitoyl transferase (CPT1) (186). CPT1 and CPT2 are necessary for the import of long chain fatty acids

(approximately 12 to 20 carbons) into the mitochondrial matrix (186,187); however, the CPT system is not effective at transporting very long-chain fatty acids (i.e. fatty acids with more than 20 carbons) (188). Peroxisomes help in this situation by oxidizing very long-chain fatty acids (188) so that CPT1 can receive a fatty acid of 20 carbons or shorter. It is through this manner that very long-chain fatty acids such as DHA can be metabolized fully and contribute to the bioenergetic capacity of the cell.

In the mitochondrial matrix, each round of FAO yields one molecule of acetyl-CoA, NADH and $FADH_2$ (189). Within the tricarboxylic acid (TCA) cycle, acetyl-CoA can be fully oxidized to yield three molecules of NADH and one molecule of $FADH_2$ (190). NADH is an excellent electron donor to the ETC, because it contains two high energy electrons that rapidly reduce flavin mononucleotide (FMN) via complex 1 (NADH:ubiquinone oxidoreductase), forming $FMNH_2$. $FMNH_2$ transfers those electrons to an iron-sulfur cluster, and those electrons are subsequently transferred to ubiquinone. During the reaction between NADH and FMN, the FMN molecule receives one proton from NADH as well as one proton from the mitochondrial matrix (189,191,192). The proton that FMN receives from the matrix is how complex 1 facilitates the pumping of protons from the matrix to the IMS. Proton pumping is essential for maintaining a transmembrane chemiosmotic gradient (191). This gradient determines the proton motive force whereby protons are shuttled from the IMS to the matrix (i.e. antegrade flow) through complex 5 (ATP synthase), resulting in the conjugation of ADP with inorganic phosphate, forming ATP (193). Complex 2, unlike complex 1, cannot pump protons from the matrix to the IMS; however, it can receive electrons from $FADH_2$ as well as the sulfide signaling gas molecule hydrogen sulfide (H_2S) (194). Within ATP synthase, several catalytic subunits regulate the synthesis of ATP. ATP synthase subunit B (ATP5B) is arguably the most important subunit for catalyzing the

synthesis of ATP, particularly because ATP5B regulates cristae formation and promotes mitochondrial elongation (195–197). The presence of subunit proteins determines the ability of ETC complexes to form, and in turn ETC complex formation determines function of the complex (198). This indicates that ETC complexes probably have different roles depending on the availability of subunit proteins and the degree to which complexes can form.

Complex 1 and complex 3 are the largest sources of superoxide ($O_2^{\cdot-}$) within the mitochondria, and therefore, they are two of the largest sources of reactive oxygen species (ROS) within the cell (199–201). Complex 1 produces superoxide when $FMNH_2$ transfers a lone electron to diatomic oxygen (partially reducing diatomic oxygen), instead of successfully transferring an electron pair to the iron-sulfur cluster (199,202). Superoxide is also produced at high levels during the reverse electron transfer of electrons to NAD^+, forming NADH, at complex 1 (203). Superoxide, as partially reduced diatomic oxygen, has an oxygen atom with one unpaired electron in its valence shell, giving the diatomic molecule a highly reactive 1^- charge. 'Superoxide' is the perfect chemical name for this molecule. The Latin etymology of superoxide ('su', 'per' and 'oxide') depicts the chemical nature of the molecule. The prefixes 'su' and 'per' translate to 'below' and 'perfect', respectively. 'Oxide' is an oxygen atom bound to another atom (e.g. could be bound to another oxygen atom). Therefore, "su-per-oxide" translates to "below-perfect-oxide," such as an oxygen atom (within diatomic oxygen) being one electron below octet valence. Henceforth it can be declared that 'superoxide' is an excellent name for the superoxide molecule.

Complex 1, through its production of superoxide, engages in in a wide array of metabolic processes including ROS signaling (203), autophagy (204), cell death execution (205) and aging (206). Superoxide has an extremely short half-life and will either undergo spontaneous

disproportionation to form the hydroxyl radical (202), or it will react with superoxide dismutase (SOD) to form H_2O_2. The hydroxyl radical is an unstable electrophile that can rapidly attack almost any molecule within the cell (207), particularly membrane lipids and DNA (208). Therefore, it is imperative that SOD2 be available to reduce superoxide to H_2O_2, in order to prevent excessive cell damage from the hydroxyl radical (202). Cytosolic SOD (copper-zinc-dependent SOD) is referred to as SOD1, while mitochondrial SOD (manganese-dependent) is referred to as SOD2 (202). H_2O_2 can then be converted to H_2O and O_2 by catalase (CAT), glutathione peroxidase (GPx), peroxinredoxin (PRX) and other antioxidant systems (209,210).

1.14 Investigating mitochondrial membrane potential

Studies from Dr. Buck Hales, Dr. Karen Hales and Dr. John Allen, have shown that the maintenance of a high mitochondrial membrane potential is essential for steroid biosynthesis in MA-10 tumor Leydig cells (211). They showed that a variety of substances can be used to deplete mitochondrial membrane potential and thereby inhibit steroid biosynthesis. So, how can mitochondrial membrane potential be measured? Tetramethylrhodamine ethyl ester (TMRE) is a lipophilic cation that rapidly accumulates in the mitochondrial matrix due to TMRE's attraction to negatively charged environments (212). The accumulation of TMRE in the matrix is a general measure of cellular respiration, such that more TMRE accumulation can be expected when cellular respiration is more active (due to a strong negative charge). Somewhat different from the concept of absolute charge is the concept of 'mitochondrial (inner-) membrane potential'. The membrane potential is an expression of the mitochondria's total capacity to conduct oxidative phosphorylation (OXPHOS) (213). Membrane potential is the strength of the charge differential from the mitochondrial matrix to the IMS. The TMRE experiment is designed to allow an estimate of this charge differential, which is an estimate of the transmembrane potential referred

to as “delta psi” (ΔΨ) (212). The transmembrane potential is directly correlated with proton motive force or chemiosmotic force.

1.15 De novo fatty acid synthesis

In animals, acetyl-CoA cannot be converted to pyruvate; therefore, in mitochondria, acetyl-CoA must be oxidized to citrate in the first step of the TCA cycle (190). Citrate is an essential substrate for *de novo* fatty acid synthesis. The *de novo* fatty acid synthetic pathway is a cytosolic pathway. This process begins when mitochondrial citrate effluxes to the cytosol through the citrate transporter. In the cytosol, ATP citrate lyase (ACYL) reacts with citrate and CoA to yield acetyl-CoA again. Acetyl-CoA can then be activated by acetyl-CoA carboxylase (ACC) to form malonyl-CoA (214) which is the substrate used to form palmitate (C16:0) via the pleiotropic enzyme fatty acid synthase (FASN) (215). Palmitate can then be readily elongated via the elongation enzyme called fatty acid elongase 6 (ELOVL6) (216) and/or desaturated by the desaturation enzyme called sterol CoA desaturase 1 (SCD1) (217), to rapidly generate C16:1n7, C18:0 and/or C18:1n9 depending on the cell’s needs for saturated or monounsaturated fatty acids. Sterol regulatory element binding protein 1 (SREBP1) is the primary transcription factor regulating the expression of lipogenic genes (e.g. ACYL, ACC, FASN, SCD1, etc) (218). Non-cancerous tissues depend mainly on the systemic circulation for the delivery of fatty acids, and as such, *de novo* fatty acid synthesis is not upregulated in most normal tissues (215). However, cancerous tissues display exceptional upregulation of *de novo* lipogenesis to meet their lipid needs (215,219). Tumors of many kinds (including ovarian tumors) have upregulated *de novo* fatty acid synthesis to support their proliferative demand for lipid encapsulation (215,219). Not only does the membrane of a mitotic cell requires lipid encapsulation, but so does all of the new intracellular organelle mass. It has been argued that SREBP1 is required for the growth of

ovarian tumors (220). PUFAs are specific, negative regulators of *de novo* fatty acid synthesis (221–225). In mouse liver, PUFAs such as C18:2ω6, C20:5ω3 and C22:6ω3 negatively regulate the maturation of SREBP1 coinciding with reduced transcription of lipogenic genes such as ACC, FASN, ACLY and SCD1 (218). The processes that regulate cellular respiration within the mitochondria are also distinctly coupled to mechanisms that regulate cell death (226).

1.16 E-cadherin, CDH1, microRNA-200a-3p and collective migration in ovarian cancer

In 1980, E-cadherin was first identified as a cell-surface adhesion molecule in liver hepatocytes of chickens, referred to as liver-cell adhesion molecule (L-CAM) (227). The following year, in 1981, researchers characterized a similar protein in mice (they called it Uvomorulin) that displayed Ca^{2+} dependent properties (228). In 1983, further cloning and specific characterization of the 124kDa chicken protein (L-CAM) (229) and 120kDa murine protein (Uvomorulin) were performed. It was through the works of these different labs that physiologists became aware that a wide array of calcium-dependent adherins junction molecules (i.e. 'cadherins') exist and share vast similarity.

E-cadherin ('epithelial cadherin') is the name for the physical cadherin protein, while *CDH1* ('cadherin 1') is the name of the gene for E-cadherin. E-cadherin is a type-1 transmembrane glycoprotein composed of a large extracellular domain, a transmembrane segment and a highly conserved cytosolic domain (230). The extracellular portion of E-cadherin consists of five extracellular cadherin domain repeats (referred to as EC domains) that encompass four Ca^{2+} binding sites. Upon Ca^{2+} binding the EC domains can engage in homophilic protein interactions with other cadherins, whether on opposing cells or with adjacent cadherins inserted in the same plasma membrane (231–233). Ultimately, these protein interactions form cadherin junctions that permit the formation of epithelial membranes that define the extent of an epithelial tissue.

Through cell adhesion, cadherins promote several process that drive cellular development and morphogenesis; those process are ‘adhesion tension’, ‘adhesion signaling’ and ‘adhesion coupling’ (234).

We now understand that advanced tumor malignancies are not restricted to mesenchymal phenotypes. Instead, advanced tumors commonly express differentiated epithelial states, at least in combination with mesenchymal features (235). For example, E-cadherin and members of the microRNA-200 (miR-200) family are strongly upregulated in epithelial ovarian cancers of White Leghorn laying hens and humans (14,236–238). Our lab has shown that the WF diet reduces the expression of miR-200a, miR-200b and miR-429 in laying hen ovarian tumors (14); however, it is unknown if these effects are based on flaxseed’s oil component, non-oil component, or perhaps based on a synergy of both components. The miR-200 family regulates *CDH1* transcription by inhibiting the protein translation of zinc finger E-box binding homeobox 1 (ZEB1) protein. ZEB1 is a canonical inhibitor of the *CDH1* promoter; therefore, miR-200a expression is often directly correlated with *CDH1* expression (239,240). Members of the miR-200 family are canonically considered regulators of the epithelial-to-mesenchymal transition (EMT) through a ZEB1/*CDH1* axis (239,240). The growing field of “mechano-biology” is setting the stage for a new metabolic appreciation of E-cadherin and the miR-200 family that transcends canonical discussions of EMT (241).

Collective cell migration is the process by which metastases often extravasate from the primary ovarian tumor (237,242). Furthermore, collective cell migration is a very dynamic process. The process of cancer cell collective migration often requires cells to collectively penetrate extracellular matrices in order to leave a primary tissue of origin and/or to invade a distal tissue location (243). This collective process requires cells to maintain sticky junctions. E-

cadherin-positive ovarian cancer cells (OVCAR5 cells) were shown to collectively migrate through 3D extracellular matrices in a serine protease dependent fashion, while maintaining cell-to-cell contacts (244). A study of the murine mammary carcinoma cell line, 4T1, illustrated that a partial reduction (but not total knockdown) of E-cadherin expression correlated with increased collective cell migration, suggesting that moderate E-cadherin expression is still required for collective migration in some cell types (245). A collectively migrating unit of cells expresses a front-to-rear polarity via cell-to-cell and cell-to-ECM contacts that transduce tensional signals through the actin cytoskeleton (246). It has been shown that a "leader cell" is responsible for remodeling the matrix through which a group of collectively migrating cancer cells must transit, and that the leader cell carries a bulk of the energetic burden (247,248). Complimentary to the leader cell concept, a "front" of cells on the progressing side of the collective migratory unit is responsible for making biphasic, high-tension focal adhesion contacts with the ECM, leading to activation of a viniculin/integrin/actin signal transduction cascade, followed by cellular restructuring and ECM remodeling (249,250). The collective movement of the cellular aggregate appears to depend upon a pulling force exerted by frontal cells, instead of a pushing force from the distal/back cells (251). Frontal cells pull the distal/back cells in their forward-leading direction, enabling the aggregate to move as a group (252). In order for these mechanisms to work the cell must maintain its collective nature which requires the continued expression of adherins junction molecules like E-cadherin (253).

Mitochondrial respiration and mitochondrial fission/fusion machinery are determinants of ovarian tumor progression (254–256). Ovarian cancer mitochondria display a high degree of morphological plasticity (i.e. fluctuation between states of fission and fusion) especially during proliferation and stress (256–258). However, little is known about mitochondrial metabolism in

laying hen ovarian tumors or the effect that flaxseed has on mitochondria within hen ovarian tumors. Accumulating evidence suggests that E-cadherin and the miR-200 family regulate core metabolic components including energy sensing, mitochondrial morphology, inorganic phosphate transport into mitochondria, mitochondrial DNA replication, and cell respiration (241,259–262). Furthermore, miR-200a has been specifically shown to regulate mitochondrial morphology by promoting mitochondrial elongation (via fusion), thus enhancing cellular respiration in cancer cells (260,263). The metabolic role of E-cadherin and the miR-200 family might be affiliated with their distinct role in regulating collective migration in ovarian cancer cells. Analysis of epithelial ovarian cancer cells in 3D culture revealed that E-cadherin and the miR-200 family (mostly miR-200a, miR-200b, and miR-429) were upregulated within inclusion cyst formations (242), suggesting that E-cadherin and the miR-200 family could be indispensable during the collective migration of ovarian cancer cells. Still, it is unknown if E-cadherin and the miR-200 family play a bioenergetic role concomitant with a migration-regulating role. Our lab has shown that dietary flaxseed downregulates the expression of miR-200a, miR-200b and miR-429, in laying hen ovarian tumors (14,264). If these downregulatory effects influence inclusion cyst formation, then our lab has likely identified a flaxseed-based mechanism that blunts the severity of ovarian cancer and reduces the risk of metastasis, in hens.

1.17 Soluble E-cadherin and cancer

Soluble E-cadherin (i.e. 80kDa E-cadherin) represents the extracellular portion of full-length E-cadherin. The full length protein has a molecular weight of approximately 120kDa (229,265), making it no surprise that the complimentary fragment to 80kDa E-cadherin is a 37 to 38kDa protein (266). In the early 1990s, clinical researchers observed elevated levels of soluble E-cadherin in the blood serum of patients with gastric cancer and hepatocellular carcinoma (267).

In their analysis, the majority of cancer patients had elevated soluble E-cadherin in blood compared to controls, suggesting that tumors exhibit enhanced proteolysis of E-cadherin. Since that time researchers have come to understand that soluble E-cadherin acts as an autocrine or paracrine signaling molecule that drives invasion and metastasis in a myriad of cancer types, including ovarian cancer (266). In ovarian tumors, soluble E-cadherin localizes to the surface of exosomes and heterodimerizes with VE-cadherin on endothelial cells thereby promotes the malignancy of ascites fluid and spread of the disease throughout the peritoneum (268). In skin squamous cell carcinoma, soluble E-cadherin (i.e. the 80kDa fragment) coimmunoprecipitated with receptor tyrosine kinases (RTKs) such as HER1, HER2 and IGF-1R, indicating the physical interaction between soluble E-cadherin and RTKs (269). Those authors further displayed that the physical interaction between soluble E-cadherin and RTKs promoted MAPK pathway activation and PI3K/Akt/MTOR activation, in both mouse and human tissues. The concentrations of soluble adhesion molecules (i.e. soluble ICAM-1, soluble CD44std and soluble E-cadherin) within ovarian cyst fluids are useful for distinguishing borderline and malignant ovarian tumors from ovarian cystadenomas (270). Similar results were observed by a group that observed higher soluble E-cadherin levels in malignant ovarian tumors versus benign ovarian cysts (271). These results indicate that soluble E-cadherin levels are elevated in the context of ovarian cancer pathogenesis, thus providing a rationale for further study of soluble E-cadherin in ovarian cancer.

Our model allows us to study the expression of several E-cadherin fragments, each bearing a unique molecular weight (i.e. 37kDa, 80kDa and 120kDa). The C-terminus of cadherin molecules is highly conserved in vertebrate species (272), meaning that an antibody that is antigenic for the C-terminus of E-cadherin has a good chance of positively detecting E-cadherin in different vertebrate animal models. Our lab has used a human antigenic C-terminus antibody

to detect E-cadherin protein in chicken ovaries (236). The fragments that have not been studied in laying hen ovarian cancer are the 37kDa and 80kDa fragments of E-cadherin. We recently received a very generous gift of 10mg of lyophilized rabbit polyclonal anti-chicken E-cadherin IgG, from Dr. Warren J. Gallin who recently retired at the University of Alberta, Canada. Dr. Gallin is one of the co-discoverers and co-characterizers of E-cadherin, although at the time they still referred to it as L-CAM (227,229). This E-cadherin antibody was designed to be polyclonal to the extracellular domain of E-cadherin (273). A diagram illustrating the molecular weights of E-cadherin that can be detected in hen ovarian tumors with our C-terminal and N-terminal antibodies can be seen in Figure 1.3.

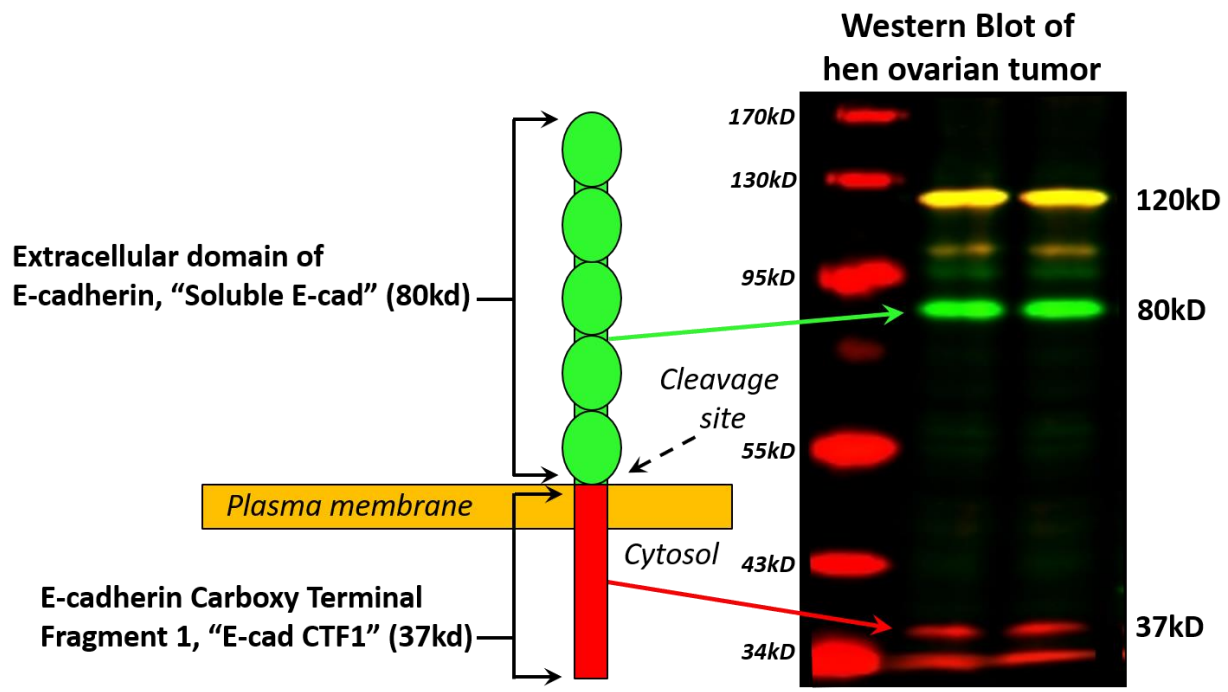

Figure 1.3. Schematic diagram of western blot for the detection of the 37kDa, 80kDa and 120kDa fragments of chicken E-cadherin, using antibodies for the C-terminus and N-terminus. The 37kDa intracellular, transmembrane domain of E-cadherin (i.e. CTF1) is detected in our model with a mouse IgG that is monoclonal to a proprietary amino acid sequence in the C-terminus of E-cadherin (shown in the western blot in red at 37kDa). The 80kDa extracellular domain of E-cadherin is detected with a rabbit IgG that is polyclonal to Ecadherin's extracellular domain (shown in the western blot in green at 80kDa). Notice that the rabbit IgG and the mouse IgG are both immunogenic for the full-length 120kDa E-cadherin protein (shown in the western blot in yellow at 120kDa).

CHAPTER 2

SPECIFIC AIMS AND HYPOTHESES

STUDY 1: The effect of flaxseed on one-carbon metabolism, lifespan and reproductive capacity in White Leghorn laying hens

Problem statement: Our lab is aware that flaxseed improves the health of laying hens, but we are unaware of the exact metabolic pathways that facilitate this health improvement.

Hypothesis: The flaxseed diet induces a transsulfuration blockade that modifies one-carbon metabolism in a manner that associates with enhanced lifespan and enhanced reproductive capacity in White Leghorn laying hens.

Specific aim 1: Conduct complex biological systems analysis (utilizing LC-MS/MS-derived blood plasma metabolomics data) to test a rationale that the flaxseed diet increases homocysteine flux into the methionine cycle and thereby boosts S-adenosylmethionine levels.

Specific aim 2: Evaluate lifespan and reproductive capacity via statistical analysis and/or metabolomics analysis to determine if lifespan and reproductive capacity are regulated by flaxseed.

Specific aim 3: Develop a model that conveys the most probable one-carbon metabolic processes that are happening during flaxseed dieting in White Leghorn laying hens.

STUDY 2: The effect of dietary polyunsaturated fatty acids (PUFAs) on mitochondrial metabolism and mir-200a/Cdh1/E-cadherin expression in laying hen ovarian tumors.

Problem statement: We a rough understanding of how miR-200a/*CDH1*/E-cadherin are regulated by PUFAs in hen ovarian tumors, but we want to extend this understanding to include the effects of PUFAs on mitochondrial metabolism in the hen ovarian tumor microenvironment.

Hypothesis: Dietary PUFAs regulate the expression of *de novo* lipogenic genes as well as the

levels of fatty acids, in ovarian tumors of the hen.

Specific Aim: Determine the expression of *de novo* lipogenic genes within hen ovarian tumors and then determine the concentration of fatty acids within that same set of tumors. *Hypothesis:* Dietary PUFAs elevate the expression of nuclear and mitochondrial genes that associate with mitochondrial electron transport chain activity (i.e. OXPHOS), in ovarian tumors of hens.

Specific Aim: Determine the expression of genes that are associated with mitochondrial ETC activity, ATP synthesis and oxidative stress response within hen ovarian tumors.

Hypothesis: Dietary PUFAs reduce the expression of microRNA-200a-3p, CDH1 and E-cadherin, in ovarian tumors of the hen.

Specific Aim: Determine the expression of miR-200a, CDH1 and E-cadherin in hen ovarian tumors, and then evaluate the expression of miR-200a and CDH1 in human ovarian cancer cells after incubation with PUFAs.

Hypothesis: Mitochondrial metabolism in human ovarian surface epithelial cells is regulated by the presence of the 80kDa E-cadherin fragment (i.e. soluble E-cadherin) during incubation with laying hen ascites fluid.

Specific Aim: Determine mitochondrial membrane potential and oxygen consumption in IOSE80 cells that have been treated with hen ascites fluid that either contains or does not contain the 80kDa E-cadherin fragment.

CHAPTER 3

MATERIALS AND METHODS

3.1 Animal studies and diet descriptions

325-day diet study in 2.5-year-old hens: Single-comb White Leghorn laying hens (*Gallus gallus*) with 2.5 years of age were assigned to one of six isocaloric diets for 325 days. Diets included a control feed diet (CTL), 10% defatted flaxseed (DF), 15% whole flaxseed (WF), 5% flaxseed oil (FXO), 5% corn oil (CRN) and 5% fish oil (FSH), for 325 days. Dietary ingredients as well as the calculated energy contents of diets can be seen in Table 3.1 and Table 3.2, respectively. Daily mortality was monitored throughout the 325-day study by the animal care facility. Causes of death before the 325th day are unknown (i.e. necropsy not conducted). Eggs were collected from hens within each diet group every day of the study. Sample sizes of hens for each diet were as follows: CTL (*n*=182), DF (*n*=161). WF (*n*=161), FXO (*n*=161), CRN (*n*=175), FSH (*n*=165). Hens were housed in the animal care facility at the University of Illinois in Urbana-Champaign, in pecks of 5 hens with a 17h/7h light/dark cycle. On the 24th week of the study, a light-restriction molt was implemented via a light/dark cycle of 8h/16h for three weeks. Food was not restricted during the molt. Animal care, diet protocols and necropsy methods were approved by the Institutional Animal Care and Use Committees (IACUC) at both Southern Illinois University, Carbondale and University of Illinois at Urbana-Champaign.

9-week diet study of 2-year-old hens: In this animal study we assigned 30 single-comb White Leghorn laying hens (*Gallus gallus*) to one of seven isocaloric diets for nine weeks (210 hens total). The diets and their composition can be seen in Table 3.3 and Table 3.4. All of the animal model protocols were the same as we used in the 325-day study. One of the major exceptions is that we did not observe any tumors in the hens from this study during necropsy (which was to be

expected given the young age of these hens at harvest; ie 2 years and 9 weeks of age).

Table 3.1. Diets and associated ingredients (g/100g), 325-day study.

	Diet					
Ingredient	Control	10% Defatted Flaxseed Meal	15% Whole Flaxseed	5% Flax Oil	5% Corn Oil	5% Menhaden Fish Oil
Corn	67.40	54.90	47.58	52.00	52.00	52.00
Flaxseed (whole)			15.00			
Corn Gluten Meal	3.00			5.00	5.00	5.00
Corn Oil					5.00	
Flax Oil				5.00		
Fish Oil						5.00
Defatted Flax Meal		10.00				
Qual Fat		3.80	2.50			
Solka Floc	0.30	2.00	5.62	8.70	8.70	8.70
Each diet received the following in g/100g of diet: Soybean meal (18.3), Limestone (8.75), Dical (1.5), Salt (0.3), Vitamin mix[1] (0.2),Mineral mix[2] (0.15),and DL-Methionine (0.1)						

[1]Vitamin premix (per kg of diet): retinyl acetate, 4,400 IU; cholecalciferol, 25 mg; DL-a-tocopheryl acetate, 11 IU; vitamin B12, 0.01 mg; riboflavin, 4.41 mg; D-Capantothenate, 10 mg; niacin, 22 mg; and menadione sodium bisulfite, 2.33 mg.

[2]Mineral premix (mg/kg of diet): Mn, 75 from MnO; Fe, 75 from FeSO4·7H2O; Zn, 75 from ZnO; Cu, 5 from CuSO4·5H2O; I, 0.75 from ethylene diamine dihydroiodide; and Se, 0.1 from Na2SeO3.

Table 3.2. Calculation of nutrient percentages and total energy of diets (325-day study).

	Diet					
Calculated Analysis	Control	10% Defatted Flaxmeal	15% Whole Flaxseed	5% Flax Oil	5% Corn Oil	5% Fish Oil
TME[1], kcal/kg	2,816	2,816	2,815	2,815	2,815	2,815
CP[2], %	16.56	17.04	16.50	16.49	16.49	16.49
Calcium, %	3.73	3.77	3.75	3.73	3.73	3.73
aPhosphorus, %	0.38	0.40	0.38	0.37	0.37	0.37
Met + Cys, %	0.67	0.72	0.64	0.67	0.67	0.67
[1]TME= total metabolizable energy, [2]CP= crude protein						

Table 3.3. List of diets showing the ingredients and the percentage of calories derived from those ingredients (9-week study).

Ingredient	Diet						
	Control	15% Defatted Flaxmeal	15% Whole Flaxseed	5% Flax Oil	5% Corn Oil	5% SDA Soy Oil	5% Soy Oil
Corn	67.40	51.90	47.58	52.00	52.00	52.00	52.00
Flaxseed (whole)			15.00				
SBM	18.30	18.30	18.30	18.30	18.30	18.30	18.30
Corn Gluten Meal	3.00			5.00	5.00	5.00	5.00
Corn Oil					5.00		
Soy Oil							5.00
SDA Soy Oil						5.00	
Flax Oil				5.00			
Qual Fat		3.80	2.50				
Defatted Flax Meal		15.00					
Solka Floc	0.30		5.62	8.70	8.70	8.70	8.70
Each diet received the following percentage of calories from: Soybean meal (18.3%), Limestone (8.75%), Dical (1.5%), Salt (0.3%), Vitamin mix[1] (0.2%),Mineral mix[2] (0.15%),and DL-Methionine (0.1%)							

[1]Vitamin premix (per kg of diet): retinyl acetate, 4,400 IU; cholecalciferol, 25 mg; DL-a-tocopheryl acetate,11 IU; vitamin B12, 0.01 mg; riboflavin, 4.41 mg; D-Capantothenate, 10 mg; niacin, 22 mg; and menadione sodium bisulfite, 2.33 mg.
[2]Mineral premix (mg/kg of diet): Mn, 75 from MnO; Fe, 75 from FeSO4·7H2O; Zn, 75 from ZnO; Cu, 5 from CuSO4·5H2O; I, 0.75 from ethylene diamine dihydroiodide; and Se, 0.1 from Na2SeO3.

Table 3.4. Calculation of nutrient percentages and total energy of diets (9-week study).

Calculated Analysis	Diet						
	Control	15% Defatted Flaxmeal	15% Whole Flaxseed	5% Flax Oil	5% Corn Oil	5% SDA Soy Oil	5% Soy Oil
TME[1], kcal/kg	2,816	2,816	2,815	2,815	2,815	2,815	2,815
CP[2], %	16.56	18.49	16.50	16.49	16.49	16.49	16.49
Calcium, %	3.73	3.77	3.75	3.73	3.73	3.73	3.73
aPhosphorus, %	0.38	0.40	0.38	0.37	0.37	0.37	0.37
Met + Cys, %	0.67	0.72	0.64	0.67	0.67	0.67	0.67
[1]TME= total metabolizable energy, [2]CP= crude protein							

3.2 Animal necropsy and tissue collection

Hens surviving to the completion of the 325-day study were prepared for manual necropsy.

Necropsy was not performed on hens that died prior to the completion of the study. Body weight was recorded in kilograms before sacrifice. Hens were sacrificed via carbon dioxide asphyxiation and cervical dislocation. Whole blood was collected from hens via heart puncture. Peritoneal pathologies were determined via manual necropsy, primarily looking for the presence of ovarian cancer, ascites fluid, GI cancer, oviductal cancer, liver cancer, and metastatic spread throughout the peritoneal cavity. Stages of ovarian cancer were assigned according to the International Federation of Gynecology and Obstetrics (FIGO) staging criteria (cancer.org). Tissue samples of each hen's ovary, oviduct, and liver, were then collected and flash frozen in liquid nitrogren. In hens with ovarian cancer, tissue samples from ovarian tumors, ascites fluid, and/or peritoneal metastases were collected. Harvested tissues were flash frozen in liquid nitrogen at collection and stored at -80 Celsius at Southern Illinois University.

3.3 LC-MS/MS analysis of blood plasma metabolites

Blood plasma was collected from hens on the 210th day of the 325-day study via wing vein puncture, centrifuged and flash frozen with liquid nitrogen. Regarding plasma collection, the sample sizes from each diet group were as follows: CTL (*n*=6), DF (*n*=5), WF (*n*=6), FXO (*n*=6), CRN (*n*=6) and FSH (*n*=4). Blood plasma samples were analyzed via liquid chromatography tandem mass spectrometry (LC-MS/MS) at the Lipid and Metabolite Mass Spectrometry Facility of the University of Texas Southwestern Medical Center. The procedure for LC-MS/MS analysis was previously described in detail (274). In summary, a targeted metabolite profiling approach was conducted by separating metabolites on a Phenomenex Synergi Polar-RP HPLC column with a Nexera Ultra High Performance Liquid Chromatography (UHPLC) system. An AB QTRAP 5500 mass spectrometer was used with electrospray ionization (ESI) source set to multiple reaction monitoring (MRM) mode. MRM data were

acquired using Analyst 1.6.1 software. MultiQuant 2.1 software was used to review chromatograms and peak areas. Peak areas were normalized for each detected metabolite against the total ion count of that sample to correct for any variations introduced by sample handling through instrument analysis and then converted to Variable of Importance Projection (VIP) scores. VIP scores are arbitrary units that are not representative of translatable concentrations. VIP scores, heat map and partial least squares-discriminant analysis (PLS-DA), were calculated using the software SIMCA-P (Version 13.0.1, Umetrics).

3.4 Reanalysis of microarray feature data from a previous laying hen study

A separate, earlier diet study using 387 single–comb White Leghorn hens (2.5-years old at study initiation) was previously conducted and published (14). Hens were provided either a 10% whole flaxseed diet or a control diet for one year. Details of dietary ingredients and methods for tissue harvesting and processing were described in (19). Animal care, diet protocol and necropsy method were approved by the Institutional Animal Care and Use Committees (IACUC) at both Southern Illinois University, Carbondale and University of Illinois at Urbana-Champaign. Ovarian tissues from stage-matched hens were sampled from each of the following: whole flax normal (WFN) hens (n=6); whole flax cancer (WFC) hens (n=6), control normal (CTLN) hens (n=6), and control cancer (CTLC) hens (n=6). These ovaries were used for RNA extraction, labeling, hybridization and microarray analysis as described in (14). Two-tailed T-tests were performed to calculate fold-change expression differences of microarray features between groups (i.e. WFN versus CFN and WFC versus CTLC). In our present paper, we reanalyze those T-tests and illustrate the percentage of features that were downregulated or upregulated at the $p<0.10$, $p<0.05$ and $p<0.01$ levels of significance.

3.5 Protein Assay (blanket protocol for all protein assay work)

BCA reagent A (Pierce, 23228), BCA reagent B (Pierce, 1859078) and 2mg/mL BSA standard (Pierce, 23209), were used to conduct protein assays in 96-well plates. Protein standard concentrations were loaded in duplicate on each plate. Unknowns were also loaded in duplicate on each plate. The plate protocol was set as: temperature 37 degrees Celsius, shake plate for 5 seconds, incubate plate for 30 minutes in reader (i.e. 30 minute read delay) and then measure absorbance at 562nm, using a Biotek Synergy plate reader.

3.6 Gas chromatography analysis of fatty acids in hen ovarian tumors

Fatty acid isolation: 50mg samples of ovarian tumor tissue were isolated on dry ice and added to 5mL round bottom tubes. 1mL of 1mM Tris base was added to the tube and then homogenized with a tissue homogenizer. 100µL of this tissue homogenate was aloquated for BCA protein assay of the sample (to determine the ug of protein per microliter of sample). 200µL of the tissue homogenate was added to a fresh test tube and 100µL of 2mg/mL C17:0 (heptadecanoic acid) was added to the tube (total volume in tube = 300µL), C17:0 was used as an internal control to control for pipetting error. Then, add 1mL of chloroform to the tube (total volume in tube = 1.3mL) and vortex. Add another 1mL of chloroform to the tube (total volume in tube = 2.3mL) and vortex. Two phases should be apparent now, with the lipid phase appearing in the bottom of the tube and the polar phase appearing in the top of the tube. Centrifuge tubes at 3400rpm for 10 minutes at 4 degrees Celsius (this is Tube A). NOTE: I refer to the word “tube” in the singular case for simplification purposes, but you would have more than one tube if preparing more than one fatty acid sample. Prepare sodium sulphate filtration pipettes (with 5-inch Pasteur pipettes) according to the diagram in Figure 3.1. In short, inserting a small piece of tissue paper into the main cylinder of pipette. Push this piece of paper down the cylinder of the pipette until it can

travel no further. The goal is to “clog” the pipette so that sodium sulphate and large solids cannot pass through the pipette. Next, add a 1.5-inch stack of sodium sulfate on top of the tissue paper. The purpose of the sodium sulfate is to allow the polar substrate (i.e. sodium sulfate) to extract polar molecules from the lipid/chloroform phase. Next, use a pipette to slowly add the lipid/chloroform phase that appeared at the bottom of Tube A after centrifuging. The lipid/chloroform phase will pass through the sodium sulphate and tissue paper in the pipette and be collected in a new tube. Use a new tube with a screw cap to catch the filtrate (this is Tube B). Add one more mL of chloroform to the previous test tube from which the lipid/chloroform phase was extracted (i.e. Tube A). Vortex Tube A and centrifuge at 3400xG for 10 minutes. Repeat the procedure where the lipid/chloroform phase is pipetted through the sodium sulfate in the Pasteur pipette, and collect the filtrate again in Tube B. The volume in Tube B should be close to 1.5 to 2mL of filtered lipid/chloroform. This is a good stopping point for the day if necessary. If stopping for the day, be sure to parafilm wrap Tube B for overnight storage at -20 degrees Celsius.

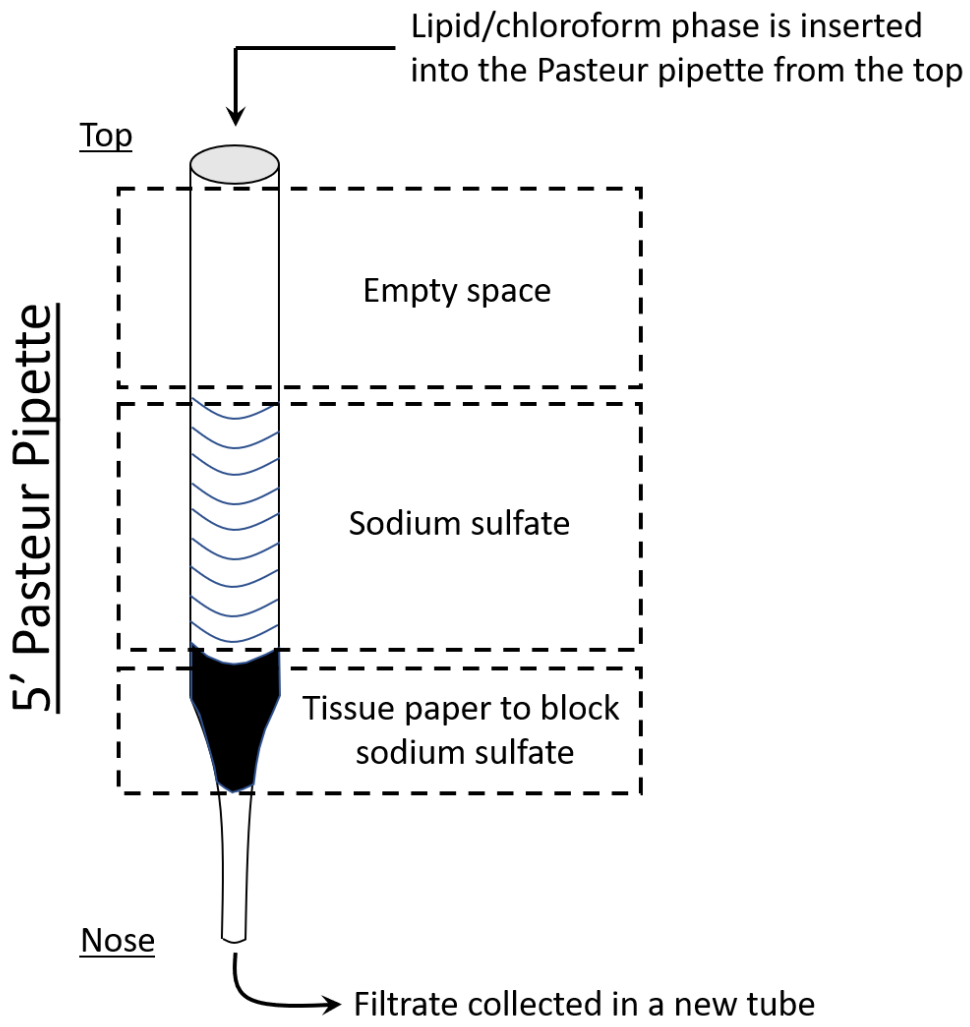

Figure 3.1. Pasteur pipette used for filtering lipid/chloroform phase through sodium sulfate.

Fatty acid methyl ester (FAME) preparation: To make the methylating reagent, slowly add 5.6mL of acetyl chloride to 112mL of methanol. Do this with a magnetic stirring rod mixing the solutions. Evaporate the chloroform from Tube B with nitrogen gas. Be sure to ethanol wash the nitrogen gas nodule before inserting it into Tube B. After the chloroform is evaporated from Tube B, add 1mL of the freshly prepared methylating reagent into Tube B, return the screw cap to the tube and vortex. Then incubate Tube B in an oven at 70 degrees Celsius for one hour.

After incubation is complete, add 500uL of methanol to Tube B if it experienced complete evaporation of methylating reagent.

Isolation of methylated fatty acids: Add 2mL of hexane to Tube B and vortex. Add 1mL of milli-Q water to Tube B and vortex. Add 1mL of hexane to Tube B and vortex. Screw the cap back onto Tube B and centrifuge the tube at 3750xG for 10 minutes at 4 degrees Celsius. After centrifuging, a lipid/hexane layer should appear on the top of Tube B. Pipette this lipid/hexane layer to a new tube (this is Tube C). Evaporate the hexane from Tube C with nitrogen gas. Add 150µL of hexane to Tube C and vortex. Put a 250µL glass insert into a 9mm chromatography autosampler vile, and then transfer 125µL of the lipid hexane from Tube C to the glass insert that is in the chromatography autosampler vile. Screw the lid onto the chromatography vile. This is also a good stopping point if necessary. Wrap the chromatography vile in parafilm wrap and store at -20 degrees Celsius, if stopping for the day.

Gas chromatograph analysis of methylated fatty acids: Fatty acids in the chromatography vile were analyzed using a Shimadzu GC-2020 gas chromatography instrument (Shimadzu Scientific Instruments Inc., Columbia, MD). This instrument utilizes a Supelco 100-m SP-2560 fused silica capillary column and a flame ionization detector. The linear velocity of the helium carrier gas was held constant at 23cm/s with a split ratio of 10:1. Oven temperature was set to 150 degrees Celsius for 80 minutes and incrementally increased by 3 degrees Celsius per minute until reaching a ceiling of 249 degrees Celsius. The temperature was held there for 10 minutes. Injector and detector temperatures were both held at 255 degrees Celsius. PUFA1 (Supelco, 47033) and PUFA3 (Supelco, 47085-U) fatty acids were used as standards to identify unknown peaks in the ovarian tumor samples. These standards were included with every iteration with the gas chromatography instrument. Hexane was used to clear the column every 5 samples that were

analyzed. Peaks in the data were observed by contrasting unknown sample peaks with the peaks of a PUFA No. 1 standard (47033, Supelco) and a PUFA No. 3 standard (47085-U, Supelco). The area under the curve of each new peak was then normalized to the peak of the C17:0 internal control, and then normalized to the protein concentration that was determined for the sample during BCA analysis of the original tissue homogenate.

3.7 Protein isolation

5 cryotubes containing frozen hen ovarian tumor tissue were randomly selected from each diet group. All stage 2, stage 3 and stage 4 ovarian tumors were eligible for selection, so stage was treated as a stochastic variable (with the exclusion of stage 1 samples that are often borderline tumors). Microsoft Excel's random number generating tool was used to generate random numbers. Non-parametric Kruskal-Wallis ANOVA (with Dunn's post-hoc test, $p<0.05$) was conducted to ensure that stages were not significantly clustered in any diet before proceeding. Approximately 50mg of hen ovarian tissue was collected from cryotubes containing frozen ovarian tissue; collected samples were then placed in 5mL round bottom, snapcap test tubes. Samples were immediately homogenized in a tissue homogenizer in 1mL of ice-cold lysis buffer. The lysis buffer consisted of (per 10mL) 8.9mL water, 1mL 1% SDS diluted in PBS, and 0.1mL of 100x HALT protease and phosphatase inhibitor cocktail (ThermoFisher, 78440). After homogenizing samples, each sample was transferred to a 1.5mL Eppendorf tube and centrifuged at 3000xG for 5 minutes at 4 degrees Celsius. The supernatant was collected, aliquoted and frozen at -80 degrees Celsius.

3.8 RNA isolation

For normal hen ovaries, 9 cryotubes containing frozen hen ovary samples were randomly selected from each diet group. Microsoft Excel's random number generating tool was used to

generate random numbers. For cancerous hen ovaries, 9 cryotubes containing frozen ovary samples were randomly selected from each diet independent of cancer stage (i.e. all stages were eligible for selection). Non-parametric Kruskal-Wallis ANOVA (with Dunn's post-hoc test, $p<0.05$) was conducted to ensure that stages were not significantly clustered in any diet before proceeding. For RNA isolation from hen ovaries, approximately 25mg of ovarian tissue was collected from cryotubes containing frozen ovarian tissue; collected samples were then placed in 5mL round bottom, snapcap test tubes. 1mL of Trizol reagent (Thermofisher, 15596026) was added to each test tube, and then tissues were homogenized. For cell culture collections, cells were washed twice with 2mL of 1X Dulbecco's phosphate-buffered saline (Corning, 20030CV), and then 1mL of Trizol reagent was added to each dish. Trizol was pipetted in each dish until cells were noticeably digested (i.e. a thick mucous-like homogenate was formed from all cells). From this point forward, I used the same steps for both hen ovary homogenates and cell culture homogenates. Homogenates (from ovaries or cells) were transferred to 1.5mL Eppendorf tubes and kept at room temperature (RT) for five minutes. 0.2mL of chloroform was added to each test tube, lightly mixed and then tubes were incubated at RT for 10 minutes. Tubes were then centrifuged at 12,000xG for 15 minutes at 4 degrees Celsius. After centrifuging, the top (aqueous phase) was transferred to a new 1.5mL Eppendorf tube, and 0.5mL of isopropynol was added to each new tube. New tubes were incubated at RT for 10 minutes and then centrifuged at 12,000xG for 12 minutes at 4 degrees Celsius. The supernatant was then poured off from each tube, and the RNA pellet was retained. 1mL of 70% ethanol was added to each tube (in order to wash RNA pellets), and tubes were centrifuged at 12,000xG for 15 minutes at 4 degrees Celsius. Supernatant from each tube was then poured off, and tubes were allowed to air dry at RT for 15 minutes. 100µL of milli-Q water was then added to each tube, and tubes were then incubated in a

water bath at 55 degrees Celsius for 10 minutes. RNA pellets were visually inspected to ensure that they were fully dissolved after water bath incubation. RNA was then precipitated in each tube by adding 125mL of 4 molar ammonium acetate and 300µL of 100% ethanol; tubes were lightly vortexed and then allowed to incubate at -80 degrees Celsius for 20 minutes. After incubation, tubes were centrifuged at 12,000xG for 10 minutes at 4 degrees Celsius. Supernatant was poured off from each tube, and 1mL of 70% ethanol was added to each tube; tubes were then centrifuged at 12,000xG for 10 minutes at 4 degrees Celsius. Supernatant was poured off, and RNA pellet was allowed to air dry at RT for 15 minutes. RNA pellets were resuspended in 100µL of milli-Q water, and the concentration of RNA was measured by detecting the 260nm/280nm ratio with a Nanodrop (Thermofisher). All RNA samples above 4000ng/µL were diluted to approximately 2000ng/µL, to ensure that the RNA concentration of the sample was in the detectable range of the Nanodrop.

3.9 RNA quality check (agarose formaldehyde gel electrophoresis)

10X MOPS preparation: 500mL of 10X morpholino-propanesulfonic acid (MOPS) was prepared by combining 20.93 grams of 200mM MOPS, 2.05 grams of 50mM sodium acetate, and 1.86 grams of 10mM ethylenediaminetetraacetic acid (EDTA). These reagents were suspended in 250mL of milli-Q water and stirred with an electric stirring rod, and the pH was set to 7.0 with 5M NaOH (final volume of 10X MOPS = 500mL). 10X MOPS was wrapped in aluminum foil and protected from light.

1.2% agarose preparation: 400 mL of 1.2% agarose gel was created by combining the following reagents: 4.8 grams of electrophoresis grade agarose, 325mL of milli-Q water, and 40mL of 10X MOPS.

Laying the 1.2% agarose gel: Boil the 1.2% agarose in a microwave for 4 minutes and allow

to cool to 65 degrees Celsius. Add 91.25mL of 1.2% agarose gel to a beaker and then add 9mL of 37% formaldehyde and 5uL of 10mg/mL ethidium bromide (EtBr). Mix these together with a glass stirring rod. Pour the gel mixture into a horizontal electrophoresis apparatus, add the lane "comb" and allow to solidify.

Preparing the running buffer: Combine 100mL of 10X MOPS, 87mL of 37% formaldehyde, and 813µL of milli-Q water. Final volume = 1 liter.

Preparing the samples and running the electrophoresis gel: Sample buffer includes the following, per sample: 7.5µL of Formamide, 2.5µL of 0.5mg/µL EtBr, 2.5µL milli-Q water, 1.5µL of 10X MOPS, 1.5µL of 0.1% bromophenol blue (diluted in 50% glycerol), and 1.3µL of 37% formaldehyde. Thaw RNA samples on ice and use Nanodrop to determine the volume required for 1 microgram (µg) of RNA. Add 1µg of RNA to 15µL of sample buffer. Heat each sample at 65 degrees Celsius for five minutes and then immediately place the sample on ice. Load 15µL of each sample into lanes of the 1.2% agarose gel and cover the gels with running buffer. Electrophorese the samples at 100V until the blue dye reaches the opposite end of the gel. Gels were then visualized using the EtBr setting on a Gel Doc EZ Imaging System™ (Bio-Rad, 170-8270). 18S and 28S lanes were observed to evaluate the quality of the RNA sample. A prominent, well defined band for 18S and 28S RNA was investigated to determine the integrity of the RNA sample. RNA samples with indeterminant bands were re-isolated from their given tissue or cell culture sample. All other RNA samples were retained for further analysis (e.g. retained for cDNA synthesis).

3.10 cDNA synthesis

For mRNA analysis: RNA samples were thawed gently on ice, and the volume required to obtain 2ug of RNA was determined using a Nanodrop. cDNA synthesis samples included: 2µg of

sample RNA, 1µL DNAse and 1µL DNAse buffer (brought up to a total volume of 10µL with nuclease-free water). Samples were incubated in a thermocycler at 37 degrees Celsius for 30 minutes. Samples were then treated with 1µL of DNAse stop solution (total volume 11µL), and samples were incubated in a thermocycler for at 65 degrees Celsius for 10 minutes. Reverse transcriptase master mix was then prepared, using (per sample) 3.2µL of nuclease-free water, 2µL of 10x reverse transcriptase buffer, 2µL of 10x reverse transcriptase primers, 1µL of Multiscribe^{TM} reverse transcriptase (Applied Biosystems, 4311235), and 0.8µL of 100mM dNTP mix. The reverse transcriptase buffer, primers and dNTP mix were part of a cDNA synthesis kit (A&B Biosystems, 4368814). 9µL of the reverse transcriptase master mix was added to each 11µL sample containing freshly DNAse'd RNA (total volume 20µL now). These 20µL samples were incubated in a thermocycler using the following protocol: 25 degrees Celsius for 10 minutes, 37 degrees Celsius for 90 minutes, 37 degrees Celsius for 30 minutes, 85 degrees Celsius for 5 minutes, and then immediately cooled to 4 degrees Celsius. cDNA samples were then diluted 10 times with nuclease-free water and stored at -20 degrees Celsius.

For microRNA analysis: RNA samples (same RNA samples used for mRNA analysis) were gently thawed on ice. RNA samples were then diluted to 5ng/µL using nuclease-free water. cDNA master mix was prepared using the Universal cDNA^{TM} Synthesis Kit (Exiqon, 203301). From this kit, 2µL of 5x reaction buffer, 5µL of nuclease-free water and 1µL of enzyme mix, were prepared per cDNA synthesis reaction (total volume = 8µL of master mix). These 8µL of master mix were added to 2µL of 5ng/µL RNA (total volume 10uL), and each sample was incubated in a thermocycler, using the following protocol: 42 degrees Celsius for 60 minutes, 95 degrees for 5 minutes, and then immediately cooled to 4 degrees Celsius. Stored at -20 degrees Celsius.

3.11 qPCR analysis

Oligonucleotide primer design: Primers were designed using NCBI's Primer Designing Tool (available at: https://www.ncbi.nlm.nih.gov/tools/primer-blast/). In general, oligonucleotides were designed so that the PCR product would be between 90 and 100 nucleotides in length. The primer melting temperatures were attempted to be as close as possible, with melting temperatures never being more than 2-degrees Celsius variable between forward and reverse primers. 60 degrees Celsius was the average melt temperature sought. Oligonucleotides were blasted against the human (*Homo sapiens*) genome for human gene analysis and against the chicken (*Gallus gallus*) genome for chicken gene analysis. The max number of guanine or cytosine nucleotides (i.e. GC) permitted in the final five nucleotides of the 5' end was three, in order to stabilize annealing strength. Nucleotide repeats exceeding four nucleotides (e.g. TTTT) were generally considered a disqualifying criterion. Otherwise, the default settings were utilized on the Primer Designing Tool, and the highest-ranking oligonucleotide pairs with minimal self-binding were purchased. All oligonucleotide pairs for mRNA analysis were ordered from Eurofins Genomics (eurofinsgenomics.com). Once received, all oligonucleotide primers were diluted to a concentration of 100 micromolar and stored at -20 degrees Celsius. A list of human (*Homo sapiens*) oligonucleotide primers can be seen in Table 3.5, and a list of chicken (*Gallus gallus*) oligonucleotide primers can be seen in Table 3.6.

Oligonucleotide primer efficiency analysis: For the analysis of cDNA amplification from mRNA-based samples, the goodness of fit of the 2(-Delta Delta C(T)) method for each oligonucleotide primer set was determined by creating amplification efficiency curves for the oligonucleotide primer set. A serial cDNA dilution was created (seven serial 2-fold dilutions) was used as the input template. In order to meet the efficiency requirments, the Ct values across

the dilutions needed to have an R-squared of at least 0.98. The percent efficiency of each oligonucleotide primer set, calculated as "(2^-(1/slope of Ct amplification))-1)", needed to range between 95% and 110% in order to meet amplification efficiency requirements. All Ct values and melt peaks were analyzed using the CFX Manager™ software.

qPCR analysis for measuring cDNA from messenger-RNA: Thaw the SsoFast™ EvaGreen® Supermix (Bio-Rad, 1725203) and protect it from light. Thaw the cDNA template samples (stored at -20 degrees Celsius) and the relevant oligonucleotide primer sets. This qPCR protocol uses 10µL reactions in a 384-well plate. Each 10uL qPCR reaction received 0.1µL of 100uM forward oligonucleotide primer (50nM forward primer), 0.1µL of 100µM reverse oligonucleotide primer (i.e. 50nM reverse primer), 5µL of SsoFast™ EvaGreen® Supermix (Bio-rad, 1725203), and 3.8µL of nuclease-free water, and 1µL of cDNA template (total reaction volume = 10µL). Also included in each plate were negative control samples that included forward and reverse oligonucleotide primers, EvaGreen® Supermix, and nuclease free water (total volume 10µL). All reactions were performed using a Bio-Rad CFX384™ thermocycler. The Evagreen was activated at 95 degrees Celsius for 10 minutes. Each round of amplification underwent 15 seconds of denaturation at 95 degrees Celsius and 20 seconds of annealing and extending at the appropriate annealing temperature (the annealing temperature was set to two degrees Celsius below the lowest melting temperature among the oligonucleotide primer pair). A photo was taken of the fluorescence following the completion of each round of amplification. A melt curve analysis was used after the completion of amplification, consisting of a 0.5-degree Celsius step from 65 degrees Celsius to 95 degrees Celsius, with a five second hold at each step and a photo of fluorescence. All Ct values and peaks were analyzed using the CFX Manager™ software.

qPCR analysis for measuring cDNA from micro-RNA: Thaw the Exilent Sybr Green PCR™ master mix (Exiqon, 203401) on ice and protect it from light. Thaw cDNA samples on ice and prepare dilutions of each cDNA containing 1:79 cDNA:nuclease-free water (i.e. add 5µL of cDNA to 395µL of nuclease-free water, total volume 400µL). Each qPCR reaction receives 5µL of master mix, 1uL of PCR primer mix (0.5uL miR-200a-3p primer and 0.5µL miR-455-5p primer), and 4uL of the 1:79 diluted cDNA template (total volume = 10µL per qPCR reaction). Each reaction was analyzed in a Bio-Rad CFX384™ thermocycler using 40 rounds of cDNA amplification. The DNA polymerase was activated at 95 degrees Celsius for 10 minutes. Each round of amplification underwent 10 seconds of denaturation at 95 degrees Celsius and 1 minute of annealing and extending at 60 degrees Celsius. A photo was taken of the fluorescence following the completion of each round of amplification. A melt curve analysis was used after the completion of amplification, consisting of a 0.5-degree Celsius step from 65 degrees Celsius to 95 degrees Celsius, with a five second hold at each step and a photo of fluorescence. All Ct values and peaks were analyzed using the CFX Manager™ software.

qPCR data analysis: All Ct values and melt peaks were analyzed using the CFX Manager™ software. All qPCR data were analyzed using the 2(-Delta Delta C(T)) method as described in (275). For chicken samples, Glyceraldehyde 3-phosphate dehydrogenase (*GAPDH*) was used as a reference gene. For human samples, Tata-box binding protein (*TBP*) was used as a reference gene.

Table 3.5. List of oligonucleotide primers used in qPCR analysis of human samples.

Abbreviation	Gene name	5' to 3' sequence
CDH1	Cadherin-1	F: TGTGCTGGATGTGAATGAAG
		R: GCAGTGTAGGATGTGATTTC
HO1	Heme Oxygenase 1	F: CCAGAAGAGCTGCACCGCAA
		R: CGCTGCATGGCTCGTGTGTA
NQO1	NAD(P)H Quinone Dehydrogenase 1	F: TGACAAAGGACCCTTCCGGAGT
		R: TCATGTCCCCGTGGATCCCT
SNAI1	Snail	F: GGTTCTTCTGCGCTACTGCT
		R: GTTAGGCTTCCGATTGGGGT
SNAI2	Slug	F: TGGGCTGGCCAAACATAAGCA
		R: GGCGCCCAGGCTCACATATT
TBP	Tata-box Binding Protein	F: GAGGATAAGAGAGCCACGAA
		R: GGACTGTTCTTCACTCTTGG
VIM	Vimentin	F: AACTTAGGGGCGCTCTTGTC
		R: CGCTGCTAGTTCTCAGTGCT
ZEB1	Zinc Finger E-Box Binding Homeobox 1	F: CCTGCCAACAGACCAGACAGT
		R: CTTGCCCTTCCTTTCCTGTGTCA

Table 3.6. List of oligonucleotide primers used in qPCR analysis of chicken samples.

Abbreviation	Gene name	5' to 3' sequence
ACC	Acetyl CoA Carboxylase	F: CCGCTGTACCGAGACGG
		R: GGCCGCACTTCCTCTGG
ACYL	ATP Citrate Lyase	F: GACAGAACCGCCCGTCACA
		R: AGCAGACACCAGAAGTCGGAG
ATP5A1	ATP Synthase F1 Subunit Alpha 1	F: AAGCTGAAGGAAATAGTCACAAA
		R: TGATGGAGAGCACATAACAACA
ATP5B	ATP Synthase Subunit 5B	F: CGGTTATTCGGTGTTCGCTG
		R: CCTGCGTGAAGCGGAAAATG
CAT	Catalase	F: CCATCCTTCATCCATAGCCAGA
		R: AGACTCAGGGCGAAGACTCA
CDH1	Cadherin-1	F: GCAGAAGATCACGTACCGCAT
		R: ATGTACTGTTGATGGCGTGC
DNM1L	Dynamin 1 Like (DRP1)	F: GTGACCCGAAGACCCCTTAT
		R: AGCATCTATCTCATTTTCATCTCCA
FASN	Fatty Acid Synthase	F: CAACAGCCAGCTTGGAATGG
		R: TACCACCTCCCACTCTTGGT
GAPDH	Glyceraldehyde-3-Phosphate Dehydrogenase	F: ACAGCAACCGTGTTGTGGAC
		R: CAACAAAGGGTCCTGCTTCC
MT-ATP6	ATP Synthase Subunit 6, mitochondrial	F: AATTCTCAAGCCCCTGCCTA
		R: AGGAGGCCTAGGAGGTTAAT
MT-ATP8	ATP Synthase Subunit 8, mitochondrial	F: ATGCCCCAATTAAACCCAAAC
		R: TTAGGTTCATGGTCAGGTTCA
MT-COX1	Cytochrome C Oxidase Subunit 1, mitochondrial	F: TCCTTCTCCTACTAGCCTCA
		R: AGGAGTAGTAGGATGGCAGT
MT-COX2	Cytochrome C Oxidase Subunit 2, mitochondrial	F: AGGCTTTCAAGACGCCTCAT
		R: GTGAGATCAGGTTCGTCGAT
MT-COX3	Cytochrome C Oxidase Subunit 3, mitochondrial	F: TAGTTGACCCAAGCCCATGA
		R: GTAGGCCCTTTTGGACAGTT
MT-CYTB	Cytochrome B, mitochondrial	F: TGCCTCATGACCCAAATCCT
		R: AGTGTGAGGAGGAGGATTACT
MT-ND2	NADH:Ubiquinone Oxidoreductase Core Subunit 2, mitochondrial	F: AGCATAACCAACGCCTGATC
		R: GATGTTAGGAGGAGGAGTGT
NOS2	Inducible Nitric Oxide Synthase	F: ACCCTGCAAGTGTGGAGTTC
		R: GATCTTGGCCGTTTGCTTGG
PPARG	Peroxisome Proliferator Activated Receptor Gamma	F: TTGGCCCGTTAATTTTGGA
		R: GAAAAATCAACAGTGGTAAATGG
SCD1	Sterol CoA Desaturase 1	F: CTGGTACGCAAACACCCAGA
		R: ATCTCCGCTGGAACATCACC
SLC25A4	ADP/ATP Translocase	F: GACCGGCTCCCAGCATGAGT
		R: GGGCGACAGCCGTCTTGGAG
SOD2	Superoxide Dismutase 2	F: ACCTAAGTGGAAACGCACAC
		R: ACCAGCTACTACCAAAGACGA
SREBP1	Sterol Regulatory Element Binding Protein 1	F: GTGCTTTTCGGATGCGTTGG
		R: CAGGCCAGAGCTGATGGAC

3.12 Western blot analysis

Gel preparation: SDS-PAGE gels were electrophoresed using Mini-PROTEAN Tetra Cell vertical gel system, 1mm gel (Bio-rad, 1658005EDU). For 9.7% resolving gels, we used the following: 1.665mL 30% acrylamide, 1.425mL Tris buffer (8.8 pH), 2mL milli-Q water, 50µL 10% APS, 5µL TEMED and 25µL trichloroethanol (TCE). TCE was added for the purpose of quantifying the total protein in the sample via fluorescent imaging. For stacking gels, we used the following: 450µL of 30% acrylamide, 660uL of Tris buffer (6.8pH), 1.5mL milli-Q water, 15µL 10% APS and 3µL TEMED.

Sample preparation and electrophoresis: 30µg of protein were mixed into a 2X Laemmli buffer solution and loaded into separate lanes in the gel. This buffer was derived from a 4X Laemmli buffer consisting of 2.5mL of 0.25M Tris-HCl (pH 6.8), 2mL of 2-mercaptoethanol, 0.8 grams of SDS, 2mL of glycerol, and 80uL of 0.1% bromophenol blue that was diluted to 2x in 50% glycerol. Samples were randomized on blots so as to reduce inter-blot bias. Loading controls were used in each blot in order to intercalibrate blot densitometry values. Electrophoresis was conducted using a running buffer consisting of 900mL milli-Q water and 100mL of 10X buffer (1X buffer contained 14.4g glycine, 3g Tris-base and 1g SDS). Proteins were electrophoresed at 100 volts through the stacking lane until a thin horizontal blue lane formed at the foot of the stacking gel. Proteins were then electrophoresed at 120 volts through the separating gel. Electrophoresis continued until the proteins reached the foot of the separating gel. EZ-Run™ protein ladder (Fisher, BP3603-500) was used in all protein electrophoresis work to identify the molecular weight of protein bands. In 9.7% resolving gels, the visible weights in the protein ladder were 170kDa, 130kDa, 95kDa, 72kDa (usually difficult to see), 55kDa, 43kDa, 34kDa and sometimes a small amount of 26kDa.

Gel transfer and primary antibody incubation: Gels were then removed from the electrophoresis apparatus and placed in transfer cassettes, using transfer membranes and PVDF membrane to facilitate the transfer. Transfers were performed in a horizontal transfer apparatus using a transfer buffer consisting of 700mL milli-Q water, 200mL methanol, and 100mL of buffer (1L of buffer contains 30g Tris-base, 144g glycine and 1g SDS). Transfers were performed at 100 volts for 1 hour at RT, using an ice-cold block to control temperature rise. PVDF membranes were then washed in 1X TBS 3 times for 5 minutes. PVDF membranes were then visualized in the Gel Doc EZ Imaging System (Bio-Rad, 170-8270) using the gel setting for TCE in order to quantify the total protein per lane of the membrane. PVDF membranes were then blocked using 30% soy milk in 1X TBST (TBS with 0.01% Tween 20), for 20 minutes. Blocking solution was then poured off and membranes were incubated overnight at 4 degrees Celsius in the appropriate dilution of primary antibody in 30% soymilk + 1X TBST (total volume of primary incubating solution, 5mL). A list of primary antibodies used in this research can be seen in Table 3.7. The polyclonal E-cadherin antibody was a gratefully received gift from Dr. Warren J. Gallin's lab. This antibody was generated against a fusion protein that encompassed the majority of E-cadherin's extracellular domain (273), thus making this antibody ideal for studying the expression of the 80kDa E-cadherin fragment (because the 80kDa fragment is the extracellular domain of E-cadherin).

Table 3.7. List of primary antibodies used.

Name	Host animal	Antigen species	Antigen location	Dilution	Source
E-cadherin	Mouse, monoclonal	Human	C-terminus	1:2000	BD Transduction Lab, #610181
E-cadherin	Rabbit, polyclonal	Chicken	N-terminus	1:1000	Dr. Warren J. Gallin (273)

Secondary antibody incubation and visualization of fluorescence: The following day, the primary antibody was poured off and the membrane was washed in 10mL of TBST three times for five minutes. The membrane was then incubated in DyLight™ 680 conjugated goat anti-mouse IgG antibody (H&L) and/or DyLight™ 800 conjugated goat anti-rabbit IgG antibody (H&L) secondary antibody at a concentration of 1:4000 in TBST, for one hour. Secondary antibody was then poured off and the membrane was washed in 10mL of TBST three times for five minutes. After the last wash, the membrane was imaged for infrared signal using Odyssey CLx imaging system (LI-COR Biosciences). Densitometry analysis was also conducted using this software.

3.13 Immunoprecipitation of 80kDa E-cadherin fragment from hen ascites fluid and hen ovarian tumor

Ascites fluid preparation: Ascites fluid from a hen with ovarian cancer was thawed and filtered using a syringe with a 0.2µL filter to ensure the removal of solid matter and cellular fraction from ascites fluid. 5mL of the ascites fluid was then added to a protein concentrator with a 30kDa filtration cutoff (Pierce, 2162598) and centrifuged at 3750xG for 25 minutes. The filtrate was discarded, and the portion containing molecules greater than 30kDa was retained in Eppendorf tube aliquots.

Magnetic bead wash: 300uL of protein A magnetic beads (Pierce, 88845) was combined with 300µL of 1X TBST (TBST with pH = 6.8) and gently hand-mixed for one minute and repeated once. Protein A beads are being used due to the high affinity between protein A and rabbit IgG. A magnet was then used to pull beads to the side of the tube, so that TBST wash fluid could be aspirated and discarded. All steps involving the removal of fluid (i.e. supernatant) from tubes containing magnetic beads necessarily require the usage of a magnet, otherwise beads would be

lost with the supernatant. This TBST wash step was repeated once. Beads were then washed with 300µL of milli-Q water to remove remnant detergent.

Magnetic bead conjugation with either rabbit E-cadherin IgG or rabbit Control IgG: Two separate conjugations were prepared with magnetic beads; one bead conjugation was with a rabbit polyclonal chicken E-cadherin antibody, and the other bead conjugation was with a rabbit control IgG antibody. For the E-cadherin IgG-conjugated magnetic beads, 24µL of 10µg/µL rabbit polyclonal chicken E-cadherin IgG was added to washed beads and brought to a final volume of 300µL with a bead blocking solution (consisting of 5% BSA plus 0.05% NP40 diluted with 1XPBS). For the Control IgG-conjugated beads, 48µL of 5µg/µL rabbit Control IgG (Invitrogen, 026102) was added to washed beads and brought to a final volume of 300µL with bead blocking solution (also consisting of 5% BSA plus 0.05% NP40 diluted with 1XPBS). Beads were then incubated overnight on a roller at 4 degrees Celsius. After completing overnight incubation, the supernatant containing the blocking buffer and unbound antibody was discarded. The beads were then washed (gently mixed) 5 times with 300µL of milli-Q water to remove residual antibody and blocking solution. The final wash was discarded, and the immunoprecipitation step was started immediately.

Immunoprecipitation: 300µL of concentrated chicken ascites fluid was thawed and added to magnetic beads already conjugated with the chicken E-cadherin IgG (this is Tube A). Another 300µL of concentrated chicken ascites fluid was thawed and added to beads already conjugated with the Control IgG (this is Tube B). Also, as a positive control, 50µL of hen ovarian tumor homogenate was thawed and added to magnetic beads already conjugated with E-cadherin IgG (this is Tube C). Each of these tubes was incubated at RT on a roller for one hour. After incubation, the ascites fluids were aspirated from tubes A and B and frozen at -80 degrees

Celsius. The ovarian tumor homogenate in tube C was discarded. The beads from tubes A, B and C were retained. The ascites fluid from tubes A and B represent the experimental treatment (i.e. E-cadherin depleted fluid) and control treatment (i.e. E-cadherin retained fluid), respectively. The ascites fluids from tube A and B are intended for use in TMRE experiments and Seahorse experiments that will be described later in the methods.

The beads that were collected from tubes A, B and C, were boiled in 100uL of 2X Laemmli sample buffer for five minutes at 100 degrees Celsius. The eluates (i.e. what separates from the beads during boiling) from beads A, B and C, were collected, aliquoted and frozen at -80 degrees Celsius. The eluates from beads A, B and C, will be used in western blotting to validate the efficiency of the E-cadherin depletion. The eluates from beads A and C will be used in proteomics to conduct peptide mass fingerprinting of the 80kDa molecular weight (to try to validate that we are investigating the 80kDa fragment of chicken E-cadherin). The results of the immunoprecipitation can be seen in Figure 3.2. In that figure, the last two 80kDa bands on the right (i.e. E-cadherin IgG ascites eluate & ovarian tumor homogenate eluate) are representations of the two 80kDa bands that were submitted for MALDI-MS peptide mass analysis.

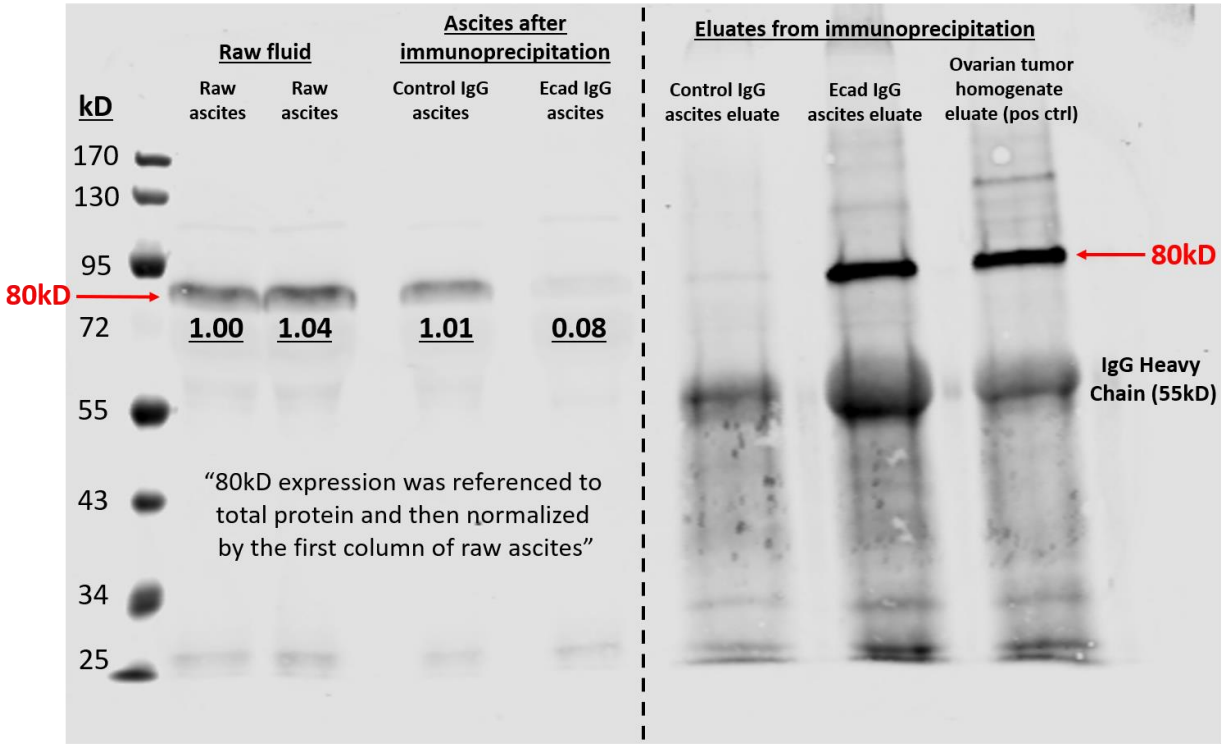

Figure 3.2. Western blot verification of immunoprecipitation results. After completing the immunoprecipitation of hen ascites fluid with the E-cadherin IgG and the Control IgG, the aspirated ascites fluids (left side of blot) and the associated bead eluates (right side of blot) were electrophoresed in a 9.7% gel. The rabbit polyclonal chicken E-cadherin primary antibody was used with a rabbit 800nm secondary streptavidin fluorophore (the blot is the visualization of the blot at 800nm). The gel was preloaded with TCE so that protein expressions could be normalized to the total protein content. This is important, because the "Control IgG ascites" sample was underloaded.

3.14 Proteomics analysis for 80kDa E-cadherin fragment

SDS-PAGE gel separation, Coomassie staining, western blotting and cutting of the band of interest: The goal here was to visualize the eluates from beads A and beads C, in order to identify the 80kDa band of interest (via Coomassie stain) and cut it out for proteomics analysis.

In brief, two gels were run in tandem; one gel was intended for western blot analysis to visualize the 80kDa E-cadherin band of interest, while the other gel was intended for Coomassie staining and protein band excision. The rationale for these two gels is that the 80kDa band needed to be visualized via western blot before performing the cutting of the band from the Coomassie stained gel. This tandem gel approach adds more reliability in the cut from the Coomassie gel.

The eluate from beads A should contain the ascites proteins that were bound to chicken E-cadherin IgG. Similarly, the eluate from beads C should contain the ovarian tumor proteins that were bound to chicken E-cadherin IgG. Said concisely, the 80kDa E-cadherin protein should be present in both eluates. For the SDS-PAGE gel separation, we utilized our western blot protocol for a 9.7% gel. 40μL of eluate from beads A and beads C were loaded into separate lanes on two different gels and electrophoresed at 120 volts until the bromophenol blue reached the foot of the gel. The gel intended for Coomassie staining was then transferred to 20mL of fixing solution that contained 25% isopropanol, 10% acetic acid and 65% milli-Q water, and incubated in this solution on a rocker at RT for 60 minutes. The fixing solution was then poured off and replaced with 20mL of Coomassie stain solution containing 10% acetic acid and 60mg/L of Coomassie Blue R-250 stain (Sigma, R-250). This is a more conservative Coomassie staining approach that allows more sensitive detection of proteins while limiting overstaining. The gel was incubated in this stain solution for two hours. The stain solution was then poured off and replaced with 20mL of destaining solution consisting of 10% acetic acid and 90% milli-Q water. The gel was destained on a rocker at RT for six hours. The destaining solution was then poured off, and the gel was stored in 7% acetic acid at 4 degrees Celsius, until the western blot protocol was complete on the second gel. That said, the second gel was processed through the western blot protocol (using rabbit polyclonal chicken E-cadherin IgG as the primary antibody, conjugated

with rabbit 800nm secondary fluorophore) to visualize the location of the 80kDa band in the eluates from beads A and beads C. The images from that western blot were used to target the location in the Coomassie-stained gel where the 80kDa band of interest was cut out with a sterile razor blade. The excised Coomassie-stained bands were stored in 1.5mL Eppendorf tubes and covered in 300µL of milli-Q water and frozen at -80 degrees Celsius, until transferred for proteomics analysis.

Proteomics analysis of 80kDa bands of interest: The frozen bands of interest from beads A and beads C were transferred to the SIUC mass-spectrometry facility (operated by Dr. Mary Kinsel), so that peptide mass fingerprinting analysis could be performed. The bands were digested overnight with trypsin. 7µL of 1% formic acid was added to each sample to stop the action of trypsin. The supernatant containing tryptic peptides was spun down, transferred to a 0.5mL Eppendorf tube and placed on ice until analysis. 1µL of supernatant was spotted with 1µL of matrix (5mg α-cyano-4-hydroxycinnamic acid in 50:50 acetonitrile: 0.1% trifluoroacetic acid) and allowed to dry at room temperature. The mass spectra of the tryptic peptides were acquired in the positive ion mode using a Bruker Daltonics MicroflexLR Time-of-Flight mass spectrometer. The tryptic peptide ion signals were searched against the SwissProt (updated 2017_11) database using Protein Prospector MS-FIT (University of California San Francisco). The search parameters allowed two trypsin missed cleavages and included oxidation of methionine (+16Da) and carbamidomethylation on cysteine (+57Da) as variable modifications. The taxonomy was limited to *Gallus gallus*. The Pfactor (partial factor) of 0.3 was used to change weighting for missed cleavages. One unique protein was represented in the search results. Note, MOWSE protein scores greater than 63 ($p < 0.05$).

3.15 Cell lines and cell culture conditions

The BG1 cell line was obtained from Dr. Ken Korach's lab at National Institute of Environmental Health Sciences (NIEHS) (276,277). BG1 cells were originally isolated from a woman with ovarian adenocarcinoma, and they are an E-cadherin positive ovarian cancer cell line. The Immortalized Ovarian Surface Epithelial 80 (IOSE80) cell line was obtained from Dr. Joanna Burdette's lab at the University of Illinois at Chicago (278,279). IOSE80 cells were isolated from a non-cancerous human ovary and immortalized via SV-40; they do not express E-cadherin. HyClone DMEM cell culture medium, containing phenol red, 4mM glutamine, 25mM glucose and 1mM pyruvate, was utilized during the culturing of all cell lines (ThermoFisher, SH30604.02). BG1 cells were cultured in HyClone DMEM plus 10% fetal bovine serum and 0.5% 1:1 penicillin:streptomycin. IOSE80 cells were cultured in Hyclone DMEM plus 10% fetal bovine serum, 0.5% 1:1 penicillin:streptomycin, and 11ng/100mL recombinant Epidermal Growth Factor (e.g.F) protein (Sigma, E5160). The rationale for using EGF was based on guidance from Dr. Joanna Burdette's lab, from whom we received the IOSE80 cell line. Cells were cultured in 100mm dishes with a seeding density of $3x10^6$ cells per well, and CO_2 was fixed at 5% and the temperature was fixed at 37 degrees Celsius. The passaging of cells was conducted using 0.25% trypsin-EDTA (Corning, MT25053CI). Extra cells were frozen down in cryotubes using 10% DMSO.

3.16 DHA treatment experiments using BG1 ovarian cancer cells

BG1 cells were seeded at a density of $3X10^5$ cells per well, in six-well (35mm well) plates and cultured using the aforementioned culture medium for BG1 cells. After 24 hours of seeding, the medium was aspirated and replaced with medium containing DMEM supplemented with 10% fetal bovine serum and a DHA concentration of either 0µM, 25µM or 50µM DHA. DHA

was initially solubilized to 100mM with dimethyl sulfoxide (DMSO). Each of these DHA concentrations was applied in duplicate in the six-well plate. Cells were incubated for 24 hours in their respective treatments and cells were harvested for RNA isolation. The experiment was repeated four times on separate days (*n*=4).

3.17 Mitochondrial membrane potential in IOSE80 cells treated with ascites fluid

Description of TMRE protocol for estimating mitochondrial membrane potential: A researcher first treats cells with TMRE and quantifies red wavelength (550nm excite / 590nm emit) to get an absolute measure of charge (call this "TMRE_1"). The researcher next depolarizes the mitochondria by treating the cells with a proton ionophore such as carbonyl cyanide 3-chlorophenylhydrazone (CCCP). CCCP forces the retrograde transport of protons (i.e. H^+) from the IMS to the matrix (280). This retrograde flow of protons forces the efflux of TMRE from the matrix (i.e. TMRE ejection to the cytosol). The assumption is that TMRE efluxing from the matrix will be removed from the cell culture when the cells are washed and aspirated again. After washing and aspirating, the researcher measures the red wavelength (550nm excite / 590nm emit) again to obtain a surrogate estimate of the depolarized charge (call this "TMRE_2"). The actual estimate of membrane potential, or $\Delta\Psi$, is the mathematical difference between TMRE_1 and TMRE_2 (212). This value is the $\Delta\Psi$. In almost all cases, TMRE_1 will be larger than TMRE_2, which will generate a positive value for $\Delta\Psi$. If $\Delta\Psi$ is considerably negative, this could be an example of hyperpolarization; however, hyperpolarization is generally elicited by inhibitors such as oligomycin.

Initial cell seeding: IOSE80 cells were seeded in 96-well plates at a density of 10,000 cells per well, using 50µL of the aforementioned culture medium for IOSE80 cells, and incubated overnight at 37 degrees Celsius with 5% CO_2.

Serum and EGF starvation: After overnight incubation, the culture medium was aspirated, and the cells were washed twice with 50µL of 100% DMEM. Wells were then filled with 50µL of 100% DMEM (i.e. serum-starved and EGF-starved) and incubated at 37 degrees Celsius for 24 hours. The rationale for removing serum and EGF from the culture medium is that we were trying to test the effects of the 80kDa E-cadherin (i.e. soluble E-cadherin) on the mitochondrial bioenergetics of the IOSE80 cells. Previous research illustrated that soluble E-cadherin has putative binding of receptor tyrosine kinases (RTKs) such as IGFR and EGFR (269); therefore, we wanted to remove serum growth factors and EGF for 24 hours prior to testing the effects of soluble E-cadherin treatment.

Ascites fluid treatment: After 24 hours of serum and EGF starvation, the culture medium was aspirated and replaced with DMEM containing, either: 1) *E-cadherin-depleted ascites* [ie ascites immunoprecipitated with rabbit polyclonal chicken E-cadherin IgG], or 2) *E-cadherin-non-depleted ascites* [ie ascites immunoprecipitated with rabbit isotype control IgG]. The ascites treatments consisted of 30µL of the following: 0% ascites (100% DMEM), 1:159 ascites (99.375% DMEM), 1:79 ascites (98.75% DMEM) and 1:39 ascites (97.5% DMEM). Each of the ascites fluid treatments (e.g. 1:159, 1:79, 1:39) was tested in four replicates per plate. Ascites treatments were allowed to incubate for 24 hours at 37 degrees Celsius and 5% CO_2.

Mitochondrial membrane potential measurement: After 24 hours of incubation, the ascites treatments were aspirated, and the cells were treated with 50µL of 30nm TMRE in DMEM and incubated for 5 minutes at RT and atmospheric CO_2. Protect the 96-well plate from light during this incubation (i.e. perform your work with the hood light off if possible). After the 5-minute incubation, aspirate the medium and wash the cells twice with 100µL of 1X PBS. After the final wash, fill each well with 100µL of 1X PBS and measure fluorescence using a 96-well plate

reader (550nm excite / 590nm emit). After measuring fluorescence, aspirate the 1X PBS and fill all treatment wells with 50µL of 2.5µM CCCP (Tocris, 04-525-00) in DMEM. CCCP was suspended in DMSO. Once the CCCP treatments are added, incubate the cells for 20 minutes at 37 degrees Celsius and 5% CO_2. After this incubation, aspirate the medium and wash twice with 1X PBS, and measure the fluorescence in a 96-well plate reader (550nm excite / 590nm emit). Next, aspirate the medium and very gently lyse the cells with 10µL of 0.1% SDS. Conduct a protein assay on the cells to determine the protein concentration (µg/µL) of each sample. Also included in the plate were cells receiving CCCP only (in 100% DMEM) and TMRE only (also in 100% DMEM), in order to subtract the effect of reagent treatment on background fluorescence.

Experimental sample size: Each of these experiments was conducted 4 times on 4 separate days.

CCCP dose finding experiment: Before conducting the above TMRE experiment, we conducted dose response experiments to identify the optimal CCCP concentration to depolarize the mitochondria. We used the same cell culture conditions (i.e. serum starvation and EGF starvation) and applied a gradient of 0µM, 0.5µM, 1µM, 2.5µM, 5µM, 10µM and 20µM CCCP to identify the optimal dose at which the mitochondrial display maximum depolarization. This was decided as being 2.5µM CCCP.

3.18 Oxygen consumption in IOSE80 cells treated with ascites fluid

Seahorse miniplate cell seeding: IOSE80 cells were seeded in Seahorse XFp (8-well) miniplates at 6,000 cells per well and cultured overnight at 37 degrees Celsius and 5% CO_2, using 50uL of culture medium for IOSE80 cells. Two miniplates were seeded simultaneously. In both miniplates, well 1 and well 8 were not seeded with any cells (they were used as treatment background wells). Only wells 2 through 6 were seeded with cells (i.e. 6,000 cells per well).

Miniplates were then shaken in a 2-dimensional, horizontal cell shaker for one minute to ensure even cell distribution in each well.

Serum and EGF starvation: The following day, the culture medium was aspirated, and the cells were washed twice with 50µL of 100% DMEM. Wells were then filled to a final volume of 50µL with 100% DMEM, and the cells were incubated for 24 hours at 37 degrees Celsius and 5% CO_2. These steps were performed for both miniplates.

Determining extracellular flux in response to an ascites dose gradient: 24 hours after serum starvation, the medium was aspirated from each well. The following treatment protocol was used to determine the dose response effect of ascites on extracellular flux. Wel1s 1 and 8 were used to measure extracellular background flux. Well 2 was filled with 100% DMEM (i.e. vehicle). Wells 3, 4, 5, 6, and 7, received 1:159, 1:79, 1:39, 1:19 and 1:9 ascites fluid, respectively.

Determining extracellular flux in response to a specific ascites fluid concentration: 24 hours after serum starvation, the medium was aspirated from each well. The following treatment protocol was used to determine the effect of a single ascites concentration on extracellular flux. Wel1s 1 and 8 were used to measure extracellular background flux. Wells 2 and 3 were filled with 30µL of 100% DMEM (i.e. vehicle). Wells 4 and 5 were filled with 30µL of a predefined concentration (i.e. 1:159) of E-cad-depleted ascites; while wells 6 and 7 were filled with a predefined concentration (i.e. 1:159) of Ctrl IgG-treated ascites.

Seahorse assay: After 24-hours of incubating miniplates, the medium was aspirated from all wells, and each well was washed twice in 200µL of Seahorse assay medium (pH of 7.4 +/- 0.1pH; containing 4mM glutamine, 1mM pyruvate and 25mM glucose). Each well was then filled with 80µL of Seahorse assay medium, and the miniplate was allowed to incubate at 37 degrees Celsius at atmospheric CO_2 for one hour. This was performed for both miniplates.

Seahorse assay cartridges were prepared to provide a final well concentration of 1µM Oligomycin, 0.5µM CCCP and 0.5uM Rotenone/Antimycin A. Oligomycin (Fisher, AAJ61898MA), CCCP (Tocris, 04-525-00), Rotenone (Sigma, R-8875) and Antimycin A (A-8674) were suspended in DMSO. The Seahorse XFp instrument was utilized to measure basal oxygen consumption in triplicate time measurements; oligomycin-treated oxygen consumption in triplicate time measurements; CCCP-treated oxygen consumption in triplicate time measurements; and Rotenone/Antimycin A-treated oxygen consumption in triplicate time measurements. After the Seahorse assay was complete, all wells were aspirated, and cells were lysed in 10µL of 0.1% SDS. Culture miniplates were wrapped in parafilm and allowed to freeze overnight at -20 degrees Celsius prior to conducting BCA protein assay. These steps were performed for both miniplates.

Experimental sample size: All of the above experimental steps were performed for three different cell passages (i.e. $n = 3$ experiments). For example, in the first experiment, two miniplates were used with passage one ($n = 4$ replicates per treatment). In the second experiment, two miniplates were used with passage two ($n = 4$ replicates per treatment). In the third experiment, two miniplates were used with passage three ($n = 4$ replicates per treatment). For statistical purposes, each treatment received $n = 12$ replicates.

Data analysis: Seahorse Wave Desktop Software was used to calculate protein normalized oxygen consumption for each well.

3.19 Statistical analysis

Statistical analysis was performed with R Statistical Software (version 4.0.3). Significant differences between diet groups were determined via One-way ANOVA and Duncan's Multiple Range post-test (significant at $p<0.05$). When Bartlett's statistic was significant at $p<0.05$, the

data were $\log_{10}$ transformed prior to conducting ANOVA. Non-parametric Kruskal-Wallis ANOVA with Dunn's post-hoc test were used in a few instances during this study ($p<0.05$). Odds ratio analysis was used to calculate the risk of stage 4 ovarian cancer. Regarding metabolomics analysis, all VIP data are shown in graphs as normalizations to the CTL diet (i.e. the CTL is always set to 1.00, while the other diets are shown as fold changes to CTL). In some metabolites, significant outliers were removed using a z-score method of detecting significant outliers ($p<0.05$). Dendrogram clustering analysis was conducted via R package 'dendextend', using the default k-means algorithm. Kaplan-Meier survival analysis and Cox proportional hazard (Coxph) analysis were conducted via R packages 'survival' and 'survminer' (significant at $p<0.05$). Student's T-test using Welch's correction was used to compare cancerous body weights versus non-cancerous body weights; this test was also used to conduct two group comparisons of miR-200a expression (two-tailed, $p<0.05$).

3.20 Power analysis

Based on preliminary observations, analysis of hen ovarian tumor homogenates requires a sample size of 7 to achieve a statistical power of 0.8 during one-way ANOVA analysis (6 group comparison, effect size=0.62, $\alpha=0.05$).

CHAPTER 4

RESULTS

4.1 STUDY 1: FLAXSEED'S PARADOXICAL ROLE IN EXTENDING LIFESPAN AND REPRODUCTIVE CAPACITY IN WHITE LEGHORN LAYING HENS

4.1.1 Metabolomics: heatmap and partial least squares discriminant analysis (PLSDA)

A targeted LC-MS/MS metabolomics approach was used to evaluate the dietary regulation of one-carbon metabolism within specific pathways. Tandem mass spectrometry analysis indicated 108 significantly detected metabolites. A heat map depicting the standardized metabolite VIP scores can be seen according to dendrogram clustering in Figure 4.1.1. The heat map is organized according to two distinct dimensions. Dendrogram A organizes individual metabolites according to the correlations of their standardized VIP scores across diets, whereas dendrogram B organizes individual diet samples according to the correlation of their standardized VIP scores across metabolites (Figure 4.1.1). Two major families of metabolites emerged in dendrogram A, and two major families of diets emerged in dendrogram B. A partial least squares discriminant analysis (PLSDA) of standardized VIP scores was conducted to visualize clustering of individual diet samples on a two-dimensional quadrant (Q) surface (Figure Appendix S1).

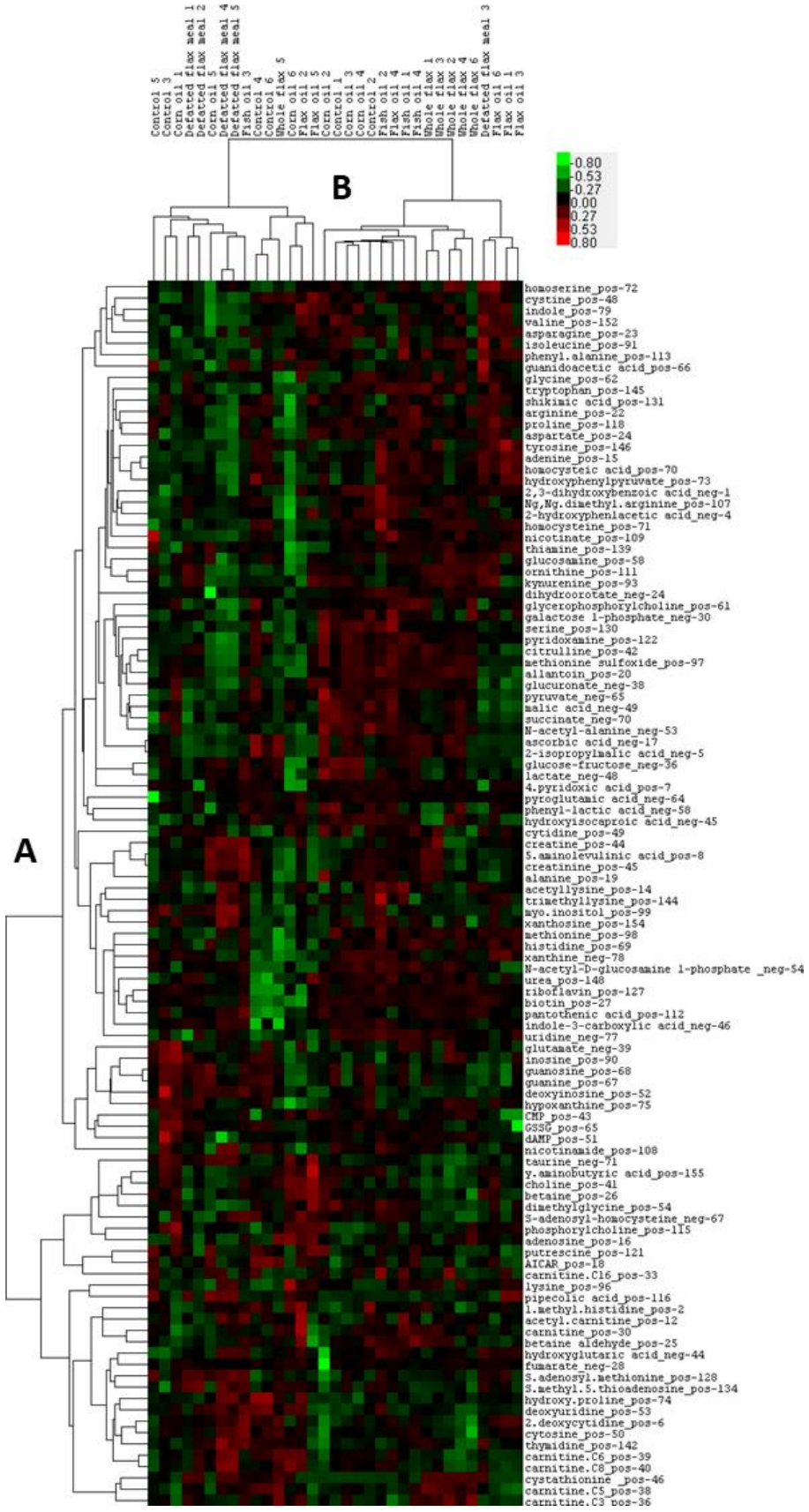
Control 5
Control 3
Corn oil 1
Defatted flax meal 1
Defatted flax meal 2
Corn oil 5
Defatted flax meal 4
Defatted flax meal 5
Fish oil 3
Control 4
Control 6
Whole flax 5
Corn oil 6
Flax oil 2
Flax oil 5
Corn oil 2
Control 1
Corn oil 3
Corn oil 4
Control 2
Fish oil 2
Flax oil 4
Fish oil 4
Flax oil 1
Whole flax 1
Whole flax 3
Whole flax 2
Whole flax 4
Whole flax 6
Defatted flax meal 3
Flax oil 6
Flax oil 1
Flax oil 3
B
-0.80
-0.53
-0.27
0.00
0.27
0.53
0.80
A
homoserine_pos-72
cystine_pos-48
indole_pos-79
valine_pos-152
asparagine_pos-23
isoleucine_pos-91
phenyl.alanine_pos-113
guanidoacetic acid_pos-66
glycine_pos-62
tryptophan_pos-145
shikimic acid_pos-131
arginine_pos-22
proline_pos-118
aspartate_pos-24
tyrosine_pos-146
adenine_pos-15
homocysteic acid_pos-70
hydroxyphenylpyruvate_pos-73
2,3-dihydroxybenzoic acid_neg-1
Ng,Ng.dimethyl.arginine_pos-107
2-hydroxyphenlacetic acid_neg-4
homocysteine_pos-71
nicotinate_pos-109
thiamine_pos-139
glucosamine_pos-58
ornithine_pos-111
kynurenine_pos-93
dihydroorotate_neg-24
glycerophosphorylcholine_pos-61
galactose 1-phosphate_neg-30
serine_pos-130
pyridoxamine_pos-122
citrulline_pos-42
methionine sulfoxide_pos-97
allantoin_pos-20
glucuronate_neg-38
pyruvate_neg-65
malic acid_neg-49
succinate_neg-70
N-acetyl-alanine_neg-53
ascorbic acid_neg-17
2-isopropylmalic acid_neg-5
glucose-fructose_neg-36
lactate_neg-48
4.pyridoxic acid_pos-7
pyroglutamic acid_neg-64
phenyl-lactic acid_neg-58
hydroxyisocaproic acid_neg-45
cytidine_pos-49
creatine_pos-44
5.aminolevulinic acid_pos-8
creatinine_pos-45
alanine_pos-19
acetyllysine_pos-14
trimethyllysine_pos-144
myo.inositol_pos-99
xanthosine_pos-154
methionine_pos-98
histidine_pos-69
xanthine_neg-78
N-acetyl-D-glucosamine 1-phosphate _neg-54
urea_pos-148
riboflavin_pos-127
biotin_pos-27
pantothenic acid_pos-112
indole-3-carboxylic acid_neg-46
uridine_neg-77
glutamate_neg-39
inosine_pos-90
guanosine_pos-68
guanine_pos-67
deoxyinosine_pos-52
hypoxanthine_pos-75
CMP_pos-43
GSSG_pos-65
dAMP_pos-51
nicotinamide_pos-108
taurine_neg-71
y.aminobutyric acid_pos-155
choline_pos-41
betaine_pos-26
dimethylglycine_pos-54
S-adenosyl-homocysteine_neg-67
phosphorylcholine_pos-115
adenosine_pos-16
putrescine_pos-121
AICAR_pos-18
carnitine.C16_pos-33
lysine_pos-96
pipecolic acid_pos-116
1.methyl.histidine_pos-2
acetyl.carnitine_pos-12
carnitine_pos-30
betaine aldehyde_pos-25
hydroxyglutaric acid_neg-44
fumarate_neg-28
S.adenosyl.methionine_pos-128
S.methyl.5.thioadenosine_pos-134
hydroxy.proline_pos-74
deoxyuridine_pos-53
2.deoxycytidine_pos-6
cytosine_pos-50
thymidine_pos-142
carnitine.C6_pos-39
carnitine.C8_pos-40
cystathionine _pos-46
carnitine.C5_pos-38
carnitine.C3_pos-36

Figure 4.1.1. Heatmap illustrating grouped hierarchies of metabolites and diet group observations. Metabolites (n=108) from hen plasma were analyzed via LC-MS/MS and organized based on the clustering of their VIP scores across diet. Metabolites are organized according to similarity with other metabolites across the diet samples (**A**). The diet samples are organized according to similarity with other diet samples across the metabolites (**B**). Green illustrates below average expression and red illustrates above average.

4.1.2 Vitamin B6 antagonism concomitant with transsulfuration inhibition: the trigger

Vitamin B6 metabolism in the blood plasma was perturbed by the two diets containing the linatine molecule, DF and WF. The biggest effect appeared in 4-pyridoxic acid (4PA) which was significantly reduced by DF and almost ($p<0.07$) reduced by WF (Figure 4.1.2). Pyridoxamine, an inactive vitamin-B6 vitamer, was decreased by DF in contrast to FSH (Figure 4.1.2). We estimated glomerular filtration rate (GFR) by evaluating urea and creatinine metabolism and observed no effect across diets (Figure Appendix S2). TS activity was extensively perturbed in DF and WF hens, according to a 15.4-fold and 16.6-fold increase in cystathionine, respectively, in contrast to CTL hens (Figure 4.1.3). On average, the DF and WF hens exhibited approximately 190-fold, 200-fold and 20-fold elevated cystathionine versus FXO, CRN and FSH hens, respectively. In other words, cystathionine was elevated in DF and WF hens on an order(s) of magnitude scale depending on the reference group used. Cystine (a di-cysteine molecule used for transmembrane passage of cysteine) was not affected by diet (Figure 4.1.3). Among other thiol amino acids that are produced downstream of TS, taurine was significantly decreased by the WF diet (Figure 4.1.3). This might be expected given a TS perturbation due to flaxseed. Neither reduced glutathione (GSSG) nor homocysteic acid were affected by diet (Figure 4.1.3).

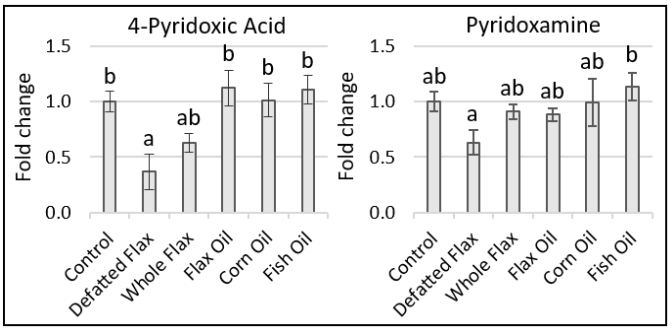

Figure 4.1.2. Plasma markers of vitamin B6 metabolism. Hen blood plasma samples measured via LC-MS/MS. VIP scores of metabolites were analyzed via one-way ANOVA (Duncan's post-test, $p<0.05$). Groups without a similar letter are significantly different. *n*=4 to 6 plasma samples from different hens per diet group. Error bars are +/- SEM.

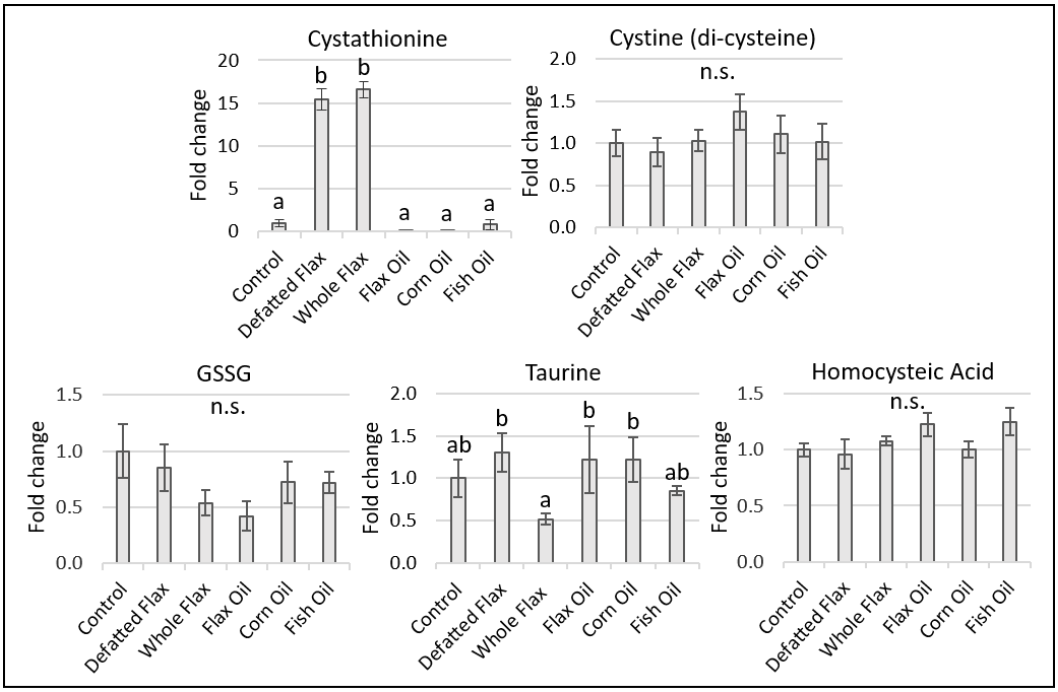

Figure 4.1.3. Plasma estimate of transsulfuration and subsequently produced sulfur metabolites. Hen blood plasma samples measured via LC-MS/MS. VIP scores of metabolites were analyzed via one-way ANOVA (Duncan's post-test, $p<0.05$). Groups without a similar letter are significantly different. *n*=4 to 6 plasma samples from different hens per diet group. Error bars are +/- SEM.

4.1.3 The new fate of Hcy: increased flux of Hcy into the Met cycle, causing increased SAM synthesis

Interestingly, neither DF nor WF displayed hyperHcy despite 15-fold elevated cystathionine, because Hcy was stable across all diets (Figure 4.1.4A). Met was slightly increased in FSH hens versus CTL and CRN hens (Figure 4.1.4A). After observing that neither Hcy nor Met were affected by DF or WF, an exceptionally large 1.9-fold increase of SAM appeared in DF hens. Similarly, the SAM:SAH ratio (a proxy for the methylation capacity of the cell) was increased in DF versus all diets except WF (Figure 4.1.4B). It is meaningful to observe that the SAM:SAH ratio was statistically similar between DF and WF. Methyl 5-thioadenosine (MTA), a pan-methyltransferase inhibitor (281) that is produced after decarboxylated SAM (*dc*SAM) participates in polyamine synthesis, was also significantly higher in DF hens (Figure 4.1.4D). SAH, the byproduct of SAM-driven methyltransferase reactions, was slightly decreased in WF hens when compared to FXO and FSH (Figure 4.1.4A). The activities of methionine cycle enzymes were also estimated by using ratios of relevant metabolites. The ratio of Hcy:SAH (a proxy for SAHH activity) was increased in WF above all other diets (Figure 4.1.4B). Parallel with this observation, the ratio of adenosine:SAH (another proxy for SAHH activity) was elevated in WF hens (Figure 4.1.4C). This is a consistent indication that the rate of SAH hydrolysis via SAHH might be exceptionally increased in WF hens. No effect on the ratio of Met to Hcy (a proxy for BHMT and/or MS-B12 activity) was observed; however, the ratio of SAM to Met (a proxy for MAT activity) was elevated in DF (Figure 4.1.4B). This suggests that as soon as Hcy was remethylated to Met, the Met was rapidly adenosylated to SAM.

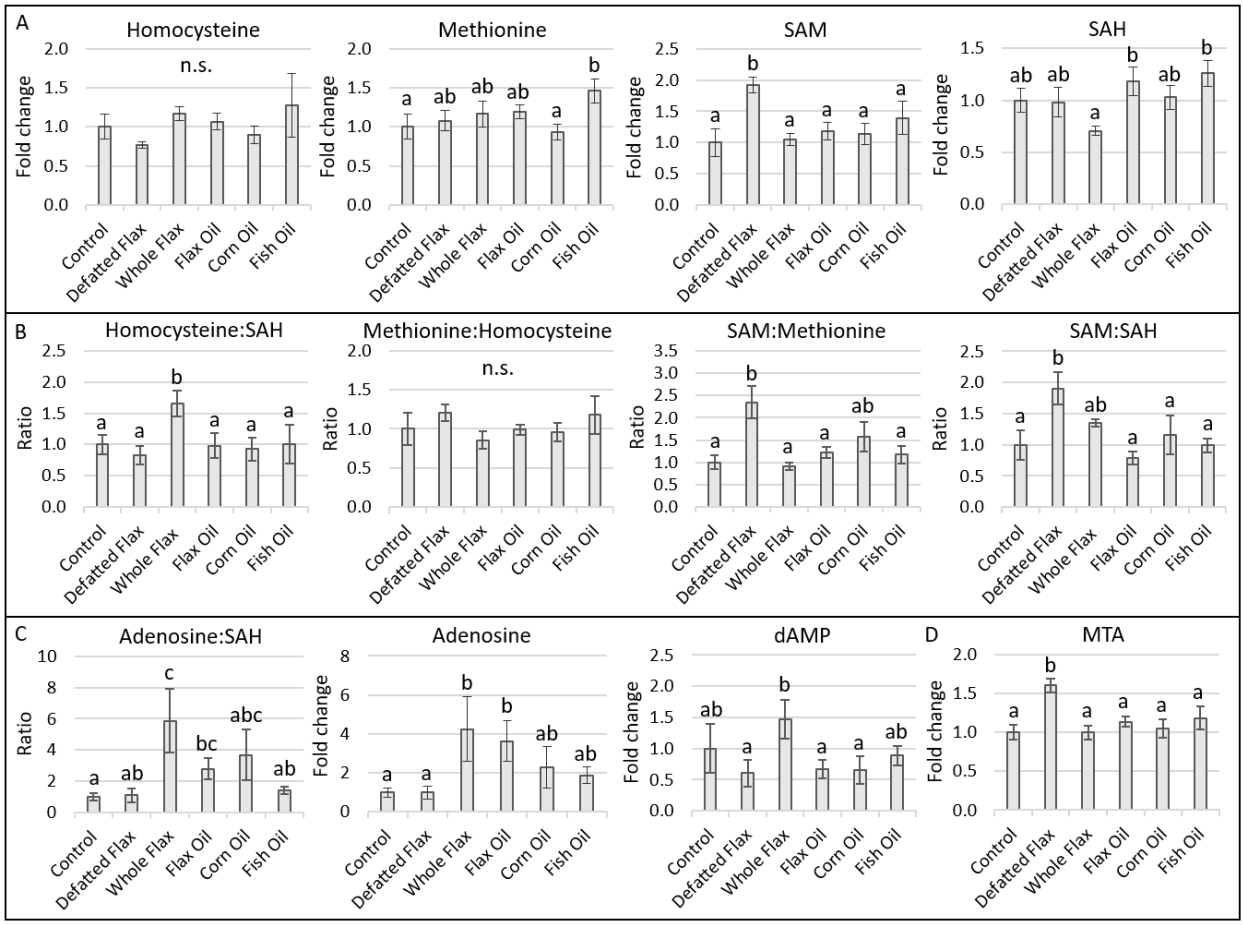

Figure 4.1.4. Plasma estimate of methionine cycle metabolites and subsequently associated metabolites. Hen blood plasma samples measured via LC-MS/MS. VIP scores of metabolites were analyzed via one-way ANOVA (Duncan's post-test, $p<0.05$). Groups without a similar letter are significantly different. *n*=4 to 6 plasma samples from different hens per diet group. Error bars are +/- SEM. The four methionine cycle metabolites (**A**) as well as their ratios (**B**) are depicted. Possible indication of SAHH activity (**C**) as well as MTA (**D**) is shown.

4.1.4 Vast downregulation of microarray features in ovaries of 10% whole flax-fed hens

After seeing an increased SAM:SAH ratio in the blood plasma of flaxseed-fed hens, we hypothesized that flaxseed might influence mRNA levels at the global scale within the ovary of the hen. To challenge this, we reanalyzed a microarray feature dataset that was previously used

to measure microarray feature expression within the ovaries of 10% WF-fed hens versus control diet hens (14). This microarray dataset was designed to make two mean comparisons (i.e. T-test comparisons), to determine if a given microarray feature was significantly upregulated or significantly downregulated in 10% WF hens versus control-fed hens. The T-test results were filtered at different p-value cutoffs ($p<0.10$, $p<0.05$ and $p<0.01$), and the percentage of features, total features and average fold per feature, are shown in Table 4.1.1. We observed that, at these given p-value cutoffs, approximately 60-80% of features were downregulated in 10% WF hens versus control-fed hens, and the average downregulation ranged from about -1.6 to -2.0-fold change. This strong pattern of microarray feature downregulation persisted in both normal and cancerous hen ovaries, with a slightly more pronounced effect in normal ovaries (Table 4.1.1).

Table 4.1.1. Feature expression in laying hen ovaries (10% WF versus CTL diet).

Ovarian tissue type*	p-value cutoff of T-test	Total features (n)		Percentage		Avg fold change per feature	
		Downregulated	Upregulated	Downregulated	Upregulated	Downregulated	Upregulated
Normal	p < 0.10	3601	1587	69.4%	30.6%	-1.66	+1.66
	p < 0.05	1720	532	76.4%	23.6%	-1.79	+1.78
	p < 0.01	129	29	81.6%	18.4%	-2.06	+2.04
Cancerous	p < 0.10	1744	1256	58.1%	41.9%	-1.60	+1.57
	p < 0.05	774	438	63.9%	36.1%	-1.75	+1.70
	p < 0.01	121	38	76.1%	23.9%	-2.01	+1.90

*n=6 hens per group (e.g. 6 normal ovaries from WF-fed hens; 6 normal ovaries from CTL-fed hens; 6 cancerous ovaries from WF-fed hens; and 6 cancerous ovaries from CTL-fed hens).

4.1.5 Methyl group donors required for the BHMT reaction

We suspect that the DF and WF hens leveraged the BHMT and MS-B12 reactions to maintain stable Hcy levels. BHMT and MS-B12 must be leveraged in order to prevent hyperHcy when Hcy is unable to exit the metabolism through TS. To evaluate the hypothesis that BHMT activity was increased we measured the levels of methyl group donors that fuel the BHMT reaction,

specifically choline and betaine. Choline was 39-52% lower in WF compared to all other diets except DF. Meanwhile, choline was reduced by DF in comparison to FXO (Figure 4.1.5). In other words, choline was decreased in both of the linatine-containing diets (i.e. DF and WF) versus FXO. The methyl group donor betaine was reduced by WF in contrast to FXO, while DF had no effect on betaine (Figure 4.1.5). The ratio of Met to betaine (a proxy for BHMT activity) was increased in WF compared to CTL and CRN (Figure 4.1.5).

Choline is a relatively limited nutrient, in its soluble form, because the majority of choline is stored in the form phosphatidylcholine (PC). Knowing that BHMT activity drives choline oxidation we wanted to contrast the body weights of hens with the levels of choline. We perceive that increased choline oxidation might be tightly coupled with PC catabolism, and therefore, increased BHMT activity might strongly correlate with hen body weight (i.e. increased choline oxidation = lower body weight). The post-hoc test results for hen body weight were nearly identical to the post-hoc test results for plasma choline, especially for the body weights of 'ALL hens' (Figure 4.1.6A). Body weight in the WF diet was significantly lower than all other diets, even lower than DF hens. DF hens weighed less than FXO hens when 'ALL hens' was considered. For 'normal hens', DF hens weighed less than CTL, FXO and CRN hens (Figure 4.1.6A). Cancer itself reduced body weight when diets were aggregated; however, diet did not induce an effect on body weight during cancer (Figure 4.1.6A). The mean choline level in each diet showed a high, positive correlation with mean body weight. For 'ALL hens' and 'normal hens' the Pearson correlation between choline and body weight was R=0.94 and R=0.92, respectively (Figure 4.1.6B).

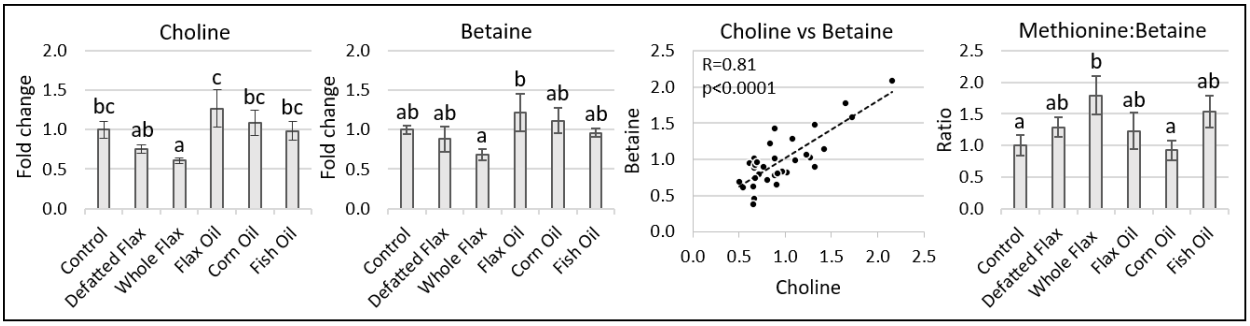

Figure 4.1.5. Methyl group donors in support of BHMT activity. Hen blood plasma samples measured via LC-MS/MS. VIP scores of metabolites were analyzed via one-way ANOVA (Duncan's post-test, $p<0.05$). Groups without a similar letter are significantly different. *n*=4 to 6 plasma samples from different hens per diet group. Error bars are +/- SEM.

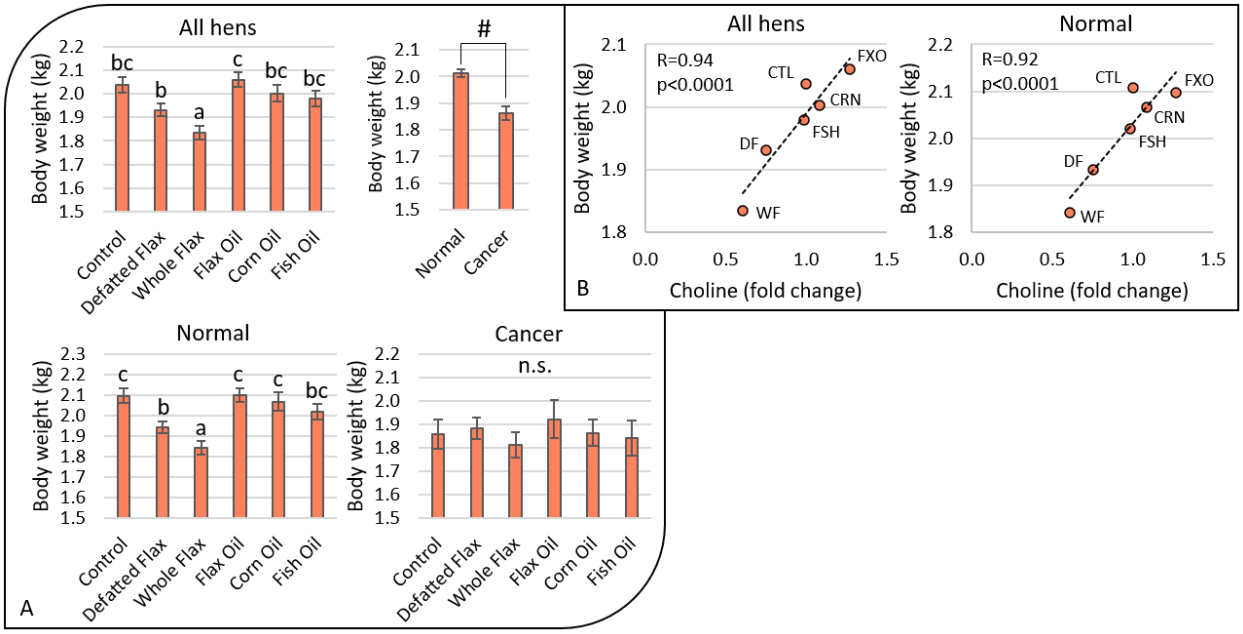

Figure 4.1.6. Hen body weight and the correlation between plasma choline and body weight. Hen body weights were recorded for all surviving hens on the 325th day of the study. Body weight was grouped by cancer status (normal, cancer and all hens) and analyzed via one-way ANOVA (Duncan's post-test, $p<0.05$) Groups without a similar letter are significantly different ($p<0.05$). Body weight was also compared between normal cancer hens, using Welch's T-test (two-tailed, $p<0.05$) (**A**). For body weights of ALL hens, the sample sizes (*n*) were as followes: CTL=123; DF=115; WF= 107; FXO=103; CRN=108; FSH=108. For body weights of Normal hens, the sample sizes (*n*) were as follows: CTL=88; DF=88; WF=72; FXO=84; CRN=62; FSH=73. For body weights of Cancer hens, the sample sizes (*n*) were as follows: CTL=29; DF=20; WF=22; FXO=22; CRN=29; FSH=21. Cancer was determined as any form of peritoneal cancer identified (e.g. ovarian, GI, oviductal, liver, etc). Scatterplots illustrate the linear correlations between average body weight and average choline content across diets (**B**).

4.1.6 Methyl group donors required for MS-B12 activity

Plasma DMG content was reduced 37% and 33% in DF and WF hens, respectively, in contrast to all other diets (Figure 4.1.7). DMG is a methyl group donor that is catabolized in the folate cycle via DMGDH to produce 5,10-CH_2THF. DMG catabolism via DMGDH is essential for preventing the inhibition of BHMT, because DMG accumulation will shut down the BHMT reaction. SAM and MTA are also negative regulators of BHMT. Table 4.1.2 summarizes the estimate of BHMT inhibition according to SAM and DMG content. Through this perspective, WF hens should exhibit much higher BHMT activity while DF hens should experience moderately increased BHMT activity. Serine, a methyl group donor that yields 5,10-CH_2THF in the folate cycle, was lower in DF hens compared to CRN hens (Figure 4.1.7). Perhaps more meaningfully, the ratio of serine to glycine was reduced in DF hens versus CRN hens, without any effect on glycine itself (Figure 4.1.7). The ratio of serine to glycine is relevant for estimating SHMT1 or SHMT2 activity in the folate cycle. Histidine, a methyl group donor that indirectly yields 5,10-CH_2THF, was lower in DF and CTL hens in contrast to FSH hens (Figure 4.1.7). Thymidine, the nucleoside consumed in the dTMP salvage pathway via thymidine kinase (TK), was significantly higher in DF hens in contrast to all diets but FSH (Figure 4.1.7).

We wanted to test how the hens from each diet group clustered according to the carbon donors involved in the BHMT pathway (i.e. choline, betaine and Met:betaine ratio) simultaneously with the carbon donors involved in 5,10-CH_2THF synthesis (i.e. serine, DMG, glycine, histidine and serine:glycine ratio). To evaluate this pattern, we conducted k-means clustering analysis and visualized the results via dendrography (Figure 4.1.8). The different letter groups represent significantly different clusters. Several dietary clusters emerged during this analysis. All FSH samples and five out of six CRN samples grouped into two adjacent clusters

(Figure 4.1.8A and B). DF distinguished itself by grouping within a single cluster (Figure 4.1.8D). Notably, 16 out of 17 samples related to the flaxseed diet (i.e. DF, WF or FXO) were grouped into two adjacent clusters (Figure 4.1.8D and E). The CTL hens expressed high dispersion overall given that two CTL hens were unique enough to form distinct clusters on their own (Figure 4.1.8C and F).

Table 4.1.2. Estimate of BHMT inhibition, via blood plasma level of SAM, MTA and DMG.

BHMT inhibiting molecule	Diet					
	Control	Defatted Flax	Whole Flax	Flax Oil	Corn Oil	Fish Oil
SAM	Moderate	High	Moderate	Moderate	Moderate	Moderate
MTA	Moderate	High	Moderate	Moderate	Moderate	Moderate
DMG	Moderate	Low	Low	Moderate	Moderate	Moderate
Net inhibition	**No change**	***Increased***	***Decreased***	**No change**	**No change**	**No change**

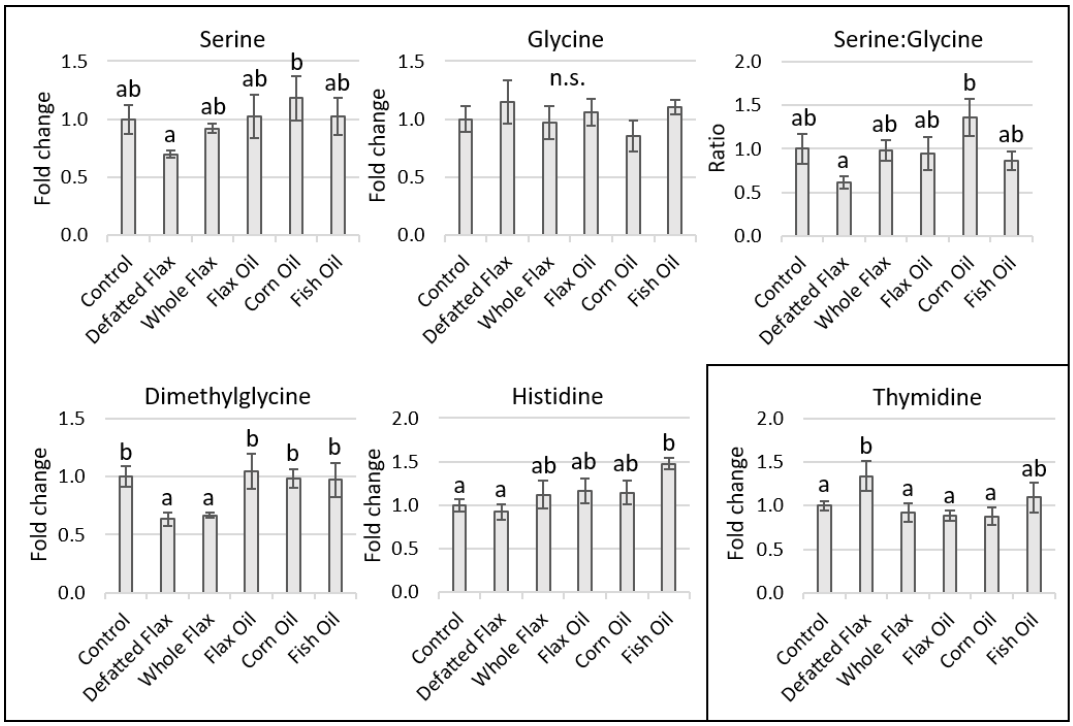

Figure 4.1.7. Folate cycle carbon donors as well as the thymidine content. Hen blood plasma samples measured via LC-MS/MS. VIP scores of metabolites were analyzed via one-way ANOVA (Duncan's post-test, $p<0.05$). Groups without a similar letter are significantly different. *n*=4 to 6 plasma samples from different hens per diet group. Error bars are +/- SEM.

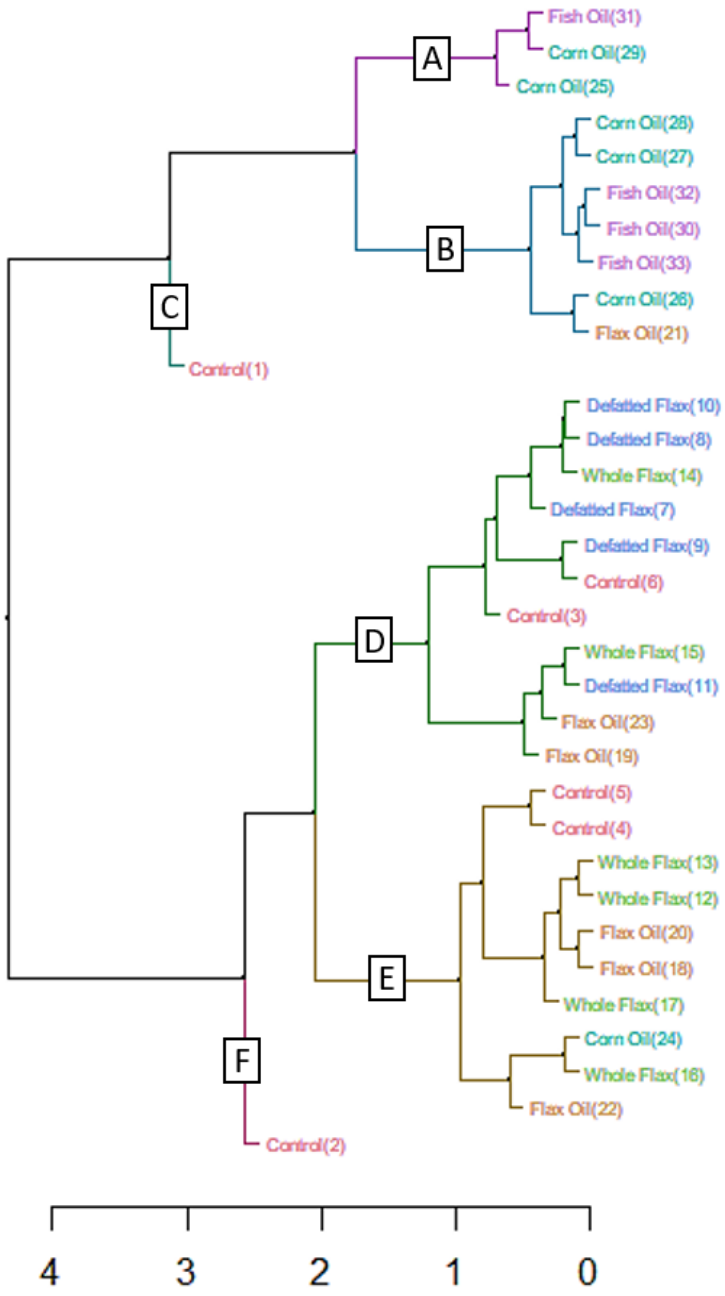

Figure 4.1.8. Dendrogram showing K-means clustering of one-carbon donating molecules. K-means clustering analysis was performed using Dendextend package in R. The VIP scores for choline, betaine, serine, glycine, DMG, histidine, Met:betaine ratio and serine:glycine ratio, were converted to Z-scores prior to conducing the K-means clustering analysis (k=6). Significantly different clusters are represented by different letters (**A-F)**.

4.1.7 Indication of a glucagon-like phenotype in flaxseed-fed hens: plasma pyruvate, plasma C3, C5, C6 and C8-carnitine, and blood serum FFA

WF hens and DF hens exhibited HbA1c values of 6.2% and 5.3%, respectively, versus CTL hens that had 1.9% HbA1c (previously published in (2)). In other words, flaxseed resulted in approximately 3-fold elevated HbA1c! These HbA1c values exceed those of hummingbirds (161), possibly making the HbA1c value of a flaxseed-fed hen the highest HbA1c ever observed in a bird! In chickens, glucagon stimulates glycogenolysis, gluconeogenesis and lipolysis, with the effect of achieving systemic hyperglycemia and hyperlipidemia (166). We provide additional evidence that flaxseed induces a glucagon-like phenotype in hens. Firstly, we observed reduced plasma pyruvate in DF and WF hens (Figure 4.1.9A), possibly acting as a good proxy for gluconeogenesis. WF hens also exhibited elevated C3-carnitine (propionylcarnitine) and C5-carnitine (isovalerylcarnitine), while DF hens displayed elevated C8-carnitine (octinoylcarnitine) (Figure 4.1.9B). C3, C5 and C8-carnitines were previously observed as markers of elevated blood glucose in humans (282). Birds could have a specialized tolerance for hyperglycemia, possibly because most birds biosynthesize ascorbic acid. Ascorbic acid has been shown to reduce the rate of protein glycation in humans (283) which might be one of the reasons why ascorbic acid might protect birds from advanced glycation end products. We detected an interesting pattern where ascorbic acid was highest in WF hens but lowest in DF hens (Figure 4.1.9C). Next, we evaluated blood serum FFA levels in hens from (2). We observed that hens consuming either DF or WF had elevated serum levels of oleic acid (C18:1ω9), linoleic acid (C18:2ω6) and docosahexaenoic acid (C22:6ω3), versus hens consuming either CTL or FXO (Figure 4.1.9D). Serum linolenic acid (C18:3ω3) was similar in hens consuming either DF, WF or FXO (Figure 4.1.9D). Why is it meaningful that DF hens had high levels of serum FFAs? It is meaningful

because the DF diet included flaxseed that underwent cold-press fat extraction. The DF diet has 50% less C18:2ω6 compared to the WF or FXO diets, and 80% less C18:3ω3 compared to the WF or FXO diets (Figure 4.1.9E). Simply put, the DF hens consumed far less dietary fatty acid than the hens that consumed WF or FXO, but yet, DF hens had 2-fold elevated serum C18:1ω9, C18:2ω6 and C22:6ω3, as well as equivalent serum 18:3ω3 (Figure 4.1.9D). Very meaningfully, the hens that we report in Figure 4.1.9D are the same exact hens that were previously published with nearly 3-fold elevated HbA1c (2). In other words, the DF and WF hens from our previous study concomitantly had elevated long term blood sugar and elevated blood lipids. Given the effect that glucagon has on serum FFAs and serum glucose in chickens (166), our observations (ie Figure 4.1.9A, B and D) support a hypothesis that flaxseed elevates glucagon secretion in hens. (166)

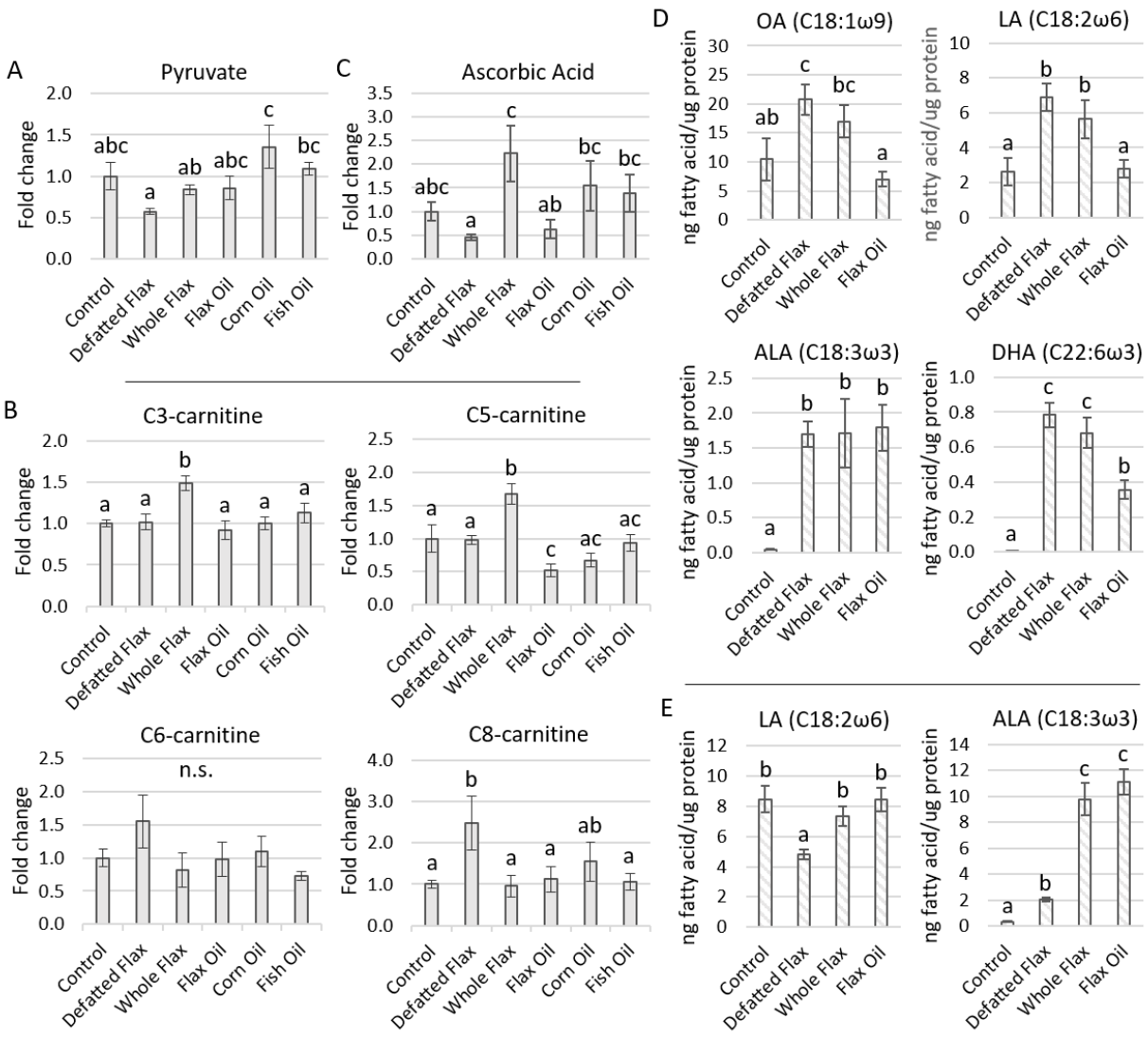
A
Pyruvate
Fold change
abc
a
ab
abc
c
bc
C
Ascorbic Acid
abc
a
c
ab
bc
bc
B
C3-carnitine
a
a
b
a
a
a
C5-carnitine
a
a
b
c
ac
ac
C6-carnitine
n.s.
C8-carnitine
a
b
a
a
ab
a
Control
Defatted Flax
Whole Flax
Flax Oil
Corn Oil
Fish Oil
D
OA (C18:1ω9)
ng fatty acid/ug protein
ab
c
bc
a
LA (C18:2ω6)
a
b
b
a
ALA (C18:3ω3)
a
b
b
b
DHA (C22:6ω3)
a
c
c
b
E
LA (C18:2ω6)
b
a
b
b
ALA (C18:3ω3)
a
b
c
c

Figure 4.1.9. Plasma pyruvate, plasma ascorbic acid, plasma acyl-carnitines, blood serum lipids and dietary lipid content. Plasma pyruvate (**A**), plasma ascorbic acid (**B**) and plasma C3, C5, C6 and C8-carnitine (**C**), were measured via LC-MS/MS in hens from the 325-day study. Blood serum lipids were quantified via gas chromatography in hens from the 9-week study (previously unreported in (2)) (**D**). We also quantified the level of C18:2ω6 and C18:3ω3 within the diets from the 9-week study, to illustrate how lipid-depleted the DF diet is versus the WFX and FXO diets (**E**). VIP scores of plasma metabolites and the areas of gas chromatograph peaks were analyzed via one-way ANOVA (Duncan's post-test, $p<0.05$). Sample sizes for **A**, **B** and **C**, range from $n=4$ to 6. Sample size for **D** is $n=4$. Sample size for **E** is $n=5$. Groups without a similar letter are significantly different. Error bars are +/- SEM.

4.1.8 Hen survival and egg laying performance

Hen survival was monitored at the daily timescale throughout the 325-day study. Total survival and average egg laying performance are shown in Table 4.1.3. Single-integer percentage shifts are biologically meaningful in this study, because each diet began with an average of 168 hens. Thus, a 1% shift in survival equaled 1.68 hens, on average. DF hens displayed better survival than all other diet groups by a range of 3.8% to 9.7% improved survival. Simultaneously, CRN exhibited lowest survival among diet groups, while CTL, WF, FSH and FXO displayed intermediate survival. We also observed daily egg laying performance as an indicator of biological vitality within animals (Table 4.1.3). Egg laying was significantly higher in WF hens versus all diets except FSH. Intermediate egg laying was observed in DF hens, while lowest egg laying occurred in CTL, FXO and CRN (Table 4.1.3). We developed a composite ranking system that integrated survival with reproductive performance as an indication of overall vitality (Table 4.1.4). Through this perspective, we observed an interesting pattern where the

"absolute difference" between survival ranking and egg laying ranking was equal to 2, for the top four best performing diets (i.e. DF, CTL, WF and FSH). FXO and CRN hens exhibited low survival concomitant with low reproductive capacity (Table 4.1.4). Overall, the DF and WF hens were tied for the best biological vitality by expressing the highest composite ranks for survival and egg laying (Table 4.1.4).

Kaplan-Meier survival analysis was conducted to compare survival patterns between diet groups (Figure 4.1.10). DF hens maintained a pattern of best cumulative survival except for several moments (i.e. a week or several days) when WF and FXO hens momentarily exhibited top survival. After the 28^{th} day of the study, DF hens maintained better cumulative survival than CTL hens until study completion. DF was the only diet to outperform CTL as such. A significantly reduced Cox proportional hazard ($\exp\{coef\} = 0.685$, $p<0.05$) was detected in DF hens when compared to CRN hens (Table 4.1.5 and Figure 4.1.10). Table 4.1.5 shows the proportional hazard of survival in each diet versus the corn oil diet (i.e. the corn oil diet is used as the reference). This Cox proportional hazard model meets the proportional hazard assumption that a global risk trend does not exist across time, according to a non-significant Schoenfeld test statistic ($p=0.39$).

Mortality in CRN hens started to accelerate at around day 150 and continued accelerating until day 190. This window of time coincided with the molting phase of the study, during which time egg laying declined and entered recovery in all diets. Although CRN hens displayed a negative response to the molt, molting is a natural physiological process that laying hens experience annually. Furthermore, hens across all diets were exposed to identical conditions during molt (i.e. light restriction but with full food access).

We observed two specific metabolites (i.e. glucuronate and glycerophosphorylcholine) and

one specific metabolite ratio (i.e. Met sulfoxide:Met ratio) that associate with increased lifespan and healthspan in human and non-human animal models (284–287). In DF hens, the Met Sulf:Met ratio was decreased concomitant with decreased glucuronate and decreased glycerophosphorylcholine (Figure 4.1.11). This pattern provides a biochemical validation of improved lifespan and healthspan in DF hens, because each of these markers has previously been used to evaluate lifespan and/or systemic oxidative stress.

Table 4.1.3. Survival percentage and egg laying performance.

Diet	Survival			Daily eggs per hen*
	Total survival *(%)*	Starting hens *(n)*	Surviving hens *(n)*	*(egg/day/hen)*
Defatted Flax	71.4%	161	115	0.384^{b} +/- 0.005
Control	67.6%	182	123	0.365^{c} +/- 0.004
Whole Flax	66.5%	161	107	0.401^{a} +/- 0.005
Fish Oil	65.5%	165	108	0.394^{ab} +/- 0.005
Flax Oil	64.0%	161	103	0.359^{c} +/- 0.005
Corn Oil	61.7%	175	108	0.355^{c} +/- 0.004
Average	66.1%	168	111	0.376 +/- 0.005

*Statistical values determined via one-way ANOVA (Duncan's Multiple Range post-test, $p<0.05$). Groups without a similar letter are significantly different. +/- SEM.

Table 4.1.4. Composite ranking of biological performance, via total survival and egg laying capacity.

Diet	Rank of survival percentage	Rank of daily egg laying	Absolute difference of ranks	Overall ranking of survival and egg laying (i.e. biological vitality)
	(**A**)	(**B**)	Abs(**A**-**B**)	Rank(median(**A**+**B**))
Defatted Flax	1	3	2	1
Control	2	4	2	2
Whole Flax	3	1	2	1
Fish Oil	4	2	2	2
Flax Oil	5	5	0	3
Corn Oil	6	6	0	4

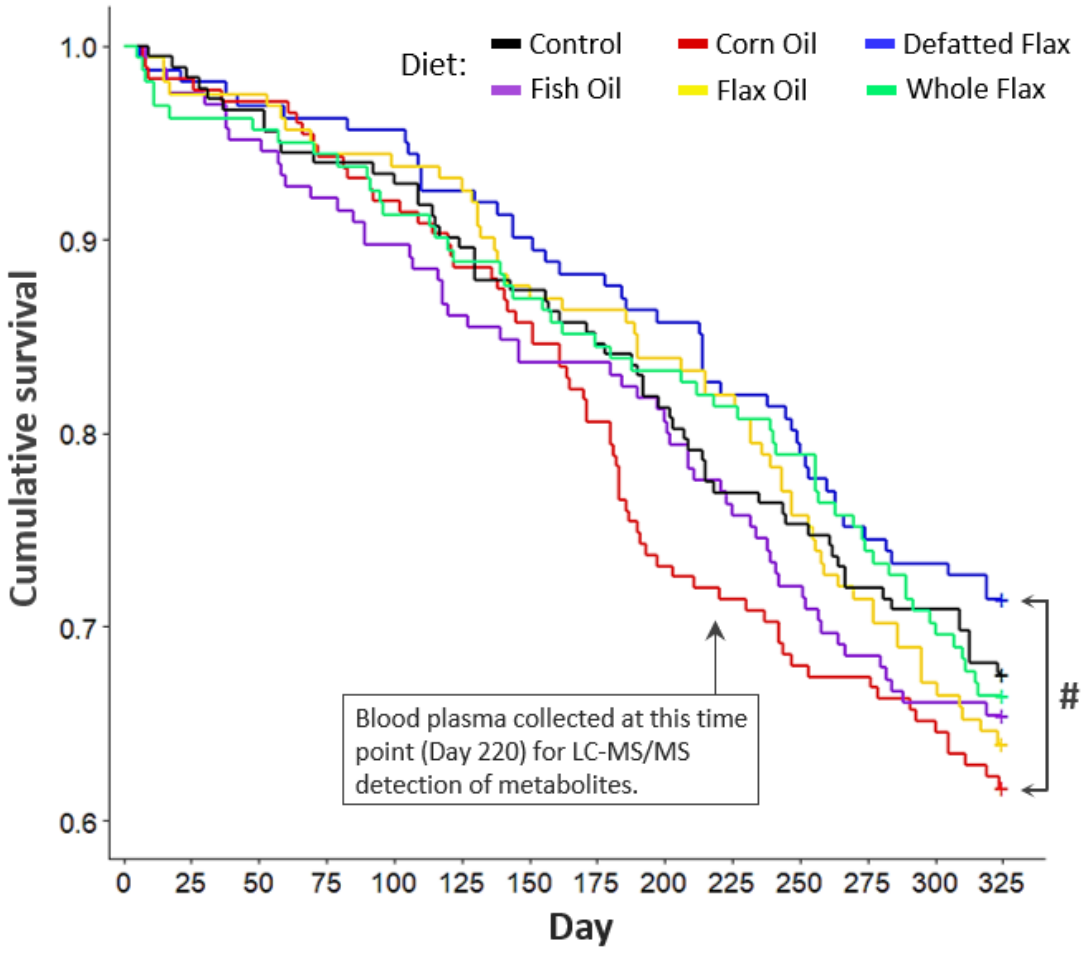

Figure 4.1.10. Kaplan-Meier survival analysis and Cox proportional hazard determination. Kaplan-Meier survival analysis was conducted on the rate of mortality within each diet group for the entire 325-day study. The # indicates a significantly different Cox proportional hazard between DF hens and CRN hens. Also shown in the graph is the timepoint at which we collected blood plasma for metabolomics analysis.

Table 4.1.5. Cox proportional hazard analysis of hen survival (using the corn oil diet as reference)

Diet[Ψ]	exp(coef)[#]	95% c.i.	p-value
Defatted Flax	0.685*	0.471 to 0.997	0.048
Control	0.805	0.567 to 1.143	0.230
Whole Flax	0.825	0.577 to 1.181	0.293
Fish Oil	0.885	0.622 to 1.260	0.500
Flax Oil	0.888	0.625 to 1.263	0.508

[Ψ] The corn oil diet was used as a reference group during Cox proportional hazard analysis (i.e. all hazards are referenced to the survival of hens consuming the corn oil diet)

[#] An "exp(coef)" below 1.0 indicates improved survival probability

* Significantly reduced Cox proportional hazard ($p<0.05$)

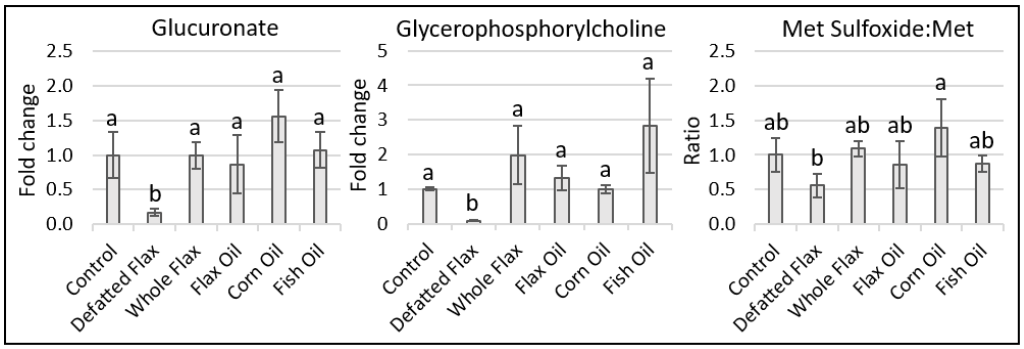

Figure 4.1.11. Metabolites indicating the process of aging and longevity. Hen blood plasma samples measured via LC-MS/MS. VIP scores of metabolites were analyzed via one-way ANOVA (Duncan's post-test, $p<0.05$). Groups without a similar letter are significantly different. *n*=4 to 6 plasma samples from different hens per diet group. Error bars are +/- SEM.

4.1.9 Physiological model of one-carbon metabolism in flaxseed-fed hens

We report for the first time of a TS blockade correlating directly with increased flux of Hcy toward SAM, correlating with enhanced survival and/or enhanced reproductive capacity in a vertebrate animal. Overall, our research indicates that the linatine molecule of flaxseed (via 1ADP) severely perturbs hepatic TS, likely via inhibiting the B6-dependent enzymes CBS and

CSE. However, instead of inducing hyperHcy our data suggest that this TS perturbation forces an increased flux of Hcy toward Met (i.e. increased Hcy remethylation) that subsequently boosts SAM. In order to sustain this flux, our data possibly indicate elevated catabolism of the methyl group donors (i.e. choline) that drive the BHMT reaction and the MS-B12 reaction. A baseline model illustrating the core pathways (i.e. methionine cycle, folate cycle, phospholipid catabolism and TS) behind our research can be seen in Figure 4.1.12.

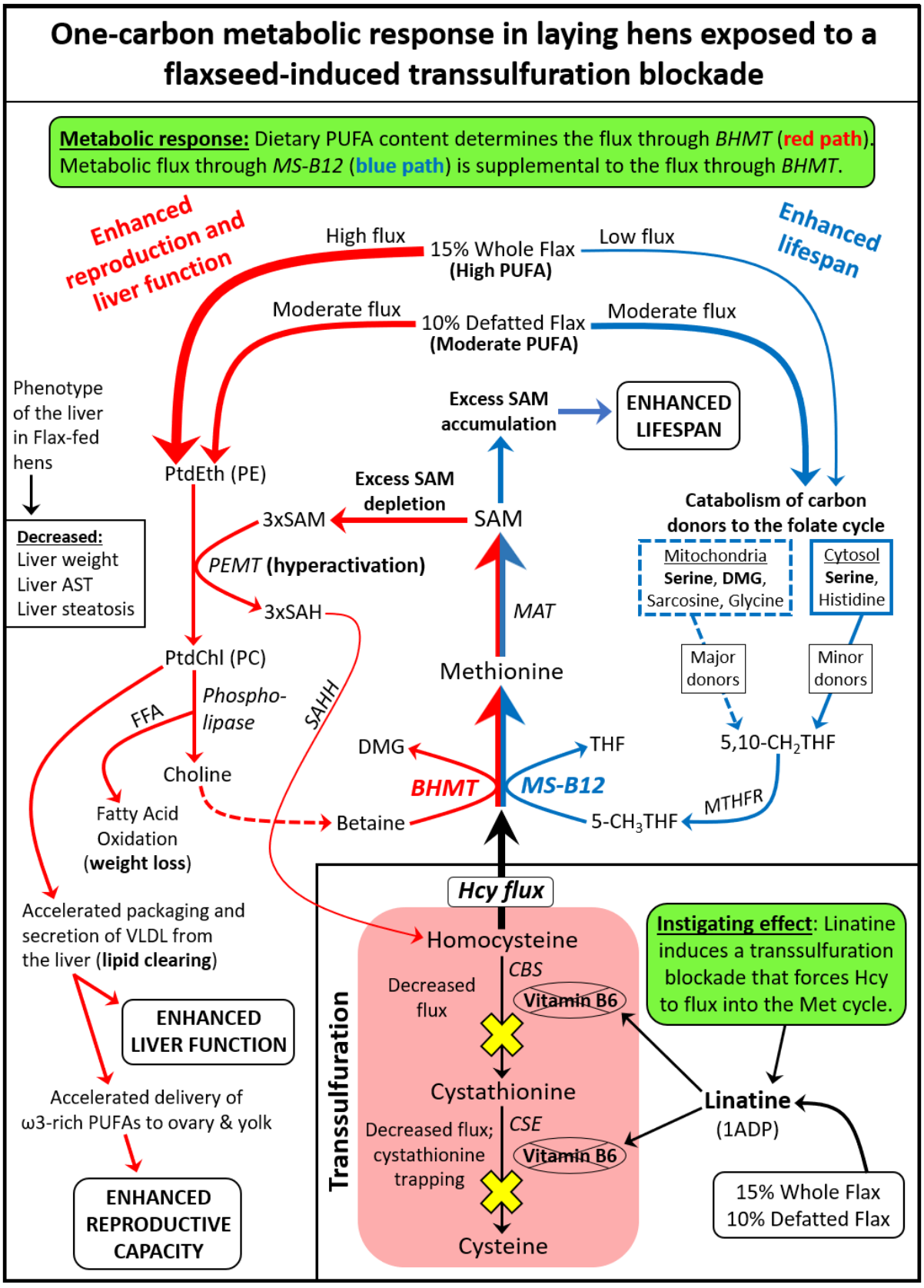
One-carbon metabolic response in laying hens exposed to a flaxseed-induced transsulfuration blockade
Metabolic response: Dietary PUFA content determines the flux through BHMT (red path). Metabolic flux through MS-B12 (blue path) is supplemental to the flux through BHMT.
Enhanced reproduction and liver function
High flux
15% Whole Flax (High PUFA)
Low flux
Enhanced lifespan
Moderate flux
10% Defatted Flax (Moderate PUFA)
Moderate flux
Phenotype of the liver in Flax-fed hens
Excess SAM accumulation
ENHANCED LIFESPAN
PtdEth (PE)
Excess SAM depletion
SAM
3xSAM
Catabolism of carbon donors to the folate cycle
Decreased:
Liver weight
Liver AST
Liver steatosis
PEMT (hyperactivation)
Mitochondria
Serine, DMG, Sarcosine, Glycine
Cytosol
Serine, Histidine
3xSAH
MAT
PtdChl (PC)
Methionine
Major donors
Minor donors
FFA
Phospho-lipase
SAHH
DMG
THF
5,10-CH2THF
Choline
BHMT
MS-B12
MTHFR
Fatty Acid Oxidation (weight loss)
Betaine
5-CH3THF
Hcy flux
Accelerated packaging and secretion of VLDL from the liver (lipid clearing)
Homocysteine
Instigating effect: Linatine induces a transsulfuration blockade that forces Hcy to flux into the Met cycle.
CBS
Decreased flux
Vitamin B6
ENHANCED LIVER FUNCTION
Cystathionine
Linatine
(1ADP)
Accelerated delivery of ω3-rich PUFAs to ovary & yolk
Decreased flux; cystathionine trapping
CSE
Vitamin B6
Transsulfuration
15% Whole Flax
10% Defatted Flax
ENHANCED REPRODUCTIVE CAPACITY
Cysteine

Figure 4.1.12. Model for one-carbon metabolism in hens consuming the WF or DF diets. The image illustrates a model by which flaxseed affects one-carbon metabolic activity in White Leghorn laying hens. The initial effect (bottom right quadrant) is instigated when linatine exerts an anti-vitamin B6 effect and reduces CBS and CSE activity. In turn this reduces flux through TS and causes cystathionine accumulation. An increased flux of Hcy into the Met cycle requires increased activity from BHMT and/or MS-B12. WF hens, having a high PUFA content, can synthesize a high level of PtdEth (PE). This means that WF hens have high access to the primary substrate for the PEMT reaction, which is PE. Therefore, WF hens should have increased capacity to hyperactivate PEMT. This capacity to hyperactivate PEMT is the suspected reason why SAM is not elevated in WF hens (i.e. excess SAM was consumed by PEMT). PEMT hyperactivation would then, in turn, enable BHMT hyperactivation and support increased flux of Hcy into the Met cycle. BHMT hyperactivation would require elevated choline synthesis (i.e. elevated PEMT activity), because choline is oxidized to make BHMT's substrate, betaine. In other words, BHMT hyperactivation is likely contingent upon PEMT hyperactivation, especially in the context of fixed nutrient dieting. PEMT hyperactivation could be expected to accelerate the packaging and secretion of VLDL into the blood stream, because PC (the product of PEMT) is rate limiting for VLDL packaging and secretion. Accelerated delivery of VLDL into the blood stream might be required for accelerated egg yolk formation, because egg yolk lipids are derived from systemic VLDL. In turn this might enhance the egg laying capacity of the hen. Given the moderate PUFA content of the DF diet, DF hens would be expected to have only moderately elevated flux through PEMT, and therefore, only moderately elevated egg laying capacity. Due to the high PUFA content of the WF diet, WF hens would be expected the have high flux through PEMT, and therefore, have highly elevated egg laying capacity. Likewise, WF hens and

DF hens would be expected to have high flux and moderate flux through BHMT, respectively. High flux through BHMT would facilitate the majority of Hcy remethylation and thereby prevent exceptionally elevated flux into the folate cycle. However, a moderate flux through BHMT (as was suspected in DF hens) would cause a residual level of hyperHcy. Therefore, DF hens would require increased catabolism of one-carbon donating molecules (i.e. serine and DMG) into the folate cycle, so that MS-B12 could provide supplemental support for Hcy remethylation. Increased one-carbon input into the folate cycle would elevate 5,10-CH_2THF synthesis and subsequently elevated 5-CH_3THF synthesis, via MTHFR. 5-CH_3THF then supports Hcy remethylation via MS-B12. The accumulation of excess SAM in DF hens might be the result of only moderately elevating PEMT hyperactivation, because highly elevated PEMT hyperactivation would be expected to deplete all excess SAM (as we suspect happened in WF hens). The accumulation of SAM in DF hens associates with increased lifespan, possibly via SAM-mediated changes in DNA, RNA or histone methylation. Overall, the entire cascade of events is instigated by linatine, and the resulting metabolic fluxes are determined by the total PUFA content of the diet.

4.2 STUDY 2: THE EFFECT OF DIETARY POLYUNSATURATED FATTY ACIDS (PUFAS) ON LIPID METABOLISM, MITOCHONDRIAL BIOENERGETICS AND E-CADHERIN EXPRESSION IN LAYING HEN OVARIAN TUMORS

4.2.1 Cancer outcomes and cancer risks in hens according to diet

Upon the completion of our 325-day study, we conducted necropsy on all surviving hens. The number of hens that survived in each diet group and what this represents as a survival percentage can be seen in Table 4.2.1. Hens that died prior to study completion were not inspected. We recorded the presence of ovarian cancer, gastrointestinal (GI) cancer, liver cancer and oviduct

cancer, in all animals that lived until study completion. The frequency and percentage of hens with peritoneal cancers can also be seen in Table 4.2.1. CTL hens and DF hens displayed elevated risk of total ovarian cancer, stage 3&4 ovarian cancer, liver cancer and cancers with multiple organ involvement. CTL hens also displayed elevated risk of GI cancer. Cancer was just really bad in CTL hens, to be frank. All of the peritoneal cancer risks (except for oviductal cancer) were reduced by treatment diets versus CTL diet. The risk of ovarian cancer and the risk of stage 4 ovarian cancer were lowest in diet groups that were supplemented with the pure oil component (i.e. FXO, FSH and CRN). Furthermore, the risk of stage 4 ovarian cancer was lowest in FXO hens versus CTL hens, again suggesting that ovarian cancer burden might be decreased by dietary PUFA enrichment, particularly with ALA enrichment. The risk of ovarian cancer and the risk of stage 3&4 ovarian cancer were elevated when the dietary PUFA supplement was either non-existent (i.e. CTL) or mostly diminished (i.e. DF). Interestingly, CTL hens and DF hens displayed the 1st and 2nd highest ovarian tumor incidence, respectively, concomitant with the 2nd and 1st highest animal survival, respectively (Table 4.1.3). Inversely, CRN hens displayed lowest ovarian tumor incidence (tied with FSH hens), concomitant with lowest animal survival (Table 4.2.1). Said concisely, we detected a noticeable pattern where animal survival and ovarian cancer risk were paradoxically, positively correlated. The likelihood of observing stage 4 ovarian cancer was lowest in diet groups with lowest animal survival (i.e. FXO, FSH and CRN hens). Flaxseed, in general displayed a cluster of moderate ovarian cancer risk, because ovarian cancer risk was moderate in DF, WF and FXO hens. WF hens and FXO hens displayed identical total ovarian cancer risk (i.e. R.R. of 0.72). The percentage of hens with GI cancer were very similar in WF and FXO hens (7% in WF and 8% in FXO), suggesting that the flaxseed oil might similarly influence the risk of ovarian cancer and GI cancer, in hens.

Table 4.2.1. Peritoneal tumors recorded in hens at the time of necropsy.

Diet	**Surviving hens (i.e. hens eligible for tumor collection)***	**Peritoneal cancers by site**										**Multiple peritoneal tumors involved**
		Ovarian cancer**							GI cancer	Liver cancer	Oviduct cancer	
		Total OvCa			*Stage 1&2*	*Stage 3*	*Stage 4*	*Stage 3&4*				
	n / %[+]	*n*	*%*	*R.R.*[#]	*%*	*%*	*%*	*%*	*%*	*%*	*%*	*%*
Control	123 / 67.6	22	18	1.00	4	3	11	14	11	3	1	10
Defatted Flax	115 / 71.4	16	14	0.78	2	3	9	12	3	2	1	4
Whole Flax	107 / 66.5	14	13	0.72	3	0	10	10	7	1	1	3
Flax Oil	103 / 64.0	13	13	0.72	3	6	4	10	8	1	3	2
Fish Oil	108 / 65.5	12	11	0.61	2	4	5	9	5	1	0	1
Corn Oil	108 / 61.7	12	11	0.61	1	4	6	10	2	0	4	3
Average	111 / 66.1	15	13	0.69	3	3	8	11	6	1	2	4

***** These are the hens that we were able to conduct necropsy on (i.e. potentially collect tumors from)

****** Ovarian cancer stages determined according to FIGO staging criteria (amp.cancer.org).

[+] All percentages (%) in this table are based on normalization to the number of surviving hens.

[#] R.R. is relative risk (calculated as a treatment diet's total OvCa % divided by the control diet's total OvCa %).

[†] Two of these hens (in control diet) died just prior to CO_2 asphyxiation.

4.2.2 Fatty acid metabolism in hen ovarian tumors

Genes representing the *de novo* lipogenic pathway were measured in laying hen ovarian tumor homogenates to challenge the hypothesis that dietary PUFAs regulate lipid metabolism in hen ovarian tumors. FXO, CRN and FSH exerted a strong (~70%) downregulation of fatty acid synthase (*FASN*) in hen ovarian tumors, while WF downregulated *FASN* by about 55% (Figure 4.2.1). *FASN* expression in DF hens was similar to WF hens, but *FASN* expression was higher in DF hens compared to FXO, CRN and FSH hens. Simultaneously, there was no difference in *FASN* between CTL hens and DF hens. CRN was the only diet to reduce the expression of *ACC* and *SCD1*, by about 50% each. Neither *ACYL* nor *SREBP1* were affected by diet. Ovarian tumors from FSH hens displayed higher transcripts for *PPARg* in contrast to the control diet (Figure 4.2.1).

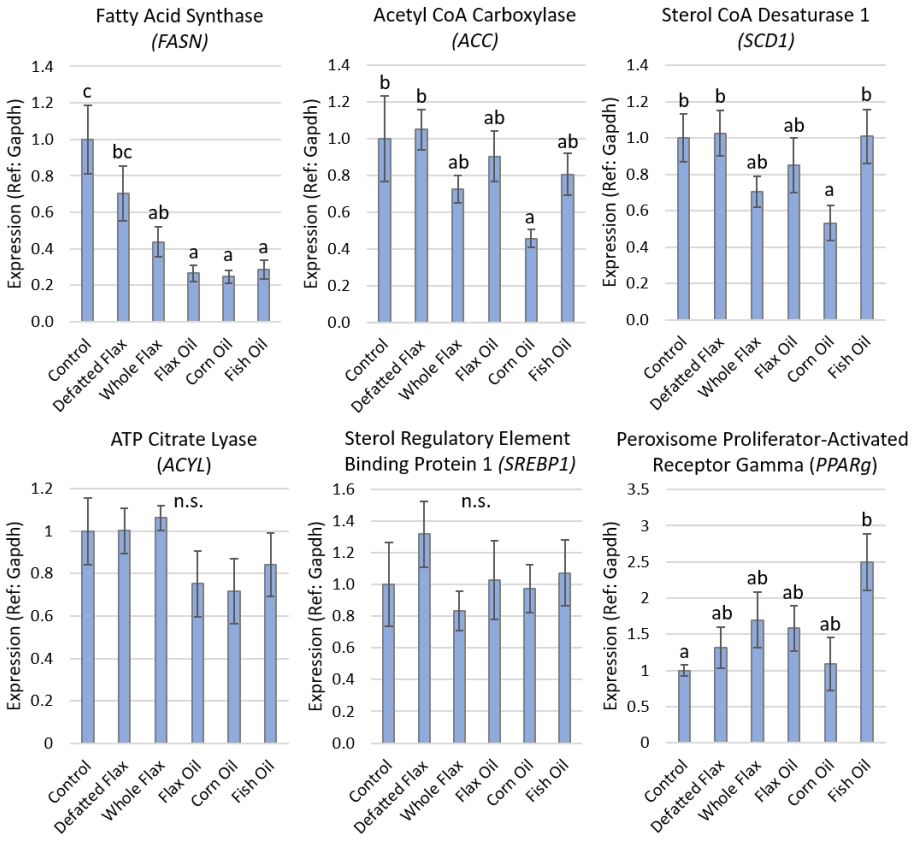

Figure 4.2.1. Gene expression markers of *de novo* fatty acid synthesis and *PPARg*, in hen ovarian tumors. cDNA expression was calculated using ddCT values obtained from RT-qPCR for each gene. Statistical values were determined using one-way ANOVA (Duncan's post hoc test, $p<0.05$). Groups without a similar letter are significantly different. Sample sizes ranged from $n = 7$ to 9 per diet group. Error bars are +/- SEM.

Gas chromatography analysis of hen ovarian tumors was conducted to assess the levels of fatty acid methyl esters within ovarian tumors (Figure 4.2.2). We observed that each diet's dominant PUFA was most upregulated in hen ovarian tumors. For example, LA (C18:2ω6) was upregulated in the ovarian tumors of hens consuming the CRN diet, and this particular PUFA consists of nearly 50% of the PUFA content of corn oil. ALA (C18:3ω3) was first and second-most upregulated in the ovaries of hens consuming the FXO and WF diets, respectively, and

linolenic acid comprises 50% of the PUFA content of flaxseed oil. C22:6ω3 was upregulated in the ovaries of hens consuming the FSH diet, and this PUFA comprises about 10% of the oil content in menhaden fish oil. We did not see any effect of diet on C20:5ω3 (EPA), although this PUFA is most enriched in the FSH diet. Furthermore, just like CTL diet, the DF diet had no significant effect on any PUFAs.

One of our goals of conducting gas chromatography analysis was to measure the concentrations of fatty acids that are canonically related to *de novo* lipid synthesis, and we were not able to detect any effect of diet on most of these species (i.e. C16:0, C16:1ω7, C18:0, C18:1ω9, or C20:0). The WF diet was able to slightly reduce the concentration of C20:1n11 in ovarian tumor homogenates. Other than C20:1ω11, there were no effects of diet on lipids associated with *de novo* lipogenesis (Figure 4.2.2).

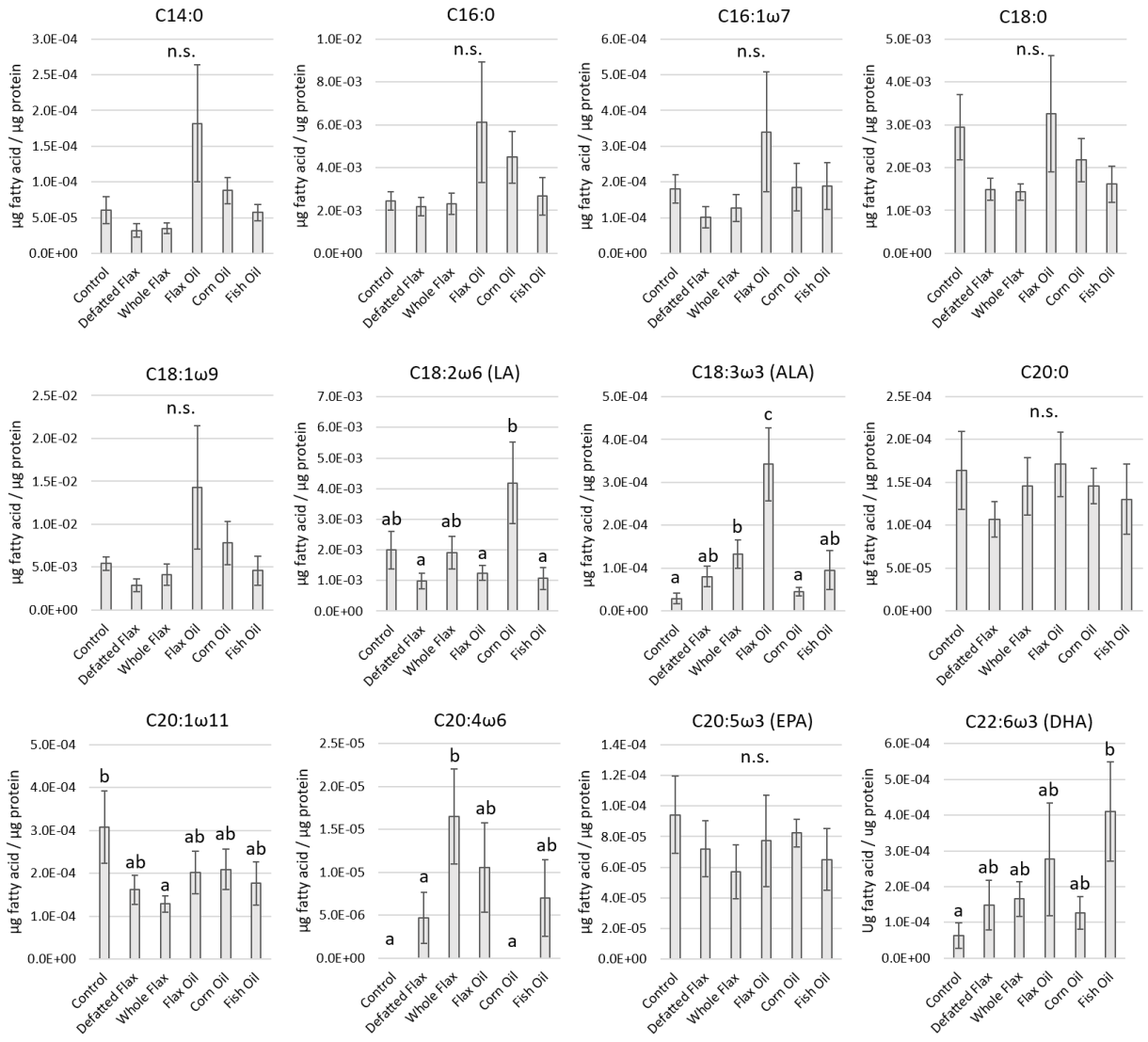

Figure 4.2.2. Fatty acid concentrations in hen ovarian tumors. Gas chromatography was utilized to measure PUFA concentrations in hen ovarian tumors. Cancerous ovaries were collected from 3.5-year-old hens that were provided 46-week diets. Sample sizes in this 46-week analysis ranged from *n* = 6 to 8 ovaries per diet group. PUFAs were measured as fatty acid methyl esters (FAME). C17:0 was used as an internal control, and all samples were normalized to total protein. One-way ANOVA and Duncan's Multiple Range Test ($p<0.05$). Groups without a similar letter are significantly different. Sample sizes ranged from *n* = 6 to 8 per diet group. Error bars are +/- SEM.

4.2.3 Gene transcripts associated with mitochondrial respiration

Our hypothesis also included the notion that dietary PUFAs would boost the level of genes that promote mitochondrial ETC activity (i.e. OXPHOS activity) with ovarian tumors of the hen. The transcription of mitochondrial genes that are most strongly associated with complex 3 catalytic activity (i.e. *MT-CYTB*) and complex 4 catalytic activity (i.e. *MT-COX1*, *MT-COX2* and *MT-COX3*) were vastly upregulated by dietary enrichment with PUFAs (Figure 4.2.3). Specifically, these mitochondrial genes were upregulated by WF, FXO, CRN and FSH. The DF diet only slightly increased the expression of *MT-CYTB* and *MT-COX3*, without affecting *MT-COX1* or *MT-COX2*. The expression of *ATP5B*, a gene associated with oxidative phosphorylation capacity and mitochondrial cristae formation, was strongly upregulated by WF, FXO, CRN and FSH. The largest enrichments of *ATP5B* were observed in FXO and CRN diets. Complementing this finding, the expression of ADP/ATP translocase 1 (*SLC25A4*) was upregulated in the ovarian tumors of FXO hens (Figure 4.2.3). Overall, this was a strong transcriptional message that nuclear and mitochondrial mRNA levels for ETC subunits might be heavily increased by dietary PUFAs.

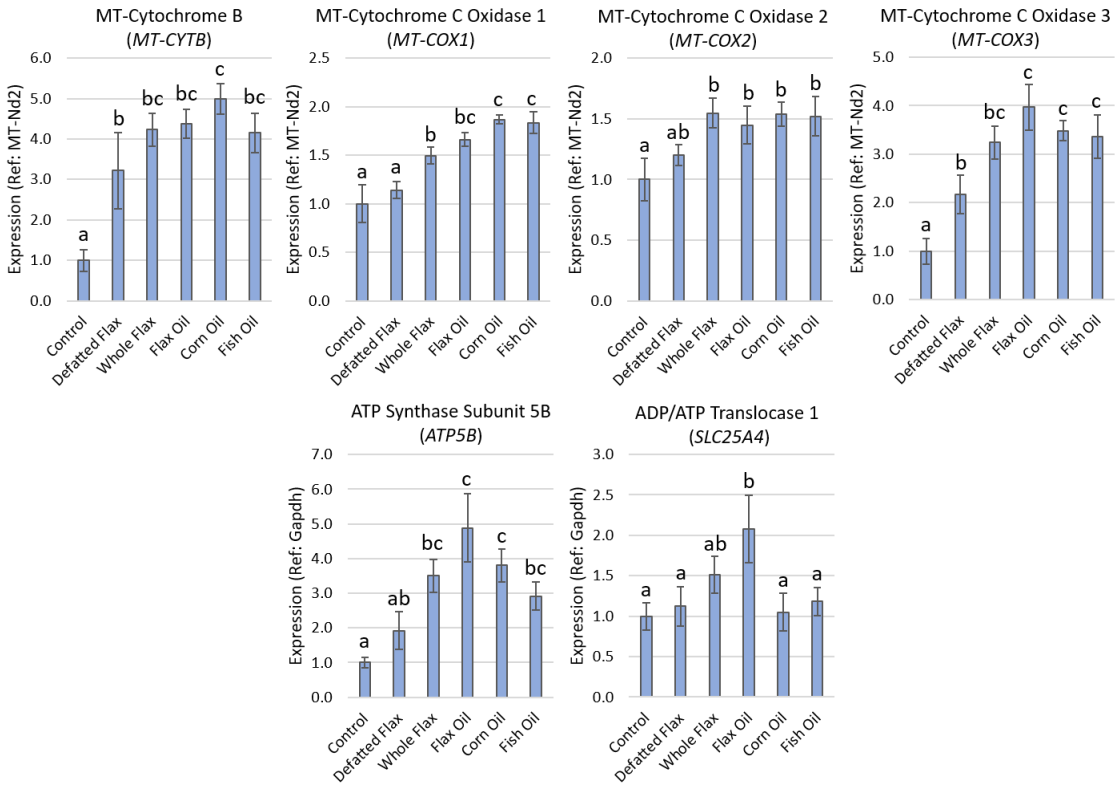

Figure 4.2.3. Gene expression markers of mitochondrial respiration and oxidative phosphorylation, in hen ovarian tumors. cDNA expression was calculated using *dd*CT values obtained from RT-qPCR for each gene. Statistical values were determined using one-way ANOVA (Duncan's post hoc test, $p<0.05$). Groups without a similar letter are significantly different. Sample sizes ranged from n = 7 to 9 per diet group. Error bars are +/- SEM.

4.2.4 Genes transcripts associated with oxidative stress response

Overall, it seemed that dietary PUFA enrichment decreased the expression of phase 2 antioxidant response enzyme genes in hen ovarian tumors (Figure 4.2.4). *SOD2*, *CAT* and inducible nitric oxide synthase (*NOS2*), were concomitantly lower in WF, FXO, CRN and FSH hens. *SOD2* and *NOS2* were also decreased in DF hens, while there was no effect of DF on *CAT*. Dynamin-like protein 1 (*DNM1L*), the gene for a protein commonly known as "*DRP1*" (which

regulates mitochondrial fission), was reduced by all treatment diets, including DF (Figure 4.2.4). The F_1/F_0-ATP synthase complex is influenced by the redox state of the cell (288), so we found it novel to include ATP synthase subunit 5A1 (*ATP5A1*), mitochondrial ATP synthase subunit 6 (*MT-ATP6*) and mitochondrial ATP synthase subunit 8 (*MT-ATP8*), in the same figure as *SOD2, CAT, NOS2* and *DNM1L* (mostly because of the similar pattern of expression). A consistent reduction of *ATP5A1, MT-ATP6* and *MT-ATP8,* was observed in ovarian tumors from most treatment diets, including DF (Figure 4.2.4).

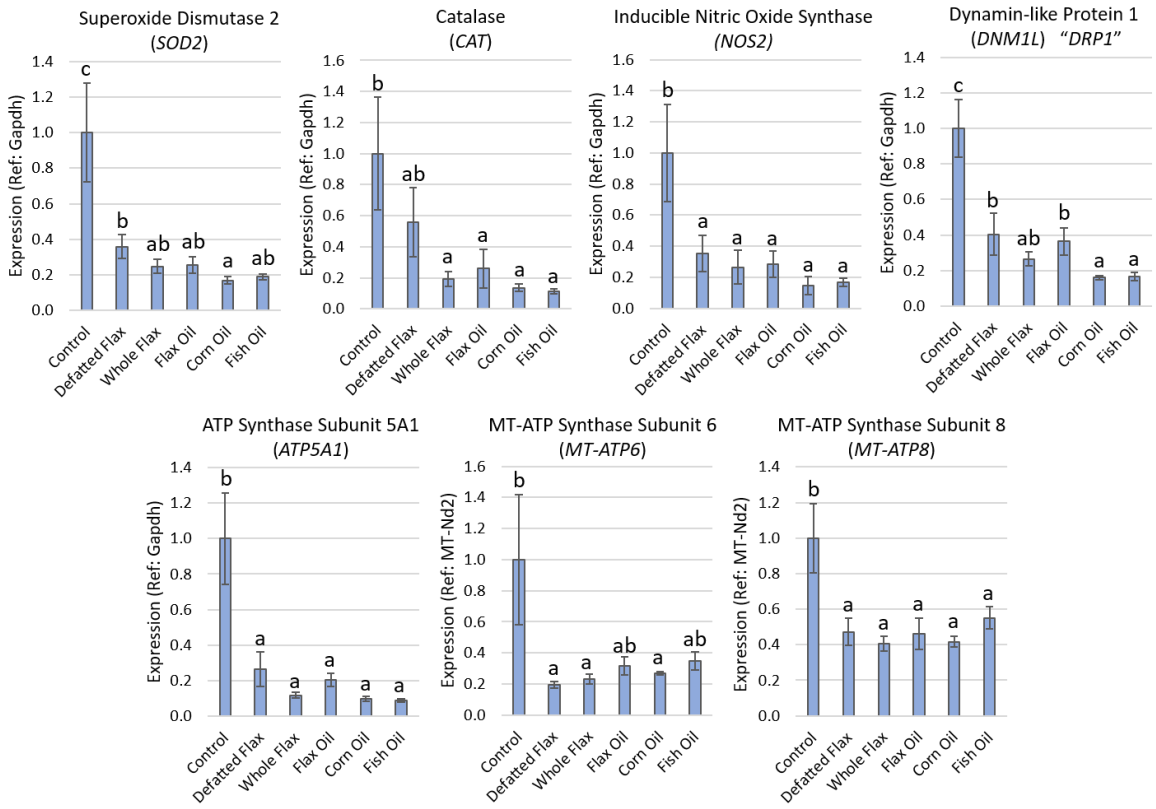

Figure 4.2.4. Gene expression markers of oxidative stress and associated ATP synthase subunits, within hen ovarian tumors. cDNA expression was calculated using ddCT values obtained from RT-qPCR for each gene. Statistical values were determined using one-way ANOVA (Duncan's post hoc test, $p<0.05$). Groups without a similar letter are significantly different. Sample sizes ranged from n = 7 to 9 per diet group. Error bars are +/- SEM.

4.2.5 MicroRNA-200a-3p and CDH1 expression in hen ovarian tumors

To test our hypothesis that dietary PUFA enrichment downregulates the expression of miR-200a and *CDH1* in hen ovaries, we conducted qPCR analysis of normal and cancerous hen ovaries after feeding these animals various PUFA enriched diets (Figure 4.2.5). The exception here is that the normal ovaries were from 2-year-9-week-old hens and the cancerous ovaries were from 3.5-year-old hens. A benefit to using 2-year-9-week-old hens is that these hens are much

less likely to have ovarian cancer; whereas the 3.5-year-old hens are well into the window of risk for ovarian cancer (18).

Each of the treatment diets, except WF, decreased the level of miR-200a in normal ovaries of the hen, with the most pronounced effect occurring in hens consuming SDA Soybean Oil (SDA Soy Oil) (Figure 4.2.5A). miR-455-5p was used as a reference microRNA when determining miR-200a transcript levels. SDA Soybean Oil is derived from a variety of soybean that possesses a delta-6 desaturase knock-in, allowing the soybean to generate stearidonic acid (SDA, C18:4ω3). SDA soybean-derived oil is beneficial for boosting the levels of EPA and DHA within the animal (289,290). Wild type plants cannot synthesize SDA; therefore, SDA Soy provides greater unsaturated oil content. In general, the data indicate that dietary exposure to PUFAs reduces the level of miR-200a in normal hen ovaries (Figure 4.2.5A); however, no effect of diet was observed on the level of miR-200a in ovarian tumors of hens (Figure 4.2.5B). The level of miR-200a in ovarian tumors was almost 15-fold higher than miR-200a expression in normal hen ovaries (Figure 4.2.5C). Ovarian tumor samples from Figure 4.2.5D were separated according to tumor stage (stage 2, 3 and 4), and then miR-200a levels were measured statistically in ovarian tumors according to stage 2, 3 or 4. The expression of miR-200a was increased in stage 4 ovarian tumors versus stage 2 ovarian tumors (Figure 4.2.5D). Lastly, BG1 ovarian cancer cells were incubated with 50μM DHA, and the level of miR-200a was measured. 50uM DHA elicited a small but significant decrease in the level of miR-200a in BG1 ovarian cancer cells (Figure 4.2.5E).

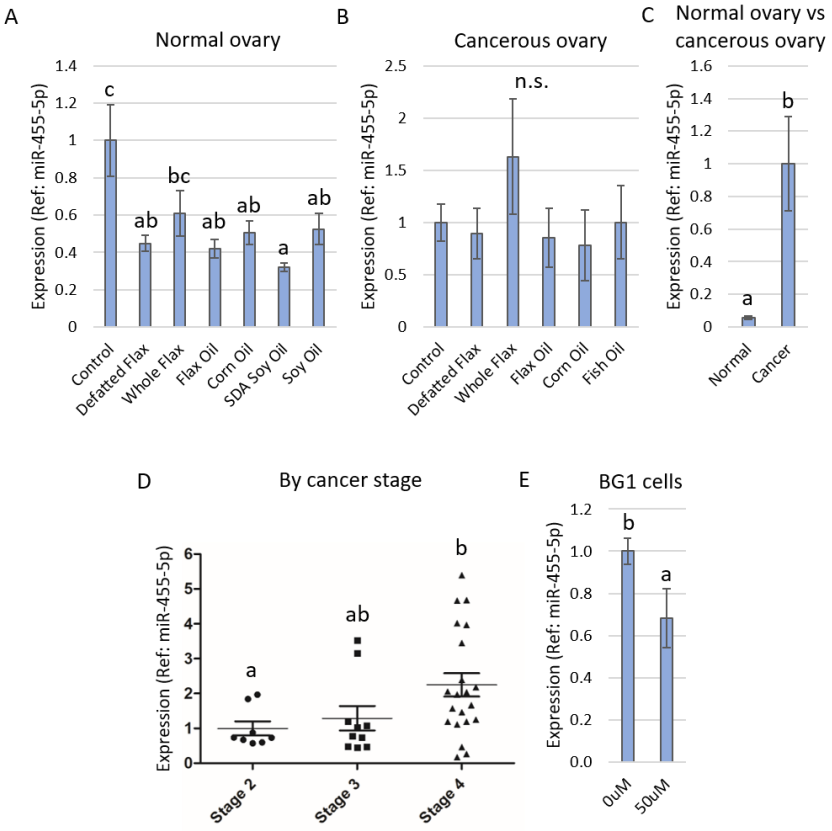
A
Normal ovary
Expression (Ref: miR-455-5p)
c
ab
bc
ab
ab
a
ab
Control
Defatted Flax
Whole Flax
Flax Oil
Corn Oil
SDA Soy Oil
Soy Oil
B
Cancerous ovary
n.s.
Control
Defatted Flax
Whole Flax
Flax Oil
Corn Oil
Fish Oil
C
Normal ovary vs cancerous ovary
a
b
Normal
Cancer
D
By cancer stage
a
ab
b
Stage 2
Stage 3
Stage 4
E
BG1 cells
b
a
0uM
50uM

Figure 4.2.5. miR-200a-3p expression in hen ovaries, hen ovarian tumors and human ovarian cancer cells. Expression of microRNA was analyzed in microRNA cDNA libraries via qPCR for each sample. miR-200a was evaluated in 2-year-old normal hen ovaries (**A**) and in 3.5-year-old cancerous hen ovaries (**B**); all values were normalized to their respective control diets. In A and B, sample sizes ranged from n = 5 to 7 per diet group. miR-200a expression was compared between normal ovaries of 2-year-old hens and cancerous ovaries of 3.5-year-old hens (both groups receiving the control diet); n= 7 per group (**C**). The effect of ovarian cancer stage on the expression of miR-200a was evaluated in hen ovarian tumors; all values are normalized to stage 2 tumors (**D**). Sample sizes in **D** ranged from n=8 for stage 2; n=10 for stage 3; and n=21 for stage 4 (**D**). Lastly, the effect of DHA treatment on miR-200a expression was evaluated in BG1 ovarian cancer cells; all values normalized to 0μM DHA (**E**). Statistical values in **A, B** and **D** were determined using one-way ANOVA (Duncan's post hoc test, $p<0.05$). Statistical values for **C** and **E** were determined used T-test with Welch's correction. Groups without a similar letter are significantly different. Error bars are +/- SEM.

We then looked at *CDH1* expression in normal and cancerous hen ovaries. *CDH1* levels were reduced 60-80% in the normal ovaries of 2-year-old hens by all treatment diets (Figure 4.2.6A). In normal ovaries of 3.5-year-old hens, *CDH1* levels were reduced in hens consuming FSH versus hens consuming WF (Figure 4.2.6A). In ovarian tumors of 3.5-year-old hens, *CDH1* levels were reduced by the FXO and FSH diets, by about 65% (Figure 4.2.6A). We detected an age effect on *CDH1* levels in ovaries, when *CDH1* increased about 5-fold in 3.5-year-old normal ovaries compared to 2-year-old normal ovaries (both groups fed CTL diet). *CDH1* expression might be increased in early neoplastic ovaries, because we detected increased *CDH1* levels in suspicious (i.e. early neoplastic) ovaries of 3.5-year-old hens versus normal ovaries. *CDH1*

increased again when going from suspicious ovaries to ovaries dominated by frank carcinoma (Figure 4.2.6B). Overall, it seemed obvious that the density of *CDH1* transcripts increases in cancerous ovarian tissue, and FXO and FSH were able to downregulate this.

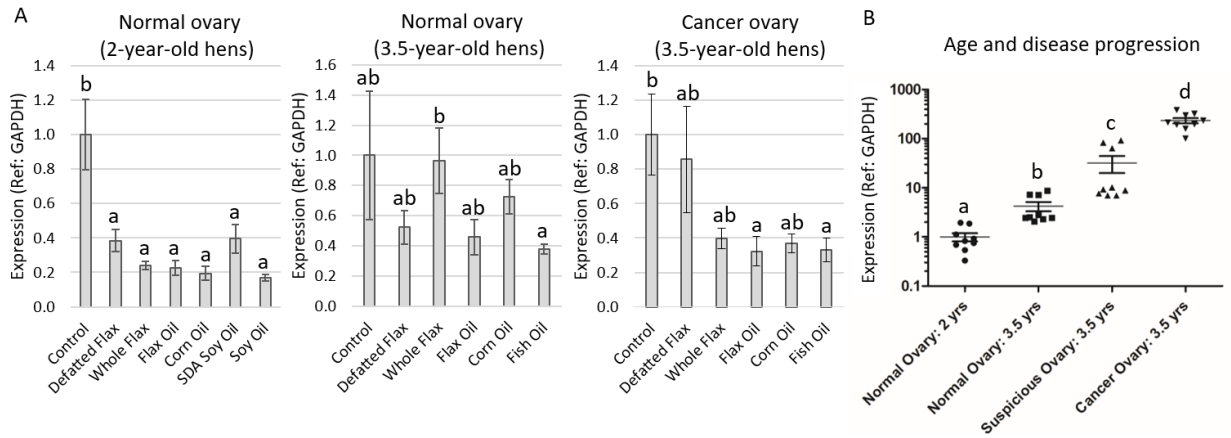

Figure 4.2.6. *CDH1* expression in normal and cancerous hen ovaries, by diet and age. Expression of *CDH1* was measured in mRNA cDNA libraries constructed from normal and cancerous hen ovary homogenates, via qPCR. *CDH1* was measured in normal and cancerous hen ovaries (**A**). *CDH1* expression was also compared across ages (i.e. 2-year hen versus 3.5-year hen) and by degree of severity (i.e. normal, suspicious and frank carcinoma) (**B**). Suspicious ovaries were identified via H&E staining, specifically looking for anomalies such as hyper-nucleation, increased gland formation and reduced endothelial/stromal compartment within the ovary. Statistical values were determined using one-way ANOVA (Duncan's post hoc test, $p<0.05$). Groups without a similar letter are significantly different. Sample sizes ranged from n=7 to 9 per diet group. Error bars are +/- SEM.

4.2.6 Effect of DHA treatment on genes regulating epithelial phenotype and redox response in BG1 cells

After observing that FSH reduces *CDH1* transcript levels within hen ovarian tumors we

wanted to investigate the effect of 24-hour DHA treatment on *CDH1* levels in BG1 human ovarian cancer cells. In addition to *CDH1*, we included several genes that are known to negatively regulate epithelial phenotype (i.e. *SNAI1*, *SNAI2*, *ZEB1* and *VIM*) and also regulate redox response (*NQO1* and *HO1*). We observed a significant downregulation of *CDH1* at both 25uM and 50uM DHA, and *SNAI2* was downregulated at 50uM DHA (Figure 4.2.7). The redox response gene *NQO1* was elevated at both 25uM and 50uM, and the redox response gene *HO1* was elevated at 50uM (Figure 4.2.7).

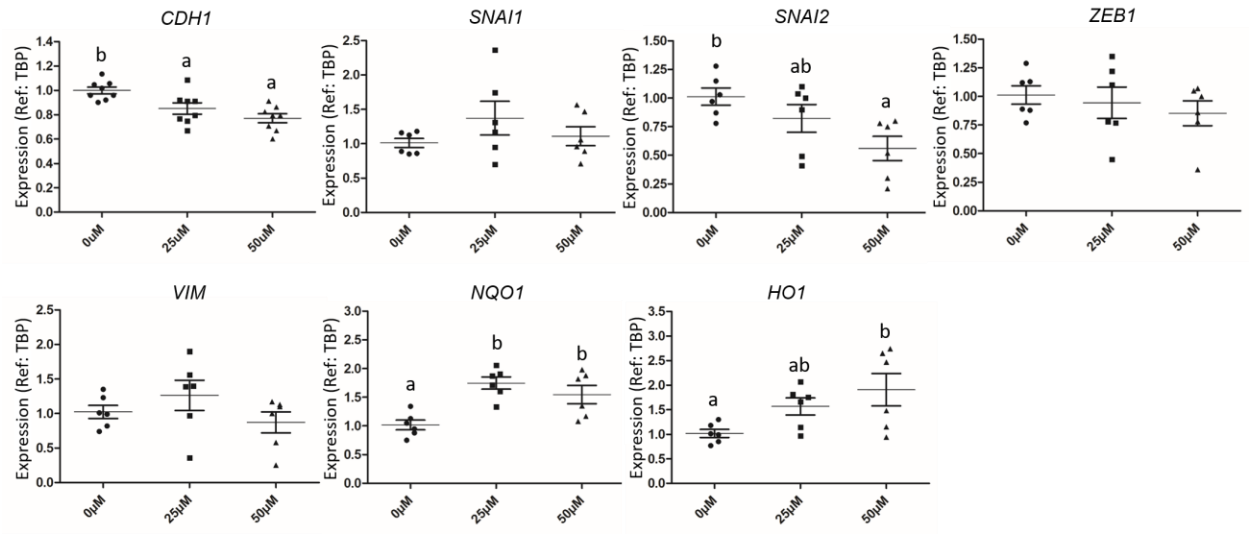

Figure 4.2.7. Effect of DHA treatment on the expression of genes regulating epithelial phenotype and redox response. RT-qPCR assay was conducted on BG1 cells that were treated with DHA for 24 hours in medium containing DMEM and 10% FBS. Tata-Box Binding Protein (*TBP*) was used as a reference gene. Four independent experiments (*n*=4) were conducted (in technichal duplicate per experiment) for the determination of *CDH1*. Three independent experiments (*n*=3) were conducted (in technical duplicate per experiment) for the determinantion of all other genes. Data in the graphs are normalized to 0μM DHA. One-way ANOVA and Duncan's Multiple Range Test ($p<0.05$) were used to identify statistically significant differences between groups. Groups without a similar letter are significantly different. Central lines represent mean, and the error bars are +/- SEM.

4.2.7 E-cadherin protein expression in hen ovarian tumors

We measured the level of 37kDa, 80kDa and 120kDa E-cadherin protein in hen ovarian tumors according to diet (Figure 4.2.8A). The 37kDa protein level was largely reduced by FXO and FSH, while the 80kDa protein was reduced by all treatment diets, with the biggest reduction of the 80kDa protein occurring in FXO hens. FXO and FSH were the only diets to reduce 37kDa

and 80kDa E-cadherin in ovarian tumors simultaneously. FXO exhibited a unique capacity to reduce the expression of 120kDa E-cadherin; however, this was versus WF hens, so it might be hard to interpret the meaning of that. Compositely, the FXO diet had the biggest effect on the expression of all molecular weights of E-cadherin (Figure 4.2.8A). All treatment diets reduced the ratio of 37kDa to 80kDa E-cadherin, while the ratio of 80kDa to 120kDa E-cadherin was not affected by diet (Figure 4.2.8B). The odds ratio of a hen having stage 4 ovarian cancer was significantly reduced by the FXO diet (O.R. = 0.32, c.i. 0.10 to 0.99, p=0.048), referenced to CTL hens. This distinguished the FXO diet, because no other diets displayed a significantly reduced risk of stage 4 ovarian cancer (Figure 4.2.8C). We then conducted non-parametric (Kruskal-Wallis) ANOVA on 37kDa and 80kDa E-cadherin in hen ovarian tumors (in order to appropriately compare 37kDa and 80kDa protein levels with the non-parametric odds ratio test), and the FXO diet was the only diet with a significantly reduced mean rank for the level of 37kDa and 80kDa E-cadherin, compared to CTL hens (Figure 4.2.8D). Said concisely, FXO hens exhibit reduced risk of stage 4 ovarian cancer concomitant with reduced levels of 37kDa and 80kDa E-cadherin.

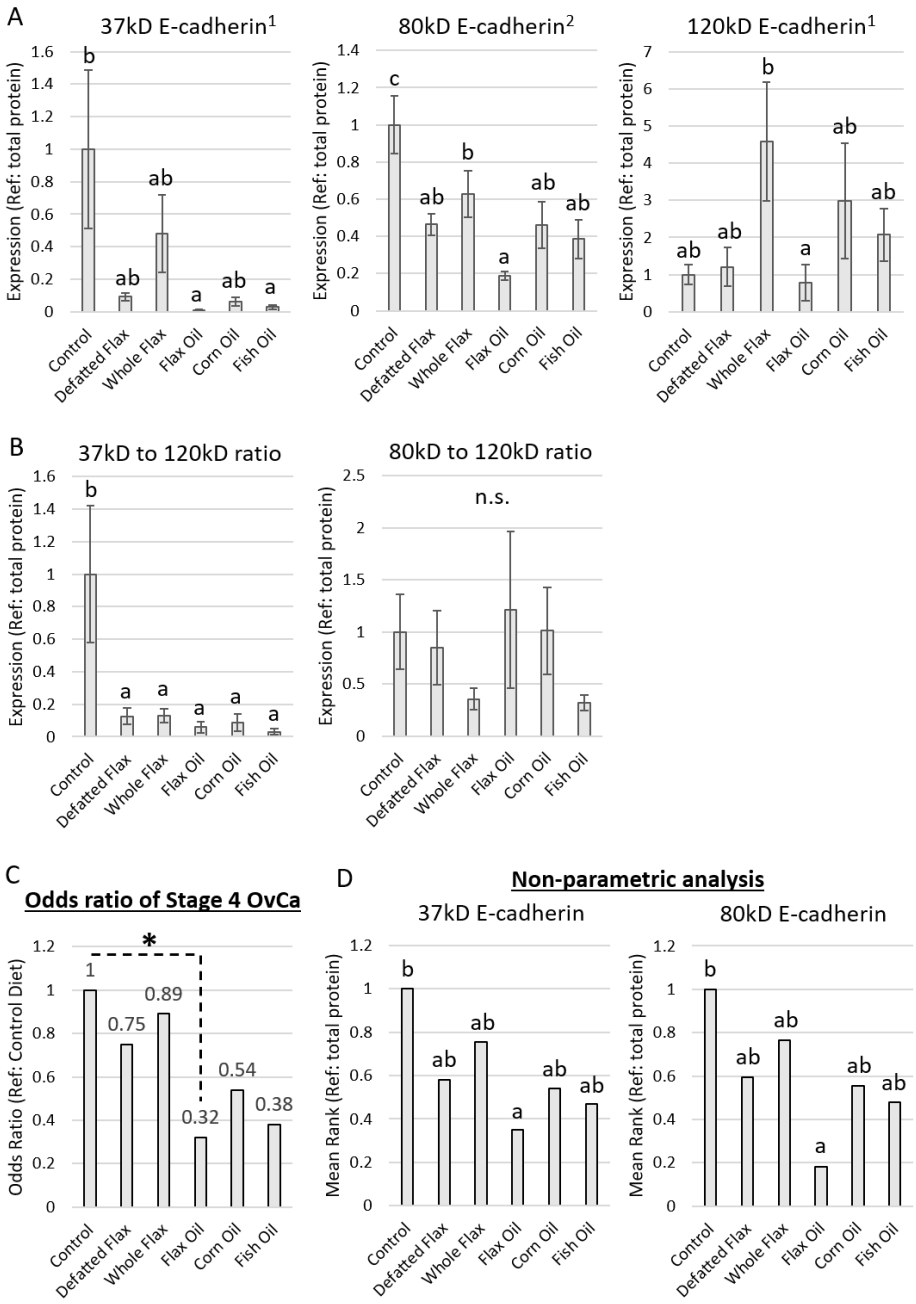
A
37kD E-cadherin1
80kD E-cadherin2
120kD E-cadherin1
Expression (Ref: total protein)
b
ab
ab
a
ab
a
c
ab
b
a
ab
ab
ab
ab
b
a
ab
ab
Control
Defatted Flax
Whole Flax
Flax Oil
Corn Oil
Fish Oil
B
37kD to 120kD ratio
80kD to 120kD ratio
n.s.
C
Odds ratio of Stage 4 OvCa
Odds Ratio (Ref: Control Diet)
*
1
0.75
0.89
0.32
0.54
0.38
D
Non-parametric analysis
37kD E-cadherin
80kD E-cadherin
Mean Rank (Ref: total protein)

Figure 4.2.8. Expression of E-cadherin protein in hen ovarian tumors. E-cadherin protein was measured in hen ovarian tumor homogenates via western blot (n=5 per diet group). The 37kDa and 120kDa E-cadherin proteins were evaluated with the mouse[1] IgG for E-cadherin, and the 80kDa E-cadherin protein was evaluated with the rabbit[2] IgG for E-cadherin (**A**). The ratio of the fragment to the full-length protein were then measured (**B**). One-way ANOVA with Duncan's post-hoc test ($p<0.05$) was used in A and B. Odds ratio analysis was conducted, evaluating the odds of a hen having stage 4 OvCa normalized by the odds of a hen not having stage 4 ovarian cancer, referenced to the CTL diet (**C**). In order to appropriately compare the odds ratio of stage 4 OvCa with the expression of 37kDa and 80kDa E-cadherin proteins, we conducted non-parametric Kruskal-Wallis ANOVA on 37kDa and 80kDa E-cadherin (Dunn's post-hoc test, $p<0.05$), in (**D**). Non-parametric ANOVA was used here, because odds ratio analysis is also non-parametric. Groups without a similar letter are significantly different. "*" denotes significantly reduced odds ratio. Error bars in A and B are +/- SEM.

4.2.8 Proteomics analysis of the 80kDa band in hen ascites fluid and hen ovarian tumor

One-dimensional electrophoresis was performed on a hen ascites sample and on a hen ovarian tumor, and the 80kDa protein band from both of these samples was analyzed via peptide mass fingerprinting. The results of that work can be seen in Table 4.2.2. Overall, seven peptide masses were detected. 7 out of 7 of these peptide masses were identified in the hen ascites sample, and 5 out of 7 of these peptide masses were identified in the ovarian tumor. Only two of the detected peptides (with masses of 718.233 and 1201.796) were within +/- 3 daltons of the *in silico* predicted peptide masses of the 80kDa E-cadherin protein. We used the amino acid sequence of the 80kDa extracellular domain for *in silico* trypsinized peptide mass prediction. If all two of these peptides are considered as hits, then we would only have 3.5% sequence coverage.

Table 4.2.2. Peptide mass fingerprint results from MS analysis of the 80kDa protein band from hen ascites fluid and hen ovarian tumor homogenate.

Peptide mass detected via MALDI-MS (Da)	Was the peptide detected in the 80kDa band from hen ascites fluid?	Was the peptide detected in the 80kDa band from hen ovarian tumor?	Nearest *in silico* predicted peptide mass that is within +/- 3 daltons of the detected peptide mass (Da)
674.893	detected	not detected	none
718.233	detected	detected	720.864
863.999	detected	not detected	none
1201.796	detected	detected	1201.408
1634.058	detected	detected	none
2261.290	detected	detected	none
2688.726	detected	detected	none

4.2.9 Mitochondrial membrane potential and oxygen consumption rate in ascites-treated IOSE80 cells

After hen ascites fluids were immunoprecipitated, we determined that the Control IgG ascites still contained the same concentration of 80kDa E-cadherin as the raw ascites fluid, whereas the E-cadherin IgG ascites fluid had only 8% of remnant 80kDa E-cadherin (Figure 3.2). We wanted to see the mitochondrial effects of using hen ascites fluid (with or 'almost without' the 80kDa fragment) on IOSE80 cells. We chose the IOSE80 cell line, because it is negative for E-cadherin (confirmed in our lab) while also being positive for EGFR (291). Most cells express receptor tyrosine kinases (RTKs), and this is the proposed receptor family for which 80kDa (i.e. soluble) E-cadherin is a putative activating ligand (269).

Mitochondrial membrane potential was measured in IOSE80 cells that were treated with Control IgG ascites or E-cadherin depleted ascites. Figure 4.2.9 illustrates the protein normalized fluorescence of IOSE80 cells that were treated with TMRE and CCCP, according to pre-incubation with Control IgG ascites or E-cadherin depleted ascites. Figure 4.2.9 was designed to allow the visualization of the values that are used to calculate Delta Psi ($\Delta\Psi$), specifically this

figure allows the visualization of the “TMRE only” fluorescence and the “TMRE + CCCP” fluorescence. The mathematical difference between “TMRE only” and “TMRE+CCCP” is how we determined the actual ΔΨ. The ΔΨ values can be seen in Figure 4.2.10. Treatment with 1:159 E-cadherin-depleted ascites increased the ΔΨ by 25%, in comparison to cells treated with 1:159 Control IgG ascites. ΔΨ was also slightly elevated by 1:159 E-cadherin-depleted ascites, versus vehicle-treated cells. According to Figure 4.2.9, the reduction of ΔΨ in 1:159 E-cadherin-depleted ascites was mainly due to a decrease of the “TMRE+CCCP” fluorescence. Treatment of cells with 1:39 E-cadherin-depleted ascites caused a 25% reduction of ΔΨ, in comparison to treatment with 1:39 Control IgG ascites. The 1:39 E-cadherin-depleted ascites also decreased ΔΨ versus the vehicle treatment. According to Figure 4.2.9, the reduction of ΔΨ in 1:39 E-cadherin-depleted ascites was mainly due to a decrease of the “TMRE only” fluorescence. Lastly, neither of the ascites fluids affected ΔΨ at the 1:79 concentration.

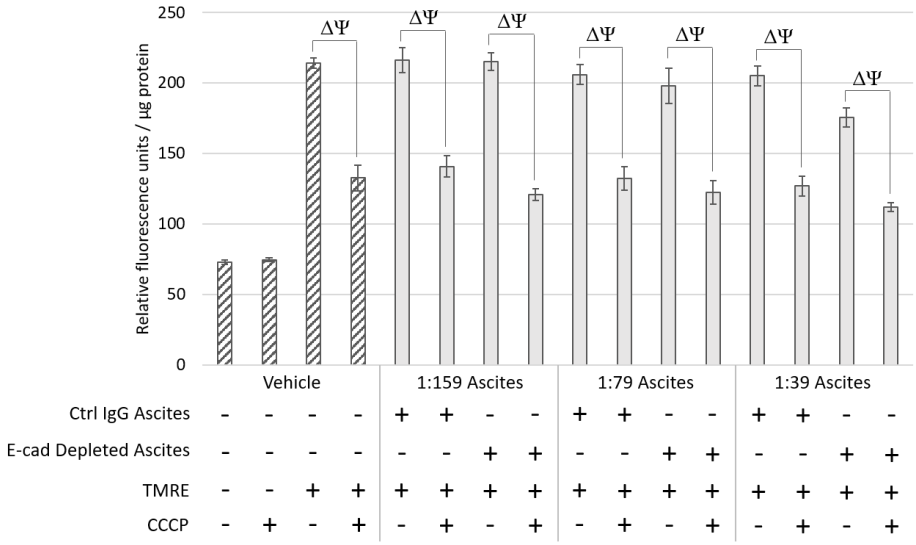

Figure 4.2.9. Analysis of mitochondrial membrane potential (using TMRE and CCCP) in IOSE80 cells treated with different concentrations of either Ctrl IgG-treated ascites or E-cad depleted ascites. IOSE80 cells were serum-starved for 24 hours and then treated with Control IgG ascites or E-cad IgG ascites for 24 hours at different concentrations (i.e. 1:159, 1:79 and 1:39). Mitochondrial membrane potential (ΔΨ) was then measured by calculating the difference between the TMRE-treated fluorescence and the TMRE+CCCP-treated fluorescence. All fluorescence values were normalized to total protein. The purpose of this figure is to allow a visualization of the baseline fluorescence (i.e. TMRE only) and the depolarized fluorescence (i.e. TMRE+CCCP) in IOSE80 cells, according to the concentration of ascites that was used to treat the cells. Each experiment was conducted four times with four technical replicates per treatment group (*n*=16 per treatment, in total). Error bars are +/- SEM.

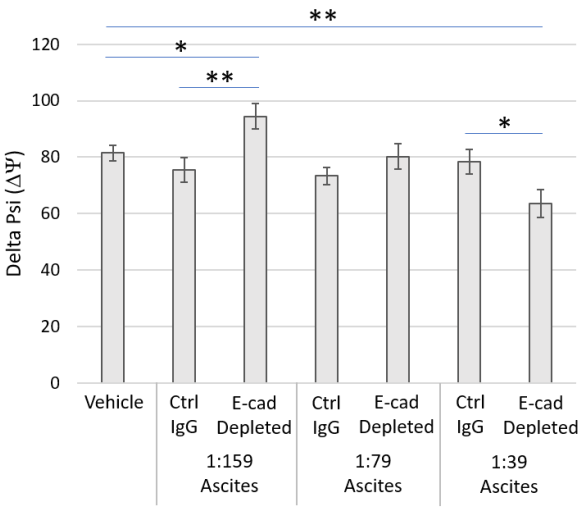

Figure 4.2.10. Calculation of Delta Psi (ΔΨ) in IOSE80 cells treated with either Control IgG ascites or E-cad depleted ascites. The ΔΨ values from Figure 4.2.9 were evaluated to determine the effects of ascites fluid on ΔΨ within IOSE80 cells. Statistical comparisons are between treatment groups of the same concentration (e.g. "Ctrl IgG 1:159" versus "E-cad IgG 1:159") or between treatment groups and the vehicle group (e.g. "E-cad IgG 1:159" versus "Vehicle"). Statistical comparisons were not made between treatments with different ascites concentrations (e.g. 1:159 versus 1:79). T-tests were used to detect differences between groups. Welch's correction was used when variances were unequal between groups. "*" denotes $p<0.05$, and "**" denotes $p<0.01$. Each experiment was conducted four times with four technical replicates per treatment group (n=16 per treatment, in total). Error bars are +/- SEM.

We conducted a dose response curve with each concentration of ascites fluid to determine the effect on mitochondrial oxygen consumption rate (OCR) in IOSE80 cells. The range of OCR appeared to be different for cells that were treated with E-cadherin IgG ascites (i.e. E-cadherin-depleted ascites) versus cells that were treated with Control IgG ascites (Figure 4.2.11A). For example, the OCR range for E-cadherin-depleted ascites cells was from 2pmol/min to

9pmol/min, whereas the OCR range for IgG Control ascites cells was from 0.5pmol/min to 3.5pmol/min. Due to this difference in OCR range between the acites treatments, we decided to normalize all OCR values to the vehicle and utilize these normalized values for the graphing of basal OCR, ATP Synthase-associated OCR, proton leak, uncoupling, coupling efficiency and total mitochondrial OCR. In general, we observed that ascites fluid concentrations at 1:159 and 1:79 had very comparable effects as compared to DMEM (vehicle), while ascites fluid concentrations of 1:39, 1:19 and 1:9, inhibited OCR in IOSE80 cells (Figure 4.2.11). The inhibitory effects on OCR increased substantially when going from ascites concentrations of 1:39 to 1:9. Specifically, mitochondrial coupling efficiency and mitochondrial uncoupling were stable at 1:159 and 1:79, while mitochondrial coupling efficiency declined and mitochondrial uncoupling increased when going from 1:39 to 1:9 ascites. Coupling efficiency can be defined as the proportion of ratio of ATP Synthase-dependent OCR divided by basal OCR, and uncoupling can be defined as non-mitochondrial OCR divided by basal OCR. Although this experiment (i.e. Figure 4.2.11) was only conducted one time, it helped us to realize that mitochondrial oxygen consumption is mostly stable at 1:159 and 1:79 ascites fluid concentrations. Given this, in addition to the observed effect of 1:159 E-cadherin-depleted ascites on $\Delta\Psi$, we chose to conduct further OCR analysis in IOSE80 cells treated with 1:159 ascites for 24 hours (i.e. Figure 4.2.12). In this experiment, the OCR parameters (e.g. basal respiration, ATP production, proton leak, coupling efficiency, uncoupling and mitochondrial OCR) were all normalized to vehicle before running statistical tests. Treatment with 1:159 Control IgG ascites increased the mitochondrial coupling efficiency and decreased mitochondrial uncoupling in IOSE80 cells, in contrast to vehicle (Figure 4.2.12). No further effects of 1:159 Control IgG ascites was detected. Given that we observed an effect of 1:39 ascites on $\Delta\Psi$, we also decided to conduct OCR analysis of 1:39

ascites. We were not able to detect any effect of 1:39 ascites on basal OCR, mitochondrial OCR or non-mitochondrial OCR (Figure 4.2.13).

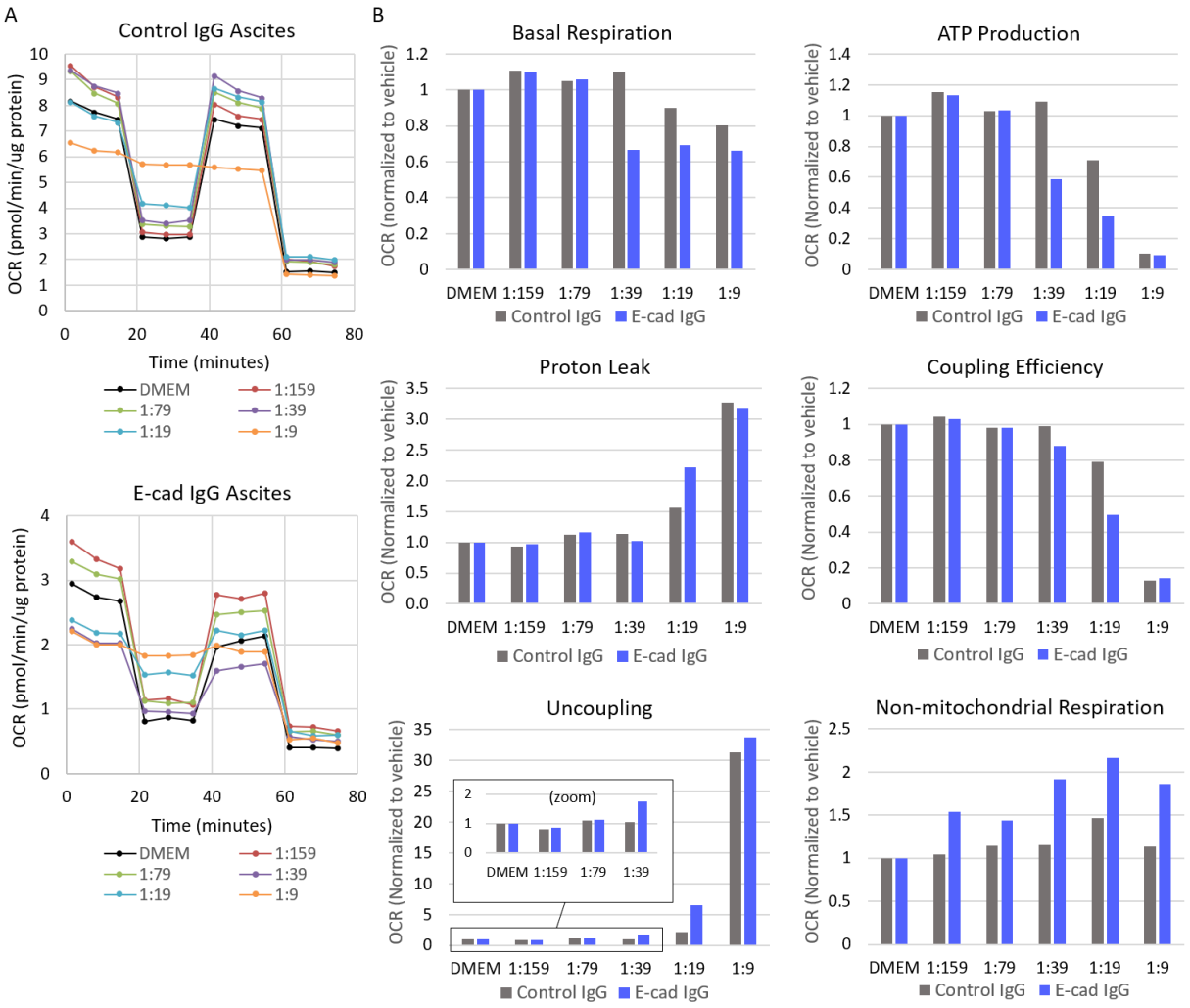

Figure 4.2.11. Dose response in IOSE80 cells treated with a gradient of ascites fluid. The Mitochondrial Stress Test was performed to evaluate the metabolic response of IOSE80 cells exposed to a series of 2-fold ascites fluid dilutions (n=1 experiment). The Seahorse line graphs show the protein normalized OCR values in response these serial dilutions of ascites fluid (**A**). Different cell respiratory parameters were calculated using the protein normalized OCR values in A, to illustrate the mitochondrial response in IOSE80 cells exposed to hen ascites fluid (**B**).

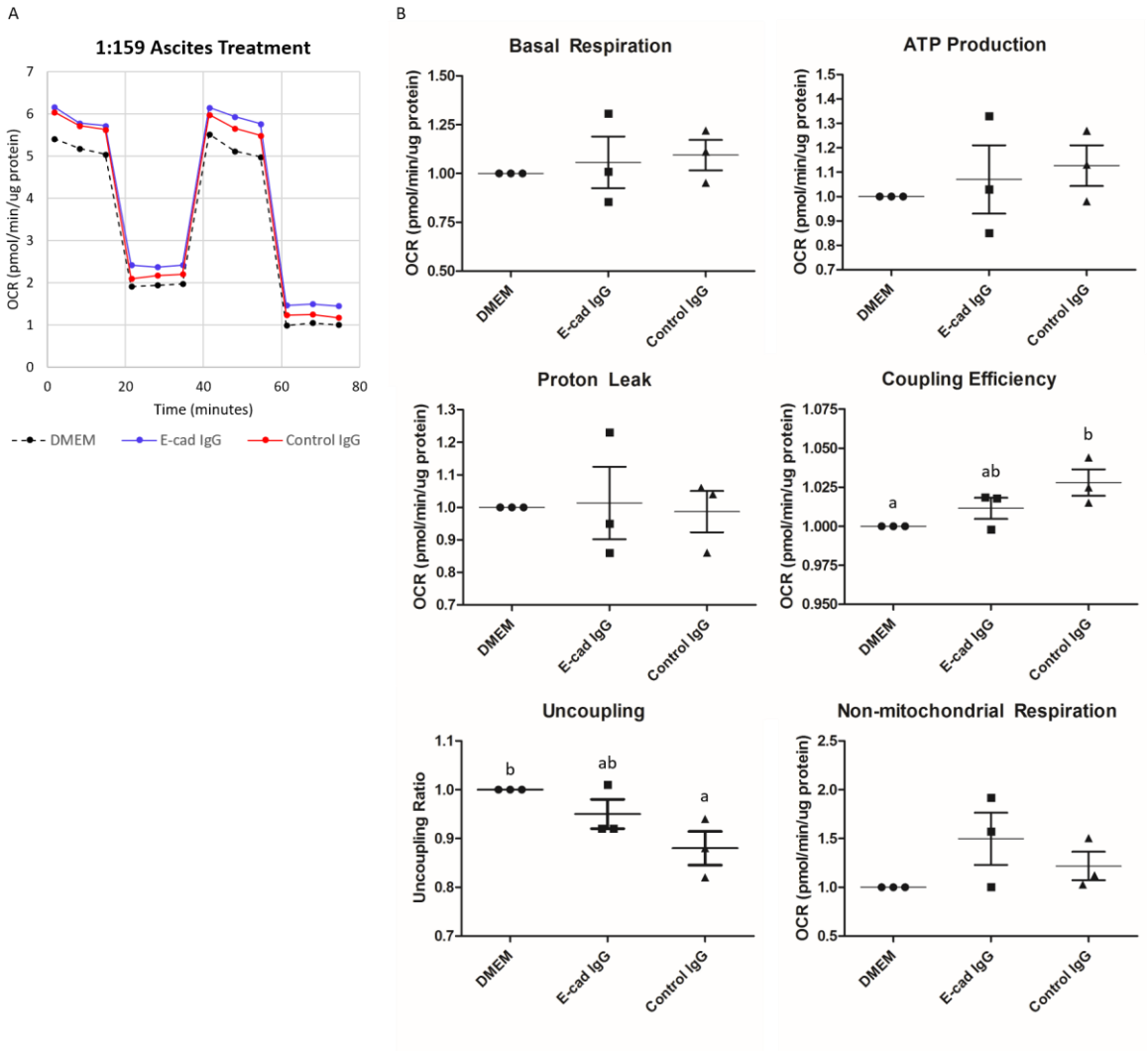

Figure 4.2.12. Metabolic response of IOSE80 cells treated with 1:159 ascites. The Mitochondrial Stress Test was performed to evaluate the metabolic response of IOSE80 cells exposed to a 1:79 dilution of hen ascites fluid (n=3 experiments). The line graphs show the protein normalized OCR values of IOSE80 cells given this treatment (**A**). Different cell respiratory parameters were calculated using the protein normalized OCR values in A, to illustrate the mitochondrial response in IOSE80 cells exposed to hen ascites fluid (**B**). One-way ANOVA with Duncan's post-hoc test was used ($p<0.05$). Graphs show means with error bars representing +/- SEM.

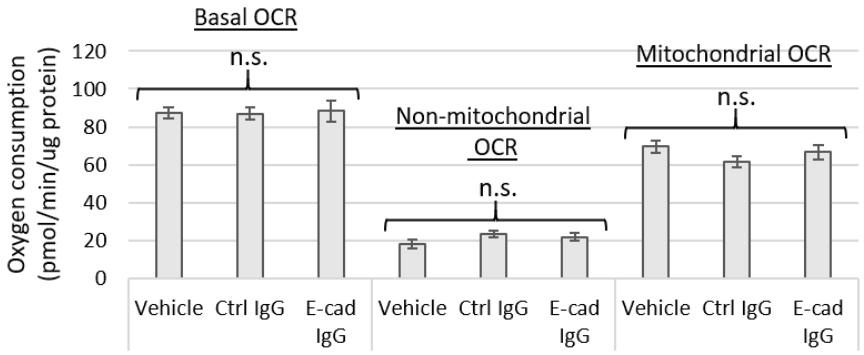

Figure 4.2.13. Oxygen consumption in IOSE80 cells treated with either 1:39 Control IgG ascites or 1:39 E-cad IgG ascites. IOSE80 cells were serum-starved for 24 hours and then treated with 5% ascites fluid (either Control IgG or E-cad IgG) and incubated for 24 hours, prior to conducting oxygen consumption analysis with Seahorse. The basal, non-mitochondrial and mitochondrial oxygen consumption rates were recorded for each treatment. Each experiment was conducted three times (*n*=3) in technical duplicate. One-way ANOVA with Duncan's post-hoc test was used ($p<0.05$). Error bars are +/- SEM.

4.2.10 Final model for the effects of dietary PUFAs within laying hen ovaries and human ovarian surface epithelial cells

We developed a final model for lipid metabolism, mitochondrial gene expression and phase 2 antioxidant gene expression, in hen ovarian tumors (Figure 4.2.14). Next, we developed a model that illustrates the effect of dietary PUFAs on miR-200a, *CDH1* and E-cadherin expression, in laying hen ovaries. This model also indicates the effect that reduced levels of the 80kDa E-cadherin protein have on mitochondrial membrane potential and oxygen consumption in IOSE80 cells (Figure 4.2.15).

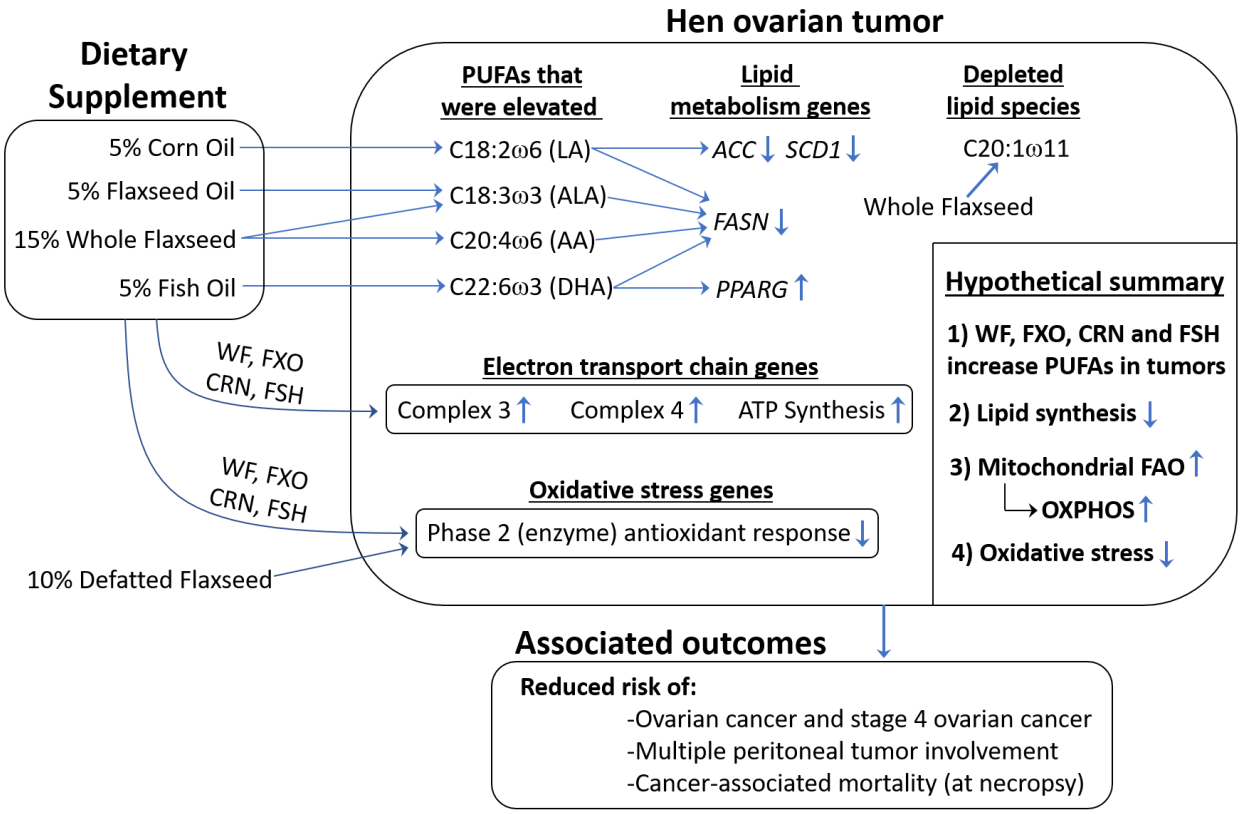

Figure 4.2.14. Model for the dietary regulation of fatty acid content, lipid metabolism, mitochondrial respiration and oxidative stress, in hen ovarian tumors.

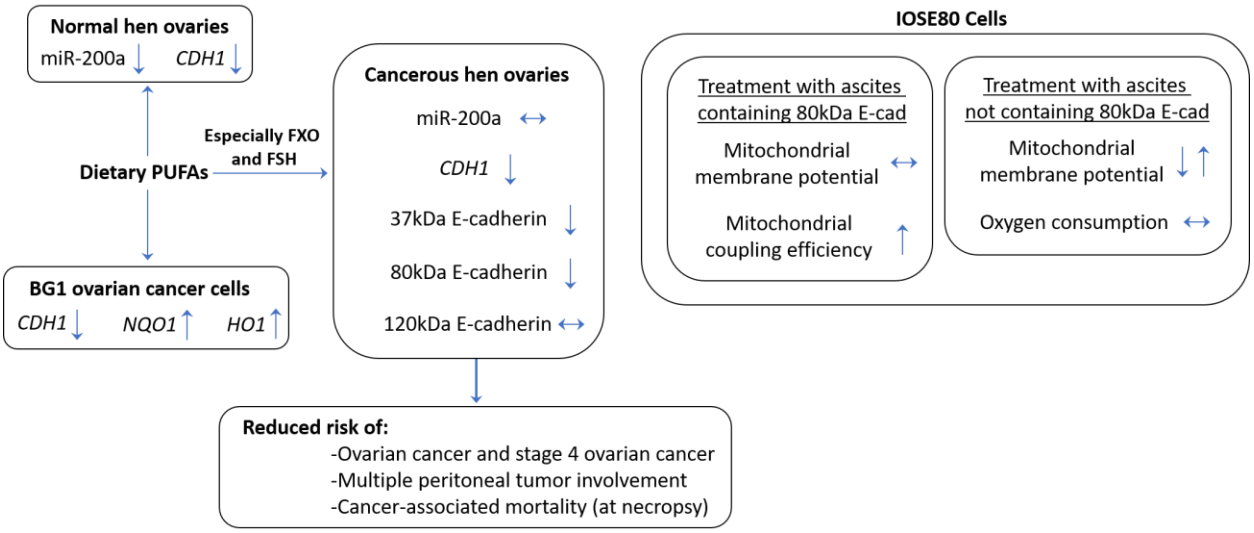

Figure 4.2.15. Model of dietary PUFA effects on miR-200, *CDH1* and E-cadherin in laying hen ovarian tumors. Also shown: the effect of 80kDa E-cadherin on mitochondrial bioenergetics in ovarian surface epithelial cells (IOSE80 cells).

CHAPTER 5

DISCUSSION & FUTURE DIRECTIONS

5.1 STUDY 1: FLAXSEED'S PARADOXICAL ROLE IN EXTENDING LIFESPAN AND REPRODUCTIVE CAPACITY IN WHITE LEGHORN LAYING HENS

5.1.1 Linatine: the "Trojan horse" that initiated the effect

Our hypothesis is that the anti-vitamin B6 molecule 'linatine' enhances lifespan and reproductive capacity in White Leghorn laying hens. Linatine is found in the cotyledon compartment of flaxseed (i.e. it can be found in DF and WF) (59). Therefore, our general hypothesis is that DF and WF enhance lifespan and/or reproductive capacity in laying hens through the effects of the linatine molecule. Our specific aims were to: 1) build a metabolic map that elucidates linatine's effects on one-carbon metabolism in laying hens, and 2) develop a rationale that either refutes or supports the hypothesis that linatine increases lifespan and/or reproductive capacity in laying hens. In brief, we observed daily mortality, daily egg laying and endpoint body weights in hens consuming one of six isocaloric diets for 325 days. On the 210th day of the study we collected blood plasma samples from hens and utilized LC-MS/MS to measure 108 plasma metabolites. We have conducted several previous studies where we used flaxseed with White Leghorn hens, and the results of those studies are used to help us interpret our current plasma metabolomics-based study.

5.1.2 Decreased vitamin B6 concomitant with a transsulfuration blockade: the canonical effect of linatine

Researchers propose using a combination of direct vitamin B6 markers (i.e. PLP, PL, etc) and functional B6 markers (i.e. cystathionine, glycine, etc) when evaluating a patient's vitamin B6 status (292). The reason for using direct markers and functional markers is that other factors such

as glomerular filtration might obscure a single B6 marker. During our analysis, plasma 4-pyridoxic acid (4PA) was decreased concomitant with elevated cystathionine, in DF and WF hens. Therefore, we have evidence of direct and functional effects associated with variation of vitamin B6. The plasma 4PA perturbation was strongest in DF hens, while this effect was near significant ($p<0.07$) in WF hens. Regardless of significance, the cystathionine elevation in DF or WF hens exceeded 15-fold versus CTL hens and approached 200-fold versus FXO and CRN hens. Said concisely, cystathionine was elevated by 'order(s) of magnitude' in DF and WF hens. Other researchers have observed a similar pattern of effect in rats consuming synthetic 1ADP (1). We did not assay the concentration of linatine in our DF or WF diets at the time of our study (year 2014); however, other researchers confirmed via UPLC-MS that linatine is a naturally-occurring molecule in flaxseed, independent of geographic cultivar (293). Our 10% DF diet and 15% WF diet were calibrated to provide a similar mass of flaxseed's non-oil component (i.e. the hull, lignan, fiber, cotyledon portion that contains linatine). 4PA and cystathionine were stable in FXO hens, supporting a lack of effect in our most appropriate negative control group (i.e. FXO hens). Cystine (a di-cysteine molecule) did not appear to be affected by diet; however, flaxseed's natural cysteine content (35,294) might appropriately supplement cysteine and prevent cysteine depletion. Researchers in rats observed that cysteine was not affected by high dose 1ADP (1), similar to our work with flaxseed-fed animals. Our data also suggested that glycine (an amino acid that is essential for glutathione synthesis) was not affected by diet. This is without surprise because flaxseed is a rich source of glycine (35). We can argue that flaxseed should not inhibit glutathione synthesis in hens, because we see no effect at the level of cystine or glycine. More research is needed to determine if flaxseed reduces TS flux to an extent that makes cysteine an 'essential' amino acid that must be acquired through the diet. In our metabolomics, the level of

reduced glutathione (i.e. GSSG) was not affected by diet, but GSSG alone cannot provide sufficient information about the total glutathione content. Further work would need to be performed to determine flaxseed's effects on glutathione synthesis, but preliminarily it seems that flaxseed does not insult key anabolic substrates used in glutathione synthesis (namely cystine and glycine). Interestingly, taurine was slightly lower in WF hens. Taurine biosynthesis requires two additional B6-dependent reactions beyond *CBS* and. In other words, taurine synthesis requires four B6-dependent reactions including those of the TS pathway, suggesting that taurine might be lower in WF hens due to anti-B6 burden. Another possibility is that taurine, as a facilitator of oxidative reactions such as fatty acid oxidation (FAO) in mitochondria (295), might be lower in WF hens due to increased taurine catabolism supporting mitochondrial FAO. Future work needs to evaluate if taurine is regulated more so by catabolic or anabolic processes. This would also help researchers to understand taurine because the taurine-related literature is fairly lacking.

A comparison of our study with previous work conducted in rats led us to suspect that transsulfuration might be more easily perturbed in laying hens versus rats. Our DF hens displayed 63% reduced 4PA levels with 15-fold elevated cystathionine. Rats consuming the anti-B6 molecule 1ADP displayed 68% reduced 4PA levels but only 4-fold elevated cystathionine (1). More information is needed, but this introduces the notion that chicken CSE and chicken CBS might have lower binding affinities for PLP compared to rat, and therefore, slight perturbations of B6 might have dramatic effects on TS activity in chickens.

The researchers in (1) also showed that 1ADP-fed rats have 4-fold elevated cystathionine with 1.4-fold elevated Hcy (1). If 4-fold elevated cystathionine can correlate with 1.4-fold elevated Hcy, then it seems very expected that 15 to 16-fold elevated cystathionine (as we saw in DF and

WF hens) would be accompanied with elevated Hcy. However, we saw no elevation of Hcy in DF and WF hens, giving us reason to suspect that Hcy is fluxing back into the Met cycle.

5.1.3 The new fate of Hcy: increased flux of Hcy into the Met cycle (causing elevated SAM)

HyperHcy did not accompany the vastly elevated cystathionine in DF and WF hens. Murine studies suggest that hyperHcy is a common outcome of TS inhibition (1,66,296–298). In the absence of hyperHcy, and without any indication of Hcy fluxing toward SAH, the most probable outcome appears to be an increased flux of Hcy into the Met cycle (i.e. increased Hcy remethylation). This Hcy flux is similar to the idea of "thiol recycling" within the Met cycle, presumably at a rate that is inversely proportional to TS flux. A key effect of this flux of Hcy remethylation appears to be elevated SAM production in DF and WF hens. DF hens exhibited the first evidence of this flux, with 1.9-fold elevated SAM. DF hens also displayed a 1.9-fold elevated SAM:SAH ratio. The SAM:SAH ratio was statistically similar between WF hens and DF hens, suggesting that methylation capacity might be somewhat similar between DF and WF hens.

All diets were supplemented with equal DL-Met (i.e. 0.1% calories as DL-Met), so hens consumed a comparable level of Met across diets. Our DF diet had a marginally higher calculated Met+Cys content (i.e. 0.72% TME versus 0.67% TME, as Met+Cys). Previous work in laying hens indicates that this percentage difference in Met+Cys does not elicit appreciable differences in amino acid profiles, feed intake, feed efficiency, egg production or weight gain, in chickens (299). Furthermore, this slight difference in Met+Cys is a "calculated difference" and might not have an actual metabolic effect.

In the metabolomics, why is SAM not elevated in WF hens? If linatine induces a flux of Hcy into the Met cycle, we would expect SAM to be elevated in WF hens as well as DF hens. We

suspect that excess SAM was catabolized by PEMT, in WF hens. We discuss this in much greater detail in sections referring specifically to the role of PEMT.

5.1.4 Anecdotal evidence of increased methylation capacity in flaxseed-fed hens

We observed several anecdotal phenomena that complement our observation of 1.9-fold elevated SAM:SAH ratio in hens consuming 10% DF. Firstly, during our current reanalysis of microarray features previously published in (14), we detected a high percentage of significantly downregulated microarray features in normal and cancerous ovaries when hens consumed 10% WF. Those hens also displayed sharply downregulated microRNA-200 family members (miR-200a, 200b, and 429) in cancerous ovaries (14). In other words, laying hens consuming 10% WF display a concomitant downregulation of microarray features and microRNA species. This suggests that flaxseed regulates the levels of RNA molecules either pre-transcriptionally and/or post-transcriptionally. The increased methylation capacity of a flaxseed-fed hen might play into this process. Histone protein methylation (300,301) and DNA methylation (68) are specific means by which one-carbon metabolism regulates RNA expression pre-transcriptionally. Scientists are also becoming more aware of the post-transcriptional regulation of RNA molecules via the abundant N6-methyladenosine mark that can guide RNA molecules (mostly mRNA) through the YTHDF2-mediated RNA decay pool (108,302). The N6-methyladenosine mark also guides mRNA molecules through the YTHDF1 and YTHDF3-mediated protein translation pathways. In light of these processes, we can hypothesize that the methylation capacity of a flaxseed-fed hen influences chromatin structure, transcriptional binding, RNA half-life and protein translation, in the ovary of the hen (independent of pathology) and culminates in widely downregulated RNA transcription and/or decreased RNA half-life.

Our lab previously observed that dietary flaxseed boosts the level of 2-methoxyestradiol (2-

MOE) in the serum of hens (16). This finding might indicate higher methylation capacity in flaxseed-fed hens, given that 2-MOE is produced during the SAM-dependent methylation reaction between catechol-O-methyltransferase (COMT) and 2-hydroxyestradiol. The 2-hydroxylated carbon of 2-hydroxyestradiol is methylated by COMT to a 2-methyl carbon, forming 2-methoxyestradiol (303). Our lab has also illustrated that 2-MOE induces proapoptotic and antiangiogenic effects in laying hen ovarian cancer and in human ovarian cancer cell lines (21). 2-MOE has been implemented in several human cancer clinical trials with tolerable effects and positive results (304).

5.1.5 The BHMT pathway: supporting increased flux of Hcy into the Met cycle

Betaine can be derived directly from the diet or it can be synthesized via choline oxidation. In the liver, a large amount of choline is irreversibly oxidized to support betaine synthesis. Betaine drives the BHMT reaction that culminates in the remethylation of Hcy. We observed a high correlation between choline and betaine in our metabolomics (r=0.81), suggesting that choline oxidation might be increased in support of betaine synthesis. Increased BHMT activity in WF hens was suggested by their elevated Met:betaine ratio (Met is output of BHMT). Therefore, the vastly lower choline level and slightly lower betaine level in WF hens might be the result of elevated oxidation of choline in support of BHMT activity. In WF hens, the expression pattern of BHMT's negative regulators (DMG, SAM and MTA) favor net loss of inhibition of BHMT (i.e. gain of function), which compliments the increased Met:betaine ratio in WF hens. Altogether, the metabolomics provide a surrogate indication that BHMT activity might be increased in WF hens. In DF hens, choline was slightly decreased while betaine was not affected. Given that DF hens had only slightly reduced choline and no effect on betaine, we feel that DF hens had moderate flux through BHMT. The expression pattern of BHMT's negative regulators suggest a

net gain of inhibitory capacity against BHMT, which fits in line with the finding that choline was only slightly reduced while betaine was not affected. The fact that choline was lower in both WF and DF hens versus FXO hens suggests that the "non-oil compartment" (i.e. linatine compartment) of flaxseed might be responsible for reducing choline levels in hens. Interestingly, the negative effect on choline was noticeably larger than the negative effect on betaine, possibly reflecting the specialized ability of hepatocytes to store betaine thus making it harder to deplete betaine. Soluble choline, on the other hand, would be easier to spontaneously deplete. Choline depletion has been shown to activate PEMT, the master regulator of *de novo* PC synthesis (81,89,305). The observation of 39% reduced choline in WF hens helped us to consider the possibility of elevated PEMT activity.

Choline is likely undergoing net catabolism in WF and DF hens: This is an important point to make, because our model suggests that choline is being oxidized to support BHMT. Therefore, it behooves of us to strengthen our argument that choline is undergoing net catabolism. The complete oxidation of choline culminates in numerous reactions that produce "dissipative structures" that can readily contribute to mass loss. Those specific reactions are shown here, with dissipative structures underlined in **bold**:

Betaine aldehyde dehydrogenase: Betaine Aldehyde → Betaine + NAD**H**

Dimethylglycine dehydrogenase: Dimethylglycine + THF → Sarcosine + 5,10-CH_2THF + **e^- (Ub pool)**

Sarcosine dehydrogenase: Sarcosine + THF → Glycine + 5,10-CH_2THF + **e^- (Ub pool)**

Glycine cleavage system: Glycine + THF + NAD^+ → 5,10-CH_2THF + **CO_2** + **NH_3** + NAD**H** + **H^+**

In line with Ilya Prigogine's Nobel prize-awarded theory of dissipative structures in biological systems (306,307), the outputs of choline oxidation can dissipate from the physical body in the form of metabolic water, CO_2, NH_4^+ or radiant heat, and thereby contribute to mass

reduction from the organism. This perspective assumes that NADH has a high capacity for oxidation at complex 1 of the ETC, yielding NAD^+, e^-, and H^+ (with e^- and H^+ ultimately forming metabolic water). In our study, the positive correlation between hen body weight and choline was strong across diet groups (R=0.94). Choline oxidation is also tightly coupled to the oxidation of de-esterified free fatty acids (FFAs) originating from the PC molecule. One molecule each of NADH, $FADH_2$, and acetyl-CoA, is created for every two acyl carbons that are consumed via mitochondrial beta-oxidation. NADH and $FADH_2$ each contribute an 2 electrons into the ETC, while acetyl-CoA can be oxidized in the TCA to generate 3NADH and $FADH_2$. These molecules can then contribute to mass reduction from the body, primarily in the form of metabolic water and CO_2. It is likely that the correlation between choline and body weight is a surrogate correlation between the beta-oxidation of PC-derived FFAs and body weight, because the mobilization of choline from PC probably generates a significant pool of FFAs that must be oxidized by the mitochondria in order to prevent intracellular lipotoxicity.

Regardless, choline oxidation is a contributor to mass reduction. We think that the level of choline observed in WF and DF hens indicates net increased catabolism of choline, particularly given the correlation between choline and physiological weight of the hen. In our previously published study of 2-year-old hens (2), the body weights of WF and DF hens were 14% and 7% lower than control hens, respectively. In our current study of 3.5-year-old hens, the body weights of WF and DF hens were 10% and 5% lower than control hens, respectively. These results indicate that younger hens might lose more weight than older hens when consuming a flaxseed diet, but the ratio of weight loss is approximately 2:1 for WF hens versus DF hens, at either age.

5.1.6 MS-B12 in our model: supplemental help to BHMT

The metabolomics suggests that DF hens might have slightly elevated BHMT activity. After

observing how strongly WF hens might be utilizing BHMT, we think it is very reasonable to predict that DF hens need slightly elevated MS-B12 activity in order to supplement Hcy flux into the Met Cycle. Our assumption is that the Hcy burden in WF and DF hens is similar, given the similarly high cystathionine in both groups of hens. After accounting for all factors (i.e. urinary loss of DMG in addition to the complete oxidation of DMG to glycine), one molecule of DMG might culminate in the methylation of 0.25 to 0.50 molecules of Hcy via MS-B12. In DF hens, this would not be enough remethylation support from MS-B12 to prevent hyperHcy, and therefore, additional 5,10-CH_2THF input from carbon donors such as serine would be required. We predict that a moderate flux through MS-B12 combined with a moderate flux through BHMT might be the way in which DF hens maintain stable Hcy levels. WF hens, contrarily, might be hyperactivating BHMT to a degree that diminishes the need for supplemental support from MS-B12. Accelerated MS-B12 activity would likely require increased flux of one-carbon units into the folate cycle in order to yield more 5,10-CH_2THF as substrate for MTHFR. In DF hens, we observed lower DMG levels, slightly lower serine levels, slightly lower serine:glycine ratio and possibly lower histidine levels. It is powerful to see this entire group of metabolites decreased in this manner, because we would predict increased catabolism of these molecules in support of 5,10-CH_2THF synthesis (to drive enhanced MS-B12 activity), in DF hens. The decreased DMG levels observed in DF and WF hens might represent increased DMG catabolism via DMGDH, which would indicate increased 5,10-CH_2THF synthesis. The slightly lower serine level and slightly lower serine:glycine ratio in DF hens might suggest enhanced SHMT1 and/or SHMT2 activity in support of 5,10-CH_2THF synthesis. The challenge here is that flaxseed (via linatine) moderately affects B6 levels, and SHMT1 and SHMT2 are B6-dependent enzymes. We observed 63% reduced 4PA levels in DF hens, and we do not know whether PLP (active B6) was

perturbed in either DF or WF hens. Research in rats suggests that plasma PLP can be statistically stable even when plasma 4PA is reduced by 68% (in rats consuming B6 sufficient diets) (1). According to our results, flaxseed perturbs B6 metabolism within healthy animals; however, the effect might not cause significantly perturb the 'active B6 vitamer', PLP. Research suggests that human SHMT2 maintains catalytic activity in the presence of moderate B6 deficiency (140,308). If SHMT2 can resist moderate B6 deficiency, then it might not be possible for a 15% WF diet or 10% DF diet to perturb SHMT2 in animal models. And therefore, SHMT2 activity might be fully in-tact in flaxseed-dieting hens, and the decreased level of serine and the decreased serine:glycine ratio in DF hens might be the result of increased SHMT2 consumption of serine. This could lead to a large contribution of one-carbon units toward the synthesis of 5,10-CH_2THF, which would help to elevate Hcy flux through MS-B12.

Interestingly, DF hens had increased thymidine levels. Thymidine is the substrate for thymidine kinase (TK). TK supplements Thymidylate Synthase (TYMS) when dTMP needs cannot be met solely by TYMS alone. Therefore, if thymidine is being spared due to reduced TK activity that might suggest increased TYMS activity, in DF hens. Two specific factors might be driving elevated TYMS activity in DF hens. In other words, the elevated thymidine in DF hens might be the result of elevated flux of 5,10-CH_2THF through the folate cycle. Elevated 5,10-CH_2THF flux through the folate cycle could be the result of increased SHMT activity contributing to the synthesis of 5,10-CH_2THF, in DF hens. Another explanation for increased TYMS activity could be the role of SAM as an MTHFR inhibitor, forcing increased flux of 5,10-CH_2THF through TYMS. Increased flux through TYMS might allow ample dTMP synthesis, thus keeping TK activity low and thymidine levels high, in DF hens. Perhaps both phenomena (i.e. increased SHMT activity and increased MTHFR inhibition) might be occurring

simultaneously in DF hens, and that might explain the statistically higher level of thymidine.

5.1.7 Clustering of diets according to one-carbon donor molecules

K-means hierarchical clustering analysis was performed to illustrate how individual plasma samples cluster according to one-carbon donating molecules. Nearly all (16 of 17) plasma samples from hens consuming either DF, WF or FXO were grouped into two adjacent clusters, suggesting a global similarity of flaxseed's effect on one-carbon donors. DF hens formed a tight cluster, suggesting a unique effect of flaxseed's "non-oil" component. Several WF hens were closely related to DF hens, further indicating a unique effect of flaxseed's "non-oil" component. FXO hens were more distanced from DF hens, and we found this to be sensible because DF has low oil content. WF and FXO hens were generally clustered, indicating a somewhat unique effect of flaxseed's oil component. CRN hens and FSH hens were grouped into two clusters that were distant from all flax-based clusters, suggesting that CRN and FSH had similar effects on one-carbon donors but those effects were quite different from the effects observed in flax-based diets.

5.1.8 PEMT: an unexpected 'juggernaut' in flaxseed-dieting hens?

Our suspicion is that PEMT hyperactivation drove the depletion of excess SAM in WF hens. PEMT was recently elucidated as the primary SAM consumer in physiology, with PEMT'*s* substrate, PE, acting as the primary 'sink' for excess SAM (77). PEMT consumes up to 50% of all physiological SAM, with PEMT and Guanidinoacetate Methyltransferase (GAMT; ie creatine synthesis) compositely accounting for 85% of total SAM consumption (78,79,104,309). We observed no indication that GAMT activity was affected by diet (Figure Appendix S3), and therefore, PEMT would be the most probable enzyme to explain why SAM was not elevated in WF hens.

5.1.9 Phenotypic evidence of PEMT hyperactivation in flaxseed-fed hens

As far as we know, we are the first lab to observe that flaxseed might induce PEMT hyperactivation in a wild-type vertebrate animal model. We observed three examples of phenotypic evidence that the flaxseed diet induces PEMT hyperactivation in hens.

1) Flaxseed hens have a high PC:PE ratio: A high PC:PE ratio is a canonical marker of elevated PEMT activity. In laying hens, a WF diet elevates the hepatic PC:PE ratio to 3.78 (310). Anyone who is familiar with physiological PC:PE ratios would recognize that 3.78 is somewhat high. However, when the researchers in (310) added a choline supplement on top of the WF diet, the PC:PE fell from 3.78 to 2.31 due to 39% less hepatic PC (310). This 39% reduction of hepatic PC is tremendously eye-opening, because our WF hens had 39% lower plasma choline compared to hens consuming our CTL diet. Did the choline supplement from (310) fill a '39% choline deficit' in WF-fed hens and thereby provide a 39% negative feedback to PEMT, causing PC synthesis to decline 39%? Choline deficiency is already known to stimulate PEMT activity, simply because PEMT is the only enzyme that can biosynthesize choline (81,89). Therefore, we hypothesize that, "the flaxseed diet, by forcing increased oxidation of choline to support elevated BHMT activity, queues PEMT to produce a proportionally higher amount of PC (i.e. 39% more PC)." Interestingly, a 39% decrease in hepatic PC (as was observed in (310)) is also analogous to the inhibition of PEMT, because PEMT normally provides 30% of hepatic PC (88). The researchers in (310) also observed severe liver pathology in their WF-fed hens that were provided a choline supplement, supporting the notion that the 39% decrease of hepatic PC was likely due to PEMT inhibition. PEMT, as a synthesizer of PC, is critical for the packaging and secretion of VLDL from the liver, illustrating why PEMT inhibition vastly elevates the risk of hepatic steatosis (311–314). This might be precisely what the researchers in (310) experienced

with their WF-fed hens that were provided a choline supplement.

2) Improved liver health concomitant with elevated blood glucose: Recent work shows that wild-type mice have exceptionally improved liver health with the offsetting effect that blood sugar rises, particularly when mice consume a high fat diet (314,315). Our lab has already shown that our 15% WF diet and (to a slightly lesser extent) our 15% DF diet promotes excellent liver health in hens (2). Both the WF and DF hens presented with 80% lower hepatic AST levels, while the WF hens also had 29% lower liver weight and overall decreased scores for hepatic steatosis and non-alcoholic fatty liver disease (NAFLD) (2). Simultaneously, the WF and DF hens had 6.23% and 5.34% glycated hemoglobin (HbA1c) levels compared to 1.90% in control diet hens (2). In other words, flaxseed caused a 3-fold elevation of long-term blood glucose in hens. This elevation in HbA1c is higher than the HbA1c values observed in hummingbirds (161), meaning that flaxseed converts the metabolism of the chicken to a hummingbird-like metabolism. This phenotype of improved liver function with elevated blood glucose is similar to the phenotype of $PEMT^{+/+}$ mice (314,315), where hepatic health was improved at the cost of increased blood glucose during high fat dieting. We did not measure HbA1c in the hens from our current study; however, the DF and WF hens were previously observed with nearly 3-fold elevated HbA1c. In our current study, the DF and WF hens displayed slightly reduced pyruvate (possibly indicating gluconeogenesis), concomitant with elevated C3-carnitine (propionylcarnitine), C5-carnitine (isovalerylcarnitine) and C8-carnitine (octinoylcarnitine). C3, C5 and C8-carnitine are markers of elevated HbA1c in diabetic humans (282), suggesting that blood glucose might be elevated in the WF and DF hens in accordance with elevated acyl carnitines. We do have some evidence that liver function was improved by flaxseed in our current study; the WF hens from our current study exhibited 40 to 60% lower blood AST (316).

3) The WF diet appears to induce SAHH activity: SAHH is the enzyme that hydrolyzes SAH into the byproducts Hcy and adenosine. In our current study, the Hcy:SAH ratio and the adenosine:SAH ratio were simultaneously elevated in WF hens, suggesting increased hydrolysis of SAH by SAHH. The levels of adenosine and dAMP (dAMP is formed from adenosine) were also elevated in WF hens, further supporting increased SAHH output. Accelerated SAH hydrolysis via SAHH is essential to sustaining elevated PEMT activity, because SAH functions as a potent inhibitor of methyltransferases (110). It is already known that PEMT is a major activator of SAHH given the tremendous amount of SAH produced by PEMT (79,317). PEMT hyperactivation increases *SAHH* mRNA and SAHH protein levels in eukaryotic cells, likely in support of accelerated SAH hydrolysis (77).

5.1.10 Laying hens are a good animal model for studying PEMT, because PEMT is positively regulated by estrogen

Postmenopausal women and all men are at higher risk of organ (e.g. liver) pathology associated with choline deficiency, whereas premenopausal women have lower risk of choline deficiency (318). The idea behind this is that the human *PEMT* DNA locus has been shown to be positively regulated by estrogen (likely via estrogen response elements, EREs) (319,320). The notion that *PEMT* is regulated by estrogen originated (although unknowingly at the time) from a study of White Leghorn hens and roosters in 1940, when blood phospholipid levels increased following treatment with natural and synthetic estrogens (321). Similar results were repeated in 1981 when synthetic estrogen stimulated PC synthesis in roosters (322). Our lab identified (via NCBI Genbank) a complete ERE palindrome +424bp from the transcription start site of chicken (*Gallus gallus*) *PEMT* including five AP-1 enhancers between -1,510bp and +42,485bp from the start site (Figure 5.1.1). Further studies are needed to investigate the functionality of these

potential binding sites. Laying hens have diurnal LH surges every 24 hours (323), aligning diurnal estrogenic activity with daily egg laying tempo. It is possible that PEMT is a critical enzyme for supporting the daily egg laying tempo of laying hens.

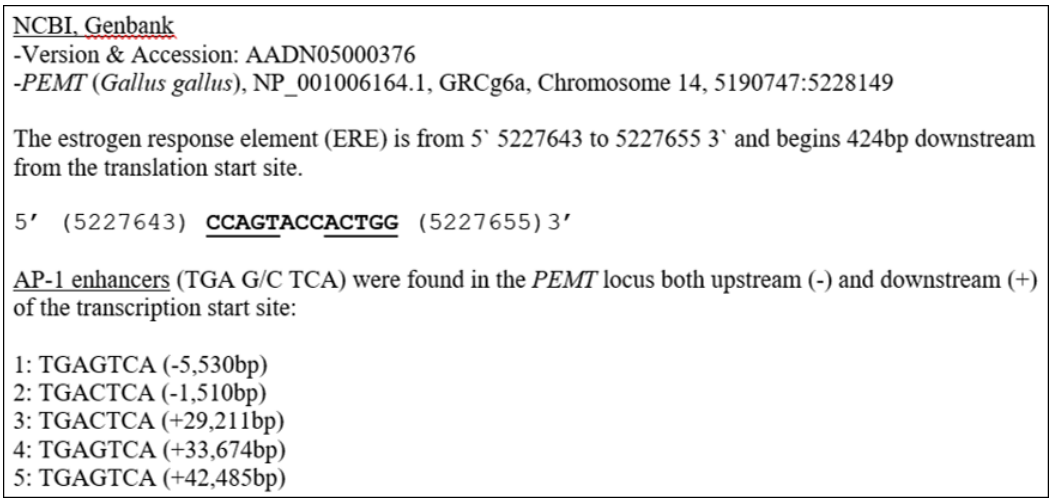
NCBI, Genbank
-Version & Accession: AADN05000376
-*PEMT* (*Gallus gallus*), NP_001006164.1, GRCg6a, Chromosome 14, 5190747:5228149

The estrogen response element (ERE) is from 5` 5227643 to 5227655 3` and begins 424bp downstream from the translation start site.

5′ (5227643) **CCAGTACCACTGG** (5227655) 3′

AP-1 enhancers (TGA G/C TCA) were found in the *PEMT* locus both upstream (-) and downstream (+) of the transcription start site:

1: TGAGTCA (-5,530bp)
2: TGACTCA (-1,510bp)
3: TGACTCA (+29,211bp)
4: TGAGTCA (+33,674bp)
5: TGAGTCA (+42,485bp)

Figure 5.1.1. Estrogen response element (ERE) and AP-1 enhancers within the locus of *PEMT* (*Gallus gallus*). The *PEMT* locus (*Gallus gallus*) was investigated for EREs and AP-1 enhancers. A complete ERE is located 424bp downstream of the transcriptions start site. Chicken *PEMT* is coded on the reverse strand. Also, two AP-1 enhancers were identified upstream of the start site, and three AP-1 enhancers were identified downstream of the start site but within the *PEMT* locus.

5.1.11 Glucagon-like phenotype in DF and WF hens

Glucagon is a strong stimulator of glycogenolysis, gluconeogenesis and lipolysis in hens (162). In a previous study (2), the DF and WF hens from nearly 3-fold elevated HbA1c. Complimenting this, in our current study the DF and WF hens exhibited slightly reduced blood plasma pyruvate concomitant with elevated C3, C5 and C8-carnitine. Interestingly, blood FFA

levels (i.e. C18:1ω9, C18:2ω6 and C22:6ω3) were elevated in DF and WF hens concomitantly with 3-fold elevated HbA1c! This is furthermore surprising given the substantially lower fatty acid content of the DF diet. Therefore, knowing that blood glucose and blood FFAs are regulated primarily by glucagon in chickens (166), we can derive that flaxseed probably increases glucagon secretion in hens. It could also be important to determine if flaxseed influences glucocorticoid metabolism, because this could have significant effects on blood sugar levels. Another important consideration is whether flaxseed influences the secretion of somatostatin from the pancreas, because somatostatin is critical for negatively regulating glucagon release in hens (165). Also notable was the observation of increased plasma ascorbic acid in WF hens. Ascorbic acid might be important for protecting WF hens from the pathological effects of advanced protein glycosylation. Ascorbic acid has been shown to reduce protein glycosylation in humans (283); therefore, the natural ability of birds to biosynthesize ascorbic acid might serve a protective role during flaxseed dieting.

5.1.12 Brief note about feed intake in flaxseed-fed hens

On the topic of "feed intake," numerous research groups provide evidence that flaxseed-fed laying hens have higher feed intake and lower body weight (324–326). You read that correctly; flaxseed-fed hens eat more and weigh less. Therefore, the result of body weight reduction in a flaxseed-fed hen is probably not the result of decreased prandial food consumption. We want to make this point regarding feed intake, because we did not directly measure feed intake in our animals.

5.1.13 Lifespan and methylation capacity in flaxseed-fed hens

Since the mid-1990s, animal class aves has been proposed as a model for the investigation of lifespan and aging (327). Birds live longer than equal-sized mammals, and they manage

oxidative stress and advanced glycation end products more efficiently (156,328). We analyzed hen survival over a 325-day period using 2.5-year-old hens. Our survival analysis is strengthened by the large sample size of animals, as well as the frequent occurrence of mortality (i.e. 35%) across diets. On average, each diet included 168 hens at study onset; therefore, a whole integer shift (i.e. 1% shift) in survival percentage is equivalent to 1.68 hens, meaning that survival differences can be interpreted to a resolution of 0.7% difference in survival percentage. DF hens displayed the highest cumulative survival with 71.4% survival. Prior to that study, our lab observed strikingly similar survival results (i.e. 72.1% survival) in 2.5-year-old White Leghorn hens consuming 10% WF (19). The 0.7% difference of survival between WF hens (72.1%) and DF hens (71.4%) is equivalent to approximately one animal. Something similar might be taking place in the metabolism of hens consuming either 10% DF or 10% WF.

DF hens displayed improved daily survival compared to CRN hens, according to a significantly reduced Cox proportional hazard. Very notably, from day 30 until day 325, the cumulative survival of DF hens was higher than CTL hens. No other diet accomplished this feat. Between day 70 to day 325, WF hens and FXO hens were the only animals to momentarily replace DF hens for top survival, suggesting that flaxseed-related diets performed well, in general.

Organism lifespan has been shown to be regulated by histone methylation, DNA methylation and RNA methylation (107,329–331). Future research should investigate linatine's biochemical role in regulating methyltransferase reactions involving histones, DNA and/or RNA. Mechanistically, the focus should be to determine if linatine influences methyltransferase activity at the level of SAM. Are the products of methyltransferase reactions elevated in flaxseed-fed hens? For example, do flaxseed-fed hens have increased PC:PE ratio, increased 5-CH_3Cytosine

in DNA and increased Ω6-CH_3Adenosine in RNA? Our prediction is that linatine boosts methyltransferase activity of the hen by inducing a flux of Hcy into the Met cycle which in turn boosts SAM content and thereby boosts the SAM:SAH ratio.

Soaking ground flaxseed in water for 24 hours nullifies the bioactivity of linatine within the bird (62,63); therefore, an appropriate investigation would be the comparison of the effects of ground flaxseed that has been soaked in water for 24 hours versus ground flaxseed that was not soaked in water. Another investigative option would be to determine the enzyme that is responsible for generating linatine within flaxseed and to develop a heterozygote or knockout flax strain. This type of information on flaxseed is currently unknown, so it might be advisable for current researchers to propose developing grants to identify the means by which flaxseed produces linatine. These hypotheses could be challenged in a linatine knockout (or linatine heterozygote) variety of flaxseed, and we could compare outcomes with the parental wild-type flaxseed. Advisors should be advised that linatine concentration vary slightly between flaxseed cultivars (293), so researchers should control for cultivar within experimental designs.

5.1.14 Metabolic markers of improved lifespan and healthspan, in DF hens

Our study is the first to demonstrate that a TS blockade concomitant with elevated SAM synthesis corresponds with elevated lifespan and elevated reproductive capacity in hens. Augmentation of TS, caloric intake and/or Met consumption are means by which other researchers have achieved lifespan extension in model animal systems. Experiments in fruit flies indicate that lifespan is increased via elevated TS flux (332); however, our work suggests that TS flux is dispensable for increased lifespan, in hens. Caloric restriction models show promise toward improving lifespan and healthspan in humans and non-human primates (333–335), and Met restriction models have been used to increase lifespan and healthspan in murine animals

(336,337). However, calorie restriction and Met restriction are not relevant to our study. We observed that a high SAM:SAH ratio correlated with increased lifespan in DF hens. An increased SAM:SAH ratio has not been previously determined to serve as a marker of extended lifespan; therefore, our work might be among the first to suggest that an increased methylation capacity promotes longevity. Decreased glucuronic acid is associated with increased lifespan and healthspan in mice and humans (285), and we detected vastly lower glucuronate (deprotonated glucuronic acid; essentially the same molecule) in DF hens. A metabolomics study in humans indicated that low glycerophosphorylcholine (GPC) levels reflect healthy aging in centenarians who are at least 100 years of age (286), and we detected vastly lower GPC in DF hens. Clinical researchers suggest that the ratio of Met sulfoxide to non-oxidized Met is a potential clinical biomarker of oxidative stress in humans (287), and we noticed that the Met Sulfoxide:Met ratio was lower in DF hens in comparison to CRN hens. Similarly, we also observed a significantly lower serine:glycine ratio in DF hens versus CRN hens. Given that DF hens had significantly reduce Cox hazard compared to CRN hens, it might be deduced that a lower Met Sulfoxide:Met ratio and a lower serine:glycine ratio indicate reduced aging in laying hens. Altoghether, glucuronate and GPC as well as the ratios of SAM:SAH and Met Sulfoxide:Met, in DF hens, support findings in the literature regarding aging and lifespan. These metabolites might be useful for assessing longevity in avian species, particularly in laying hens.

5.1.15 Reproductive capacity (egg laying performance)

We measured egg laying performance in advanced-age hens that were already one-year beyond their reproductive prime when the study began. Therefore, the improvements in reproductive capacity that we observed in WF, FSH and DF hens, are likely exceptional. WF hens and FSH hens exhibited best egg laying during the study, indicating that OM3-PUFAs and

particularly long-chain ω3-PUFAs such as EPA and DHA assist egg laying capacity. We already know that EPA and DHA are enriched in the livers and eggs of WF-fed hens (338,339), including the livers of hens consuming our 15% WF diet (2). To no surprise, hens consuming fish oil also display elevated EPA and DHA in egg yolk (340). FSH hens have the advantage of consuming EPA and DHA directly through the diet. WF hens, on the other hand, need to generate EPA and DHA via desaturation and elongation of ALA in the endoplasmic reticulum of hepatocytes. The need to desaturate and elongate ALA would pose a time delay in terms of enriching egg yolks with EPA and DHA, in WF hens. Accelerated VLDL trafficking of lipids to the egg yolk might be necessary to compensate for this time delay. In order to accelerate VLDL packaging and secretion it would be necessary to accelerate PC synthesis, because PC availability is rate-limiting for VLDL biosynthesis. This is primarily because PC represents 60-80% of the phospholipid within the external phospholipid leaflet of VLDL (341,342). In other words, PC is essential for VLDL encapsulation. This is where PEMT hyperactivation would serve a paramount role in WF hens. Mice that lack PEMT secrete 70% less VLDL-TG when fed a high fat diet (311). Similarly, TAG and apoB100 secretions are reduced 50-70% in mouse hepatocytes lacking PEMT (312). DF hens displayed moderately improved egg laying performance, but it was not as high as WF hens. Our opinion is that DF hens might only have moderately elevated PEMT activity, and therefore, DF hens would have moderately elevated access to PC. This would in turn moderately elevate VLDL secretion to support egg yolk formation, culminating in the moderate enhancement of egg laying in DF hens. A strength of our study is that we observed egg laying capacity in aged hens that are well beyond their prime years of egg laying, meaning that the acute effects of the diet could be more apparent.

5.1.16 Overall ranking of biological vitality (i.e. survival and reproductive capacity) in hens

Biology displays two common priorities: 1) do not die right now, and 2) if you did not die, then maybe consider reproduction. A simple physiological metaphor could be the duality of fight and flight versus rest and digest. This perspective suggests that an overall scoring of biological vitality should consider animal survival as well as reproductive capacity. Although none of the hens in our study were provided the opportunity to experience oocyte fertilization, we might gain insight from using unfertilized egg laying capacity as a surrogate for hen reproductive capacity. Through this lens we observed an interesting pattern in which the absolute value of the difference between a diet group's survival rank and egg laying rank was equal to 2, suggesting a common "trade off magnitude" or compensation between survival performance and reproductive performance. For example, the DF hens exhibited #1 survival and #3 egg laying (absolute difference of 2). This pattern of "trade off" was apparent for DF, WF, CTL and FSH hens (absolute difference of 2), validating the notion that survival and egg laying might combine as a valid indication of total biological vitality. The general biological well-being of FXO hens and CRN hens seemed to have deteriorated to a level where survival and reproduction suffered, with the most pronounced effect appearing in CRN hens. This observation suggests that dietary enrichment with flaxseed oil or corn oil, alone, is not beneficial to the well-being of hens. Given the low performance of CRN hens, we might also suggest that dietary enrichment with omega-6 PUFA is not a desirable approach with aged hens. After factoring survival rank and egg laying rank together, the animals with #1 biological vitality were DF and WF hens. We argue that it might be the synergistic relationship between linatine and OM3-PUFA that allows flaxseed-fed hens to display superior biological vitality, in direct relationship with forcing a flux of one-carbon unit inputs into the Met cycle and providing the hen with greater access to the master

methylating molecule SAM. In the future, researchers should measure the linatine concentration of the flaxseed cultivar that they utilize, because variations between studies might be due to different concentrations of linatine across cultivars. That said, a linatine effect should be expected independent of cultivar, as previously indicated by HPLC-MS/MS analysis (293).

5.2 STUDY 2: THE EFFECT OF DIETARY POLYUNSATURATED FATTY ACIDS (PUFAS) ON LIPID METABOLISM, MITOCHONDRIAL BIOENERGETICS AND E-CADHERIN EXPRESSION IN LAYING HEN OVARIAN TUMORS

5.2.1 Overall cancer risks

The enrichment of the diet with PUFAs (either ω-3 or ω-6) had a particularly strong anti-cancer effect in hens. Total ovarian cancer risk, liver cancer risk, multiple peritoneal tumor risk, and the risk of stage 3&4 ovarian cancer, were all highest in the CTL and DF diet groups. CTL and DF also had the lowest oil content of all diets, suggesting that a diet with lower dietary PUFA content associates with increased risk of morbidity from ovarian cancer or otherwise peritoneal cancer, in hens. If our model captured true cancer risk, then we would argue that the pure oil component (independent of omega-3 or omega-6 PUFA) exerts the most powerful anti-ovarian cancer effect. The diet groups with greatest hen survival were most likely to have a higher percentage of hens with ovarian cancer, suggesting that ovarian cancer risk in our study might be biased by survival. Our data suggest that ovarian cancer-associated mortality might be lowest in diet groups with highest overall survival. For example, the risk of ovarian cancer-associated mortality might be decreased in CTL, DF and WF hens, because these animals displayed the best survival despite having the greatest risk of stage 4 ovarian cancer. This possibly indicates that CTL hens, DF hens and WF hens, lived longer with late-stage ovarian cancer. Inverse to this pattern, FXO hens, FSH hens and CRN hens, might have significantly

elevated ovarian cancer-associated mortality given that they displayed the lowest overall survival concomitant with the lowest percentage of hens with stage 4 ovarian cancer.

However, our model is challenged by the fact that we do not know the cause of death of any animal that died before the completion of our study. Approximately 33.9% of our hens died prior to study completion, or 341 out of 1005 hens. This certainly limits our ability to infer cancer risk or cancer-associated mortality risk. Future work could repeat our research model with the modification of analyzing cause of death in all birds that die during the study, otherwise it is difficult to make inferences with confidence. The uncertainty within our inferences is particularly high (i.e. 33.9% of animals have no known cause of death); furthermore, we detected significantly different Cox proportional survival hazards between some of our diets (i.e. DF versus CRN).

Despite the presence of uncertainty within our data, it seemed that the diets with lower PUFA content were at greater risk of stage 4 ovarian cancer and greater risk of ovarian cancer in general. Another interpretation is that ovarian cancer risk was biased by overall survival, causing a higher percentage of hens to be found with tumors when the diet enhanced survival in hens. This perspective also suggests that fewer tumors are likely to be found when the diet displays low survival.

5.2.2 Lipid metabolism in hen ovarian tumors

A big takeaway from our analysis is that the WF diet, FXO diet, CRN diet and FSH diet, were able to accumulation fatty acids in ovarian tumors if those fatty acids were already enriched in the diet (e.g. C18:3ω3 accumulation in ovarian tumors of FXO-fed hens). This is a helpful "case in point" type of rationale, helping us to make the argument that the PUFAs form the diet serve a bioactive role in ovarian tumors of the hen. The dietary effects on lipid metabolism within these

tumors might be the result of specific lipid species accumulating with the tumor. WF hens also exhibited an increase in arachidonic acid (C20:4ω6), which is the elongation and desaturation product of LA (C18:2ω6). In other words, WF hens had elevated C18:3ω3 as well as C20:4ω6.

PUFAs have been suggested for quite some time as negative regulators of lipogenic gene transcription in liver (218) and in glioma cancer cells (343); however, not so much is known about the influence of PUFAs on *de novo* lipogenic gene transcription within solid tumors. The broad downregulation of *FASN* expression seen in WF, FXO, CRN and FSH hens, indicates that dietary PUFAs (omega-3 and omega-6) might exert negative feedback on *FASN* expression in ovarian tumors of hens. Intriguingly, *FASN* expression in these tumors, by diet, was very similar to the risk of total ovarian cancer across the diets, where risk decreased as the PUFA content of the diet increased. CRN hens also exhibited a capacity to downregulate *ACC* and *SCD1*, in addition to *FASN*, suggesting a superior role of C18:2ω6 in the downregulation of genes in the *de novo* lipogenic pathway.

Although we observed dietary effects on *de novo* lipogenic gene expression in hen ovarian tumors, we did not observe any effect of diet on the fatty acid species that are canonically regulated in the *de novo* lipogenic pathway (e.g. C16:0, C18:0 and C18:1). The only effect was a small decrease in C20:1ω11 within tumors of WF hens. WF hens also had elevated C20:4ω6 which can exert anti-lipogenic effects along with other PUFAs such as C18:3ω3. Therefore, it is possible that WF hen are expressing negative feedback to *de novo* lipogenesis due to lower levels of C20:1ω11.

In FSH hens, the expression of *PPARg* and the concentration of DHA were concomitantly higher in ovarian tumors. Dietary omega-3 PUFA enrichment, in general, encouraged higher average *PPARg* expression, although the FSH diet was the only diet to significantly elevate

PPARg. PPARs have been referred to as lipid sensors (344), and long-chain PUFAs function as ligand-like activators of PPARα and PPARg (345,346). EPA and DHA are suggested to function as activators of PPARs in a ligand-dependent manner (347,348). DHA positively regulates PPARg activity in peripheral blood mononuclear cells (PBMCs) of humans with T2DM (349). *PPARg* expression might be higher in ovarian tumors of FSH hens due to DHA's ability to activate PPARg. Future works should investigate how dietary PUFAs regulate PPAR binding to PPAR response elements within hen ovarian tumors and test how this effects PPAR-dependent gene transcription.

5.2.3 Gene transcripts associated with mitochondrial respiration

In the 1920s, Otto Warburg postulated that tumors have dysfunctional mitochondrial respiration ("injured mitochondria"), such that tumors leverage glucose fermentation at a high rate despite oxygen tension being ample (350,351). This is the basis for the concept of aerobic glycolysis. In the 1950s, Joanna Budwig theorized that Warburg's so-called mitochondrial injury was the result of mitochondria having insufficient access to respiratory substrates such as fatty acids and sulfhydryl groups (352). It was from this perspective that researchers such as Joanna Budwig and Bill Henderson advocated including flaxseed oil as a primary constituent of the anti-cancer diet (352,353). Up front, our data suggest that PUFAs upregulate the transcripts for ETC complex 3, 4 and 5 as well as the ADP/ATP translocase were elevated in the PUFA-enriched diets (especially the FXO diet). Interestingly, the FXO hens also exhibited reduced odds ratio of stage 4 ovarian cancer, indicating that they had a boost in OXPHOS-related genes as well as a significantly reduced risk of late-stage disease. This observation suggests that PUFAs might reduce ovarian cancer risk in an ETC dependent manner, and this would not be a surprise because the mitochondrial beta oxidation of PUFAs would necessarily increase ETC activity.

Our results support the recommendations of Budwig and Henderson, both of whom believed that the dietary consumption of flaxseed oil can help to amplify mitochondrial function in tumors (352,353).

Why are we observing elevated OXPHOS genes in the ovarian tumors of hens consuming either WF, FXO, CRN or FSH? Our strongest evidence is that these four diets were effective at concentrating their corresponding PUFA (i.e. C18:2ω6 for CRN hens) within ovarian tumors, and the concentration of these PUFAs might amplify mitochondrial beta-oxidation. In turn, beta-oxidation (in combination with the TCA) would yield a tremendous amount of NADH and $FADH_2$ that elevate the need for ETC complex formation. A substantial elevation of beta-oxidation within tumors has been considered by other researchers as the "reversal of the Warburg Effect," whereby tumors reduce their glycolytic activity in favor of mitochondrial beta-oxidation (354). This is our workflow for postulating why OXPHOS-related genes are heavily amplified in the ovarian tumors of hens consuming either WF, FXO, CRN or FSH.

The expression of *FASN* was opposite to the expression of *MT-CYTB*, *MT-COX1*, *MT-COX2*, *MT-COX3*, *ATP5B* and *SLC25A4*, in hen ovarian tumors. This could be an expected outcome, because FASN represents lipid anabolism (i.e. *de novo* lipid synthesis), whereas increased OXPHOS would be stimulated by lipid catabolism (i.e. increased mitochondrial FAO). Anabolic lipid programs and catabolic lipid programs are not simultaneously upregulated (or downregulated) within the cell. For example, it is commonly known that malonyl CoA (the substrate utilized by FASN to make C16:0) is a potent CPT1 inhibitor, meaning that *de novo* lipid synthesis inhibits the transport of long-chain fatty acids into the mitochondria (thereby inhibiting mitochondrial beta-oxidized in the matrix) (355). Therefore, our gene transcript data regarding OXPHOS and *de novo* lipid synthesis are physiologically congruent.

5.2.4 Gene transcripts associated with oxidative stress response

In the mitochondria, SOD2 converts superoxide to hydrogen peroxide. Then, throughout the cell, CAT converts hydrogen peroxide to water and oxygen. These two enzymes provide a significant amount of the cell's phase 2 (i.e. enzyme-mediated) antioxidant response. The lower expression of *SOD2* might suggest lower superoxide production in ovarian tumors from hens consuming DF, WF, FXO, CRN or FSH. Similarly, the lower level of Cat might suggest reduced production of hydrogen peroxide in the tumors of hens consuming WF, FXO, CRN or FSH. The proteins for inducible nitric oxide synthase (NOS2) and SOD2 have been shown to be simultaneously elevated in AIDS-related Kaposi sarcomas (356), suggesting a direct correlation between nitration stress response and oxidative stress response in cancer. As such, our results suggest that protein nitration stress might be lower in the ovarian tumors of hens consuming DF, WF, FXO, CRN or FSH. Furthermore, just as was observed in (356), we detected elevated *SOD2* and *NOS2* in ovarian tumors of our CTL hens. *DNM1L* (also known as *DRP1*) is a master regulator of mitochondrial fission (357). *DNM1L* is activated post-translationally by phosphorylation and (via the promotion of mitochondrial fragmentation) acts as an important step by which cancer cells upregulate oxidative stress and mitophagy (358).

Cancer cells utilize antioxidant defense systems to protect themselves from aberrantly high levels of ROS (359). Meanwhile, cancer cells also utilize ROS-associated oxidative stress to promote metastasis away from the primary tumor (360). The F_1/F_0-ATP synthase complex, which produces the vast majority of cellular ATP, is tightly regulated by the redox status of the cell (288). Cysteine 294 of canine ATP5A1 (the α-subunit of the F_1 complex) can be modified by disulfide bond formation, S-glutathionylation or S-nitrosation, depending on the redox status of the mitochondria (361). This observation very closely relates ATP synthase function with redox

environment. Furthermore, the activity of ATP synthase depends on the structural association of 17 different proteins (193,362). It has been suggested that the function of inner membrane complexes (such as ATP synthase) depends on the availability of subunit proteins, because the availability of subunit proteins informs the degree to which inner membrane complexes can be fully assembled (198). The F_1 catalytic domain of ATP synthase consists of α, β, γ, δ and ε subunits, and these subunits occur with a stoichiometry of 3:3:1:1:1, in mammals (363). The transcripts for *ATP5B* (the F_1 β-subunit) were 3 to 5-fold higher in ovarian tumors of hens consuming WF, FXO, CRN or FSH, while the transcripts for *ATP5A1* (i.e. the F_1 α-subunit) were concomitantly 80% to 90% lower in those same diets. This idea a flip-flop between ATP5A1 and ATP5B expression might be an indicator of metastatic risk and/or tumor severity, according to published work. In humans, colon tumor metastases have high ATP5A1 expression compared to primary tumors of origin (364), and more advanced colon tumors have reduced ATP5B expression (365,366). High ATP5A1 expression concomitant with low ATP5B expression might be a marker of increased tumor severity and/or metastatic burden, in hens. The ovarian tumors of hens consuming our CTL diet had high ATP5A1 expression and low ATP5B expression. Our CTL hens also suffered the worst ovarian cancer morbidity (i.e. 18% of CTL hens had ovarian cancer) as well as the highest rate of multiple peritoneal organ involvement (i.e. 10% of CTL hens had multiple organs involved). *MT-ATP6* and *MT-ATP8* are mitochondrially encoded genes for ATP synthase subunits 6 and 8. These two subunits help to anchor the stalk of ATP synthase into the mitochondrial inner-membrane (193,362). Mutations in *MT-ATP6* and *MT-ATP8* have been shown to influence ROS production specifically in the context of cancer and cell function (367–369).

Future research should evaluate the protein expression of ATP5A1, ATP5B, MT-ATP6 and

MT-ATP8. Our data suggest that dietary PUFA enrichment decreases the expression of ATP5A1, MT-ATP6 and MT-ATP8, while increasing the expression of ATP5B. This apparent flip flow in ATP synthase subunit expression might have specific relevance to the redox status of the cell.

5.2.5 CDH1 and miR-200a-3p expression in hen ovaries and BG1 cells

We illustrated that the DHA concentration of hen ovarian tumors is increased by the FSH diet. In addition to fish oil, flaxseed can also enhance DHA concentrations via the stepwise elongation and desaturation of C18:3ω3. Our results suggest that omega-3 PUFAs downregulate *CDH1* levels in normal and cancerous hen ovaries. We also saw an age-dependent effect on *CDH1* in normal hen ovaries, suggesting that *CDH1* expression might increase with greater age of the animal. This is not the first age-dependent effect that we observed in our animal model. Our lab has observed an age-dependent increase in prostaglandin E2 (PGE2) in the ovaries of laying hens (370), possibly correlating PGE2 regulation with miR-200/*CDH1*/E-cadherin regulation.

CDH1 levels were decreased by 25μM DHA and 50μM DHA in BG1 ovarian cancer cells, suggesting that dietary PUFAs (specifically omega-3 PUFAs) might reduce *CDH1* levels in human ovarian cells. miR-200a was also decreased at 50μM (we did not measure effects at 25μM), indicating that the decrease of *CDH1* might be in response to decreased miR-200a levels. miR-200a is a known inhibitor of ZEB1 which is transcriptional repressor of the *CDH1* promoter. *NQO1* was decreased at 25uM and 50uM DHA while *HO1* was decreased at 50μM DHA, suggesting that *CDH1* levels might decline in response to cellular redox response. We have already observed that BG1 ovarian cancer cells have intact mitochondrial respiration during oxygen consumption analysis with Seahorse XF_p; therefore, they would be expected to

efficiently oxidize DHA in the mitochondria. DHA treatment might elevate mitochondrial FAO in BG1 cells, which could in turn enhance ETC activity and result in an upregulation in *NQO1* and *HO1*. NQO1 is one of the most redox sensitive enzymes in the cell (371), and we noticed that the transcripts for *CDH1* and *NQO1* were simultaneously decreased at 25µM and 50µM DHA, while *HO1* levels were not affected until 50µM. HO1 provides negative feedback to heme-dependent metabolism, and also helps to increase the availability of carbon monoxide, iron, biliverdin and bilirubin, as antioxidants (372). Furthermore, the transcription of *NQO1* and *HO1* is mostly regulated by NRF2, a transcription factor that is activated when redox-sensitive cysteine residues on the sequestering protein, KEAP1, are modified by electrophilic attack from molecules such as H_2O_2 (373). The modification of these cysteine residues leads to the stabilization of NRF2 and the subsequent nuclear translocation of NRF2 where it binds to antioxidant response elements, such as those for *NQO1* and *HO1*. We cannot speculate further on this mechanism, but we suspect that dietary PUFAs might regulate *CDH1* in ovarian tumors by increasing FAO and thereby inducing a redox response that affects *CDH1* expression. Future studies should attempt to utilize glutathione-boosting supplements such as N-acetyl cysteine (NAC) to test if the effect of DHA on *CDH1* expression in BG1 cells is dependent upon redox status.

We also detected decreased levels of miR-200a in BG1 cells that were treated with 50µM DHA (we did not test the effects of 25µM DHA on miR-200a expression in BG1 cells). miR-200a increases the transcription of *CDH1* by inhibiting the *CDH1* inhibitor ZEB1. Therefore, future studies should also investigate the role of redox sensitive systems in regulating the expression of miR-200a in ovarian tumors. We did not detect an effect of diet on miR-200a expression in ovarian tumors of the hen. Our lab previously indicated that miR-200a levels are

decreased in hen ovarian tumors during 10% WF dieting (14); however, we could not repeat those results. One possibility is that the authors in (14) ensured that all hen ovarian tumor samples were stage-matched (i.e. all stage 4), while we analyzed a random mixture of ovarian tumor stages in our current study. PUFA-enriched diets downregulated miR-200a detection in preneoplastic (i.e. normal) hen ovaries; however, the expression of miR-200a was much lower in normal versus cancerous tissues. miR-200a detection was correlated with the stage of the hen ovarian tumor, such that miR-200a was more abundant in stage 4 ovarian tumors versus stage 2 ovarian tumors. Strikingly, in humans, miR-200a is also higher in ovarian tumors versus normal ovaries, and miR-200a levels are also higher in more advanced stage ovarian tumors (374). Therefore, miR-200a expression seems to progress similarly in ovarian tumors of hens and women regarding neoplastic evolution of the tissue. Our lab previously illustrated that E-cadherin protein expression increases as the hen ovary becomes more neoplastic, just as what can be observed in human ovarian cancer (236). The works from (14,236) in combination with this current study further solidify the epithelial similarity between human ovarian cancer and laying hen ovarian cancer. More recent publications suggest that the miR-200 family and E-cadherin play a major role in the process of ovarian tumor metastasis (collective migration) (237,242). Also, in collaboration with researchers from Harvard, our lab recently elucidated the utility of miR-200 family members as blood biomarkers for the early detection of ovarian cancer (238).

5.2.6 E-cadherin protein levels in hen ovarian tumors

The analysis of E-cadherin protein in hen ovarian tumors produced some interesting results. The FXO and FSH diets were unique in their ability to reduce the level of 37kDa and 80kDa E-cadherin protein fragments, suggesting that omega-3 PUFAs might be particularly effective at reducing the cleavage of full-length (120kDa) E-cadherin in hen ovarian tumors. Previous

studies indicate that omega-3 PUFAs reduce the activity of extracellular cleavage enzymes such as matrix metalloproteinases (MMPs) and disintegrin and metalloproteinase with thrombospondin motifs (ADAMTS) (375,376). FSH hens had increased *PPARg* transcripts in hen ovarian tumors. PPARg is a known NF-kB inhibitor, and NF-kB can drive the expression of cytokines, MMPs and ADAMTS (377,378). Therefore, FSH (or specifically EPA and/or DHA) might act to decrease E-cadherin cleavage in a PPARg/NF-kB-dependent manner. Future work would need to consider the expression and activity of these cleavage enzymes in hen ovarian tumors, as they were not assessed in our current study. Our FXO hens were exceptionally unique in their ability to reduce the odds ratio of having stage 4 ovarian cancer while also having reduced 37kDa and reduced 80kDa E-cadherin during non-parametric analysis. This might suggest that the FXO diet reduces the severity of ovarian cancer by reducing the expression of the E-cadherin cleavage fragments. All of our treatment diets reduced 80kDa E-cadherin levels in hen ovarian tumors, a finding that correlates well with our observation that ovarian cancer risk was reduced by all of our treatment diets, in general. These results might indicate that PUFAs regulate the progression of ovarian cancer, because 80kDa (i.e. soluble) E-cadherin is very intimately related with the development and progression of human cancers (266,269,379). Our study indicates that PUFAs (omega-3 and omega-6) reduce 80kDa E-cadherin levels in hen ovarian tumors, and this reduction might be important for diminishing the severity of the disease. The 37kDa protein also has relevance in the context of cancer, given that the cytosolic portion of E-cadherin (i.e. 37kDa fragment) provides a scaffolding anchor for the beta-catenin complex. Cleavage of 37kDa E-cadherin can promote beta-catenin activation and subsequent downstream transcriptional activities (380,381). Perhaps inferences about beta-catenin activation could be made based on studies of either 37kDa or 80kDa E-cadherin.

5.2.7 Proteomics analysis of the 80kDa band in hen ascites fluid and hen ovarian tumor

It was helpful to observe similar peptide masses in the hen ascites fluid and the hen ovarian tumor. However, based on the low sequence coverage of the peptide mass analysis, we cannot conclude that we have strong evidence that the 80kDa band represents 80kDa E-cadherin. However, knowing that we do see the 37kDa E-cadherin fragment, we still have a very reasonable argument that we are working with 80kDa E-cadherin. We do expect to see 80kDa E-cadherin in both the tumor homogenate and in the ascites fluid, which is what our western blots indicated. Furthermore, our anti-chicken E-cadherin antibody binds to both the 80kDa fragment and the 120kDa fragment; this would be expected for an antibody that binds to the extracellular portion of the full-length E-cadherin protein. Future work might want to consider a 2-dimensional gel electrophoresis of soluble E-cadherin, in an attempt to isolate the 80kDa protein according to isoelectric focusing. The original characterization of 80kDa chicken E-cadherin indicated an isoelectric point (pI) of 4.0 to 4.5 (229). Therefore, the isoelectric focusing has already performed with our antibody in chicken tissues.

5.2.8 Mitochondrial membrane potential and OCR in ascites-treated IOSE80 cells

Hen ascites fluid seemed to harshly affect oxygen consumption at ascites fluid concentrations of 1:19 and 1:9, given the profound elevation of proton leak and mitochondrial uncoupling at 1:19 and 1:9 concentrations. Therefore, we conclude that hen ascites fluid at concentrations of 1:19 and 1:9 are toxic to IOSE80 cells. Interestingly, 1:39 ascites had mixed effects on OCR and mitochondrial membrane potential ($\Delta\Psi$), such that 1:39 E-cadherin-depleted ascites reduced $\Delta\Psi$ but had no effect on basal OCR, mitochondrial OCR or non-mitochondrial OCR. Future experiments should also evaluate the effect of 1:39 E-cadherin-depleted ascites on ATP Synthase dependent OCR, via the utilization of oligomycin. This approach might reveal that 1:39 E-

cadherin-depleted ascites does affect OCR. Otherwise, as it stands, 1:39 E-cadherin-depleted ascites has no effect on OCR despite reducing ΔΨ in IOSE80 cells.

Possibly to our observations, other studies have observed pro-apoptotic (382) and anti-angiogenic (383) properties of human ovarian cancer ascites fluid when applied *in vitro* at concentrations of 1:19 and 1:9. We suspect that hen ascites fluid imparts a negative effect on IOSE80 cells at concentrations of 1:19 and 1:9. However, other studies have observed pro-migration (384) and pro-survival (385) effects of human ovarian cancer ascites fluid *in vitro*; therefore, ovarian cancer ascites fluid is sometimes helpful and harmful to cell metabolism. Our dose response experiment revealed that OCR was stable and "healthy" at ascites concentrations of 1:159 and 1:79, indicating that 1:159 and 1:79 were likely non-toxic to IOSE80 cells. Mitochondrial membrane potential experiments supported this finding by evidencing that ΔΨ was maintained at ascites fluid concentrations of 1:159 and 1:79. Furthermore, the E-cadherin-depleted ascites fluid even increased ΔΨ at a concentration of 1:159, suggesting that a slight treatment of with E-cadherin-depleted ascites promotes mitochondrial polarization, in IOSE80 cells.

Opposite to the effect of 1:159 ascites, the E-cadherin-depleted ascites fluid at a 1:39 concentration decreased ΔΨ. These findings suggest that a slight addition of E-cadherin-depleted ascites (i.e. 1:159) boosts mitochondrial metabolism, whereas a more concentrated addition of E-cadherin-depleted ascites (i.e. 1:39) reduces mitochondrial metabolism, in IOSE80 cells. Interestingly, during extracellular flux experiments, the 1:159 concentration of Control IgG ascites reduced mitochondrial uncoupling and increased mitochondrial coupling efficiency, versus vehicle-treated cells. This might suggest that a slight addition of E-cadherin-containing ascites (i.e. 1:159) elevates mitochondrial metabolism. However, our results make it hard to

determine if the presence or absence of the 80kDa E-cadherin fragment in ascites enhances or decreases mitochondrial metabolism in IOSE80 cells. This is mainly because 1:159 E-cadherin-depleted ascites increased ΔΨ, while 1:159 Control IgG ascites increased mitochondrial coupling efficiency. These are both phenomena that indicate elevated mitochondrial metabolism. If we assume that extracellular flux analysis of OCR (which is used to determine coupling efficiency) is more definitive of mitochondrial phenotype than ΔΨ analysis, then we might suggest that a 1:159 treatment with E-cadherin-containing ascites improves ATP-dependent cellular respiration in IOSE80 cells. Regardless, it would be nice if the ΔΨ data had more parallel agreement with our extracellular flux OCR data.

Future work should also conduct immunohistochemistry with an antibody that is monoclonal to the extracellular domain of chicken E-cadherin (such as antibodies used in (229)), in order to visualize if the 80kDa chicken E-cadherin fragment colocalizes with EGFR or other RTKs such as IGF-1R. Experiments should also be conducted to evaluate the activation of these receptors and downstream Akt activation.

CHAPTER 6

CONCLUSION AND SUMMARY

6.1 STUDY 1: FLAXSEED'S PARADOXICAL ROLE IN EXTENDING LIFESPAN AND REPRODUCTIVE CAPACITY IN WHITE LEGHORN LAYING HENS

This research provides a comprehensive and integrative summary of work that has emerged from our lab over the past 12 years. Our lab has completed numerous flaxseed studies during that timeframe. We feel that it is imperative to share this information before the lab shifts its focus into new areas of research. All labs have a beginning, so all labs have an ending. A key strength in our work is that we always used the same animal and diet model (White Leghorn hens with flaxseed); therefore, we anticipate that our research is very repeatable. A vast number of hypotheses are made possible by this study. Furthermore, this work indicates that a completely paradoxical phenomenon might be possible with flaxseed-dieting in laying hens. That paradox involves the anti-vitamin B6 effects of linatine, whereby linatine severely perturbs transsulfuration and might enable a flux of Hcy into the Met cycle, thereby boosting SAM levels and possibly allowing PEMT hyperactivation. The resulting effect is increased egg laying and/or increased lifespan, depending on how much PUFA is included in the flaxseed diet. We predict that the PUFA content is the pivotal factor determining whether excess SAM is depleted (favoring egg laying) or accumulated (favoring lifespan). Previous literature indicates that the PUFA-rich nature of the WF diet should enhance the PE synthesis capacity of the animal, and PE is a rate-limiting substrate for PEMT. In the presence of excess SAM, we predict that elevated PE synthesis would fuel PEMT hyperactivation. Recent research indicates that this is precisely what should occur (77). PEMT hyperactivation would in turn provide elevated access to soluble choline, via PC synthesis. Soluble choline can then be oxidized to help facilitate Hcy

remethylation via BHMT. We suspect that PEMT hyperactivation is highest in WF hens, and this in turn would support elevated BHMT activity. We suspect that the 10% DF diet only moderately stimulated *Pemt* hyperactivation, and therefore, DF hens could only slightly elevate BHMT activity. If DF hens have only slightly elevated BHMT activity, then MS-B12 would need to facilitate the remethylation of the remaining amount of Hcy. Flux through MS-B12 requires increased carbon input to the folate cycle (e.g. increased serine catabolism via SHMT) to drive Hcy remethylation via MS-B12. Our data suggest that increased catabolism of serine might have occurred in DF hens. This perspective observes BHMT as a primary mediator of Hcy remethylation in the context of a TS blockade, and places MS-B12 in a supplemental role to facilitate remethylation that cannot be performed by BHMT. Such a perspective is interesting, because MS-B12 is responsible for conducting the majority of Hcy remethylation under normal circumstances. However, the context of a TS blockade is not a normal circumstance. These results suggest that BHMT might be able to enhance its contribution to Hcy remethylation in correlation with the degree to which the diet is enriched with PUFA. Serine might be the dominant source of carbon that is powering Hcy flux through MS-B12, in DF hens. If this is the case, then our results suggest that B6 levels are not perturbed badly enough to inhibit SHMT activity, likely referring to SHMT2. We hope that our results motivate researchers to validate our hypothetical framework in laying hens and further investigate whether these results can be duplicated with flaxseed-dieting in other animals, including humans. Future experimenters should consider using synthetic linatine (or 1ADP) alone and in combination with an ω3-PUFA supplement such as flaxseed oil, in hens. We envision the possibility of discovering a unique form of "dietary technology" that can be used to custom tailor a particular outcome in the test subject, possibly increasing lifespan, healthspan or otherwise biological performance. As a

precautionary note, researchers have observed that B6-deficient rats are susceptible to negative hepatic effects when a high concentration of 1ADP is included in the diet (1). That said, our work suggests that flaxseed does not induce a B6 difficiency, although it certainly induces some form of B6 perturbation. The TS enzymes (i.e. CBS and CSE) might be sensitive to the anti-B6 effects of linatine, suggesting that TS might be an early signal to the metabolism that vitamin or nutrient deficiency is occurring. It would make sense that the metabolism would be proactively selected by nature to provide an early warning that starvation is beginning, and TS might be a specific pathway for providing this signal (e.g. vastly elevated cystathionine). Does cystathionine elevation provide an early warning to the pancreas that a starvation-like state is present? Can the α-cells of the pancreas interpret elevated cystathionine as hyperaminoacidemia? In turn, does this promote the enhanced secretion of glucagon from α-cells? These are important questions because our work indicates that flaxseed induces a dramatic elevation of both cystathionine and HbA1c, in hens. An appreciation of avian and mammalian glucagon activity would be helpful for researchers who are comparing avian and mammalian models because most avian species have an exaggerated response to glucagon and a blunted response to insulin (compared to mammals.

In closing, we are excited about the future investigations that can be imagined given the present findings about flaxseed's metabolic effects in laying hens. Do you find it bizarre that flaxseed converts the hen's metabolism to that a hummingbird, possibly via elevating glucagon release? Or that flaxseed extends avian life, possibly via boosting the level of the master methyl donor, SAM? Or that flaxseed enhances egg laying capacity, possibly as a result of hyperactivating PC synthesis via PEMT? Future research needs to take these questions into account when designing hypotheses and specific aims; furthermore, future work needs to evaluate the effects of defatted flaxseed and whole flaxseed on a finer gradient (i.e. 5%, 7.5%,

10%, 12.5% and 15% defatted flaxseed, and the same gradient for whole flaxseed). Future research should consider the variations of linatine content that occur in flaxseed across varieties or cultivars. If the linatine concentration is not controlled for, then the results across studies will likely not be repeatable. This might be one of the biggest contributors to inconsistencies in flaxseed chicken research. A wide array of human pre-clinical, nutritional biochemistry-oriented, veterinarian-based, avian wildlife-based, agricultural, plant biological, or otherwise chemistry-based research labs, need to sink their teeth into this animal/diet model. No one has ever modelled this type of a phenomenon in a vertebrate animal, so this is the dawning of a new perspective. Researchers have used flaxseed with laying hens for a long time, but they have not been aware of the phenomena that we elucidated in this present body of work. Investigators who have already conducted research with flaxseed in chickens might want to interpret their results given this new one-carbon metabolic perspective.

6.2 STUDY 2: THE EFFECT OF DIETARY POLYUNSATURATED FATTY ACIDS (PUFAS) ON LIPID METABOLISM, MITOCHONDRIAL BIOENERGETICS AND E-CADHERIN EXPRESSION IN LAYING HEN OVARIAN TUMORS

This work indicates that dietary PUFAs associate with an accumulation of PUFAs within hen ovarian tumors. These accumulated PUFAs reflect the fatty acid composition of the diet. For example, ALA (C18:3ω3) was higher in the tumors of FXO and WF-fed hens. ALA happens to be very concentrated in flaxseed oil, so it makes sense to see highest levels of ALA in ovarian tumors of hens fed either FXO or WF. This pattern was reflected in the ovarian tumors of CRN and FSH hens also. The accumulation of PUFAs within hen ovarian tumors associated with decreased levels of transcripts for *de novo* lipogenic genes and increased levels of transcripts for genes that support OXPHOS. The interesting aspect here is that *de novo* lipogenesis reflects lipid

anabolism while OXPHOS, in this context, would more likely reflect lipid catabolism that might result from elevated beta-oxidation of PUFAs within the tumor. Therefore, we have a succinct gene transcriptional message in which lipid catabolism might be high while lipid anabolism might be decreased in ovarian tumors when the hens consume a PUFA-supplemented diet. The genes that associate with oxidative stress response (i.e. phase 2 antioxidant enzymes) were vastly lower in PUFA-supplemented ovarian tumors, possibly suggesting that oxidative stress is lower in tumors when the OXPHOS machinery is activated to a higher level. This framework might indicate that our CTL-fed hens suffered extreme oxidative stress and highly glycolytic metabolism (i.e. largely quieted OXPHOS) within ovarian tumors that exhibited a strong lipid anabolism program (i.e. to support growth and replication). Accordingly, we observed the highest ovarian cancer risk in the CTL-fed hens, as well as highest GI cancer risk, liver cancer risk and risk of presenting with multiple peritoneal tumor sites. We even observed two CTL-fed hens died at the necropsy, prior to their CO_2 asphyxiation, due to complete peritoneal cavity tumor involvement. Without equivocation, ovarian tumor severity and peritoneal tumor burden were almost exponentially worse when PUFAs were not somehow incorporated into the diet. From this perspective, we can say that dietary PUFAs reduced the risk of peritoneal cancer and also associated with a molecular phenotype that might be reminiscent of reversing the Warburg Effect. If only Joanna Budwig could be here today.

This study suggested that dietary PUFAs might not affect the level of miR-200a within hen ovarian tumors. Previous work from our lab (14) showed that WF-fed hens have reduced levels of miR-200a, 200b and 429, in ovarian tumors. One takeaway from our study suggests that miR-200a expression might increase across stages. Future work should evaluate stage-related changes in expression of the miR-200 family in hen ovarian tumors. We observed an effect of PUFAs on

miR-200a and *CDH1* within 2-year-old normal ovaries, which might suggest that PUFAs begin to regulate the early pre-neoplastic state of the ovary. Cell culture experiments indicated that *CDH1* expression might be reduced by treatment with as little as 25μM DHA, which is in the physiological range for DHA. *NQO1 and HO1* expression suggest that *CDH1* gene expression might be regulated in a redox-sensitive manner that is associated with mitochondrial FAO and OXPHOS. These results might reflect what we observed in ovarian tumors of the hen, because FXO and FSH decreased the expression of *CDH1* in those tumors. However, when we looked at the protein level, we did not detect any effect on the expression of full-length (120kDa) E-cadherin. Furthermore, although we detected an effect of 50uM DHA on miR-200a levels in BG1 cells, we did not observe any effect of diet on miR-200a expression in hen ovarian tumors.

Strikingly though, the level of the cleaved E-cadherin fragments (i.e. 37kDa and 80kDa) were decreased widely by our PUFA-enriched diets, with the biggest effects coming from FXO and FSH. Therefore, the *CDH1* level of the hen ovarian tumor correlated with the 37kDa and 80kDa E-cadherin fragments, at least in FXO and FSH hens. FSH hens also had elevated *PPARg* expression, and PPARg is a known NF-kB inhibitor. By inhibiting NF-kB this might reduce MMP and ADAMT activity and culminate in reduced cleavage of 120kDa E-cadherin. Future experiments should investigate the role of ALA and DHA in regulating the cleavage of E-cadherin and determine if this happens in a PPARg/NF-kB-dependent manner.

The low sequence coverage of our peptide mass fingerprinting probably provides little confirmation that we are working with the 80kDa E-cadherin protein. The researcher (Warren Gallin) who developed the N-terminus antibody has already conducted the 2-dimensional isoelectric focusing work (229); therefore the pI for 80kDa E-cadherin is already known. Dr. Gallin, in the middle of his recent retirement, kindly gifted us with 10mg of N-terminus

polyclonal E-cadherin antibody. We were successful at developing an 80kDa E-cadherin-depleted ascites fluid. We observed mixed results with regard to the effect of ascites fluid on mitochondrial metabolism in IOSE80 cells. E-cadherin-depleted ascites fluid increased the $\Delta\Psi$ of IOSE80 cells when the ascites concentration was small (i.e. 1:159); however the $\Delta\Psi$ of IOSE80 cells decreased when the concentration of E-cadherin-depleted ascites was higher (i.e. 1:39). The story became more mixed after observing that treatment with 1:159 ascites increases mitochondrial coupling efficiency and decreases mitochondrial uncoupling. Therefore, we observed pro-mitochondrial effects at an ascites concentration of 1:159, whether or not the E-cadherin fragment was present in the ascites. Perhaps it is more conclusive to observe increased mitochondrial coupling efficiency in IOSE80 cells treated with 1:159 Control IgG ascites, because estimates of extracellular oxygen tension reflect cell physiological function. It seems very clear that ascites concentrations of 1:19 and 1:9 are certainly toxic to IOSE80 cells, meaning that it is more helpful to conduct experiments in the 1:159 and 1:79 range of ascites fluid. Treatments at the 1:39 level might be borderline toxic and therefore difficult to interpret. Future work should focus on treatments at 1:159 and 1:79 when using the hen ovarian cancer ascites fluid that we are experimenting with. Future work should also evaluate the activation of growth factor receptors such as EGFR and IGF-1R, to see if the 80kDa fragment in hen ascites fluid activates these RTKs.

CHAPTER 7

INDIVIDUAL PERSPECTIVE

7.1 The 15% whole flaxseed diet as an ideal diet for fueling PEMT hyperactivation, in hens

The WF diet satisfies several prerequisites and conditions that promote PEMT hyperactivation (summarized in Table 7.1). The first mandatory prerequisite is excess SAM availability. We already indicate the presence of a TS blockade in the absence of hyperHcy or elevated SAH, in DF and WF hens, strongly suggesting that Hcy fluxed into the Met cycle. Supporting the existence of this flux, SAM was elevated 1.9-fold in DF hens. We propose that *Pemt* hyperactivation catalyzed the consumption of all excess SAM in WF hens. The second mandatory prerequisite for PEMT hyperactivation is enhanced PE synthesis capacity. In a study of primary rat hepatocytes, the PC created by PEMT (i.e. PC coming from PE) contained a wide variety of unsaturated acyls such as C18:1, C18:2, C20:4, C22:5 or C22:6, with a preference for longer chain PUFAs (88). What a lucky situation for flaxseed! Flaxseed is densely packed with C18:1, C18:2 and C18:3, and furthermore, C18:3 can be desaturated and elongated to C22:5 and C22:6. In White Leghorns, a 15% WF diet enriches the PE and PC fractions of egg yolks with C18:3, C20:5, C22:5 and C22:6 (338). It is commonly known that egg yolk phospholipids comes from the liver (i.e. come from liver VLDL), so the PE and PC fraction enrichments observed in (338) suggest that a 15% WF diet enriches hepatic PE and PC with long-chain PUFAs, in hens. Our 15% WF diet was already shown to elevate hepatic EPA and DHA content in White Leghorns (2), and similar results have been reported by others (339,386). We certainly expect vastly enhanced PE synthesis capacity in the livers of White Leghorns consuming 15% WF. However, we would not make this claim about our 10% DF diet. The 10% DF diet has 26.7% of the lipid content as the 15% WF diet, per gram of input (quantified by our lab via gas

chromatography). Due to nearly 75% less lipid content in the DF diet, we expect PEMT activity to become rate-limiting for DF hens at the level of PE synthesis. The predicted outcome would be less PEMT hyperactivation, and therefore, increased SAM accumulation in DF hens, as was supported by the 1.9-fold elevation in SAM.

Table 7.1. Molecules and enzymes that influence PEMT activity, including their predicted effect on PEMT activity in WF and DF hens.

Molecule or enzyme	Effect on PEMT	Status of molecule or enzyme		Favored effect on PEMT activity	
		in WF hens	in DF hens	in WF hens	in DF hens
Phosphatidyl-ethanolamine (PE)	Substrate for PEMT	Suspected to be very enhanced (due to highly elevated PUFA)	Suspected to be moderately enhanced (due to moderately elevated PUFA)	+ + +	+ (***rate limiting***)
S-adenosyl-methionine (SAM)	Substrate for PEMT	High SAM potential (due to flux of Hcy into Met cycle)	High SAM potential (due to flux of Hcy into Met cycle)	+ + +	+ + +
S-adenosyl-homocysteine (SAH)	Inhibits PEMT	Slightly lower level was detected	No change detected	+	No effect
S-adenosyl-homocysteine hydrolase (SAHH)	SAHH decreases the SAH level and thereby increases PEMT activation	High activity is suspected (due to high Hcy:SAH and Adenosine:SAH)	No change detected	+ + +	No effect
Choline	Choline depletion activates PEMT	Much lower level was detected	Slightly lower level was detected	+ + +	+
Betaine homocysteine methyltransferase (BHMT)	*Bhmt* increases choline depletion and thereby activates PEMT	High activity is suspected (due to high Met:Betaine and lower choline & betaine levels)	Slightly higher activity is suspected (due to slightly lower choline level)	+ + +	+
---------- **Summed Effect** ----------				**Highly increased PEMT activity**	**Moderately increased PEMT activity**

7.2 Model for flaxseed's induction of glucagon secretion in hens

Although we did not measure systemic glucagon in flaxseed-fed hens, our data in combination with previously published work (2) suggest phenotypically that glucagon secretion could be highly elevated in WF and DF hens. The role of glucagon is likely important in our model, because glucagon has the ability to heavily stimulate lipolysis in hens. Elevated lipolysis could be critical during flaxseed dieting in hens, because the production of soluble choline requires phospholipase activity on PC. It is unknown if glucagon stimulates phospholipase activity in hens, but this hypothetical model synergizes glucagon activity with the larger model regarding Hcy remethylation. This synergistic model can be seen in Figure 7.1.

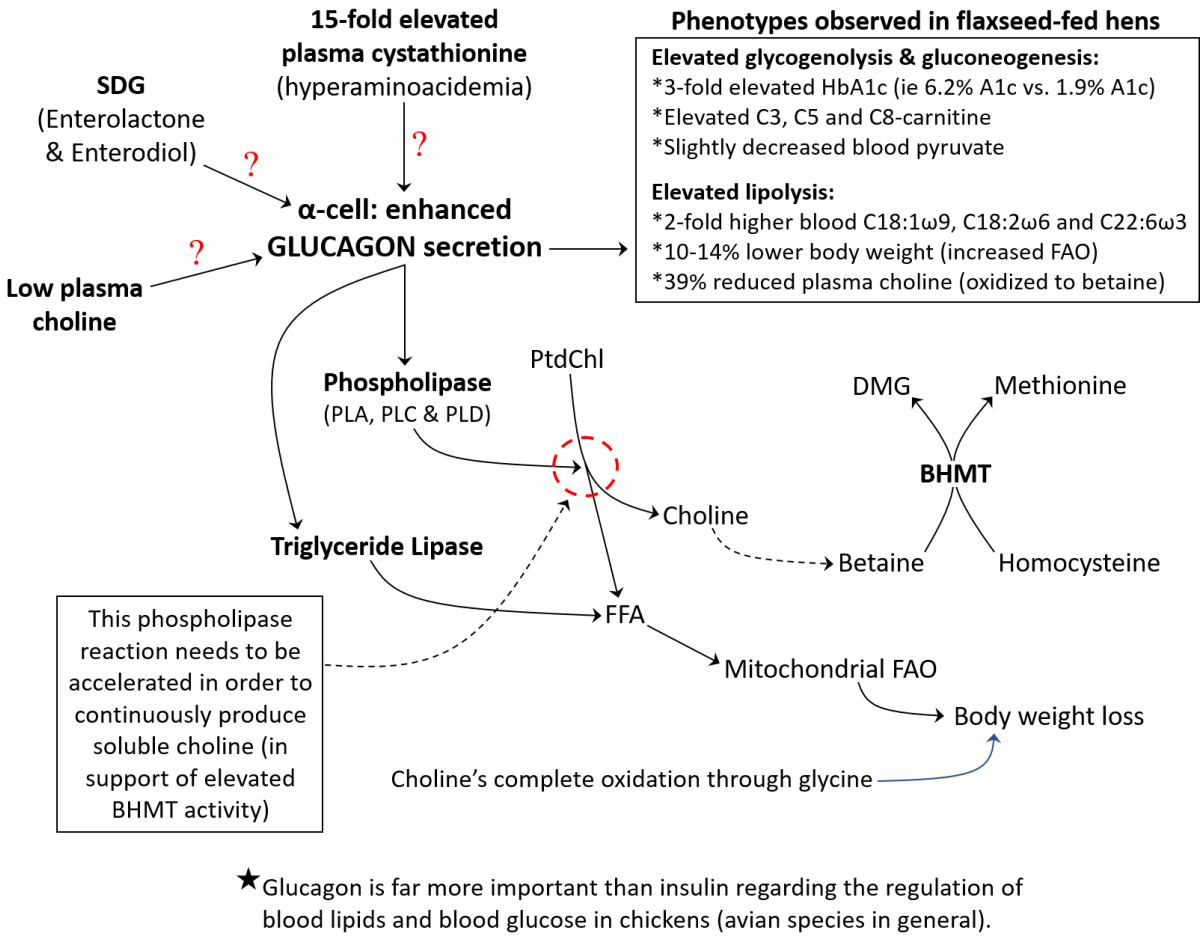

Figure 7.1. Glucagon's integration into the larger model of flaxseed's effect on one-carbon metabolism in laying hens. We have ample evidence to argue that glucagon secretion might be highly elevated in hen's consuming either DF or WFX. This evidence includes elevated HbA1c, reduced plasma pyruvate, elevated blood lipids and reduced body weight. Glucagon secretion might be accelerated in flaxseed-fed hens for several reasons, such as plasma hyperaminoacidemia, elevated plasma enterolactone or enterodiol and/or decreased plasma choline. A primary takeaway from this flow chart is that accelerated glucagon secretion might be critical for enabling accelerated phospholipase activity on PtdChl, so that soluble choline can be continuously produced in support of elevated flux through BHMT. Said concisely, this model predicts a synergy between glucagon and linatine at the level of phospholipase activity on PtdChl (in terms of producing soluble choline and allowing elevated flux of Hcy through BHMT).

7.3 What is it about flaxseed that might be causing elevated glucagon release?

A primary role of pancreatic α-cells is the monitoring of amino acid levels in the liver (387). When α-cells detect elevated amino acids (i.e. hyperaminoacidemia) they respond by strongly increasing their release of glucagon into the systemic circulation, at least in mammals (387,388). The liver has the highest level of TS activity among all organs (389); therefore, cystathionine (as a TS metabolite) might be easily detectable by pancreatic α-cells. An important question then is, "does elevated cystathionine stimulate α-cells to increase their secretion of glucagon?" This is a big question for future research to explore. If the pancreas interprets 15-fold elevated cystathionine as hyperaminoacidemia (and hyperaminoacidemia enhances glucagon secretion from α-cells), then this might explain the nearly 3-fold elevated HbA1c values in DF and WF hens.

An alternative hypothesis (alternative to the hyperaminoacidemia idea) is that glucagon secretion was increased by enterodiol (ED) and/or enterolactone (EL) in DF and WF hens. We already know that ED and EL are highly elevated concomitantly with elevated HbA1c, in DF and WF hens (2). ED and EL are phytoestrogens that are produced after the enteric fermentation of seicoisolariciresinol diglucoside (SDG) (390). Flaxseed is the richest natural source of SDG, explaining why our DF and WF hens have high blood levels of ED and EL. In mice, ED and EL have been observed to exert estrogenic effects (391), but it is unknown if ED and EL exert estrogenic effects in chickens. 17-β estradiol promotes proglucagon-derived peptide secretion from human and mouse α-cells (392), so it is possible that ED and EL might influence glucagon release in an estrogenic manner. Further studies are needed to determine if ED and EL influence glucagon release in hens. It would certainly be interesting to explore whether hyperaminoacidemia (e.g. elevated cystathionine) in conjunction with elevated ED and EL, cause highly increased glucagon secretion from avian α-cells.

Lastly, the α-cells of the pancreas might be sensitive to the choline content of the animal. If amino acid sensing is a primary function of α-cells (387), then they might be able to detect choline depletion. Choline is somewhat amino acid-like. Nonetheless, low choline levels such as those observed in WF hens (and to a lesser extent in DF hens) might contribute to enhanced glucagon secretion from the pancreas, particularly if the lipolysis enhancing effects of glucagon promote the mobilization of choline from PC (via phospholipase activity).

7.4 Could a positive feedback loop exist between cystathionine and glucagon?

Why on Earth is cystathionine elevated over 15-fold in DF and WF hens? The first, and obvious explanation, is that CSE activity was decreased due to linatine's B6 antagonizing effect, thereby reducing TS flux. However, a 15-fold elevation of cystathionine suggests the presence of

a positive feedback loop. We propose a positive feedback loop between cystathionine and glucagon, assuming that elevated cystathionine is interpreted by the pancreas as hyperaminoacidemia. As already noted, hyperaminoacidemia induces glucagon release from α-cells, at least in mammals (387,388). In turn, glucagon exposure increases *CBS* gene transcription and catalytic enzyme activity (393,394). Recall that CBS synthesizes cystathionine.

One hypothetical model is that linatine exposure stimulates an elevation of cystathionine that is interpreted by the pancreas as hyperaminoacidemia, and this activates a positive feedback loop between cystathionine and glucagon, culminating in 16-fold elevated cystathionine. Assuming that a hen just consumed a flaxseed meal (either DF or WF) and the initial anti-B6 effects have already taken place, the positive feedback loop might look like:

4-fold elevated cystathionine → more glucagon release → more hepatic CBS activity → **8-fold elevated cystathionine** → more glucagon release → more hepatic CBS activity → **16-fold elevated cystathionine** → **END OF LOOP** (blood glucose is so elevated at this point that pancreatic somatostatin blocks further glucagon release)

7.5 Are DF hens at risk of developing aggressive tumors?

This is where courage counts. The synthesis of 5,10-CH_2THF from SHMT might be elevated in DF hens, given their slightly reduced serine:glycine ratio. This would provide more one-carbon substrate for reactions within the folate cycle, especially the *Ts* reaction where dTMP is synthesized. DF hens exhibited a thymidine-sparing effect that might suggest elevated TYMS activity (as a result of reduced TK activity). Furthermore, the elevated SAM in DF hens suggests that the cytosolic 5,10-CH_2THF will preferentially react with TYMS and SHMT1. Compositely,

these observations suggest anecdotally that TYMS activity might be elevated in DF hens. Would this cause elevated dTMP synthesis, or would it simply mean decreased TK supplementation and stable dTMP synthesis? This is a complex question but important to consider in the context of cancer. dTMP must be incorporated into the DNA to ensure proper DNA replication during the S-phase of the cell cycle. As such, elevated dTMP synthesis would provide a pro-proliferative advantage to tumors. Highly active TYMS is a prognostic risk factor for reduced survival in various forms of cancer (395–397). Chemotherapeutic substances such as 5-fluorouracil (5-FU), when converted to 5-fluoro-2'deoxy-5' monophosphate, prevent TYMS from synthesizing dTMP and thereby exert anti-proliferative effects in solid tumors (398,399). Further research is needed to determine if TYMS activity is regulated by the DF diet in a manner that promotes tumor development. Ironically, if TYMS activity is upregulated in DF hens, it could make DF hens a useful animal model for studying TYMS-inhibiting drugs in the context of ovarian cancer. Some research suggests that our DF hens might be useful as a positive control for studying the refractory effects (i.e. upregulated folate cycle proteins) of platinum chemotherapy in human ovarian cancer (400).

7.6 Could serine be lower in DF hens in support of gluconeogenesis or glycogen synthesis?

We propose in our model that serine catabolism via SHMT is increased, in DF hens, in support of 5,10-CH_2THF synthesis (helping to aid in Hcy remethylation). However, we have a strong phenotypic indication that glycogenolysis and gluconeogenesis are elevated in DF and WF hens (by way of 3-fold elevated HbA1c and slightly decreased pyruvate). Is it possible that DF hens have slightly decreased serine in support of gluconeogenesis and/or glycogen synthesis (to replace rapidly broke-down glycogen). If DF hens are consuming serine in support of glucose and/or glycogen synthesis, then that might challenge our model's proposition of increased

SHMT activity in DF hens. What does the literature have to say about this?

The kidney is the primary organ for gluconeogenesis in chickens, while the liver is the primary organ for gluconeogenesis in mammals (401). In chickens, lactate carbon (via the Cori cycle) is the primary contributor to hepatic gluconeogenesis, because the cytosolic form of phosphoenoylpyruvate carboxykinase (PEPCK) is not active in chicken liver (which probably explains why chickens conduct gluconeogenesis primarily in the kidney) (402). Pyruvate and certain amino acids (glutamine, glutamate, alanine, aspartate and proline) are contributors to gluconeogenesis in the kidneys of starving chickens, while serine and glycine are not contributors (402). A different lab observed that gluconeogenesis is supported in starving chickens by administration of the following amino acids: alanine > glycine > aspartate > serine > glutamate > arginine (403). Those researchers observed that hyperglycemia was supported in starving chickens by administration of lactate, glycerol or pyruvate, in the order of lactate > glycerol > pyruvate (403). They also observed that serine administration was the only substrate that increased glycogen synthesis in starving birds (403).

Overall, it seems that serine is not a good candidate for the support of gluconeogenesis or hyperglycemia in chickens. It might be possible that the catabolism of serine is increased in support of glycogen synthesis; however, this idea would be based on previous studies that were conducted in 48 hour fasted chickens (i.e. starved animals). Those starved chickens would likely have elevated glucagon secretion. However, the animals in our study were not starved whatsoever, so we do not know how comparable starvation studies would be with our work. Nonetheless, it certainly is interesting to fathom that glycogenolysis and gluconeogenesis are upregulated in DF and WF hens (i.e. non-fasted animals). This is such a rare perspective on physiology…the ability to study upregulated glycogenolysis and gluconeogenesis in non-fasted

animals (i.e. DF and WF hens). Glycogenolysis and gluconeogenesis typically occur during the fasted state, so this might infer that flaxseed dieting induces a “fasting like” metabolic effect in hens. This would be truly paradoxical.

Future work is needed in this area to determine if the flaxseed diet causes hens to increase their catabolism of serine in support of gluconeogenesis, hyperglycemia or glycogen synthesis, in hens. From our study, there was no significant effect of diet on the following amino acids: alanine, aspartate, glutamate, arginine, asparagine or proline. Lactate was also not affected by diet. Pyruvate, however, was slightly decreased in DF hens and WF hens, suggesting a possible contribution of pyruvate toward renal gluconeogenesis. Without any affect on other major candidates, such as alanine or lactate, it seems somewhat less likely that serine catabolism was elevated in support of anabolic glucose metabolism.

7.7 Could a high SAM:SAH ratio be pathological in DF hens?

It is reasonable to ask if hypermethylation might serve a pathological role in flaxseed-fed hens. Too much methylation, particularly too much DNA methylation, induces a number of diseases in humans (404). As a counterbalance to the risk of hypermethylation, we detected significantly elevated levels of MTA in DF hens. MTA (a derivative of *dc*SAM) is a cell-permeable, pan-methyltransferase inhibitor that has been used extensively in the context of preventing histone arginine hypermethylation (115,117). MTA could serve a role in balancing the methylation capacity, and thereby prevent hypermethylation-associated pathology in DF hens. This also suggests that DF hens might be useful as an *in vivo* positive control for testing the effects of methyltransferase inhibitors.

7.8 What might this research mean about chicken metabolism, in general? Furthermore, how might Galloanserae (i.e. chickens and ducks) have survived the Cretaceous-Paleogene boundary mass extinction event 66 million years ago?

I would like to take a moment to address a key extrapolation of my research findings. It is without equivocation that we identified a paradoxical metabolic outcome in chickens that eat flaxseed. Flaxseed-fed hens display multiple predictable perturbations: one of reduced vitamin B6 level and the other of elevated cystathionine level. Up front, it is apparent that the TS pathway (where cystathionine is produced) could be an early warning that a starvation-like condition is present in the bird. And how could this be? Consider vitamin B6. Vitamin B6 is arguably one of the most important prosthetic groups (or cofactors) in biology (55), meaning that vitamin B6 is present in practically all forms of life. Given the common availability of vitamin B6 in biological organisms, it is very uncommon for a person to experience vitamin B6 deficiency when food is adequately available (405). Life eats life, so the mere act of eating is the act of consuming vitamin B6. Without attempting to sound sarcastic, a medical clinician's first question to a patient who exhibits a vitamin B6 deficiency should be, "are you eating food?" Through this perspective, one could fathom that reduced levels of B6 within an animal induce a starvation-like response. We observed starvation-like effects in flaxseed-fed hens, such that flaxseed-fed hens weighed significantly less (e.g. they weigh 10% less than control-fed hens). This likely indicates that flaxseed-fed hens increase their phospholipid catabolism, triglyceride catabolism and fatty acid oxidation, in response to the anti-vitamin B6 effects of flaxseed. Our evidence suggests that flaxseed increases lipolysis in hens, as evidenced by elevated circulating blood plasma free fatty acids. This is probably the result of increased glucagon secretion. In support of elevated glucagon secretion, our flaxseed-fed hens also had 3-fold elevated HbA1c

and slightly reduced plasma pyruvate. These were likely the result of elevated glycogenolysis and elevated gluconeogenesis. Altogether flaxseed's anti-B6 effects associated with a phenotype of elevated glucagon secretion, in hens.

The glucagon-like phenotype of flaxseed-fed hens could be a metabolic adaptation in hens (or perhaps birds, in general) that are exposed to vitamin B6 antagonism, or B6 deficiency. This informs me that the TS pathway functions as both a "sensor" and "signal" of starvation, in hens. The B6-dependent enzymes, CBS and CSE, function as "sensors" of starvation given their catalytic dependence on vitamin B6. Subsequently, an elevation of plasma cystathionine functions as a TS-mediated "signal" of starvation, because elevated cystathionine is the downstream result of insulted B6 levels within the TS pathway. This sensor and signal process might be particularly conserved within the TS pathway of ornithine species. When food availability is challenged due to seasonal disparity or due to environmental pressure, the TS pathway can serve in a capacity that announces the presence of vitamin deficiency.

Recent evidence indicates that extant birds of today (i.e. "crown birds" or members of Galloanserae such as landfowl and waterfowl) were likely alive prior to the Cretaceous-Paleogene (K-Pg) boundary event 66 million years ago. The most reliable "neo-ornithine" fossil is an in-tact, 3-dimensionally preserved skull fossil of a crown bird sharing phenotypic qualities of a turkey, duck and chicken (ie "turducken"), dating 66.7 to 66.8 million years ago (406,407). The authors of (406) provided this neornithine bird with the taxonomical name *Asteriornis maastrichtensis*; they also referred to the bird colloquially as a 'Wonderchicken' (406). The skull fossil from *A. maastrichtensis* provides evidence that this bird lived prior to the K-Pg boundary mass extinction, while also indicating phenotypically similar presentation as modern-day Galloanserae. What does this mean? It means that modern day Galloanserae (chickens and

ducks) might be very directly descended from survivors of the K-Pg boundary extinction! This is a tremendous observation.

The K-Pg boundary (precision-dated to 66.02 million years ago (408)) represents the consequences of a 10km-wide meteor impacting Earth at the Chicxulub site near the Yucatan Peninsula. The Chicxulub meteor impact forced a tremendous plumage of stratospheric soot (409) that blocked incoming solar radiation by 80-90% and caused rapid global cooling (i.e. caused Earth's "impact winter") (410). This loss of solar radiation concomitant with vast cooling elicited an 88% extinction amongst terrestrial animals, primarily due to widespread loss of plants (411,412). In other words, the K-Pg mass extinction was mostly the result of widespread starvation beginning at the level of primary producers. Birds, like other terrestrial animals, were heavily subjected to the selective pressure of mass extinction during the K-Pg boundary (413,414). It is my current opinion that modern day Galliformes (i.e. chickens) respond to vitamin B6 antagonism in a way that helps us to understand how pre-K-Pg crown birds like *Asteriornis maastrichtensis* might have responded to the tremendous selective pressure of mass starvation during the K-Pg boundary extinction. In the presence of reduced B vitamin availability (i.e. in the presence of starvation-like conditions), we would expect pre-K-Pg crown birds to exhibit reduced TS flux, elevated Hcy remethylation (via BHMT and MS-B12) and increased oxidation of PC, choline, betaine, DMG and serine. The presence of a complete ERE in the DNA locus of chicken PEMT (as we observed in our current study) is another factor that likely protects chickens (especially hens) from starvation (82). The ability of females to regulate PEMT via estrogen signaling is suspected to be a chief reason why PEMT protects females from pathologies associated with choline deficiency (82).

All of this means that pre-K-Pg crown birds would have been more protected from the risk of

starvation-induced hyperHcy. Pre-K-Pg crown birds would also be more able to maintain a viable methylation index (i.e SAM:SAH ratio) and a viable epigenome, despite exposure to the B-vitamin-deficient conditions of starvation. Therefore, crown birds would have been better adapted to deal with the severe starvation conditions that were faced by terrestrial animals in response to the Chicxulub meteor impact. Famine and B-vitamin deficiency are associated with severe pathologies such as cardiovascular diseases in humans (415,416). I am suggesting that crown birds would have been less vulnerable to the development of B-vitamin deficiency-associated pathologies, allowing crown birds to survive the extreme selective starvation pressure of the K-Pg boundary extinction. One can fathom that, in the aftermath of the K-Pg boundary extinction, crown birds would be "metabolically suited" to successfully recover their populations and fill new ecological niches.

Pre-K-Pg crown birds would not be expected to survive excessive B vitamin deprivation, so there are realistic limitations to this hypothetical framework. However, up to a certain point of B vitamin deficiency, pre-K-Pg crown birds would be expected to display a paradoxical sustainment of biological vitality (ie egg laying and lifespan). Is it tremendously wild to make metabolic assumptions about animals that lived over 66 million years ago? Yes, it is wild. It is also exciting and possible. As a scientist who is versed in environmental, biological, molecular, biochemical and geographic studies, I feel that it is within my capacity to ontologically connect biological information about extant species today and paleontological information about past species.

Biology is a continuous process of natural selection, and nothing is more selective than mass extinction. The selective pressure of mass extinction might be better understood through the term "mass starvation." The essential question is, "why have certain species survived the universe's

repeated attempts at biological eradication?" All life that exists today holds information that can help us to answer this question, especially with regard to the K-Pg boundary extinction. Animals that are alive today might be, in general, well adapted to conditions of nutrient deprivation or blatant starvation. An individual who wants to understand the biological nature of the world (as in, have true "gnosis" of biology), would do well to appreciate why certain species displayed tremendous survivorship during the K-Pg boundary extinction. Certain physiological factors such as flying ability (i.e. increased land sampling), omnivorous eating behavior and small body size, were beneficial factors that probably improved animal survival during the K-Pg boundary extinction. By no means do I discredit the importance of those factors. My argument is that certain metabolic adaptations within crown birds (i.e. the ability to tolerate B6-vitamin deficiency) were important factors that determined survival and reproductive capacity during the tremendous starvation pressure that emerged after the Chicxulub meteor impact 66 million years ago. Furthermore, if pre-K-Pg crown birds had not displayed physiological resistance to B-vitamin deficiency, I predict that more crown bird species would have fallen extinct during the K-Pg boundary extinction event (despite being small, omnivorous creatures of flight).

Future researchers should investigate the role of transsulfuration as an early-stage sensor of nutrient deprivation in birds. This might be one of the integral reasons why birds have displayed such high resilience in the face of environmental changes that would have otherwise spelled localized and/or generalized species extinction. How can humans harness this biotechnological information? Can this flaxseed-based biotechnology be used to help with the breeding of endangered vertebrate species? Zoological organizations might be able to leverage our findings to help expand endanger species populations, specifically because this natural biotechnological approach focuses on improving animal survival and animal reproductive capacity.

REFERENCES

1. **Mayengbam S, Raposo S, Aliani M, House JD.** Oral exposure to the anti-pyridoxine compound 1-amino d-proline further perturbs homocysteine metabolism through the transsulfuration pathway in moderately vitamin B6 deficient rats. *J. Nutr. Biochem.* 2015;26(3):241–249.
2. **Davis JE, Cain J, Small C, Hales DB.** Therapeutic effect of flax-based diets on fatty liver in aged laying hens. *Poult. Sci.* 2016;95(11):2624–2632.
3. **Ferlay J, Soerjomataram I, Dikshit R, Eser S, Mathers C, Rebelo M, Parkin DM, Forman D, Bray F.** Cancer incidence and mortality worldwide: Sources, methods and major patterns in GLOBOCAN 2012. *Int. J. Cancer* 2015;136(5):E359–E386.
4. **Allemani C, Weir HK, Carreira H, Harewood R, Spika D, Wang X-S, Bannon F, Ahn J V, Johnson CJ, Bonaventure A, Marcos-Gragera R, Stiller C, Azevedo e Silva G, Chen W-Q, Ogunbiyi OJ, Rachet B, Soeberg MJ, You H, Matsuda T, Bielska-Lasota M, Storm H, Tucker TC, Coleman MP.** Global surveillance of cancer survival 1995–2009: analysis of individual data for 25 676 887 patients from 279 population-based registries in 67 countries (CONCORD-2). *Lancet* 2015;385(9972):977–1010.
5. **Howlader N, Noone AM, Krapcho M, Miller D, Brest A, Yu M, Ruhl J, Tatalovich Z, Mariotto A, Lewis DR, Chen HS, Feuer EJ CK.** SEER Cancer Statistics Review, 1975-2017. *Natl. Cancer Inst.*:https://seer.cancer.gov/csr/1975_2017/.
6. **Casagrande JT, Pike MC, Ross RK, Louie EW, Roy S, Henderson BE.** "INCESSANT OVULATION" AND OVARIAN CANCER. *Lancet* 1979;314(8135):170–173.
7. **Gnagy S, Ming EE, Devesa SS, Hartge P, Whittemore AS.** Declining Ovarian Cancer

Rates in U.S. Women in Relation to Parity and Oral Contraceptive Use. *Epidemiology* 2000;11(2):102–105.

8. **McGuire V, Hartge P, Liao LM, Sinha R, Bernstein L, Canchola AJ, Anderson GL, Stefanick ML, Whittemore AS.** Parity and Oral Contraceptive Use in Relation to Ovarian Cancer Risk in Older Women. *Cancer Epidemiol. Biomarkers Prev.* 2016;25(7):1059–1063.
9. **Barua A, Bitterman P, Abramowicz JS, Dirks AL, Bahr JM, Hales DB, Bradaric MJ, Edassery SL, Rotmensch J, Luborsky JL.** Histopathology of ovarian tumors in laying hens, a preclinical model of human ovarian cancer. *Int. J. Gynecol. Cancer* 2009;19(4):531–539.
10. **Johnson PA, Giles JR.** The hen as a model of ovarian cancer. *Nat. Rev. Cancer* 2013;13:432.
11. **Hakim AA, Barry CP, Barnes HJ, Anderson KE, Petitte J, Whitaker R, Lancaster JM, Wenham RM, Carver DK, Turbov J, Berchuck A, Kopelovich L, Rodriguez GC.** Ovarian Adenocarcinomas in the Laying Hen and Women Share Similar Alterations in p53, ras, and HER-2/neu. *Cancer Prev. Res.* 2009;2(2):114 LP – 121.
12. **Hawkridge AM.** The Chicken Model of Spontaneous Ovarian Cancer. *Proteomics. Clin. Appl.* 2014;8(9–10):689–699.
13. **Giles JR, Elkin RG, Trevino LS, Urick ME, Ramachandran R, Johnson PA.** The restricted ovulator chicken: A unique animal model for investigating the etiology of ovarian cancer. *Int. J. Gynecol. Cancer* 2010;20(5):738–744.
14. **Hales KH, Speckman SC, Kurrey NK, Hales DB.** Uncovering molecular events associated with the chemosuppressive effects of flaxseed: a microarray analysis of the

laying hen model of ovarian cancer. *BMC Genomics* 2014;15(1):709.

15. **Dikshit A, Gomes Filho MA, Eilati E, McGee S, Small C, Gao C, Klug T, Hales DB.** Flaxseed reduces the pro-carcinogenic micro-environment in the ovaries of normal hens by altering the PG and oestrogen pathways in a dose-dependent manner. *Br. J. Nutr.* 2015;113(9):1384–1395.
16. **Dikshit A, Hales K, Hales DB.** Whole flaxseed diet alters estrogen metabolism to promote 2-methoxtestradiol-induced apoptosis in hen ovarian cancer. *J. Nutr. Biochem.* 2017;42:117–125.
17. **Dikshit A, Gao C, Small C, Hales K, Hales DB.** Flaxseed and its components differentially affect estrogen targets in pre-neoplastic hen ovaries. *J. Steroid Biochem. Mol. Biol.* 2016;159:73–85.
18. **Eilati E, Bahr JM, Hales DB.** Long term consumption of flaxseed enriched diet decreased ovarian cancer incidence and prostaglandin E_2in hens. *Gynecol. Oncol.* 2013;130(3):620–628.
19. **Ansenberger K, Richards C, Zhuge Y, Barua A, Bahr JM, Luborsky JL, Hales DB.** Decreased severity of ovarian cancer and increased survival in hens fed a flaxseed-enriched diet for 1 year. *Gynecol. Oncol.* 2010;117(2):341–347.
20. **Eilati E, Small CC, McGee SR, Kurrey NK, Hales DB.** Anti-inflammatory effects of fish oil in ovaries of laying hens target prostaglandin pathways. *Lipids Health Dis.* 2013;12(1):1.
21. **Pal P, Hales K, Petrik J, Hales DB.** Pro-apoptotic and anti-angiogenic actions of 2-methoxyestradiol and docosahexaenoic acid, the biologically derived active compounds from flaxseed diet, in preventing ovarian cancer. *J. Ovarian Res.* 2019;12(1):49.

22. **Zohary D.** Monophyletic vs. polyphyletic origin of the crops on which agriculture was founded in the Near East. *Genet. Resour. Crop Evol.* 1999;46(2):133–142.

23. **W. van Uden, N. Pras HJW.** Linum species (Flax): in vivo and in vitro accumulation of lignans and other metabolites. In: *Y.P.S. Bajaj (Ed.), Biotechnology in agriculture and forestry, Medicinal and aromatic plants VI, Vol. 26*. Berlin, Germany: Springer-Verlag; 1994:219–244.

24. **Oomah BD, Mazza G.** Effect of Dehulling on Chemical Composition and Physical Properties of Flaxseed. *LWT - Food Sci. Technol.* 1997;30(2):135–140.

25. **Cloutier S, Ragupathy R, Niu Z, Duguid S.** SSR-based linkage map of flax (Linum usitatissimum L.) and mapping of QTLs underlying fatty acid composition traits. *Mol. Breed.* 2011;28(4):437–451.

26. **Green A.G.** Mutation breeding for fatty acid composition in flax (Linum usitatissimum). In: *FAO/IAEA Co-ordinated Research Programme*. Bombay; 1990:2–4.

27. **Muir A and WN.** *Flax: the genus Linum*. London; 2003.

28. **Burr, G.O.; Burr MM.** Nutrition, On the nature and role of the fatty acids essential in nutrition. *J. Biol. Chem.* 1930;86:587–621.

29. **Burr GO, Burr MM, Miller ES.** ON THE FATTY ACIDS ESSENTIAL IN NUTRITION. III. *J. Biol. Chem.* 1932;97(1):1–9.

30. **Burr GO., Burr MM.** A new deficiency disease produced by the rigid exclusion of fat from the diet. *Nutr. Rev.* 1929;82:345–367.

31. **Glick NR, Fischer MH.** The Role of Essential Fatty Acids in Human Health. *J. Evid. Based. Complementary Altern. Med.* 2013;18(4):268–289.

32. **Kaur N, Chugh V, Gupta AK.** Essential fatty acids as functional components of foods- a

review. *J. Food Sci. Technol.* 2014;51(10):2289–2303.

33. **Hall C, Tulbek MC, Xu YBT-A in F and NR.** Flaxseed. In: Vol 51. Academic Press; 2006:1–97.

34. **Oomah BD, Mazza G.** Flaxseed proteins—a review. *Food Chem.* 1993;48(2):109–114.

35. **Shim YY, Gui B, Arnison PG, Wang Y, Reaney MJT.** Flaxseed (Linum usitatissimum L.) bioactive compounds and peptide nomenclature: A review. *Trends Food Sci. Technol.* 2014;38(1):5–20.

36. **Chung MWY, Lei B, Li-Chan ECY.** Isolation and structural characterization of the major protein fraction from NorMan flaxseed (Linum usitatissimum L.). *Food Chem.* 2005;90(1):271–279.

37. **V. MAN. BAK. ZVV. M.** [Nutritional value and functional properties of flaxseed]. *Vopr. Pitan.* 2012;81(3):4–10.

38. **Marambe HK, Shand PJ, Wanasundara JPD.** In vitro digestibility of flaxseed (Linum usitatissimum L.) protein: effect of seed mucilage, oil and thermal processing. *Int. J. Food Sci. Technol.* 2013;48(3):628–635.

39. **BUCKNER GD, MARTIN JH.** The Function of Grit in the Gizzard of the Chicken. *Poult. Sci.* 1922;1(4):108–113.

40. **Ames BN, Profet M, Gold LS.** Dietary pesticides (99.99% all natural). *Proc. Natl. Acad. Sci. U. S. A.* 1990;87(19):7777–7781.

41. **Ames BN, Profet M, Gold LS.** Nature's chemicals and synthetic chemicals: comparative toxicology. *Proc. Natl. Acad. Sci. U. S. A.* 1990;87(19):7782–7786.

42. **Estabrook RW.** A PASSION FOR P450s (REMEMBRANCES OF THE EARLY HISTORY OF RESEARCH ON CYTOCHROME P450). *Drug Metab. Dispos.*

2003;31(12):1461 LP – 1473.

43. **Zanger UM, Turpeinen M, Klein K, Schwab M.** Functional pharmacogenetics/genomics of human cytochromes P450 involved in drug biotransformation. *Anal. Bioanal. Chem.* 2008;392(6):1093–1108.

44. **Kajla P, Sharma A, Sood DR.** Flaxseed-a potential functional food source. *J. Food Sci. Technol.* 2015;52(4):1857–1871.

45. **Morrison O.** Europe's food safety watchdog plays down flaxseed cyanide danger. *Food Navig.* 2019. Available at: https://www.foodnavigator.com/Article/2019/08/21/Europe-s-food-safety-watchdog-plays-down-flaxseed-cyanide-danger#.

46. **Cressey P, Reeve J.** Metabolism of cyanogenic glycosides: A review. *Food Chem. Toxicol.* 2019;125:225–232.

47. **Morris D.** *Flax-A Health and Nutrition Primer*. 4th ed.; 2007.

48. **Seigler DS.** Cyanide and cyanogenic glycosides. In: *In: Rosenthal GA and Berenbaum MR (eds.) 2502 Herbivores. Their Interaction with Secondary Plant Metabolites, Vol. 1*. Academic Press; 1991:35–77.

49. **Chadha RK, Lawrence JF, Ratnayake WMN.** Ion chromatographic determination of cyanide released from flaxseed under autohydrolysis conditions. *Food Addit. Contam.* 1995;12(4):527–533.

50. **Abraham K, Buhrke T, Lampen A.** Bioavailability of cyanide after consumption of a single meal of foods containing high levels of cyanogenic glycosides: a crossover study in humans. *Arch. Toxicol.* 2016;90(3):559–574.

51. **Birch TW, György P, Harris LJ.** The vitamin B(2) complex. Differentiation of the antiblacktongue and the "P.-P." factors from lactoflavin and vitamin B(6) (so-called "rat

pellagra" factor). Parts I-VI. *Biochem. J.* 1935;29(12):2830–2850.

52. **Parra M, Stahl S, Hellmann H.** Vitamin B_6 and Its Role in Cell Metabolism and Physiology. *Cells* 2018;7(7):84.

53. **M.P. DK. DS. C.** *Handbook of Famine, Starvation, and Nutrient Deprivation*. In: Preedy. Springer; 2017. doi:10.1007/978-3-319-40007-5_81-1.

54. **Toney MD.** Pyridoxal Phosphate (PLP). 2020. Available at: https://sites.google.com/site/mdtoneylab/research/pyridoxal-phosphate-enzymes.

55. **Mooney S, Leuendorf J-E, Hendrickson C, Hellmann H.** Vitamin B6: a long known compound of surprising complexity. *Molecules* 2009;14(1):329–351.

56. **Havaux M, Ksas B, Szewczyk A, Rumeau D, Franck F, Caffarri S, Triantaphylidès C.** Vitamin B6 deficient plants display increased sensitivity to high light and photo-oxidative stress. *BMC Plant Biol.* 2009;9:130.

57. **Bilski P, Li MY, Ehrenshaft M, Daub ME, Chignell CF.** Vitamin B6 (Pyridoxine) and Its Derivatives Are Efficient Singlet Oxygen Quenchers and Potential Fungal Antioxidants. *Photochem. Photobiol.* 2000;71(2):129–134.

58. **Klosterman HJ.** Vitamin B6 antagonists of natural origin. *J. Agric. Food Chem.* 1974;22(1):13–16.

59. **Klosterman HJ, Lamoureux GL, Parsons JL.** Isolation, Characterization, and Synthesis of Linatine. A Vitamin B6 Antagonist from Flaxseed (Linum usitatissimum)*. *Biochemistry* 1967;6(1):170–177.

60. **Schlamb KF, Clagett CO, Bryant RL.** Comparison of the Chick Growth Inhibition of Unheated Linseed Hull and Cotyledon Fractions12. *Poult. Sci.* 1955;34(6):1404–1407.

61. **Bethke RM. GBHLSDC, H. EK and BHE.** The comparative nutritive value of the

proteins of linseed meal and cottonseed meal for different animals. *J. Agric. Res.* 1928;36:817–855.

62. **Kratzer FH, Williams DE.** The Improvement of Linseed Oil Meal for Chick Feeding by the Addition of Synthetic Vitamins. *Poult. Sci.* 1948;27(2):236–238.

63. **MacGregor HI, McGinnis J.** Toxicity of Linseed Meal for Chicks*. *Poult. Sci.* 1948;27(2):141–145.

64. **Kratzer FH.** The Growth Depression of Turkey Poults Caused by Linseed Oil Meal. *Poult. Sci.* 1949;28(4):618–620.

65. **Dunn WA, Aronson NN, Englard S.** The effects of 1-amino-D-proline on the production of carnitine from exogenous protein-bound trimethyllysine by the perfused rat liver. *J. Biol. Chem.* 1982;257(14):7948–7951.

66. **Mayengbam S, Raposo S, Aliani M, House JD.** A Vitamin B-6 Antagonist from Flaxseed Perturbs Amino Acid Metabolism in Moderately Vitamin B-6–Deficient Male Rats. *J. Nutr.* 2015;146(1):14–20.

67. **Xu J, Sinclair KD.** One-carbon metabolism and epigenetic regulation of embryo development. *Reprod. Fertil. Dev.* 2015;27(4):667–676.

68. **Clare CE, Brassington AH, Kwong WY, Sinclair KD.** One-Carbon Metabolism: Linking Nutritional Biochemistry to Epigenetic Programming of Long-Term Development. *Annu. Rev. Anim. Biosci.* 2019;7(1):263–287.

69. **Meier M, Janosik M, Kery V, Kraus JP, Burkhard P.** Structure of human cystathionine beta-synthase: a unique pyridoxal 5’-phosphate-dependent heme protein. *EMBO J.* 2001;20(15):3910–3916.

70. **Williams KT, Schalinske KL.** Homocysteine metabolism and its relation to health and

disease. *Biofactors* 2010;36(1):19–24.

71. **Wang L, Niu H, Zhang J.** Homocysteine induces mitochondrial dysfunction and oxidative stress in myocardial ischemia/reperfusion injury through stimulating ROS production and the ERK1/2 signaling pathway. *Exp Ther Med* 2020;20(2):938–944.

72. **Austin RC, Sood SK, Dorward AM, Singh G, Shaughnessy SG, Pamidi S, Outinen PA, Weitz JI.** Homocysteine-dependent Alterations in Mitochondrial Gene Expression, Function and Structure: HOMOCYSTEINE AND H2O2 ACT SYNERGISTICALLY TO ENHANCE MITOCHONDRIAL DAMAGE . *J. Biol. Chem.* 1998;273(46):30808–30817.

73. **Chen S, Dong Z, Zhao Y, Sai N, Wang X, Liu H, Huang G, Zhang X.** Homocysteine induces mitochondrial dysfunction involving the crosstalk between oxidative stress and mitochondrial pSTAT3 in rat ischemic brain. *Sci. Rep.* 2017;7(1):6932.

74. **Kruman II, Culmsee C, Chan SL, Kruman Y, Guo Z, Penix L, Mattson MP.** Homocysteine elicits a DNA damage response in neurons that promotes apoptosis and hypersensitivity to excitotoxicity. *J. Neurosci.* 2000;20(18):6920–6926.

75. **Ganguly P, Alam SF.** Role of homocysteine in the development of cardiovascular disease. *Nutr. J.* 2015;14:6.

76. **Dowhan W, Bogdanov MBT-NCB.** Chapter 1 Functional roles of lipids in membranes. In: *in: Vance D. E. & Vance J. E., Biochemistry of Lipids, Lipoproteins and Membranes, 4th edition.*Vol 36. Elsevier; 2002:1–35.

77. **Ye C, Sutter BM, Wang Y, Kuang Z, Tu BP.** A Metabolic Function for Phospholipid and Histone Methylation. *Mol. Cell* 2017;66(2):180-193.e8.

78. **Stead LM, Brosnan JT, Brosnan ME, Vance DE, Jacobs RL.** Is it time to reevaluate

methyl balance in humans? *Am. J. Clin. Nutr.* 2006;83(1):5–10.

79. **Jacobs RL, Stead LM, Devlin C, Tabas I, Brosnan ME, Brosnan JT, Vance DE.** Physiological regulation of phospholipid methylation alters plasma homocysteine in mice. *J. Biol. Chem.* 2005;280(31):28299–305.

80. **Sato N, Mori N, Hirashima T, Moriyama T.** Diverse pathways of phosphatidylcholine biosynthesis in algae as estimated by labeling studies and genomic sequence analysis. *Plant J.* 2016;87(3):281–292.

81. **Cui Z, Vance DE.** Expression of Phosphatidylethanolamine N-Methyltransferase-2 Is Markedly Enhanced in Long Term Choline-deficient Rats . *J. Biol. Chem.* 1996;271(5):2839–2843.

82. **Walkey CJ, Yu L, Agellon LB, Vance DE.** Biochemical and Evolutionary Significance of Phospholipid Methylation. *J. Biol. Chem.* 1998;273(42):27043–27046.

83. **Vance DE, Ridgway ND.** The methylation of phosphatidylethanolamine. *Prog. Lipid Res.* 1988;27(1):61–79.

84. **Vance DE, Walkey CJ, Cui Z.** Phosphatidylethanolamine N-methyltransferase from liver. *Biochim. Biophys. Acta - Lipids Lipid Metab.* 1997;1348(1):142–150.

85. **Vance JE.** Phospholipid synthesis in a membrane fraction associated with mitochondria. *J. Biol. Chem.* 1990;265(13):7248–7256.

86. **Åkesson B.** Autoregulation of phospholipid N-methylation by the membrane phosphatidylethanolamine content. *FEBS Lett.* 1978;92(2):177–180.

87. **Sundler R, Akesson B.** Regulation of phospholipid biosynthesis in isolated rat hepatocytes. Effect of different substrates. *J. Biol. Chem.* 1975;250(9):3359–3367.

88. **DeLong CJ, Shen YJ, Thomas MJ, Cui Z.** Molecular distinction of phosphatidylcholine

synthesis between the CDP- choline pathway and phosphatidylethanolamine methylation pathway. *J. Biol. Chem.* 1999;274(42):29683–29688.

89. **Zeisel SH, Zola T, daCosta KA, Pomfret EA.** Effect of choline deficiency on S-adenosylmethionine and methionine concentrations in rat liver. *Biochem. J.* 1989;259(3):725–729.

90. **Cantoni GL.** S-ADENOSYLMETHIONINE; A NEW INTERMEDIATE FORMED ENZYMATICALLY FROM l-METHIONINE AND ADENOSINETRIPHOSPHATE. *J. Biol. Chem.* 1953;204(1):403–416.

91. **Giordana L, Mantilla B, Santana M, Silber A, Nowicki C.** Cystathionine γ-lyase, an Enzyme Related to the Reverse Transsulfuration Pathway, is Functional in Leishmania spp. *J. Eukaryot. Microbiol.* 2014;61. doi:10.1111/jeu.12100.

92. **Macnicol PK, Datko AH, Giovanelli J, Mudd SH.** Homocysteine Biosynthesis in Green Plants: Physiological Importance of the Transsulfuration Pathway in Lemna paucicostata. *Plant Physiol.* 1981;68(3):619–625.

93. **Osborne CB, Lowe KE, Shane B.** Regulation of folate and one-carbon metabolism in mammalian cells. I. Folate metabolism in Chinese hamster ovary cells expressing Escherichia coli or human folylpoly-gamma-glutamate synthetase activity. *J. Biol. Chem.* 1993;268(29):21657–21664.

94. **Koutmos M, Datta S, Pattridge KA, Smith JL, Matthews RG.** Insights into the reactivation of cobalamin-dependent methionine synthase. *Proc. Natl. Acad. Sci.* 2009;106(44):18527 LP – 18532.

95. **Slow S, Garrow TA.** Liver Choline Dehydrogenase and Kidney Betaine-Homocysteine Methyltransferase Expression Are Not Affected by Methionine or Choline Intake in

Growing Rats. *J. Nutr.* 2006;136(9):2279–2283.

96. **Millian NS, Garrow TA.** Human Betaine–Homocysteine Methyltransferase Is a Zinc Metalloenzyme. *Arch. Biochem. Biophys.* 1998;356(1):93–98.

97. **Neece DJ, Griffiths MA, Garrow TA.** Isolation and characterization of a mouse betaine-homocysteine S-methyltransferase gene and pseudogene. *Gene* 2000;250(1):31–40.

98. **Finkelstein JD.** Methionine metabolism in liver diseases. *Am. J. Clin. Nutr.* 2003;77(5):1094–1095.

99. **Finkelstein JD.** Inborn Errors of Sulfur-Containing Amino Acid Metabolism. *J. Nutr.* 2006;136(6):1750S-1754S.

100. **Mudd SH, Brosnan JT, Brosnan ME, Jacobs RL, Stabler SP, Allen RH, Vance DE, Wagner C.** Methyl balance and transmethylation fluxes in humans. *Am. J. Clin. Nutr.* 2007;85(1):19–25.

101. **Strakova J, Gupta S, Kruger WD, Dilger RN, Tryon K, Li L, Garrow TA.** Inhibition of betaine-homocysteine S-methyltransferase in rats causes hyperhomocysteinemia and reduces liver cystathionine β-synthase activity and methylation capacity. *Nutr. Res.* 2011;31(7):563–571.

102. **Zhang Y, Zhu T, Wang L, Pan Y-H, Zhang S.** Homocysteine homeostasis and betaine-homocysteine S-methyltransferase expression in the brain of hibernating bats. *PLoS One* 2013;8(12):e85632–e85632.

103. **Finkelstein JD.** Methionine metabolism in mammals. *J. Nutr. Biochem.* 1990;1(5):228–237.

104. **Mudd SH and JRP.** Labile methyl balances for normal humans on various dietary regimens. *Metab. Clin. Exp.* 1975;24(6):721–735.

105. **McMullen MH, Rowling MJ, Ozias MK, Schalinske KL.** Activation and induction of glycine N-methyltransferase by retinoids are tissue- and gender-specific. *Arch. Biochem. Biophys.* 2002;401(1):73–80.

106. **Xia L, Ma S, Zhang Y, Wang T, Zhou M, Wang Z, Zhang J.** Daily variation in global and local DNA methylation in mouse livers. *PLoS One* 2015;10(2):e0118101–e0118101.

107. **Xue C, Zhao Y, Li L.** Advances in RNA cytosine-5 methylation: detection, regulatory mechanisms, biological functions and links to cancer. *Biomark. Res.* 2020;8(1):43.

108. **Wang X, Lu Z, Gomez A, Hon GC, Yue Y, Han D, Fu Y, Parisien M, Dai Q, Jia G, Ren B, Pan T, He C.** N6-methyladenosine-dependent regulation of messenger RNA stability. *Nature* 2014;505(7481):117–120.

109. **Männistö PT, Kaakkola S.** Catechol-O-methyltransferase (COMT): Biochemistry, Molecular Biology, Pharmacology, and Clinical Efficacy of the New Selective COMT Inhibitors. *Pharmacol. Rev.* 1999;51(4):593 LP – 628.

110. **Kerr SJ.** Competing Methyltransferase Systems. *J. Biol. Chem.* 1972;247(13):4248–4252.

111. **Cantoni G.** S-Adenosylamino Acids Thirty Years Later: 1951–1981. In: *Biochemistry of S-Adenosylmethionine and Related Compounds*. London: Palgrave Macmillan; 1982:3–10.

112. **Cantoni GL, Chiang PK.** The Role of S-Adenosylhomocysteine and S-Adenosylhomocysteine Hydrolase in the Control of Biological Methylations. In: Cavallini D., Gaull G.E. ZV (eds), ed. *Natural Sulfur Compounds*. Boston, MA: Springer; 1980:67–80.

113. **Soda K.** Polyamine Metabolism and Gene Methylation in Conjunction with One-Carbon Metabolism. *Int. J. Mol. Sci.* 2018;19(10):3106.

114. **Pegg AE, McCann PP.** Polyamine metabolism and function. *Am. J. Physiol. Physiol.* 1982;243(5):C212–C221.

115. **Zhang J, Zheng YG.** SAM/SAH Analogs as Versatile Tools for SAM-Dependent Methyltransferases. *ACS Chem. Biol.* 2016;11(3):583–597.

116. **Mavrakis KJ, McDonald ER, Schlabach MR, Billy E, Hoffman GR, deWeck A, Ruddy DA, Venkatesan K, Yu J, McAllister G, Stump M, deBeaumont R, Ho S, Yue Y, Liu Y, Yan-Neale Y, Yang G, Lin F, Yin H, Gao H, Kipp DR, Zhao S, McNamara JT, Sprague ER, Zheng B, Lin Y, Cho YS, Gu J, Crawford K, Ciccone D, Vitari AC, Lai A, Capka V, Hurov K, Porter JA, Tallarico J, Mickanin C, Lees E, Pagliarini R, Keen N, Schmelzle T, Hofmann F, Stegmeier F, Sellers WR.** Disordered methionine metabolism in MTAP/CDKN2A-deleted cancers leads to dependence on PRMT5. *Science (80-.).* 2016;351(6278):1208 LP – 1213.

117. **Kryukov G V, Wilson FH, Ruth JR, Paulk J, Tsherniak A, Marlow SE, Vazquez F, Weir BA, Fitzgerald ME, Tanaka M, Bielski CM, Scott JM, Dennis C, Cowley GS, Boehm JS, Root DE, Golub TR, Clish CB, Bradner JE, Hahn WC, Garraway LA.** MTAP deletion confers enhanced dependency on the PRMT5 arginine methyltransferase in cancer cells. *Science* 2016;351(6278):1214–1218.

118. **Marjon K, Cameron MJ, Quang P, Clasquin MF, Mandley E, Kunii K, McVay M, Choe S, Kernytsky A, Gross S, Konteatis Z, Murtie J, Blake ML, Travins J, Dorsch M, Biller SA, Marks KM.** MTAP Deletions in Cancer Create Vulnerability to Targeting of the MAT2A/PRMT5/RIOK1 Axis. *Cell Rep.* 2016;15(3):574–587.

119. **Gorelova V, Ambach L, Rébeillé F, Stove C, Van Der Straeten D.** Folates in Plants: Research Advances and Progress in Crop Biofortification. *Front. Chem.* 2017;5:21.

120. **Fowler B.** The folate cycle in human disease. *Kidney Int.* 2001;59(Suppl. 78):S221–S229.

121. **Rosenblatt DS.** *Inherited disorders in folate transport and metabolism*. in Scriver. New York: McGraw-Hill; 1995.

122. **TEFFERI A, PRUTHI RK.** The Biochemical Basis of Cobalamin Deficiency. *Mayo Clin. Proc.* 1994;69(2):181–186.

123. **Hoskins DD, Mackenzie CG.** Solubilization and Electron Transfer Flavoprotein Requirement of Mitochondrial Sarcosine Dehydrogenase and Dimethylglycine Dehydrogenase. *J. Biol. Chem.* 1961;236(1):177–183.

124. **Froese DS, Fowler B, Baumgartner MR.** Vitamin B12, folate, and the methionine remethylation cycle—biochemistry, pathways, and regulation. *J. Inherit. Metab. Dis.* 2019;42(4):673–685.

125. **Abbasi IHR, Abbasi F, Wang L, Abd El Hack ME, Swelum AA, Hao R, Yao J, Cao Y.** Folate promotes S-adenosyl methionine reactions and the microbial methylation cycle and boosts ruminants production and reproduction. *AMB Express* 2018;8(1):65.

126. **MacFarlane AJ, Liu X, Perry CA, Flodby P, Allen RH, Stabler SP, Stover PJ.** Cytoplasmic serine hydroxymethyltransferase regulates the metabolic partitioning of methylenetetrahydrofolate but is not essential in mice. *J. Biol. Chem.* 2008;283(38):25846–25853.

127. **Tramonti A, Nardella C, di Salvo ML, Barile A, Cutruzzolà F, Contestabile R.** Human Cytosolic and Mitochondrial Serine Hydroxymethyltransferase Isoforms in Comparison: Full Kinetic Characterization and Substrate Inhibition Properties. *Biochemistry* 2018;57(51):6984–6996.

128. **Wittwer AJ, Wagner C.** Identification of the folate-binding proteins of rat liver

mitochondria as dimethylglycine dehydrogenase and sarcosine dehydrogenase. Flavoprotein nature and enzymatic properties of the purified proteins. *J. Biol. Chem.* 1981;256(8):4109–4115.

129. **Kikuchi G, Motokawa Y, Yoshida T, Hiraga K.** Glycine cleavage system: reaction mechanism, physiological significance, and hyperglycinemia. *Proc. Jpn. Acad. Ser. B. Phys. Biol. Sci.* 2008;84(7):246–263.

130. **Mailloux RJ, Young A, Chalker J, Gardiner D, O'Brien M, Slade L, Brosnan JT.** Choline and dimethylglycine produce superoxide/hydrogen peroxide from the electron transport chain in liver mitochondria. *FEBS Lett.* 2016;590(23):4318–4328.

131. **Rose MG, Farrell MP, Schmitz JC.** Thymidylate Synthase: A Critical Target for Cancer Chemotherapy. *Clin. Colorectal Cancer* 2002;1(4):220–229.

132. **Anderson DD, Quintero CM, Stover PJ.** Identification of a de novo thymidylate biosynthesis pathway in mammalian mitochondria. *Proc. Natl. Acad. Sci. U. S. A.* 2011;108(37):15163–15168.

133. **Al-Madhoun A. WTSE.** The Role of Thymidine Kinases in the Activation of Pyrimidine Nucleoside Analogues. *Mini Rev. Med. Chem.* 2004;4(4):341–350.

134. **Eriksson S, Munch-Petersen B, Johansson K, Ecklund H.** Structure and function of cellular deoxyribonucleoside kinases. *Cell. Mol. Life Sci. C.* 2002;59(8):1327–1346.

135. **Arnér ESJ, Eriksson S.** Mammalian deoxyribonucleoside kinases. *Pharmacol. Ther.* 1995;67(2):155–186.

136. **Munch-Petersen B, Tyrsted G, Cloos L, Beck RA, Eger K.** Different affinity of the two forms of human cytosolic thymidine kinase towards pyrimidine analogs. *Biochim. Biophys. Acta - Protein Struct. Mol. Enzymol.* 1995;1250(2):158–162.

137. **Kabil O, Vitvitsky V, Xie P, Banerjee R.** The quantitative significance of the transsulfuration enzymes for H2S production in murine tissues. *Antioxid. Redox Signal.* 2011;15(2):363–372.

138. **Banerjee R, Evande R, Kabil Ö, Ojha S, Taoka S.** Reaction mechanism and regulation of cystathionine β-synthase. *Biochim. Biophys. Acta - Proteins Proteomics* 2003;1647(1):30–35.

139. **Zhang Z, Kebreab E, Jing M, Rodriguez-Lecompte JC, Kuehn R, Flintoft M, House JD.** Impairments in pyridoxine-dependent sulphur amino acid metabolism are highly sensitive to the degree of vitamin B6 deficiency and repletion in the pig. *animal* 2009;3(6):826–837.

140. **Lamers Y, Williamson J, Ralat M, Quinlivan EP, Gilbert LR, Keeling C, Stevens RD, Newgard CB, Ueland PM, Meyer K, Fredriksen A, Stacpoole PW, Gregory 3rd JF.** Moderate dietary vitamin B-6 restriction raises plasma glycine and cystathionine concentrations while minimally affecting the rates of glycine turnover and glycine cleavage in healthy men and women. *J. Nutr.* 2009;139(3):452–460.

141. **Davis SR, Quinlivan EP, Stacpoole PW, Gregory III JF.** Plasma Glutathione and Cystathionine Concentrations Are Elevated but Cysteine Flux Is Unchanged by Dietary Vitamin B-6 Restriction in Young Men and Women. *J. Nutr.* 2006;136(2):373–378.

142. **Lima CP, Davis SR, Mackey AD, Scheer JB, Williamson J, Gregory III JF.** Vitamin B-6 Deficiency Suppresses the Hepatic Transsulfuration Pathway but Increases Glutathione Concentration in Rats Fed AIN-76A or AIN-93G Diets. *J. Nutr.* 2006;136(8):2141–2147.

143. **Sato A, Nishioka M, Awata S, Nakayama K, Okada M, Horiuchi S, Okabe N, Sassa**

T, Oka T, Natori Y. Vitamin B6Deficiency Accelerates Metabolic Turnover of Cystathionase in Rat Liver. *Arch. Biochem. Biophys.* 1996;330(2):409–413.

144. **Wang R.** Physiological Implications of Hydrogen Sulfide: A Whiff Exploration That Blossomed. *Physiol. Rev.* 2012;92(2):791–896.

145. **Liu Y-H, Lu M, Hu L-F, Wong PT-H, Webb GD, Bian J-S.** Hydrogen Sulfide in the Mammalian Cardiovascular System. *Antioxid. Redox Signal.* 2012;17(1):141–185.

146. **Yanfei W, Xia Z, Hongfang J, Hongling W, Wei L, Dingfang B, Xiuying T, Yali R, Chaoshu T, Junbao D.** Role of Hydrogen Sulfide in the Development of Atherosclerotic Lesions in Apolipoprotein E Knockout Mice. *Arterioscler. Thromb. Vasc. Biol.* 2009;29(2):173–179.

147. **Pichette J, Gagnon J.** Implications of Hydrogen Sulfide in Glucose Regulation: How H2S Can Alter Glucose Homeostasis through Metabolic Hormones. *Oxid. Med. Cell. Longev.* 2016;2016:3285074.

148. **Fu M, Zhang W, Wu L, Yang G, Li H, Wang R.** Hydrogen sulfide (H2S) metabolism in mitochondria and its regulatory role in energy production. *Proc. Natl. Acad. Sci.* 2012;109(8):2943 LP – 2948.

149. **Hellmich MR, Szabo C.** Hydrogen Sulfide and Cancer. *Handb. Exp. Pharmacol.* 2015;230:233–241.

150. **Chakraborty PK, Murphy B, Mustafi SB, Dey A, Xiong X, Rao G, Naz S, Zhang M, Yang D, Dhanasekaran DN, Bhattacharya R, Mukherjee P.** Cystathionine β-synthase regulates mitochondrial morphogenesis in ovarian cancer. *FASEB J.* 2018;32(8):4145–4157.

151. **Bhattacharyya S, Saha S, Giri K, Lanza IR, Nair KS, Jennings NB, Rodriguez-**

Aguayo C, Lopez-Berestein G, Basal E, Weaver AL, Visscher DW, Cliby W, Sood AK, Bhattacharya R, Mukherjee P. Cystathionine beta-synthase (CBS) contributes to advanced ovarian cancer progression and drug resistance. *PLoS One* 2013;8(11):e79167–e79167.

152. **Zhu H, Blake S, Chan KT, Pearson RB, Kang J.** Cystathionine *β*-Synthase in Physiology and Cancer. Tornesello ML, ed. *Biomed Res. Int.* 2018;2018:3205125.

153. **Vitvitsky V, Thomas M, Ghorpade A, Gendelman HE, Banerjee R.** A Functional Transsulfuration Pathway in the Brain Links to Glutathione Homeostasis. *J. Biol. Chem.* 2006;281(47):35785–35793.

154. **Hazelwood RL, Lorenz FW.** Effects of fasting and insulin on carbohydrate metabolism of the domestic fowl. *Am. J. Physiol. Content* 1959;197(1):47–51.

155. **Klandorf H, Holt SB, McGowan JA, Pinchasov Y, Deyette D, Peterson RA.** Hyperglycemia and non-enzymatic glycation of serum and tissue proteins in chickens. *Comp. Biochem. Physiol. Part C Pharmacol. Toxicol. Endocrinol.* 1995;110(2):215–220.

156. **Holmes DJ, Ottinger MA.** Birds as long-lived animal models for the study of aging. *Exp. Gerontol.* 2003;38(11):1365–1375.

157. **Braun EJ, Sweazea KL.** Glucose regulation in birds. *Comp. Biochem. Physiol. Part B Biochem. Mol. Biol.* 2008;151(1):1–9.

158. **Szwergold BS, Miller CB.** Potential of Birds to Serve as Pathology-Free Models of Type 2 Diabetes, Part 2: Do High Levels of Carbonyl-Scavenging Amino Acids (e.g., Taurine) and Low Concentrations of Methylglyoxal Limit the Production of Advanced Glycation End-Products? *Rejuvenation Res.* 2014;17(4):347–358.

159. **O'DONNELL III JA, GARBETT R, MORZENTI A.** NORMAL FASTING PLASMA

GLUCOSE LEVELS IN SOME BIRDS OF PREY. *J. Wildl. Dis.* 1978;14(4):479–481.

160. **Rendell M, Stephen PM, Paulsen R, Valentine JL, Rasbold K, Hestorff T, Eastberg S, Shint DC.** An interspecies comparison of normal levels of glycosylated hemoglobin and glycosylated albumin. *Comp. Biochem. Physiol. Part B Comp. Biochem.* 1985;81(4):819–822.

161. **Beuchat CA, Chong CR.** Hyperglycemia in hummingbirds and its consequences for hemoglobin glycation. *Comp. Biochem. Physiol. Part A Mol. Integr. Physiol.* 1998;120(3):409–416.

162. **HAZELWOOD RL.** The Avian Endocrine Pancreas. *Am. Zool.* 1973;13(3):699–709.

163. **Dupont J, Dagou C, Derouet M, Simon J, Taouis M.** Early steps of insulin receptor signaling in chicken and rat: apparent refractoriness in chicken muscle. *Domest. Anim. Endocrinol.* 2004;26(2):127–142.

164. **Ruffier L, Simon J, Rideau N.** Isolation of Functional Glucagon Islets of Langerhans from the Chicken Pancreas. *Gen. Comp. Endocrinol.* 1998;112(2):153–162.

165. **HONEY RN, ARIMURA A, WEIR GC.** Somatostatin Neutralization Stimulates Glucagon and Insulin Secretion from the Avian Pancreas*. *Endocrinology* 1981;109(6):1971–1974.

166. **LANGSLOW DR, BUTLER EJ, HALES CN, PEARSON AW.** THE RESPONSE OF PLASMA INSULIN, GLUCOSE AND NON-ESTERIFIED FATTY ACIDS TO VARIOUS HORMONES, NUTRIENTS AND DRUGS IN THE DOMESTIC FOWL. *J. Endocrinol.* 1970;46(2):243–260.

167. **Grande F, Prigge WF.** Glucagon infusion, plasma FFA and triglycerides, blood sugar, and liver lipids in birds. *Am. J. Physiol. Content* 1970;218(5):1406–1411.

168. **Bernard SF, Thil M-A, Groscolas R.** Lipolytic and metabolic response to glucagon in fasting king penguins: phase II vs. phase III. *Am. J. Physiol. Integr. Comp. Physiol.* 2003;284(2):R444–R454.

169. **MITCHELL P.** CHEMIOSMOTIC COUPLING IN OXIDATIVE AND PHOTOSYNTHETIC PHOSPHORYLATION. *Biol. Rev.* 1966;41(3):445–501.

170. **Vakifahmetoglu-Norberg H, Ouchida AT, Norberg E.** The role of mitochondria in metabolism and cell death. *Biochem. Biophys. Res. Commun.* 2017;482(3):426–431.

171. **Perkins G, Renken C, Martone ME, Young SJ, Ellisman M, Frey T.** Electron Tomography of Neuronal Mitochondria: Three-Dimensional Structure and Organization of Cristae and Membrane Contacts. *J. Struct. Biol.* 1997;119(3):260–272.

172. **Mannella CA, Buttle K, Rath BK, Marko M.** Electron microscopic tomography of rat-liver mitochondria and their interactions with the endoplasmic reticulum. *BioFactors* 1998;8(3-4):225–228.

173. **Alberts, B; Johnson, A; Lewis J et al.** *Molecular Biology of the Cell*. 4th ed. New York: Garland Science; 2002. Available at: https://www.ncbi.nlm.nih.gov/books/NBK26894/.

174. **Lazzarino G, Amorini AM, Signoretti S, Musumeci G, Lazzarino G, Caruso G, Pastore FS, Di Pietro V, Tavazzi B, Belli A.** Pyruvate Dehydrogenase and Tricarboxylic Acid Cycle Enzymes Are Sensitive Targets of Traumatic Brain Injury Induced Metabolic Derangement. *Int. J. Mol. Sci.* 2019;20(22):5774.

175. **Fajardo VA, Mikhaeil JS, Leveille CF, Saint C, LeBlanc PJ.** Cardiolipin content, linoleic acid composition, and tafazzin expression in response to skeletal muscle overload and unload stimuli. *Sci. Rep.* 2017;7(1):2060.

176. **Paradies G, Paradies V, De Benedictis V, Ruggiero FM, Petrosillo G.** Functional role

of cardiolipin in mitochondrial bioenergetics. *Biochim. Biophys. Acta - Bioenerg.* 2014;1837(4):408–417.

177. **Desjardins P, Morais R.** Sequence and gene organization of the chicken mitochondrial genome: A novel gene order in higher vertebrates. *J. Mol. Biol.* 1990;212(4):599–634.

178. **Taanman J-W.** The mitochondrial genome: structure, transcription, translation and replication. *Biochim. Biophys. Acta - Bioenerg.* 1999;1410(2):103–123.

179. **Pereira S, Baker A.** Low number of mitochondrial pseudogenes in the chicken (Gallus gallus) nuclear genome: Implications for molecular inference of population history and phylogenetics. *BMC Evol. Biol.* 2004;4:17.

180. **Axelsson E, Webster MT, Smith NGC, Burt DW, Ellegren H.** Comparison of the chicken and turkey genomes reveals a higher rate of nucleotide divergence on microchromosomes than macrochromosomes. *Genome Res.* 2005;15(1):120–125.

181. **Fukuda M, Wakasugi S, Tsuzuki T, Nomiyama H, Shimada K, Miyata T.** Mitochondrial DNA-like sequences in the human nuclear genome: Characterization and implications in the evolution of mitochondrial DNA. *J. Mol. Biol.* 1985;186(2):257–266.

182. **Woischnik M, Moraes CT.** Pattern of organization of human mitochondrial pseudogenes in the nuclear genome. *Genome Res.* 2002;12(6):885–893.

183. **Knoop F.** Der Abbau aromatishcer Fettsaeuren im Tierkoerper. *Beitr. Z. Chem. Phys. Ul Pathol.* 1904;6:150–162.

184. **Demarquoy J, Le Borgne F.** Crosstalk between mitochondria and peroxisomes. *World J. Biol. Chem.* 2015;6(4):301–309.

185. **Wanders RJA, Waterham HR, Ferdinandusse S.** Metabolic Interplay between Peroxisomes and Other Subcellular Organelles Including Mitochondria and the

Endoplasmic Reticulum . *Front. Cell Dev. Biol.* 2016;3:83.

186. **Violante S, IJlst L, te Brinke H, Koster J, Tavares de Almeida I, Wanders RJA, Ventura F V, Houten SM.** Peroxisomes contribute to the acylcarnitine production when the carnitine shuttle is deficient. *Biochim. Biophys. Acta - Mol. Cell Biol. Lipids* 2013;1831(9):1467–1474.

187. **Ramsay RR.** The Role of the Carnitine System in Peroxisomal Fatty Acid Oxidation. *Am. J. Med. Sci.* 1999;318(1):28–35.

188. **Wanders RJA, Ferdinandusse S, Brites P, Kemp S.** Peroxisomes, lipid metabolism and lipotoxicity. *Biochim. Biophys. Acta - Mol. Cell Biol. Lipids* 2010;1801(3):272–280.

189. **Houten SM, Violante S, Ventura F V, Wanders RJA.** The Biochemistry and Physiology of Mitochondrial Fatty Acid β-Oxidation and Its Genetic Disorders. *Annu. Rev. Physiol.* 2016;78(1):23–44.

190. **Berg, JM; Tymoczko, JL; Stryer L.** *Section 17.2, Entry to the Citric Acid Cycle and Metabolism Through It Are Controlled*. 5th ed.; 2002. Available at: https://www.ncbi.nlm.nih.gov/books/NBK22347/.

191. **Alberts, B; Johnson, A; Lewis J et al.** *Electron-Transport Chains and Their Proton Pumps*. 4th ed, Mo. New York: Garland; 2002. Available at: https://www.ncbi.nlm.nih.gov/books/NBK26904/.

192. **Lenaz G, Fato R, Genova ML, Bergamini C, Bianchi C, Biondi A.** Mitochondrial Complex I: Structural and functional aspects. *Biochim. Biophys. Acta - Bioenerg.* 2006;1757(9):1406–1420.

193. **Jonckheere AI, Smeitink JAM, Rodenburg RJT.** Mitochondrial ATP synthase: architecture, function and pathology. *J. Inherit. Metab. Dis.* 2012;35(2):211–225.

194. **Szabo C, Ransy C, Módis K, Andriamihaja M, Murghes B, Coletta C, Olah G, Yanagi K, Bouillaud F.** Regulation of mitochondrial bioenergetic function by hydrogen sulfide. Part I. Biochemical and physiological mechanisms. *Br. J. Pharmacol.* 2014;171(8):2099–2122.

195. **Deng J, Wang P, Chen X, Cheng H, Liu J, Fushimi K, Zhu L, Wu JY.** FUS interacts with ATP synthase beta subunit and induces mitochondrial unfolded protein response in cellular and animal models. *Proc. Natl. Acad. Sci.* 2018;115(41):E9678 LP-E9686.

196. **Paumard P, Vaillier J, Coulary B, Schaeffer J, Soubannier V, Mueller DM, Brèthes D, di Rago J-P, Velours J.** The ATP synthase is involved in generating mitochondrial cristae morphology. *EMBO J.* 2002;21(3):221–230.

197. **Seo H, Lee I, Chung HS, Bae G-U, Chang M, Song E, Kim MJ.** ATP5B regulates mitochondrial fission and fusion in mammalian cells. *Animal Cells Syst. (Seoul).* 2016;20(3):157–164.

198. **Houtkooper RH, Mouchiroud L, Ryu D, Moullan N, Katsyuba E, Knott G, Williams RW, Auwerx J.** Mitonuclear protein imbalance as a conserved longevity mechanism. *Nature* 2013;497(7450):451–457.

199. **Kussmaul L, Hirst J.** The mechanism of superoxide production by NADH:ubiquinone oxidoreductase (complex I) from bovine heart mitochondria. *Proc. Natl. Acad. Sci.* 2006;103(20):7607 LP – 7612.

200. **Grivennikova VG, Vinogradov AD.** Generation of superoxide by the mitochondrial Complex I. *Biochim. Biophys. Acta - Bioenerg.* 2006;1757(5):553–561.

201. **Bleier L, Dröse S.** Superoxide generation by complex III: From mechanistic rationales to functional consequences. *Biochim. Biophys. Acta - Bioenerg.* 2013;1827(11):1320–1331.

202. **Sheng Y, Abreu IA, Cabelli DE, Maroney MJ, Miller A-F, Teixeira M, Valentine JS.** Superoxide dismutases and superoxide reductases. *Chem. Rev.* 2014;114(7):3854–3918.

203. **Scialò F, Fernández-Ayala DJ, Sanz A.** Role of Mitochondrial Reverse Electron Transport in ROS Signaling: Potential Roles in Health and Disease . *Front. Physiol.* 2017;8:428.

204. **Chen Y, Azad MB, Gibson SB.** Superoxide is the major reactive oxygen species regulating autophagy. *Cell Death Differ.* 2009;16(7):1040–1052.

205. **Madesh M, Zong W-X, Hawkins BJ, Ramasamy S, Venkatachalam T, Mukhopadhyay P, Doonan PJ, Irrinki KM, Rajesh M, Pacher P, Thompson CB.** Execution of superoxide-induced cell death by the proapoptotic Bcl-2-related proteins Bid and Bak. *Mol. Cell. Biol.* 2009;29(11):3099–3112.

206. **Hur JH, Stork DA, Walker DW.** Complex-I-ty in aging. *J. Bioenerg. Biomembr.* 2014;46(4):329–335.

207. **Sonntag C.** *The Hydroxyl Radical*. In Ed. Fre. Berlin, Heidelberg: Springer; 2006. doi:10.1007/3-540-30592-0_3.

208. **Mu T, Sun H, Zhang M, Wang C.** Chapter 2 - Sweet Potato Proteins. In: Mu T, Sun H, Zhang M, Wang CBT-SPPT, eds. Academic Press; 2017:49–119.

209. **Mailloux RJ.** Mitochondrial Antioxidants and the Maintenance of Cellular Hydrogen Peroxide Levels. *Oxid. Med. Cell. Longev.* 2018;2018:7857251.

210. **Kurutas EB.** The importance of antioxidants which play the role in cellular response against oxidative/nitrosative stress: current state. *Nutr. J.* 2016;15(1):71.

211. **HALES DB, ALLEN JA, SHANKARA T, JANUS P, BUCK S, DIEMER T, HALES KH.** Mitochondrial Function in Leydig Cell Steroidogenesis. *Ann. N. Y. Acad. Sci.*

2005;1061(1):120–134.

212. **Crowley LC, Christensen ME, Waterhouse NJ.** Measuring Mitochondrial Transmembrane Potential by TMRE Staining. *Cold Spring Harb. Protoc.* 2016;2016(12):pdb.prot087361.

213. **Zorova LD, Popkov VA, Plotnikov EJ, Silachev DN, Pevzner IB, Jankauskas SS, Zorov SD, Babenko VA, Zorov DB.** Functional Significance of the Mitochondrial Membrane Potential. *Biochem. (Moscow), Suppl. Ser. A Membr. Cell Biol.* 2018;12(1):20–26.

214. **Wang, C; Rajput, S; Cao D.** Acetyl-CoA carboxylase as a novel target for cancer therapy. *Front. Biosci.* 2010;2:515–526.

215. **Mashima T, Seimiya H, Tsuruo T.** De novo fatty-acid synthesis and related pathways as molecular targets for cancer therapy. *Br. J. Cancer* 2009;100:1369.

216. **Matsuzaka T, Shimano H.** Elovl6: a new player in fatty acid metabolism and insulin sensitivity. *J. Mol. Med.* 2009;87(4):379–384.

217. **Tracz-Gaszewska Z, Dobrzyn P.** Stearoyl-CoA Desaturase 1 as a Therapeutic Target for the Treatment of Cancer. *Cancers (Basel).* 2019;11(7):948.

218. **Yahagi N, Shimano H, Hasty AH, Amemiya-Kudo M, Okazaki H, Tamura Y, Iizuka Y, Shionoiri F, Ohashi K, Osuga J, Harada K, Gotoda T, Nagai R, Ishibashi S, Yamada N.** A Crucial Role of Sterol Regulatory Element-binding Protein-1 in the Regulation of Lipogenic Gene Expression by Polyunsaturated Fatty Acids. *J. Biol. Chem.* 1999;274(50):35840–35844.

219. **Kuhajda FP.** Fatty-acid synthase and human cancer: new perspectives on its role in tumor biology. *Nutrition* 2000;16(3):202–208.

220. **Nie L, Lu Q, Li W, Yang N, Dongol S, Zhang XIN, Jiang JIE.** Sterol regulatory element-binding protein 1 is required for ovarian tumor growth. 2013:1346–1354.

221. **Allmann DW, Gibson DM.** Fatty acid synthesis during early linoleic acid deficiency in the mouse. *J. Lipid Res.* 1965;6(1):51–62.

222. **Jump DB, Tripathy S, Depner CM.** Fatty acid-regulated transcription factors in the liver. *Annu. Rev. Nutr.* 2013;33:249–269.

223. **Jump DB, Clarke SD, Thelen A, Liimatta M, Ren B, Badin M.** Dietary polyunsaturated fatty acid regulation of gene transcription. *Prog. Lipid Res.* 1996;35(3):227–241.

224. **FUKUDA H, KATSURADA A, IRITANI N.** Effects of nutrients and hormones on gene expression of ATP citrate-lyase in rat liver. *Eur. J. Biochem.* 1992;209(1):217–222.

225. **IRITANI N.** Nutritional and hormonal regulation of lipogenic-enzyme gene expression in rat liver. *Eur. J. Biochem.* 1992;205(2):433–442.

226. **Gottlieb RA.** Mitochondria: execution central. *FEBS Lett.* 2000;482(1–2):6–12.

227. **Bertolotti R, Rutishauser U, Edelman GM.** A cell surface molecule involved in aggregation of embryonic liver cells. *Proc. Natl. Acad. Sci.* 1980;77(8):4831 LP – 4835.

228. **Hyafil F, Babinet C, Jacob F.** Cell-cell interactions in early embryogenesis: A molecular approach to the role of calcium. *Cell* 1981;26(3, Part 1):447–454.

229. **Gallin WJ, Edelman GM, Cunningham BA.** Characterization of L-CAM, a major cell adhesion molecule from embryonic liver cells. *Proc. Natl. Acad. Sci.* 1983;80(4):1038–1042.

230. **David JM, Rajasekaran AK.** Dishonorable discharge: the oncogenic roles of cleaved E-cadherin fragments. *Cancer Res.* 2012;72(12):2917–2923.

231. **Tamura K, Shan W-S, Hendrickson WA, Colman DR, Shapiro L.** Structure-Function Analysis of Cell Adhesion by Neural (N-) Cadherin. *Neuron* 1998;20(6):1153–1163.

232. **Nagar B, Overduin M, Ikura M, Rini JM.** Structural basis of calcium-induced E-cadherin rigidification and dimerization. *Nature* 1996;380(6572):360–364.

233. **Takeichi M.** CADHERINS: A MOLECULAR FAMILY IMPORTANT IN SELECTIVE CELL-CELL ADHESION. *Annu. Rev. Biochem.* 1990;59(1):237–252.

234. **Maître J-L, Heisenberg C-P.** Three functions of cadherins in cell adhesion. *Curr. Biol.* 2013;23(14):626–633.

235. **Christiansen JJ, Rajasekaran AK.** Reassessing Epithelial to Mesenchymal Transition as a Prerequisite for Carcinoma Invasion and Metastasis. *Cancer Res.* 2006;66(17):8319–8326.

236. **Ansenberger K, Zhuge Y, Lagman JAJ, Richards C, Barua A, Bahr JM, Hales DB.** E-cadherin Expression in Ovarian Cancer in the Laying Hen, Gallus Domesticus, compared to Human Ovarian Cancer. *Gynecol. Oncol.* 2009;113(3):362–369.

237. **Choi P-W, So WW, Yang J, Liu S, Tong KK, Kwan KM, Kwok JS-L, Tsui SKW, Ng S-K, Hales KH, Hales DB, Welch WR, Crum CP, Fong W-P, Berkowitz RS, Ng S-W.** MicroRNA-200 family governs ovarian inclusion cyst formation and mode of ovarian cancer spread. *Oncogene* 2020;39(20):4045–4060.

238. **Choi P-W, Bahrampour A, Ng S-K, Liu SK, Qiu W, Xie F, Kuo WP, Kwong J, Hales KH, Hales DB, Wong K-K, Norwitz ER, Chow CK, Berkowitz RS, Ng S-W.** Characterization of miR-200 family members as blood biomarkers for human and laying hen ovarian cancer. *Sci. Rep.* 2020;10(1):20071.

239. **Park SM, Gaur AB, Lengyel E, Peter ME.** The miR-200 family determines the

epithelial phenotype of cancer cells by targeting the E-cadherin repressors ZEB1 and ZEB2. *Genes Dev.* 2008;22(7):894–907.

240. **Korpal M, Kang Y.** The emerging role of miR-200 family of microRNAs in epithelial-mesenchymal transition and cancer metastasis. *RNA Biol.* 2008;5(3):115–119.

241. **Bays JL, Campbell HK, Heidema C, Sebbagh M, DeMali KA.** Linking E-cadherin mechanotransduction to cell metabolism through force mediated activation of AMPK. *Nat. Cell Biol.* 2017;19(6):724–731.

242. **Choi P-W, Yang J, Ng S-K, Feltmate C, Muto MG, Hasselblatt K, Lafferty-Whyte K, JeBailey L, MacConaill L, Welch WR, Fong W-P, Berkowitz RS, Ng S-W.** Loss of E-cadherin disrupts ovarian epithelial inclusion cyst formation and collective cell movement in ovarian cancer cells. *Oncotarget* 2016;7(4):4110–4121.

243. **Lintz M, Muñoz A, Reinhart-King CA.** The Mechanics of Single Cell and Collective Migration of Tumor Cells. *J. Biomech. Eng.* 2017;139(2):210051–210059.

244. **Kwon Y, Cukierman E, Godwin AK.** Differential expressions of adhesive molecules and proteases define mechanisms of ovarian tumor cell matrix penetration/invasion. *PLoS One* 2011;6(4):e18872–e18872.

245. **Elisha Y, Kalchenko V, Kuznetsov Y, Geiger B.** Dual role of E-cadherin in the regulation of invasive collective migration of mammary carcinoma cells. *Sci. Rep.* 2018;8(1):4986.

246. **Mayor R, Etienne-Manneville S.** The front and rear of collective cell migration. *Nat. Rev. Mol. Cell Biol.* 2016;17(2):97–109.

247. **Gaggioli C, Hooper S, Hidalgo-Carcedo C, Grosse R, Marshall JF, Harrington K, Sahai E.** Fibroblast-led collective invasion of carcinoma cells with differing roles for

RhoGTPases in leading and following cells. *Nat. Cell Biol.* 2007;9(12):1392–1400.

248. **Liu L, Duclos G, Sun B, Lee J, Wu A, Kam Y, Sontag ED, Stone HA, Sturm JC, Gatenby RA, Austin RH.** Minimization of thermodynamic costs in cancer cell invasion. *Proc. Natl. Acad. Sci.* 2013;110(5):1686 LP – 1691.

249. **Grashoff C, Hoffman BD, Brenner MD, Zhou R, Parsons M, Yang MT, McLean MA, Sligar SG, Chen CS, Ha T, Schwartz MA.** Measuring mechanical tension across vinculin reveals regulation of focal adhesion dynamics. *Nature* 2010;466(7303):263–266.

250. **Gardel ML, Sabass B, Ji L, Danuser G, Schwarz US, Waterman CM.** Traction stress in focal adhesions correlates biphasically with actin retrograde flow speed. *J. Cell Biol.* 2008;183(6):999–1005.

251. **du Roure O, Saez A, Buguin A, Austin RH, Chavrier P, Siberzan P, Ladoux B.** Force mapping in epithelial cell migration. *Proc. Natl. Acad. Sci. U. S. A.* 2005;102(7):2390 LP – 2395.

252. **Das T, Safferling K, Rausch S, Grabe N, Boehm H, Spatz JP.** A molecular mechanotransduction pathway regulates collective migration of epithelial cells. *Nat. Cell Biol.* 2015;17(3):276–287.

253. **Cousin H.** Cadherins function during the collective cell migration of Xenopus Cranial Neural Crest cells: revisiting the role of E-cadherin. *Mech. Dev.* 2017;148:79–88.

254. **Gabrielson M, Björklund M, Carlson J, Shoshan M.** Expression of Mitochondrial Regulators PGC1α and TFAM as Putative Markers of Subtype and Chemoresistance in Epithelial Ovarian Carcinoma. Agoulnik IU, ed. *PLoS One* 2014;9(9):e107109.

255. **Caneba CA, Bellance N, Yang L, Pabst L, Nagrath D.** Pyruvate uptake is increased in highly invasive ovarian cancer cells under anoikis conditions for anaplerosis,

mitochondrial function, and migration. *Am. J. Physiol. Metab.* 2012;303(8):E1036–E1052.

256. **Shin D-H, Kim YS, Shimko S, Wang H-G, Phaeton R, Hempel N.** 136 - Mitochondrial Function is Dynamically Regulated during Ovarian Cancer Progression through Alterations in Fusion/Fission. *Free Radic. Biol. Med.* 2017;112:99–100.

257. **Zhang CS, Lin SC.** AMPK promotes autophagy by facilitating mitochondrial fission. *Cell Metab.* 2016;23(3):399–401.

258. **Toyama EQ, Herzig S, Courchet J, Lewis TL, Losón OC, Hellberg K, Young NP, Chen H, Polleux F, Chan DC, Shaw RJ.** AMP-activated protein kinase mediates mitochondrial fission in response to energy stress. *Science* 2016;351(6270):275–281.

259. **Yao J, Zhou E, Wang Y, Xu F, Zhang D, Zhong D.** microRNA-200a Inhibits Cell Proliferation by Targeting Mitochondrial Transcription Factor A in Breast Cancer. *DNA Cell Biol.* 2014;33(5):291–300.

260. **Tak H, Kang H, Ji E, Hong Y, Kim W, Lee EK.** Potential use of TIA-1, MFF, microRNA-200a-3p, and microRNA-27 as a novel marker for hepatocellular carcinoma. *Biochem. Biophys. Res. Commun.* 2018;497(4):1117–1122.

261. **Goncharova EA, Goncharov DA, James ML, Atochina-Vasserman EN, Stepanova V, Hong SB, Li H, Gonzales L, Baba M, Linehan WM, Gow AJ, Margulies S, Guttentag S, Schmidt LS, Krymskaya VP.** Folliculin Controls Lung Alveolar Enlargement and Epithelial Cell Survival through E-Cadherin, LKB1, and AMPK. *Cell Rep.* 2014;7(2):412–423.

262. **Baseler WA, Thapa D, Jagannathan R, Dabkowski ER, Croston TL, Hollander JM.** miR-141 as a regulator of the mitochondrial phosphate carrier (Slc25a3) in the type 1 diabetic heart. *Am. J. Physiol. Physiol.* 2012;303(12):C1244–C1251.

263. **Lee H, Tak H, Park SJ, Jo YK, Cho DH, Lee EK.** microRNA-200a-3p enhances mitochondrial elongation by targeting mitochondrial fission factor. *BMB Rep.* 2017;50(4):214–219.

264. **Ansenberger K, Paulus A, Bahr J, Hales DB.** Flaxseed/Omega-3 Fatty Acid Suppression of E-Cadherin Expression in Ovarian Cancer in the Laying Hen: Molecular Target for Dietary Intervention. *Biol. Reprod.* 2010;83(Suppl_1):189.

265. **Peyriéras N, Hyafil F, Louvard D, Ploegh HL, Jacob F.** Uvomorulin: a nonintegral membrane protein of early mouse embryo. *Proc. Natl. Acad. Sci. U. S. A.* 1983;80(20):6274–6277.

266. **Hu Q-P, Kuang J-Y, Yang Q-K, Bian X-W, Yu S-C.** Beyond a tumor suppressor: Soluble E-cadherin promotes the progression of cancer. *Int. J. Cancer* 2016;138(12):2804–2812.

267. **Katayama M, Hirai S, Kamihagi K, Nakagawa K, Yasumoto M, Kato I.** Soluble E-cadherin fragments increased in circulation of cancer patients. *Br. J. Cancer* 1994;69(3):580–585.

268. **Tang MKS, Yue PYK, Ip PP, Huang R-L, Lai H-C, Cheung ANY, Tse KY, Ngan HYS, Wong AST.** Soluble E-cadherin promotes tumor angiogenesis and localizes to exosome surface. *Nat. Commun.* 2018;9(1):2270.

269. **Brouxhon SM, Kyrkanides S, Teng X, Athar M, Ghazizadeh S, Simon M, O'Banion MK, Ma L.** Soluble E-cadherin: a critical oncogene modulating receptor tyrosine kinases, MAPK and PI3K/Akt/mTOR signaling. *Oncogene* 2014;33(2):225–235.

270. **Daraï E, Bringuier AF, Walker-Combrouze F, Feldmann G, Madelenat P, Scoazec JY.** Soluble adhesion molecules in serum and cyst fluid from patients with cystic tumours

of the ovary. *Hum. Reprod.* 1998;13(10):2831–2835.

271. **Brännström KSKIKRMHLHM.** Higher levels of soluble E-cadherin in cyst fluid from malignant ovarian tumours than in benign cysts. *Anticancer Res.* 2001;21(1A):65–70.

272. **Nollet F, Kools P, van Roy F.** Phylogenetic analysis of the cadherin superfamily allows identification of six major subfamilies besides several solitary members11Edited by M. Yaniv. *J. Mol. Biol.* 2000;299(3):551–572.

273. **Renaud-Young M, Gallin WJ.** In the First Extracellular Domain of E-cadherin, Heterophilic Interactions, but Not the Conserved His-Ala-Val Motif, Are Required for Adhesion. *J. Biol. Chem.* 2002;277(42):39609–39616.

274. **Mullen AR, Hu Z, Shi X, Jiang L, Boroughs LK, Kovacs Z, Boriack R, Rakheja D, Sullivan LB, Linehan WM, Chandel NS, DeBerardinis RJ.** Oxidation of alpha-ketoglutarate is required for reductive carboxylation in cancer cells with mitochondrial defects. *Cell Rep.* 2014;7(5):1679–1690.

275. **Livak KJ, Schmittgen TD.** Analysis of Relative Gene Expression Data Using Real-Time Quantitative PCR and the 2−ΔΔCT Method. *Methods* 2001;25(4):402–408.

276. **Baldwin WS, Curtis SW, Cauthen CA, Risinger JI, Korach KS, Barrett JC.** BG-1 ovarian cell line: An alternative model for examining estrogen-dependent growth in vitro. *Vitr. Cell. Dev. Biol. - Anim.* 1998;34(8):649–654.

277. **Geisinger KR, Kute TE, Pettenati MJ, Welander CE, Dennard Y, Collins LA, Berens ME.** Characterization of a human ovarian carcinoma cell line with estrogen and progesterone receptors. *Cancer* 1989;63(2):280–288.

278. **Quartuccio SM, Lantvit DD, Bosland MC, Burdette JE.** Conditional Inactivation of p53 in Mouse Ovarian Surface Epithelium Does Not Alter MIS Driven Smad2-Dominant

Negative Epithelium-Lined Inclusion Cysts or Teratomas. *PLoS One* 2013;8(5):e65067.

279. **Kruk, PA; Maines-Bandiera SAN.** A simplified method to culture human ovarian surface epithelium. *Lab. Investig.* 1990;63:132–136.

280. **Kasianowicz, J; Benz, R; McLaughlin S.** The kinetic mechanism by which CCCP (carbonyl cyanide m-chlorophenylhydrazone) transports protons across membranes. *J. Biol. Membr.* 1984;82(2):179–190.

281. **Williams-Ashman HG, Seidenfeld J, Galletti P.** Trends in the biochemical pharmacology of 5′-deoxy-5′-methylthioadenosine. *Biochem. Pharmacol.* 1982;31(3):277–288.

282. **Mihalik SJ, Goodpaster BH, Kelley DE, Chace DH, Vockley J, Toledo FGS, DeLany JP.** Increased levels of plasma acylcarnitines in obesity and type 2 diabetes and identification of a marker of glucolipotoxicity. *Obesity (Silver Spring).* 2010;18(9):1695–1700.

283. **Davie SJ, Gould BJ, Yudkin JS.** Effect of Vitamin C on Glycosylation of Proteins. *Diabetes* 1992;41(2):167 LP – 173.

284. **Ogawa T, Tsubakiyama R, Kanai M, Koyama T, Fujii T, Iefuji H, Soga T, Kume K, Miyakawa T, Hirata D, Mizunuma M.** Stimulating S-adenosyl-l-methionine synthesis extends lifespan via activation of AMPK. *Proc. Natl. Acad. Sci.* 2016:201604047.

285. **Ho A, Sinick J, Esko T, Fischer K, Menni C, Zierer J, Matey-Hernandez M, Fortney K, Morgen EK.** Circulating glucuronic acid predicts healthspan and longevity in humans and mice. *Aging (Albany. NY).* 2019;11(18):7694–7706.

286. **Montoliu I, Scherer M, Beguelin F, DaSilva L, Mari D, Salvioli S, Martin F-PJ, Capri M, Bucci L, Ostan R, Garagnani P, Monti D, Biagi E, Brigidi P, Kussmann M,**

Rezzi S, Franceschi C, Collino S. Serum profiling of healthy aging identifies phospho- and sphingolipid species as markers of human longevity. *Aging (Albany. NY).* 2014;6(1):9–25.

287. **Suzuki S, Kodera Y, Saito T, Fujimoto K, Momozono A, Hayashi A, Kamata Y, Shichiri M.** Methionine sulfoxides in serum proteins as potential clinical biomarkers of oxidative stress. *Sci. Rep.* 2016;6(1):38299.

288. **Wang S-B, Murray CI, Chung HS, Van Eyk JE.** Redox regulation of mitochondrial ATP synthase. *Trends Cardiovasc. Med.* 2013;23(1):14–18.

289. **Lemke SL, Vicini JL, Su H, Goldstein DA, Nemeth MA, Krul ES, Harris WS.** Dietary intake of stearidonic acid–enriched soybean oil increases the omega-3 index: randomized, double-blind clinical study of efficacy and safety. *Am. J. Clin. Nutr.* 2010;92(4):766–775.

290. **Harris WS.** Stearidonic Acid–Enhanced Soybean Oil: A Plant-Based Source of (n-3) Fatty Acids for Foods. *J. Nutr.* 2012;142(3):600S-604S.

291. **Choi J-H, Chen C-L, Poon SL, Wang H-S, Leung PCK.** Gonadotropin-stimulated epidermal growth factor receptor expression in human ovarian surface epithelial cells: involvement of cyclic AMP-dependent exchange protein activated by cAMP pathway. *Endocr. Relat. Cancer* 16(1):179–188.

292. **Ueland PM, Ulvik A, Rios-Avila L, Midttun Ø, Gregory JF.** Direct and Functional Biomarkers of Vitamin B6 Status. *Annu. Rev. Nutr.* 2015;35:33–70.

293. **Mayengbam S, Yang H, Barthet V, Aliani M, House JD.** Identification, Characterization, and Quantification of an Anti-pyridoxine Factor from Flaxseed Using Ultrahigh-Performance Liquid Chromatography–Mass Spectrometry. *J. Agric. Food Chem.* 2014;62(2):419–426.

294. **Gutte K, Sahoo A, Ranveer DR.** Bioactive Components of Flaxseed and its Health Benefits. *Int. J. Pharm. Sci. Rev. Res.* 2015;31:42–51.

295. **Hansen SH, Andersen ML, Cornett C, Gradinaru R, Grunnet N.** A role for taurine in mitochondrial function. *J. Biomed. Sci.* 2010;17 Suppl 1(Suppl 1):S23–S23.

296. **Watanabe M, Osada J, Aratani Y, Kluckman K, Reddick R, Malinow MR, Maeda N.** Mice deficient in cystathionine beta-synthase: animal models for mild and severe homocyst(e)inemia. *Proc. Natl. Acad. Sci. U. S. A.* 1995;92(5):1585–1589.

297. **Wang H, Jiang X, Yang F, Gaubatz JW, Ma L, Magera MJ, Yang X, Berger PB, Durante W, Pownall HJ, Schafer AI.** Hyperhomocysteinemia accelerates atherosclerosis in cystathionine β-synthase and apolipoprotein E double knock-out mice with and without dietary perturbation. *Blood* 2003;101(10):3901–3907.

298. **Liqun W, Kwang-Hwan J, Xiang H, M. DP, W. JD, D. KW.** Modulation of Cystathionine β-Synthase Level Regulates Total Serum Homocysteine in Mice. *Circ. Res.* 2004;94(10):1318–1324.

299. **Carvalho TSM, Sousa LS, Nogueira FA, Vaz DP, Saldanha MM, Triginelli M V, Pinto MFVS, Baião NC, Lara LJC.** Digestible methionine+cysteine in the diet of commercial layers and its influence on the performance, quality, and amino acid profile of eggs and economic evaluation. *Poult. Sci.* 2018;97(6):2044–2052.

300. **Mentch SJ, Mehrmohamadi M, Huang L, Liu X, Gupta D, Mattocks D, Gómez Padilla P, Ables G, Bamman MM, Thalacker-Mercer AE, Nichenametla SN, Locasale JW.** Histone Methylation Dynamics and Gene Regulation Occur through the Sensing of One-Carbon Metabolism. *Cell Metab.* 2015;22(5):861–873.

301. **Yu W, Wang Z, Zhang K, Chi Z, Xu T, Jiang D, Chen S, Li W, Yang X, Zhang X,**

Wu Y, Wang D. One-Carbon Metabolism Supports S-Adenosylmethionine and Histone Methylation to Drive Inflammatory Macrophages. *Mol. Cell* 2019;75(6):1147-1160.e5.

302. **Shi H, Wang X, Lu Z, Zhao BS, Ma H, Hsu PJ, Liu C, He C.** YTHDF3 facilitates translation and decay of N(6)-methyladenosine-modified RNA. *Cell Res.* 2017;27(3):315–328.

303. **Dawling S, Roodi N, Mernaugh RL, Wang X, Parl FF.** Catechol-O-Methyltransferase (COMT)-mediated Metabolism of Catechol Estrogens. *Cancer Res.* 2001;61(18):6716 LP – 6722.

304. **J. LN, A. SM, Jurgen V, D. FW.** 2-Methoxyestradiol, a Promising Anticancer Agent. *Pharmacother. J. Hum. Pharmacol. Drug Ther.* 2012;23(2):165–172.

305. **Ridgway ND, Yao Z, Vance DE.** Phosphatidylethanolamine levels and regulation of phosphatidylethanolamine N-methyltransferase. *J. Biol. Chem.* 1989;264(2):1203–1207.

306. **Prigogine I, Lefever R.** Symmetry Breaking Instabilities in Dissipative Systems. II. *J. Chem. Phys.* 1968;48(4):1695–1700.

307. **PRIGOGINE I, LEFEVER R, GOLDBETER A, HERSCHKOWITZ-KAUFMAN M.** Symmetry Breaking Instabilities in Biological Systems. *Nature* 1969;223(5209):913–916.

308. **Perry C, Yu S, Chen J, Matharu KS, Stover PJ.** Effect of vitamin B6 availability on serine hydroxymethyltransferase in MCF-7 cells. *Arch. Biochem. Biophys.* 2007;462(1):21–27.

309. **Mudd SH, Ebert MH, Scriver CR.** Labile methyl group balances in the human: The role of sarcosine. *Metabolism* 1980;29(8):707–720.

310. **Aziza AE, Awadin W, Cherian G.** Impact of Choline Supplementation on Hepatic

Histopathology, Phospholipid Content, and Tocopherol Status in Layer Hens Fed Flaxseed. *J. Appl. Poult. Res.* 2019;28(3):679–687.

311. **van der Veen JN, Lingrell S, Gao X, Quiroga AD, Takawale A, Armstrong EA, Yager JY, Kassiri Z, Lehner R, Vance DE, Jacobs RL.** Pioglitazone attenuates hepatic inflammation and fibrosis in phosphatidylethanolamine N-methyltransferase-deficient mice. *Am. J. Physiol. Liver Physiol.* 2016;310(7):G526–G538.

312. **Noga AA, Zhao Y, Vance DE.** An Unexpected Requirement for PhosphatidylethanolamineN-Methyltransferase in the Secretion of Very Low Density Lipoproteins . *J. Biol. Chem.* 2002;277(44):42358–42365.

313. **Verkade HJ, Fast DG, Rusiñol AE, Scraba DG, Vance DE.** Impaired biosynthesis of phosphatidylcholine causes a decrease in the number of very low density lipoprotein particles in the Golgi but not in the endoplasmic reticulum of rat liver. *J. Biol. Chem.* 1993;268(33):24990–24996.

314. **Wan S, van der Veen JN, N'Goma J-CB, Nelson RC, Vance DE, Jacobs RL.** Hepatic PEMT activity mediates liver health, weight gain, and insulin resistance. *FASEB J.* 2019;33(10):10986–10995.

315. **Van Der Veen JN, Lingrell S, McCloskey N, Leblond ND, Galleguillos D, Zhao YY, Curtis JM, Sipione S, Fullerton MD, Vance DE, René JL.** A role for phosphatidylcholine and phosphatidylethanolamine in hepatic insulin signaling. *FASEB J.* 2019;33(4):5045–5057.

316. **Davis JE, Cain J, Small C, Hales DB.** Supplementation of whole flaxseed reduced hepatic steatosis in aged laying hens. *FASEB J.* 2016;30(S1):692.28-692.28.

317. **Igolnikov AC, Green RM.** Mice heterozygous for the Mdr2 gene demonstrate decreased

PEMT activity and diminished steatohepatitis on the MCD diet. *J. Hepatol.* 2006;44(3):586–592.

318. **Fischer LM, daCosta KA, Kwock L, Stewart PW, Lu T-S, Stabler SP, Allen RH, Zeisel SH.** Sex and menopausal status influence human dietary requirements for the nutrient choline. *Am. J. Clin. Nutr.* 2007;85(5):1275–1285.

319. **Resseguie ME, da Costa K-A, Galanko JA, Patel M, Davis IJ, Zeisel SH.** Aberrant estrogen regulation of PEMT results in choline deficiency-associated liver dysfunction. *J. Biol. Chem.* 2011;286(2):1649–1658.

320. **Resseguie M, Song J, Niculescu MD, da Costa K-A, Randall TA, Zeisel SH.** Phosphatidylethanolamine N-methyltransferase (PEMT) gene expression is induced by estrogen in human and mouse primary hepatocytes. *FASEB J.* 2007;21(10):2622–2632.

321. **Entenman C, Lorenz FW, Chaikoff IL.** The endocrine control of lipid metabolism in the bird. III. The effects of crystalline sex hormones on the blood lipids of the bird. *J. Biol. Chem.* 1940;134:495–504.

322. **Vigo C, Paddon HB, Millard FC, Pritchard PH, Vance DE.** Diethylstilbestrol treatment modulates the enzymatic activities of phosphatidylcholine biosynthesis in rooster liver. *Biochim. Biophys. Acta - Lipids Lipid Metab.* 1981;665(3):546–550.

323. **Liu H-K, Long DW, Bacon WL.** Preovulatory Luteinizing Hormone Surge Interval in Old and Young Laying Turkey Hens Early in the Egg Production Period1. *Poult. Sci.* 2001;80(9):1364–1370.

324. **S. LEESON, J. D. SUMMERS and LJC.** Response of Layers to Dietary Flaxseed According to Body Weight Classification at Maturity. *Appl. Poult. Sci.* 2000;9(3):297–302.

325. **Caston LJ, Squires EJ, Leeson S.** Hen performance, egg quality, and the sensory evaluation of eggs from SCWL hens fed dietary flax. *Can. J. Anim. Sci.* 1994;74(2):347–353.

326. **Novak C, Scheideler SE.** Long-Term Effects of Feeding Flaxseed-Based Diets. 1. Egg Production Parameters, Components, and Eggshell Quality in Two Strains of Laying Hens1. *Poult. Sci.* 2001;80(10):1480–1489.

327. **Holmes DJ, Austad SN.** Birds as Animal Models for the Comparative Biology of Aging: A Prospectus. *Journals Gerontol. Ser. A* 1995;50A(2):B59–B66.

328. **Travin DY, Feniouk BA.** Aging in birds. *Biochem.* 2016;81(12):1558–1563.

329. **Han S, Brunet A.** Histone methylation makes its mark on longevity. *Trends Cell Biol.* 2012;22(1):42–49.

330. **Sen P, Shah PP, Nativio R, Berger SL.** Epigenetic Mechanisms of Longevity and Aging. *Cell* 2016;166(4):822–839.

331. **Abhyankar V, Kaduskar B, Kamat SS, Deobagkar D, Ratnaparkhi GS.** Drosophila DNA/RNA methyltransferase contributes to robust host defense in aging animals by regulating sphingolipid metabolism. *J. Exp. Biol.* 2018;221(22):jeb187989.

332. **Kabil H, Kabil O, Banerjee R, Harshman LG, Pletcher SD.** Increased transsulfuration mediates longevity and dietary restriction in Drosophila. *Proc. Natl. Acad. Sci.* 2011;108(40):16831 LP – 16836.

333. **Most J, Tosti V, Redman LM, Fontana L.** Calorie restriction in humans: An update. *Ageing Res. Rev.* 2017;39:36–45.

334. **Hwangbo D-S, Lee H-Y, Abozaid LS, Min K-J.** Mechanisms of Lifespan Regulation by Calorie Restriction and Intermittent Fasting in Model Organisms. *Nutrients*

2020;12(4):1194.

335. **Smith Jr DL, Nagy TR, Allison DB.** Calorie restriction: what recent results suggest for the future of ageing research. *Eur. J. Clin. Invest.* 2010;40(5):440–450.

336. **Miller RA, Buehner G, Chang Y, Harper JM, Sigler R, Smith-Wheelock M.** Methionine-deficient diet extends mouse lifespan, slows immune and lens aging, alters glucose, T4, IGF-I and insulin levels, and increases hepatocyte MIF levels and stress resistance. *Aging Cell* 2005;4(3):119–125.

337. **Orentreich N, Matias JR, DeFelice A, Zimmerman JA.** Low Methionine Ingestion by Rats Extends Life Span. *J. Nutr.* 1993;123(2):269–274.

338. **JIANG Z, AHN DU, SIM JS.** Effects of Feeding Flax and Two Types of Sunflower Seeds on Fatty Acid Compositions of Yolk Lipid Classes. *Poult. Sci.* 1991;70(12):2467–2475.

339. **Shafey TM, Al-Batshan HA, Farhan AMS.** The Effect of Dietary Flaxseed Meal on Liver and Egg Yolk Fatty Acid Profiles, Immune Response and Antioxidant Status of Laying Hens. *Ital. J. Anim. Sci.* 2015;14(3):3939.

340. **Omidi M, Rahimi S, Karimi Torshizi MA.** Modification of egg yolk fatty acids profile by using different oil sources. *Vet. Res. forum an Int. Q. J.* 2015;6(2):137–141.

341. **Ågren JJ, Kurvinen J-P, Kuksis A.** Isolation of very low density lipoprotein phospholipids enriched in ethanolamine phospholipids from rats injected with Triton WR 1339. *Biochim. Biophys. Acta - Mol. Cell Biol. Lipids* 2005;1734(1):34–43.

342. **Skipski VP, Barclay M, Barclay RK, Fetzer VA, Good JJ, Archibald FM.** Lipid composition of human serum lipoproteins. *Biochem. J.* 1967;104(2):340–352.

343. **Natali F, Siculella L, Salvati S, Gnoni G V.** Oleic acid is a potent inhibitor of fatty acid

and cholesterol synthesis in C6 glioma cells. *J. Lipid Res.* 2007;48(9):1966–1975.

344. **Ahmadian M, Suh JM, Hah N, Liddle C, Atkins AR, Downes M, Evans RM.** PPARγ signaling and metabolism: the good, the bad and the future. *Nat. Med.* 2013;19(5):557–566.

345. **Kliewer SA, Sundseth SS, Jones SA, Brown PJ, Wisely GB, Koble CS, Devchand P, Wahli W, Willson TM, Lenhard JM, Lehmann JM.** Fatty acids and eicosanoids regulate gene expression through direct interactions with peroxisome proliferator-activated receptors alpha and gamma. *Proc. Natl. Acad. Sci. U. S. A.* 1997;94(9):4318–4323.

346. **Xu HE, Lambert MH, Montana VG, Parks DJ, Blanchard SG, Brown PJ, Sternbach DD, Lehmann JM, Wisely GB, Willson TM, Kliewer SA, Milburn M V.** Molecular Recognition of Fatty Acids by Peroxisome Proliferator–Activated Receptors. *Mol. Cell* 1999;3(3):397–403.

347. **von Schacky C.** n-3 PUFA in CVD: influence of cytokine polymorphism. *Proc. Nutr. Soc.* 2007;66(2):166–170.

348. **Neschen S, Morino K, Dong J, Wang-Fischer Y, Cline GW, Romanelli AJ, Rossbacher JC, Moore IK, Regittnig W, Munoz DS, Kim JH, Shulman GI.** n-3 Fatty Acids Preserve Insulin Sensitivity In Vivo in a Peroxisome Proliferator–Activated Receptor-α–Dependent Manner. *Diabetes* 2007;56(4):1034 LP – 1041.

349. **Naeini Z, Toupchian O, Vatannejad A, Sotoudeh G, Teimouri M, Ghorbani M, Nasli-Esfahani E, Koohdani F.** Effects of DHA-enriched fish oil on gene expression levels of p53 and NF-κB and PPAR-γ activity in PBMCs of patients with T2DM: A randomized, double-blind, clinical trial. *Nutr. Metab. Cardiovasc. Dis.* 2020;30(3):441–

447.

350. **Warburg O, Wind F, Negelein E.** THE METABOLISM OF TUMORS IN THE BODY. *J. Gen. Physiol.* 1927;8(6):519–530.

351. **Warburg O.** On the Origin of Cancer Cells. *Science (80-.).* 1956;123(3191):309 LP – 314.

352. **Mannion C, Page S, Bell LH, Verhoef M.** Components of an anticancer diet: dietary recommendations, restrictions and supplements of the Bill Henderson Protocol. *Nutrients* 2011;3(1):1–26.

353. **Budwig J.** *Flax Oil as a True Aid against Arthritis, Heart Infarction, Cancer and Other Diseases.* Vancouver, BC: Apple Publishing Company; 1994.

354. **Manley SJ, Liu W, Welch DR.** The KISS1 metastasis suppressor appears to reverse the Warburg effect by shifting from glycolysis to mitochondrial beta-oxidation. *J. Mol. Med. (Berl).* 2017;95(9):951–963.

355. **Foster DW.** Malonyl-CoA: the regulator of fatty acid synthesis and oxidation. *J. Clin. Invest.* 2012;122(6):1958–1959.

356. **Mallery SR, Pei P, Landwehr DJ, Clark CM, Bradburn JE, Ness GM, Robertson FM.** Implications for oxidative and nitrative stress in the pathogenesis of AIDS-related Kaposi's sarcoma. *Carcinogenesis* 2004;25(4):597–603.

357. **Otera H, Wang C, Cleland MM, Setoguchi K, Yokota S, Youle RJ, Mihara K.** Mff is an essential factor for mitochondrial recruitment of Drp1 during mitochondrial fission in mammalian cells. *J. Cell Biol.* 2010;191(6):1141 LP – 1158.

358. **Ježek J, Cooper KF, Strich R.** Reactive Oxygen Species and Mitochondrial Dynamics: The Yin and Yang of Mitochondrial Dysfunction and Cancer Progression. *Antioxidants*

(Basel, Switzerland) 2018;7(1):13.

359. **Gill JG, Piskounova E, Morrison SJ.** Cancer, Oxidative Stress, and Metastasis. *Cold Spring Harb. Symp. Quant. Biol.* 2016;81:163–175.

360. **Pani G, Galeotti T, Chiarugi P.** Metastasis: cancer cell's escape from oxidative stress. *Cancer Metastasis Rev.* 2010;29(2):351–378.

361. **Wang S-B, Foster DB, Rucker J, O'Rourke B, Kass DA, Van Eyk JE.** Redox regulation of mitochondrial ATP synthase: implications for cardiac resynchronization therapy. *Circ. Res.* 2011;109(7):750–757.

362. **Song J, Pfanner N, Becker T.** Assembling the mitochondrial ATP synthase. *Proc. Natl. Acad. Sci.* 2018;115(12):2850 LP – 2852.

363. **Walker JE, Fearnley IM, Gay NJ, Gibson BW, Northrop FD, Powell SJ, Runswick MJ, Saraste M, Tybulewicz VLJ.** Primary structure and subunit stoichiometry of F1-ATPase from bovine mitochondria. *J. Mol. Biol.* 1985;184(4):677–701.

364. **Chang HJ, Lee MR, Hong S-H, Yoo BC, Shin Y-K, Jeong JY, Lim S-B, Choi HS, Jeong S-Y, Park J-G.** Identification of mitochondrial FoF1-ATP synthase involved in liver metastasis of colorectal cancer. *Cancer Sci.* 2007;98(8):1184–1191.

365. **Lin P-C, Lin J-K, Yang S-H, Wang H-S, Li AF-Y, Chang S-C.** Expression of β-F1-ATPase and mitochondrial transcription factor A and the change in mitochondrial DNA content in colorectal cancer: clinical data analysis and evidence from an in vitro study. *Int. J. Colorectal Dis.* 2008;23(12):1223–1232.

366. **Cuezva JM, Krajewska M, de Heredia ML, Krajewski S, Santamaría G, Kim H, Zapata JM, Marusawa H, Chamorro M, Reed JC.** The Bioenergetic Signature of Cancer. *Cancer Res.* 2002;62(22):6674 LP – 6681.

367. **Grzybowska-Szatkowska L, Ślaska B, Rzymowska J, Brzozowska A, Floriańczyk B.** Novel mitochondrial mutations in the ATP6 and ATP8 genes in patients with breast cancer. *Mol Med Rep* 2014;10(4):1772–1778.

368. **Niedzwiecka K, Tisi R, Penna S, Lichocka M, Plochocka D, Kucharczyk R.** Two mutations in mitochondrial ATP6 gene of ATP synthase, related to human cancer, affect ROS, calcium homeostasis and mitochondrial permeability transition in yeast. *Biochim. Biophys. Acta - Mol. Cell Res.* 2018;1865(1):117–131.

369. **Weiss H, Wester-Rosenloef L, Koch C, Koch F, Baltrusch S, Tiedge M, Ibrahim S.** The Mitochondrial Atp8 Mutation Induces Mitochondrial ROS Generation, Secretory Dysfunction, and β-Cell Mass Adaptation in Conplastic B6-mtFVB Mice. *Endocrinology* 2012;153(10):4666–4676.

370. **Eilati E, Pan L, Bahr J, Hales DB.** Abstract 4616: Age dependent increase in Prostaglandin pathway coincides with onset of ovarian cancer in laying hens. *Cancer Res.* 2013;72. doi:10.1158/1538-7445.AM2012-4616.

371. **Ross D, Siegel D.** Functions of NQO1 in Cellular Protection and CoQ(10) Metabolism and its Potential Role as a Redox Sensitive Molecular Switch. *Front. Physiol.* 2017;8:595.

372. **Chau L-Y.** Heme oxygenase-1: emerging target of cancer therapy. *J. Biomed. Sci.* 2015;22(1):22.

373. **Taguchi, K.; Motohashi, H.; and Yamamoto M.** Molecular mechanisms of the Keap1–Nrf2 pathway in stress response and cancer evolution. *Genes to cells* 2011;16(2):123–140.

374. **Cao Q, Lu K, Dai S, Hu Y, Fan W.** Clinicopathological and prognostic implications of the miR-200 family in patients with epithelial ovarian cancer. *Int. J. Clin. Exp. Pathol.* 2014;7(5):2392–2401.

375. **Tsuzuki T, Shibata A, Kawakami Y, Nakagawa K, Miyazawa T.** Conjugated Eicosapentaenoic Acid Inhibits Vascular Endothelial Growth Factor-Induced Angiogenesis by Suppressing the Migration of Human Umbilical Vein Endothelial Cells. *J. Nutr.* 2007;137(3):641–646.

376. **Zainal Z, Longman AJ, Hurst S, Duggan K, Caterson B, Hughes CE, Harwood JL.** Relative efficacies of omega-3 polyunsaturated fatty acids in reducing expression of key proteins in a model system for studying osteoarthritis. *Osteoarthr. Cartil.* 2009;17(7):896–905.

377. **Vanden Berghe W., Vermeulen L., Delerive P., De Bosscher K., Staels B. HG.** *A Paradigm for Gene Regulation: Inflammation, NF-κB and PPAR*. Peroxisoma. Boston: Springer; 2003. doi:10.1007/978-1-4419-9072-3_22.

378. **Moraes LA, Piqueras L, Bishop-Bailey D.** Peroxisome proliferator-activated receptors and inflammation. *Pharmacol. Ther.* 2006;110(3):371–385.

379. **Repetto O, De Paoli P, De Re V, Canzonieri V, Cannizzaro R.** Levels of Soluble E-Cadherin in Breast, Gastric, and Colorectal Cancers. Luciani A, ed. *Biomed Res. Int.* 2014;2014:408047.

380. **Bonfim DC, Dias RB, Fortuna-Costa A, Chicaybam L, Lopes D V, Dutra HS, Borojevic R, Bonamino M, Mermelstein C, Rossi MID.** PS1/*γ*-Secretase-Mediated Cadherin Cleavage Induces *β*-Catenin Nuclear Translocation and Osteogenic Differentiation of Human Bone Marrow Stromal Cells. Ballini A, ed. *Stem Cells Int.* 2016;2016:3865315.

381. **Maretzky T, Reiss K, Ludwig A, Buchholz J, Scholz F, Proksch E, de Strooper B, Hartmann D, Saftig P.** ADAM10 mediates E-cadherin shedding and regulates epithelial

cell-cell adhesion, migration, and β-catenin translocation. *Proc. Natl. Acad. Sci. U. S. A.* 2005;102(26):9182 LP – 9187.

382. **Cohen M, Pierredon S, Wuillemin C, Delie F, Petignat P.** Acellular fraction of ovarian cancer ascites induce apoptosis by activating JNK and inducing BRCA1, Fas and FasL expression in ovarian cancer cells. *Oncoscience* 2014;1(4):262–271.

383. **Jandu N, Richardson M, Singh G, Hirte H, Hatton MWC.** Human ovarian cancer ascites fluid contains a mixture of incompletely degraded soluble products of fibrin that collectively possess an antiangiogenic property. *Int. J. Gynecol. Cancer* 2006;16(4):1536 LP – 1544.

384. **Meunier L, Puiffe M-L, Le Page C, Filali-Mouhim A, Chevrette M, Tonin PN, Provencher DM, Mes-Masson A-M.** Effect of ovarian cancer ascites on cell migration and gene expression in an epithelial ovarian cancer in vitro model. *Transl. Oncol.* 2010;3(4):230–238.

385. **Lane D, Goncharenko-Khaider N, Rancourt C, Piché A.** Ovarian cancer ascites protects from TRAIL-induced cell death through αvβ5 integrin-mediated focal adhesion kinase and Akt activation. *Oncogene* 2010;29(24):3519–3531.

386. **Bean LD, Leeson S.** Long-term effects of feeding flaxseed on performance and egg fatty acid composition of brown and white hens. *Poult. Sci.* 2003;82(3):388–394.

387. **Dean ED.** A Primary Role for α-Cells as Amino Acid Sensors. *Diabetes* 2020;69(4):542 LP – 549.

388. **Unger RH, Ohneda A, Aguilar-Parada E, Eisentraut AM.** The role of aminogenic glucagon secretion in blood glucose homeostasis. *J. Clin. Invest.* 1969;48(5):810–822.

389. **Mudd SH, Finkelstein JD, Irreverre F, Laster L.** Transsulfuration in Mammals:

MICROASSAYS AND TISSUE DISTRIBUTIONS OF THREE ENZYMES OF THE PATHWAY . *J. Biol. Chem.* 1965;240(11):4382–4392.

390. **Kitts DD, Yuan Y V, Wijewickreme AN, Thompson LU.** Antioxidant activity of the flaxseed lignan secoisolariciresinol diglycoside and its mammalian lignan metabolites enterodiol and enterolactone. *Mol. Cell. Biochem.* 1999;202(1):91–100.

391. **Damdimopoulou P, Nurmi T, Salminen A, Damdimopoulos AE, Kotka M, van der Saag P, Strauss L, Poutanen M, Pongratz I, Mäkelä S.** A Single Dose of Enterolactone Activates Estrogen Signaling and Regulates Expression of Circadian Clock Genes in Mice. *J. Nutr.* 2011;141(9):1583–1589.

392. **Handgraaf S, Dusaulcy R, Visentin F, Philippe J, Gosmain Y.** 17-β Estradiol regulates proglucagon-derived peptide secretion in mouse and human α- and L cells. *JCI insight* 2018;3(7):e98569.

393. **Jacobs RL, Stead LM, Brosnan ME, Brosnan JT.** Hyperglucagonemia in Rats Results in Decreased Plasma Homocysteine and Increased Flux through the Transsulfuration Pathway in Liver. *J. Biol. Chem.* 2001;276(47):43740–43747.

394. **Ratnam S, Maclean KN, Jacobs RL, Brosnan ME, Kraus JP, Brosnan JT.** Hormonal Regulation of Cystathionine β-Synthase Expression in Liver. *J. Biol. Chem.* 2002;277(45):42912–42918.

395. **Rahman L, Voeller D, Rahman M, Lipkowitz S, Allegra C, Barrett JC, Kaye FJ, Zajac-Kaye M.** Thymidylate synthase as an oncogene: A novel role for an essential DNA synthesis enzyme. *Cancer Cell* 2004;5(4):341–351.

396. **Pestalozzi BC, Peterson HF, Gelber RD, Goldhirsch A, Gusterson BA, Trihia H, Lindtner J, Cortés-Funes H, Simmoncini E, Byrne MJ, Golouh R, Rudenstam CM,**

Castiglione-Gertsch M, Allegra CJ, Johnston PG. Prognostic importance of thymidylate synthase expression in early breast cancer. *J. Clin. Oncol.* 1997;15(5):1923–1931.

397. **Johnston PG, Fisher ER, Rockette HE, Fisher B, Wolmark N, Drake JC, Chabner BA, Allegra CJ.** The role of thymidylate synthase expression in prognosis and outcome of adjuvant chemotherapy in patients with rectal cancer. *J. Clin. Oncol.* 1994;12(12):2640–2647.

398. **Pinedo HM, Peters GF.** Fluorouracil: biochemistry and pharmacology. *J. Clin. Oncol.* 1988;6(10):1653–1664.

399. **van Triest B, Pinedo HM, van Hensbergen Y, Smid K, Telleman F, Schoenmakers PS, van der Wilt CL, van Laar JAM, Noordhuis P, Jansen G, Peters GJ.** Thymidylate Synthase Level as the Main Predictive Parameter for Sensitivity to 5-Fluorouracil, but not for Folate-based Thymidylate Synthase Inhibitors, in 13 Nonselected Colon Cancer Cell Lines. *Clin. Cancer Res.* 1999;5(3):643 LP – 654.

400. **Ferrari S, Severi L, Pozzi C, Quotadamo A, Ponterini G, Losi L, Marverti G, Costi MP.** Chapter Seventeen - Human Thymidylate Synthase Inhibitors Halting Ovarian Cancer Growth. In: Litwack GBT-V and H, ed. *Ovarian Cycle*.Vol 107. Academic Press; 2018:473–513.

401. **M. W.** Gluconeogenesis in the chicken: regulation of phosphoenolpyruvate carboxykinase gene expression. *Fed. Proc.* 1985;44(8):2469–2474.

402. **Watford M, Hod Y, Chiao YB, Utter MF, Hanson RW.** The unique role of the kidney in gluconeogenesis in the chicken. The significance of a cytosolic form of phosphoenolpyruvate carboxykinase. *J. Biol. Chem.* 1981;256(19):10023–10027.

403. **Davison TF, Langslow DR.** Changes in plasma glucose and liver glycogen following the administration of gluconeogenic precursors to the starving fowl. *Comp. Biochem. Physiol. Part A Physiol.* 1975;52(4):645–649.

404. **Ehrlich M.** DNA hypermethylation in disease: mechanisms and clinical relevance. *Epigenetics* 2019;14(12):1141–1163.

405. **Brown, MJ, Ameer, MA, Beier K.** *StatPearls [Internet]*. Vitamin B6. Treasure Island, FL: StatPearls Publishing; 2020. Available at: https://www.ncbi.nlm.nih.gov/books/NBK470579/.

406. **Field DJ, Benito J, Chen A, Jagt JWM, Ksepka DT.** Late Cretaceous neornithine from Europe illuminates the origins of crown birds. *Nature* 2020;579(7799):397–401.

407. **Vogel G.** Oldest fossil of modern birds is a 'turducken.' *Science (80-.).* 2020;367(6484):1290 LP – 1290.

408. **Clyde WC, Ramezani J, Johnson KR, Bowring SA, Jones MM.** Direct high-precision U-Pb geochronology of the end-Cretaceous extinction and calibration of Paleocene astronomical timescales. *Earth Planet. Sci. Lett.* 2016;452:272–280.

409. **Kaiho K, Oshima N, Adachi K, Adachi Y, Mizukami T, Fujibayashi M, Saito R.** Global climate change driven by soot at the K-Pg boundary as the cause of the mass extinction. *Sci. Rep.* 2016;6:28427.

410. **Vellekoop J, Sluijs A, Smit J, Schouten S, Weijers JWH, Sinninghe Damsté JS, Brinkhuis H.** Rapid short-term cooling following the Chicxulub impact at the Cretaceous-Paleogene boundary. *Proc. Natl. Acad. Sci. U. S. A.* 2014;111(21):7537-75411. Vellekoop J, Sluijs A, Smit J, Schoute.

411. **Sheehan PF DE.** Major extinctions of land-dwelling vertebrates at the Cretaceous-

Tertiary boundary, eastern Montana. *Geology* 1992;20(6):556–560.

412. **Alvarez LW, Alvarez W, Asaro F, Michel H V.** Extraterrestrial Cause for the Cretaceous-Tertiary Extinction. *Science (80-.).* 1980;208(4448):1095 LP – 1108.

413. **Longrich NR, Tokaryk T, Field DJ.** Mass extinction of birds at the Cretaceous-Paleogene (K-Pg) boundary. *Proc. Natl. Acad. Sci. U. S. A.* 2011;108(37):15253–15257.

414. **Field DJ, Bercovici A, Berv JS, Dunn R, Fastovsky DE, Lyson TR, Vajda V, Gauthier JA.** Early Evolution of Modern Birds Structured by Global Forest Collapse at the End-Cretaceous Mass Extinction. *Curr. Biol.* 2018;28(11):1825-1831.e2.

415. **Mangge H, Becker K, Fuchs D, Gostner JM.** Antioxidants, inflammation and cardiovascular disease. *World J. Cardiol.* 2014;6(6):462–477.

416. **Loscalzo J, Handy DE.** Epigenetic modifications: basic mechanisms and role in cardiovascular disease (2013 Grover Conference series). *Pulm. Circ.* 2014;4(2):169–174.

APPENDIX A

SUPPLEMENTAL FIGURES

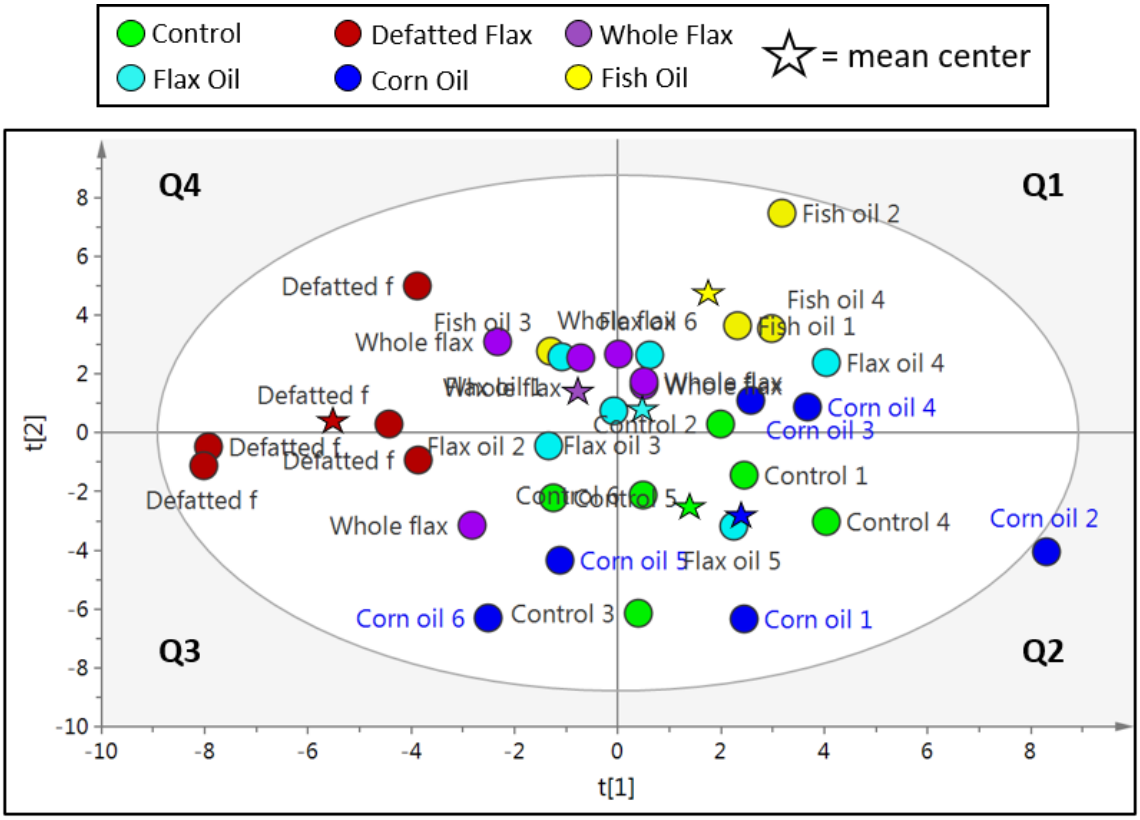

Figure Appendix S1. Partial least squares discriminate analysis (PLSDA).

VIP scores from the metabolites were used to cluster plasma samples according to PLSDA analysis. WF hens displayed the highest degree of clustering (notably, two WF samples perfectly coincident in Q1), followed by DF, FSH, FXO and CTL. DF hens were the most unique in terms separation from all other diets. Dietary enrichment with flaxseed oil (i.e. WF and FXO) caused a high degree of two-dimensional overlap. CRN was the least clustered, displaying a pattern of dispersion across Q1, Q2 and Q3. The mean center (i.e. the average XY dimension) for WF was located in Q4 near the origin (x=0, y=0). Similarly, FXO's mean center was also near the origin. DF's mean center showed a strong left shift beyond all other diets and was placed slightly into Q4. The mean centers of WF, FXO and DF (i.e. the flax diets) displayed similar horizontal y-axis alignment. The mean center of FSH extended separated itself further into Q1. Lastly, CRN and CTL displayed proximal mean centers located in Q2.

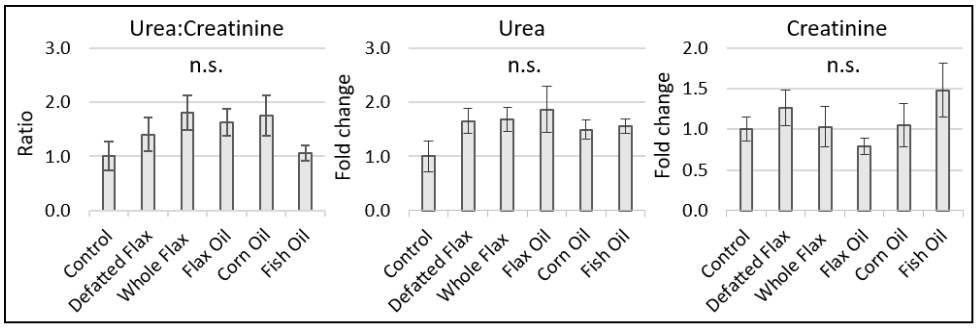

Figure Appendix S2. Plasma estimate of renal clearance. Hen blood plasma samples measured via LC-MS/MS. VIP scores of metabolites were analyzed via one-way ANOVA (Duncan's post-test, $p<0.05$). Groups without a similar letter are significantly different. *n*=4 to 6 plasma samples from different hens per diet group. Error bars are +/- SEM.

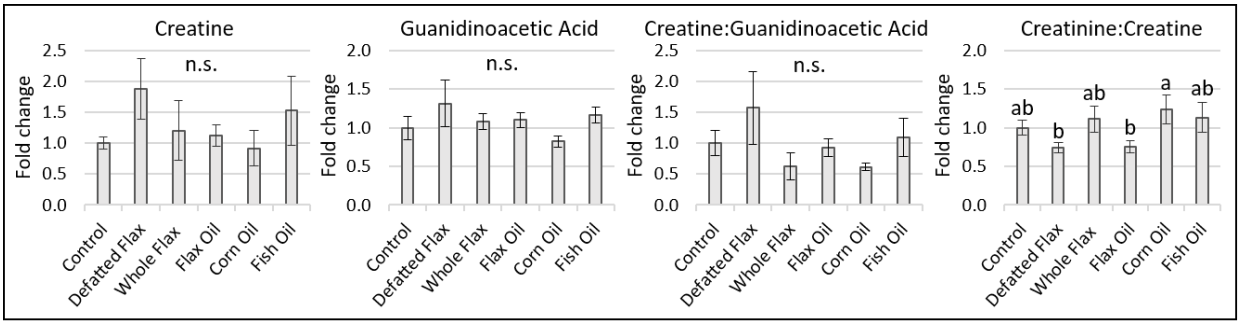

Figure Appendix S3. Creatine metabolism and estimate of GAMT activity. Hen blood plasma samples analyzed via LC-MS/MS. VIP scores of metabolites were analyzed via one-way ANOVA (Duncan's post-test). Samples without a similar letter are significantly different ($p<0.05$).

VITA

Graduate School
Southern Illinois University

William Christopher “Chris” Weston

william.c.weston1@gmail.com

Southern Illinois University Carbondale
Bachelor of Arts, German, May 2005
Bachelor of Arts, Sociology, May 2005

Southern Illinois University Carbondale
Master of Science, Geography and Geographic Information Systems, August 2012

Special Honors and Awards:
Sigma Xi Scholarship Recipient, 2016
Chandrashekar Memorial Travel Award, 2019

Dissertation Paper Title:
Flaxseed’s paradoxical role in extending lifespan and reproductive capacity in White Leghorn laying hens; and the effect of polyunsaturated fatty acids (PUFAs) on lipid metabolism, mitochondrial bioenergetics and E-cadherin expression in laying hen ovarian tumors

Major Professor: Dr. Dale B. Hales